EXPRESSION AND EDITING OF MICRORNA-376 CLUSTER IN HUMAN GLIOBLASTOMAS:

ROLE IN TUMOR GROWTH AND INVASION

YUKTI CHOUDHURY

NATIONAL UNIVERSITY OF

SINGAPORE

2011

EXPRESSION AND EDITING OF MICRORNA-376 CLUSTER IN HUMAN GLIOBLASTOMAS:

ROLE IN TUMOR GROWTH AND INVASION

YUKTI CHOUDHURY

(B.Sc., NUS)

A THESIS SUBMITTED

FOR THE DEGREE OF DOCTOR OF PHILOSOPHY

DEPARTMENT OF BIOLOGICAL SCIENCES

NATIONAL UNIVERSITY OF SINGAPORE

2011

Acknowledgements

Foremost, I would like to express my sincere gratitude to my advisor Dr. Wang Shu for his continuous support during my Ph.D studies and research, for his patience, motivation, enthusiasm, and immense knowledge. His guidance was invaluable throughout the time of research.

I thank my fellow lab-mates who have been helpful in every possible way and made time spent in the lab exciting and enjoyable. Thanks to Lam Dang Hoang and Felix Tay for their unwavering co-operation and contribution to this project. I would like to thank our collaborators at NNI, Singapore, Dr. Carol Tang and Dr. Ang Beng-Ti who have provided fruitful insights into several aspects of this work.

I would like to thank Khasali for his help during the writing of this thesis. Finally, I would like to thank my parents and my sister, for their constant encouragement, dedication and support for my endeavours through the last few years.

Table of Contents

Summary

MicroRNAs (miRNAs) are short non-coding RNAs that negatively regulate gene expression at the post-transcriptional level. The specificity of miRNA function is determined by complementary base-pairing of the 20-22 nucleotide miRNA sequence, specifically the 5'- end "seed", to target mRNAs. Adenosine-to-inosine (A-to-I) RNA editing is a mechanism that modifies the sequence of some miRNAs by replacing specific adenosine with inosine bases. miRNAs from miR-376 cluster are subject to regulated A-to-I editing and in healthy brain tissues, these miRNAs are edited to high levels at a single base in their seed sequences, which can redirect their targeting specificity. Several lines of evidence suggest that A-to-I editing is perturbed in gliomas, due to dysfunction of the editing machinery, the ADAR enzymes. Thus, in this study, it was hypothesized that the normal "programmed" level of editing of miRNAs from miR-376 cluster does not occur in gliomas and this has functional consequences related to tumor development, stemming from changes to the sequence of miRNAs.

Here, by sequencing of miRNAs from miR-376 cluster it was shown that compared to normal brain tissue, overall A-to-I editing of this cluster is significantly reduced in high-grade gliomas due to low expression of ADAR enzymes. As a result, in tumors, miRNAs are underedited or unedited. Specifically from this cluster, miR-376a* aberrantly accumulates entirely in the unedited form in glioblastomas (GBMs), the most malignant WHO grade IV gliomas. Thus, unedited miR-376a* is a tumor-specific miRNA sequence variant generated due to altered A-to-I editing in GBMs.

To investigate if aberrant accumulation of unedited miR-376a* in GBMs has functional consequences, unedited or edited miR-376a*, differing by a single base in the seed sequence were introduced in glioma cell lines. Through in vitro assays it was determined that unedited miR-376a* promotes glioma cell migration and invasion, in contrast to the edited miR-376a*, that suppresses these features.

Furthermore, through in vivo studies, expression of unedited miR-376a* in glioma cells was shown to promote aggressive growth of orthotopic gliomas, recapitulating features of human GBMs. By global gene expression profiling it was confirmed that a single base change in miR-376a*, brought about by loss of regulated A-to-I editing, is sufficient to direct its function towards an unfavorable target gene profile, consistent with aggressive glioma growth. Thus, unedited miR-376a* represents a functional miRNA sequence variant that promotes malignant properties of glioma cells.

To understand the mechanism by which unedited miR-376a* promotes glioma cell migration and invasion, target gene specificity of this miRNA was determined, through a combination of microarray analysis and computational predictions. It was established that the cellular effects of unedited miR-376a* in glioma cells are mediated by its sequence-dependent ability to target STAT3 and concomitant inability to target AMFR. These results show that a single base change in the sequence of a miRNA can have profound consequences on tumor growth and invasion through altered target gene specification. Significantly, these findings uncover a novel mechanism of miRNA deregulation in cancer, based on a tumor-specific change in miRNA seed sequence due to altered A-to-I editing.

Publications

Yukti Choudhury, Felix Chang Tay, Dang Hoang Lam, Carol Tang, Christopher B.T. Ang, and Shu Wang. Accumulation of Unedited Form of MicroRNA-376a* due to Attenuated Adenosine-to-Inosine Editing Promotes Migration and Invasion of Glioblastoma Cells. In preparation.

Yukti Choudhury, Lam Dang Hoang, and Shu Wang. MicroRNA-376a* accumulates in highly invasive glioma cells producing aggressive tumors and promotes glioma cell invasion in vitro. *5th RNAi and miRNA World Congress*. Boston. 2011. (***Winner of Best Poster Award****)*

The following are publications I have contributed to but are not included in the main body of the thesis:

Haiyan Guo, **Yukti Choudhury***, Jing Yang, Can Chen, Felix Chang Tay, Tit Meng Lim, Shu Wang Antiglioma effects of combined use of a baculoviral vector expressing wild-type p53 and sodium butyrate. *Journal of Gene Medicine* 2011; 13: 26–36**. (*co-first author**)*

Chunxiao Wu, Jiakai Lin, Michelle Hong, **Yukti Choudhury**, Poonam Balani, Doreen Leung, Lam H Dang, Ying Zhao, Jieming Zeng, and Shu Wang. Combinatorial Control of Suicide Gene Expression by Tissue-specific Promoter and microRNA Regulation for Cancer Therapy. *Molecular Therapy* 2009; 17(12):2058-66.

Chrishan J. A. Ramachandra, Mohammad Shahbazi, Timothy W. X. Kwang, **Yukti Choudhury**, Xiao Ying Bak, Jing Yang and Shu Wang, Efficient recombinase-mediated cassette exchange at the AAVS1 locus in human embryonic stem cells using baculoviral vectors. *Nucleic Acids Research* 2011; [Epub ahead of print]

List of Tables

List of Figures

List of Abbreviations

A	Adenosine
AA	Anaplastic astrocytoma
ADAR	Adenosine deaminase acting on RNA
AGO	Argonaute
AMFR	Autocrine motility factor receptor
AOA	Anaplastic oligoastrocytoma
AOG	Anaplastic oligodendroglioma
A-to-I	Adenosine-to-inosine
bp	Base pairs
BrdU	Bromodeoxyuridine
BSA	Bovine serum albumin
cDNA	Complementary DNA
CNS	Central nervous system
Ct	Threshold cycle
DAB	3,3' diaminobenzidine
DGCR8	Digeorge syndrome critical region gene 8
DMSO	Dimethyl sulfoxide
DNASe	Deoxyribonuclease
DPBS	Dulbecco's phosphate-buffered saline
dsRBD	Double-stranded RNA binding domain
dsRNA	Double-stranded RNA
ECM	Extra cellular matrix
EGF	Epidermal growth factor
EGFP	Enhanced green fluorecence protein
ELM	Experimental lung metastasis
FBS	Fetal bovine serum
FGF	Fibroblast growth factor
FITC	Fluorescein isothiocyanate
G	Guanosine
GBM	Glioblastoma
GFAP	Glial fibrillary acidic protein
GIC	Glioblastoma-initiating cell
GluR-B	Glutamate receptor subunit B
GO	Gene onotology
GO	Gene ontology
hESCs	Human embryonic stem cells
HIF	Hypoxia-inducible factor
I	Inosine
IP6	Inositol hexakisphosphate
KEGG	Kyoto Encyclopedia of Genes and Genomes
LB	Luria broth
LNA	Locked nucleic acid
MCS	Multiple cloning site
miR	Mature miRNA

miRISC	MicroRNA-induced silencing complex
miRNA	MicroRNA
miRNA*	MicroRNA-star
MMP	Matrix metalloproteinase
mRNA	Messenger RNA
NAA	Normal astrocytes
NB	Normal brain
NPC	Neural precursor cell
NSC	Neural stem cell
nt	Nucleotide
ORF	Open reading frame
PAP	Poly A polymerase
P-body	Processing body
PCR	Polymerase chain reaction
PDGF	Platelet-derived growth factor
Pol II	RNA polymerase II
Pol III	RNA polymerase III
pre-miRNA	Precursor miRNA
pri-miRNA	Primary miRNA
PTEN	Phosphatase and tensin homolog
qRT-PCR	Quantitative reverse transciptase-PCR
RISC	RNA-induced silencing complex
Rnase	Ribonuclease
rRNA	Ribosomal RNA
RT-PCR	Reverse transciptase-PCR
SD	Standard deviation
SDS	Sodium dodecyl sulphate
siRNA	Short interfering RNA
SNP	Single nucleotuce polymorphism
ssRNA	Single-stranded RNA
STAT3	Signal transducer and activator of transcription 3
TAE	Tris-acetate-EDTA
TBS	Tris -buffered Saline
TCGA	The cancer genome atlas
TGF	Transforming growth factor
TU	Transcription units
U	Uracil
ULS	Universal linkage system
UTR	Untranslated region
VEGF	Vascular endothelial growth factor
WHO	World health organization

1 CHAPTER 1. Introduction

1.1 MicroRNAs: Overview

MicroRNAs constitute an abundant family of short, non-coding RNAs that mediate posttranscriptional gene expression regulation. Based on antisense complementarity to the 3' untranslated regions (3' UTR) of messenger RNAs (mRNA), miRNAs specifically mediate negative regulation of target gene translation impacting target protein output (Bartel, 2004). miRNAs are ubiquitously present and have been found in viruses, worms, flies, plants, mammals, indeed in all metazoan eukaryotes (Bartel, 2009). In humans, >1000 miRNAs are annotated in the comprehensive miRNA registry, miRBase version 17.0 (Griffiths-Jones et al., 2008). Each mammalian miRNA is predicted to target ~200 genes (Krek et al., 2005) and based on bioinformatics analyses this amounts to a collective regulation of over 30% of all protein-coding genes (Lewis et al., 2005; Xie et al., 2005). Despite having modest effects on protein output by fine-tuning target gene expression (Baek et al., 2008; Selbach et al., 2008), miRNAs can be indispensible for cellular function and are known to regulate differentiation, apoptosis, metabolism, and neuronal development as well as pathological conditions such as cancer (Kloosterman and Plasterk, 2006).

1.2 Biogenesis of miRNAs

1.2.1 Genomics

The genomics of miRNA genes are closely linked to their biogenesis. Nearly half of the genes encoding miRNAs are found in clusters and 55 such miRNA clusters have been identified in the human genome (Kim and Nam, 2006; Yuan et al., 2009). Given their proximal genomic location, clustered miRNAs are polycistronically transcribed as long primary transcripts and presumably, are under similar regulatory influences (Kim and Nam, 2006).

miRNA genes can be located in intergenic genomic regions distinct from known transcription units where they can be clustered or monocistronic. Significantly however, the location of ~70% of known mammalian miRNAs is intragenic and overlaps with known transcription units (TUs)- either within introns of protein-coding genes, or within TUs lacking protein-coding potential, referred to as long non-coding RNAs (Rodriguez et al., 2004). Intragenic miRNAs are also often present in clustered arrangements such as the mir-106b~25~93 cluster found within the intron 13 of *MCM7* gene in humans and mice (Kim and Nam, 2006).

1.2.2 Transcription

miRNA biogenesis begins with transcription of a long primary transcript by RNA polymerase II (Pol II), while a small group of miRNAs may be transcribed by Pol III (Kim et al., 2009). Most primary miRNAs (pri-miRNAs) are capped at the 5' end and polyadenylated at the 3' end, characteristic features of all Pol II transcripts (Lee et al., 2004). The genomic location of miRNA loci dictates that intergenic miRNAs are transcribed from their own promoters while intragenic miRNAs share regulatory elements with their host genes (Bartel, 2004). In case of intronic and exonic miRNAs, the Pol II-transcribed primary transcript hosts both the pre-mRNA and the pri-miRNA.

1.2.3 Processing

Pri-miRNAs can range from hundreds to thousands of nucleotides in length and contain one or more defining local stem-loop structures (Kim et al., 2009). In the nucleus, the RNAse III-type endonuclease Drosha, cleaves both strands of the primary stem-loop at the base of the stem releasing ~60-70-nt long intermediate stem-loop structure termed the precursor miRNA (pre-miRNA) (Lee et al., 2003). Appropriate cleavage of pri-miRNAs requires the recognition of the 33-bp (double-stranded) stem and flanking single-stranded RNA segments of pri-miRNA structure by DGCR8, which then aids Drosha cleavage of both strands of the stem ~11 bp from the ssRNA-dsRNA junction (Han et al., 2006). The Drosha-generated pre-

miRNAs are characterized by a staggered base with a 5' phosphate and ~ 2-nt 3' overhang (Bartel, 2004). For intragenic miRNAs, their release from host genes is assumed to involve the action of the spliceosome machinery for intron excision prior to further processing (Kim and Kim, 2007).

The pre-miRNA is transported by exportin-5 out of the nucleus to the cytoplasm where it undergoes further processing by the RNAse III endonuclease, Dicer which cleaves both strands of the pre-miRNA stem ~22 nt from the pre-existing terminus (product of Drosha processing, which defines one end of the mature product (Bartel, 2004)) removing the loop and terminal base pairs (Bartel, 2004). Dicer generates a staggered cut with a 5' phosphate and ~ 2-nt overhang, resulting in an imperfect 16-24 nt duplex containing the mature miRNA, termed the miRNA:miRNA* duplex with 5' phosphates and ~2 nt 3' overhangs.

Following Dicer cleavage, the RNA duplex is assembled into a large ribonucleoprotein complex, known as miRNA-induced silencing complex (miRISC). One strand of the duplex remains associated with an AGO protein, from the highly conserved Argonaute family, which form the core of miRISC (Bartel, 2004). This strand is known as the guide strand. The other strand known as the passenger strand or miRNA* is degraded (Kim et al., 2009). The determination of which strand is incorporated is based on the thermodynamic stability of the two ends of the duplex. Typically, the strand with more unstable base pairs at its 5' end is preferentially incorporated into RISC (Hutvagner, 2005; Khvorova et al., 2003). Figure 1.1 summarizes the steps involved in the biogenesis of miRNAs till their loading into functional miRISCs.

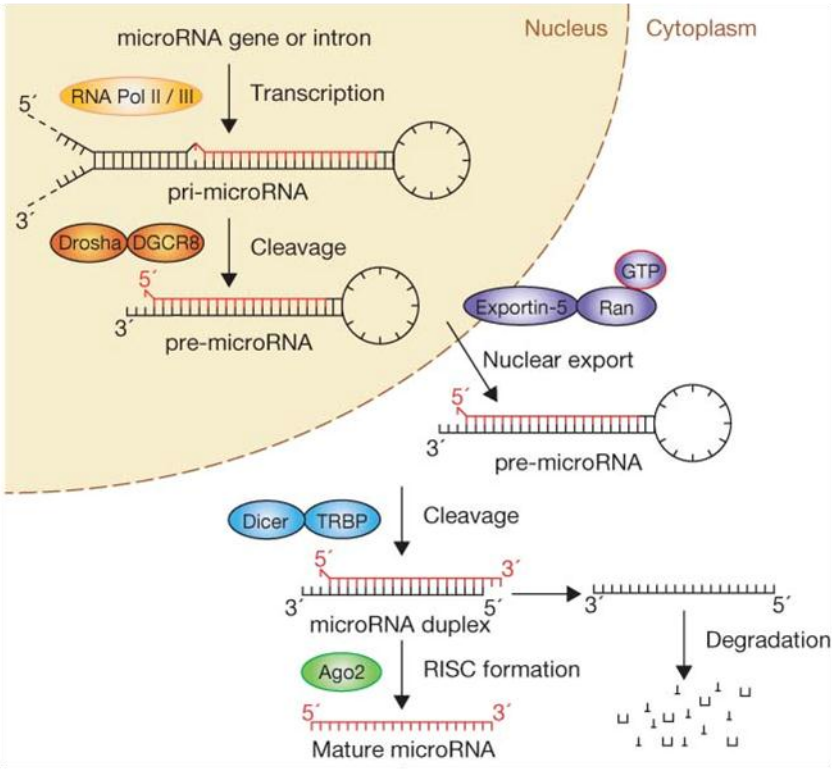

Figure 1.1 Biogenesis of miRNAs. Schematic representation of the miRNA biogenesis pathway. Following transcription by RNA polymerase II, primary miRNA (pri-miRNA) transcripts are recognized and cleaved by the nuclear Microprocessor complex consisting of Drosha and DGCR8, to produce ~60-nt precursor miRNA (pre-miRNA) transcripts with characteristic stem-loop structure. The pre-miRNA is then transported to the cytoplasm by Ran-GTP and export receptor exportin-5. The cytoplasmic RNase, Dicer then processes the pre-miRNA to ~20 bp mature miRNA duplex. One strand of the duplex, the guide strand, is selected for incorporation into RISC while the other strand is degraded. The core component, of RISC, Ago protein mediates the downstream silencing effect of the incorporated guide strand. Image taken from (Winter et al., 2009).

1.2.3.1 miRNA strands*

It is important to note that thermodynamic properties alone are unlikely to determine the choice of miRNA duplex arm incorporation into RISC because several miRNA* species are abundantly expressed and functional (Okamura et al., 2008; Yang et al., 2011), and miRNA or miRNA* incorporation and individual strand abundance can vary widely across tissues and developmental times (Griffiths-Jones et al., 2011). Some sequence determinants that dictate the preferential sorting of miRNA* strand

of the miRNA/miRNA* duplex to AGO2 proteins have been identified (Czech et al., 2009; Okamura et al., 2009).

Indeed, for several pre-miRNAs, both strands of the duplex are functional mature miRNAs. The naming of miRNA and miRNA* strands is conventionally determined by the steady-state abundance of each strand. The more abundant product of a pre-miRNA is referred to as miRNA while the rarer partner strand is referred to as miRNA* (Lau et al., 2001; Okamura et al., 2008). According to miRBase (Griffiths-Jones et al., 2008), if the ratio of expression of miRNA and miRNA* strands is not yet determined or where both strands have an approximately equal expression, the mature miRNA is named with a suffix '-5p' or '-3p' depending on the pre-miRNA strand of origin. A recent development in the miRNA nomenclature system is the move to substitute all miR:miR* nomenclature with '-5p'/'-3p' to reflect the general abundance and regulatory function of miRNA* species (Okamura et al., 2008; Yang et al., 2011).

1.2.4 Determinants of steady-state abundance of miRNAs

The steady-state abundance of a mature miRNA is determined by several posttranscriptional mechanisms and is rarely correlated to the expression or transcription rate of its precursor (Siomi and Siomi, 2010). Furthermore, although clustered miRNAs are commonly transcribed in a single transcript, their expression may not be coordinated due to regulation at the level of individual miRNAs (Guil and Caceres, 2007; Lu et al., 2007; Mineno et al., 2006). In addition to strand selection, degradation and turnover of mature miRNAs, association with target mRNAs are other posttranscriptional mechanisms that can determine the steady-state abundance of an individual miRNA (Siomi and Siomi, 2010).

1.3 Mechanism of action of miRNAs

The functional core of miRISC is AGO which execute the inhibitory effects of miRNAs. Additionally, RISC contains other regulatory factors that control RISC assembly and function (Filipowicz et al., 2008). miRNAs incorporated in the RISC assembly direct posttranscriptional gene regulation leading to repressed target protein synthesis. At least three mechanisms of miRNA function in repressing protein synthesis are currently known but the exact mechanism by which a particular miRNA may regulate a particular target is difficult to predict. During regulation of target genes, miRNAs can mediate mRNA cleavage, deadenylation or translational repression of target mRNAs (Figure 1.2).

1.3.1 mRNA cleavage

Some miRNAs can direct endonucleolytic cleavage of their targets (Davis et al., 2005; Yekta et al., 2004). This is typically determined by the extensive base-pairing between the miRNA and target mRNA and is rare given that most animal miRNAs do not have extensive complementarity to mRNAs (Valencia-Sanchez et al., 2006). For target cleavage to occur the RISC complex must contain a specific Argonaute, AGO2, which in mammalian cells is the only AGO protein known to be capable of directing cleavage through its RNase H domain (Meister et al., 2004).

1.3.2 mRNA deadenylation and decay

In a manner independent from endonucleolytic cleavage, miRNAs can induce destabilization of their target mRNAs (Figure 1.2A). This is evident from specific examples of target mRNA degradation in the absence of perfect complementarity with miRNA (Bagga et al., 2005; Wu et al., 2006), and from microarray experiments where experimentally manipulating the level of a miRNA leads to changes in the mRNA abundance of several validated and predicted targets (Krutzfeldt et al., 2005; Lim et al., 2005). miRNAs direct their targets for degradation by accelerating their deadenylation and decapping (Eulalio et al., 2008; Filipowicz et al., 2008). GW182, a

protein required for P-body integrity, interacts with AGO1 of the RISC complex, and marks mRNA for decay by recruitment of CCR4:NOT1 deadenylase complex (Filipowicz et al., 2008; Pillai et al., 2007). In addition to GW182, miRNAs, miRNA targets and AGO proteins are also detected in cytoplasmic P-bodies, where bulk mRNA degradation occurs, suggesting a model where miRNA targets are sequestered from the translational machinery and undergo decay (Eulalio et al., 2008; Valencia-Sanchez et al., 2006).

1.3.3 Translational repression

Translational repression can be mediated by miRNAs at the initiation and post-initiation stages of protein synthesis (Figure 1.2B). Translation initiation can be blocked by inhibition of cap-binding of the translation initiation factor eIF4E by direct competition with Argonaute for the mRNA 7-methylguanosine cap (Kiriakidou et al., 2007). Interaction of eIF6, a crucial factor for 60S ribosome subunit biogenesis, with the Ago2-Dicer-TRBP (RISC) complex can also prevent ribosome assembly and block translation initiation (Chendrimada et al., 2007). At the post-initiation stages, miRNAs can interfere with the polypeptide elongation step by inducing ribosome ‘drop-off’ (Maroney et al., 2006; Petersen et al., 2006). The association of repressed mRNAs with actively translating polyribosomes supports a post-initiation action of miRNA inhibition. Repressed ribosome-free mRNA aggregate may be exported to P-bodies for degradation (Behm-Ansmant et al., 2006; Pillai et al., 2007).

Recent evidence from genome-wide studies on miRNA-mediated regulation of protein and mRNA abundances, suggests that mRNA degradation alone can account for most of the repression mediated by miRNAs, at least in cell culture (Huntzinger and Izaurralde, 2011). Through such mRNA and protein level comparisons, it has been found that only a very small fraction of targets are repressed exclusively at the translational level, and this fraction also displays more limited levels of regulation (Baek et al., 2008; Hendrickson et al., 2009).

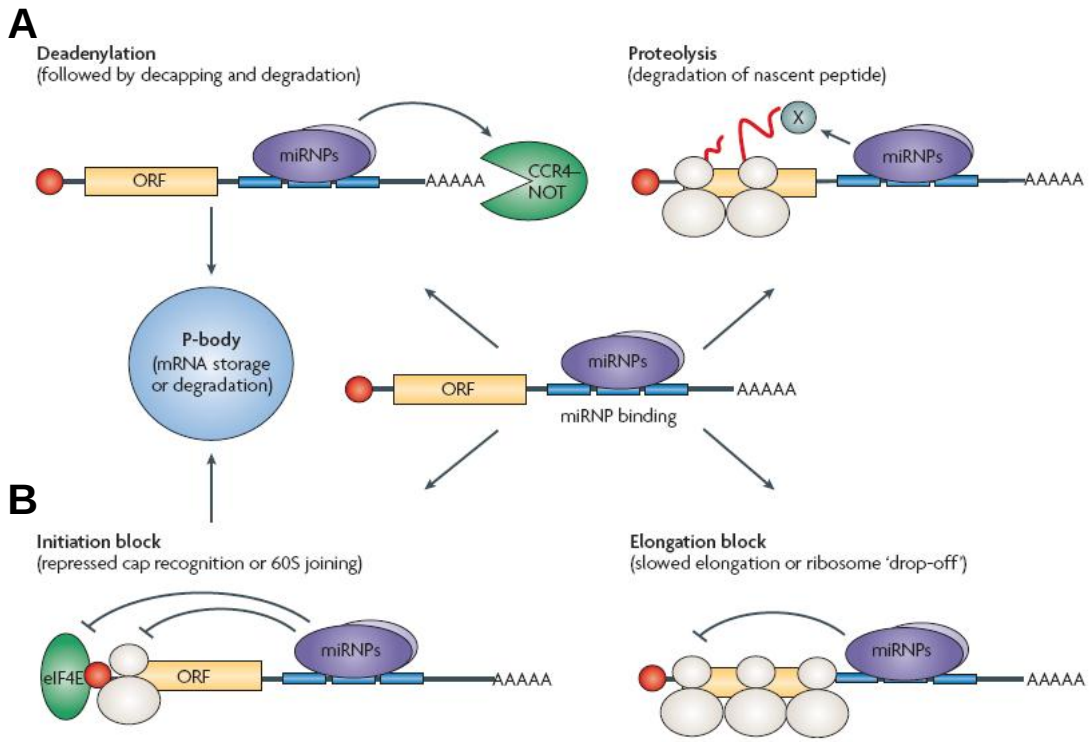

Figure 1.2 Mechanisms of posttranscriptional repression mediated by miRNAs . *A.* Binding of miRNA-loaded miRNP (miRISC) complex can lead to mRNA deadenylation and degradation through the recruitment of deadenylation complex, CCR4-NOT, right. Proteolysis of nascent polypeptide may also occur cotranslationally through an as yet unrecognized protease, left. ***B.*** miRNA targeting can lead to translational repression through an initiation block by hindering cap recognition by eIF4E or by preventing 60S subunit joining, left. Alternatively, repression can also occur at post-initiation step of translation, right. Middle, repressed mRNAs are transported to P-bodies for degradation or storage. Image from (Filipowicz et al., 2008).

1.4 Principles of miRNA target recognition

The key determinant for miRNA-mediated regulation is the miRNA sequence. In plants, miRNAs bear near-perfect complementarity with their targets and induce endonucleolytic cleavage of mRNA (Jones-Rhoades et al., 2006). In contrast, most metazoan miRNAs pair with partial complementarity to their targets. Target selection for most miRNAs is governed by a set of rules that have been experimentally and computationally determined (Brennecke et al., 2005; Doench and Sharp, 2004; Lewis et al., 2005).

1.4.1 Seed matches in 3'UTRs

At the core of miRNA target recognition is the requirement of contiguous and perfect base-pairing with nucleotides 2-8 of miRNA, termed the miRNA 'seed' sequence (Brennecke et al., 2005; Lewis et al., 2005). Lack of complementarity in the central part of the miRNA (positions 10 and 11) is also a feature of most mRNA-miRNA interactions and precludes the endonucleolytic cleavage of the target mRNA (Pillai et al., 2007). Most functional miRNA sites lie in the 3'UTR of target genes, and show high degree of conservation. The requirement for miRNA targeting sites to be restricted to the 3'UTR, is speculated to be due the potential displacement of the bound miRISC complex by ribosomes translocating through the 5' UTR and ORF regions during protein translation, precluding their selection as miRNA binding sites (Grimson et al., 2007; Gu et al., 2009).

1.4.2 Features of miRNA targeting sites

Functional miRNA target sites have been classified based on the degree of pairing with the 5'-end of miRNA (Figure 1.3A). Three classes of miRNA target sites include (i) 5' dominant canonical, (ii) 5' dominant seed, and (iii) 3' compensatory (Brennecke et al., 2005). 5' dominant canonical sites have good pairing with both 5' and 3' ends of miRNA, whereas 5' dominant seed sites tend to have good pairing with the 5' seed only with limited or no pairing with the 3' end of miRNA. Due to their extensive pairing canonical sites may function in single copies. Whereas, seed sites are speculated to be more effective when present in multiple copies. The 3' compensatory class of target sites involves compromised 5' seed pairing of 4 to 6 base-pairs, seeds of 7 or 8 bases with G:U wobbles, single nucleotide bulges or mismatches, which are then complemented by extensive pairing to the 3' end of the miRNA, especially at nucleotides 13-16.

The presence of multiple sites of the same miRNA within a given 3'UTR increases the effectiveness of miRNA targeting significantly (Brennecke et al., 2005; Nielsen et

al., 2007). The distance between the sites determines their effectiveness together, with 10-40 nt apart being most contributory to cooperative action (Grimson et al., 2007).

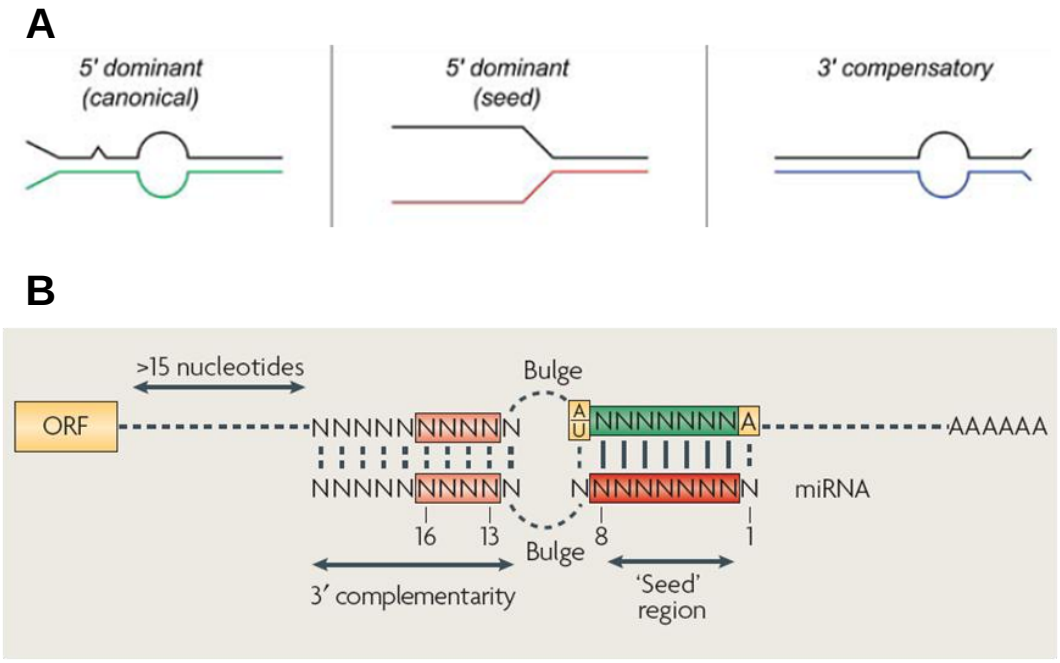

Figure 1.3 Priniciples of miRNA target recognition. ***A.*** Three classes of miRNA target sites based on extent of miRNA-mRNA interaction. mRNA target sites are the upper lines and miRNAs are the lower lines. Canonical site with good pairing of 5' and 3' ends of miRNA (left), 5' dominant seed site with extensive pairing of seed only (middle), and 3' compensatory site with compromised 5' seed pairing complemented by extensive pairing of the 3' end of miRNA (right). Image from (Brennecke et al., 2005). ***B.*** Generalized principles of miRNA interaction with targets. Contiguous base-pairing at miRNA positions 2-8, is enhanced by the presence of A at target position 1 and A or U at target position 9. Bulge at the central region of miRNA-mRNA duplex precludes endonucleolytic cleavage by Argonaute. Complementarity at 3' end of miRNA stabilizes the interaction. Image from (Filipowicz et al., 2008).

1.4.3 Contextual determinants of targeting

In addition to the targeting site itself, several contextual determinants of functional targeting have been determined. High local AU density in the immediate vicinity of the targeting site improves the effectiveness of targeting sites, presumably due to the weaker secondary structure of mRNA which increases miRNA accessibility to the targeting sites (Grimson et al., 2007). Indeed, lack of a local secondary structure near miRNA targeting site has been shown to be an essential and conserved feature

across genomes (Kertesz et al., 2007). Effective sites also lie preferentially at the ends of long 3'UTRs (>1300 nt), that is, close to the ORF or to the poly(A) tail, while the region within 15 nt of the stop codon of the ORF is generaly not suitable for targeting (Grimson et al., 2007).

Quantitative analysis of microarray data of messages down-regulated after introducing a miRNA has shown that efficacy of targeting sites follows a hierarchy: 8mer>>7mer-m8>7mer-A1>>6mer (Bartel, 2009; Grimson et al., 2007). The degree of mRNA down-regulation is therefore, to an extent determined by the type of targeting site present in the 3'UTR. The same hierarchy applies when protein levels are examined (Baek et al., 2008; Selbach et al., 2008). However, whether a given miRNA triggers mRNA decay or translation repression seems to be specified by the mRNA target (Eulalio et al., 2008). The involvement of accessory proteins, structural determinants of the miRNA-mRNA duplex may dictate the outcome (Filipowicz et al., 2008).

There are notable exceptions to many of the miRNA targeting rules. Offset 6mer sites, that is, seed matches at positions 3-8 of miRNA are variant seeds that are often conserved and functional (Friedman et al., 2009; Wu and Belasco, 2005). Contrary to expectation, some functional miRNA sites are located in the ORFs of target mRNAs rather than their 3'UTRs (Duursma et al., 2008; Forman et al., 2008; Lal et al., 2008; Tay et al., 2008). Furthermore, using artificial sensor constructs miRNA-mediated repression was shown to be effective when sites were located in the 5'UTR of the reporter (Lytle et al., 2007). The absolute requirement for Watson-Crick base-pairing in the miRNA seed sequence has been overturned by the presence of mismatches in the seed and G:U wobble pairs in functional non-seed matches in mouse and *C. elegans* targets (Didiano and Hobert, 2006; Tay et al., 2008). Furthermore, functional "seedless" target sites for a particular miRNA, miR-24 have also been identified, with no seed sequence match but extensive pairing at other regions (Lal et

al., 2009). Rather than being exceptions, these examples may represent a general scenario which is yet to be defined and is independent of seed site and conservation.

1.5 miRNAs in cancer

Majority of identified miRNAs are evolutionarily conserved in related species such as humans and mouse with some (e.g. let-7 family) being found conserved across many lineages (Bartel, 2004), suggesting critical functions for miRNAs. Studies suggest a general involvement of miRNAs in regulation of developmental pathways and differentiation of cells. At least three features of miRNA genomics and expression support a role for miRNAs in cancers:

1. Location of human miRNA genes in cancer-associated sites : about 50% of the annotated human miRNAs are located in specific cancer-associated genomic regions or fragile sites (Calin et al., 2004).
2. Tissue-specific expression profiles of miRNAs : a microarray study of 154 human miRNAs revealed that most miRNAs are expressed in a tissue-specific manner, and that adult organs (more differentiated) express many more miRNAs than embryonic tissues (Babak et al., 2004a; Babak et al., 2004b).
3. General downregulation of miRNAs in cancers : a systematic expression analysis of 217 miRNAs across multiple human cancer samples, showed that there is a general downregulation of miRNA expression in tumors compared to the normal tissue counterparts (Lu et al., 2005) and in tumor-derived cell lines (Gaur et al., 2007). A general role for down-regulated miRNA expression in tumorigenesis was supported by enhanced tumorigenesis mediated by global miRNA loss due to Dicer knockdown (Kumar et al., 2007).

Cancer-specific miRNA expression patterns, termed ‘miRNA signatures’ have been identified by miRNA expression profiling for every type of cancer analyzed (Calin and Croce, 2006). Functions of individual miRNAs have been associated with specific

cancers, populating an ever-expanding list (Table 1.1). The current model proposes a direct role of miRNAs in cancer as either oncogenes or tumor suppressors by virtue of their over- or under-expression. In this scenario, due to miRNA misexpression, several target genes become misregulated being under the negative regulatory influence of miRNAs.

	miRNA	**Alteration in cancers**	**Targets**
ONCOGENES	miR-17-92, miR-17-5p and miR-20a	Overexpressed in B-cell lymphoma and lung cancer	BIM, PTEN, CDKN1A, PTEN
	miR-106a, miR-363	Overexpressed in T-cell leukemia, colon, pancreatic and prostate tumors	Retinoblastoma protein, myosin regulatory light chain-interacting protein and retinoblastoma-binding protein 1-like
	miR-155	Overexpressed in CLL, B-cell, Hodgkin's and Burkitt lymphomas and in human breast cancer	SHIP1, CEBPB, MAF
	miR-21	Overexpressed in breast cancer, glioblastomas, CLL and in cervical cancer	SPOCK1, TPM1 and PTEN, PDCD4
	miR-221	Overexpressed in thyroid cancer, glioblastoma, pancreatic cancer and in prostate cancer	p27
	miR-372, miR-373	Overexpressed in testicular germ cell tumors with wt p53	LATS2
TUMOR SUPPRESSORS	let-7	Reduced in lung and colon cancers	H-Ras, N-Ras, K-Ras, HMGA2
	miR-15a	Lost in CLL, pituitary adenoma	Bcl-2
	miR-16-1	Lost in CLL, pituitary adenoma	Bcl-2; arginyl-tRNA synthetase
	miR-127	Reduced in various cancer cell lines	Bcl-6
	miR-29	Reduced in CLL	Tcl1, Mcl1, DNMTs
	mR-181	Reduced in CLL	Tcl1
	miR-124a	Reduced by methylation in colon and lung cancers	CDK6
	miR-17-5p	Decreased in some cancers, increased in others	E2F, AIB1
	miR-34a, miR-34b and miR-34c	Reduced in colon, lung, breast, kidney and bladder cancer	CDK4, CDK6, CCNE2, CCND1, MET, MYC, BCL-2
	miR-26a	Reduced in liver cancer	CCND2, CCNE2

Table 1.1 miRNAs associated with cancers as oncogenes or tumor suppressors. CLL: chronic lymphocytic leukemia. Adapted from (Garzon et al., 2010), (Croce, 2009) and (Gartel and Kandel, 2008).

1.5.1 miRNAs involved in metastasis and invasion

In addition to their involvement in cancer as classical tumor suppressors or oncogenes, miRNAs may regulate cancer cell migration, invasion and metastasis. miRNAs that have been found shown to promote invasion and metastasis in breast cancer include miR-10b, miR-373 and miR-520c, while others suppressing metastasis and invasion include miR-335, miR-206 and miR-146a/b (Aigner, 2011; Dykxhoorn, 2010). Some miRNAs can be specifically involved in metastatic development and not linked to primary tumor development, such as miR-31 (Valastyan et al., 2009). A key regulator of metastasis is miR-103/107 family that regulates Dicer expression by targeting its 3'UTR and through this induces a global down-regulation of miRNAs during breast cancer progression (Martello et al., 2010). Like other differentially expressed miRNAs, most metastatic-promoting or suppressing miRNAs have been identified by their differential expression in highly metastatic cancer cell lines to parental non-metastatic cell lines through profiling studies (Ma et al., 2007; Tavazoie et al., 2008; Valastyan et al., 2009). Furthermore, in these studies the two major aspects of metastatic behaviour that have been shown to be governed by miRNAs are cellular motility and invasion (Hurst et al., 2009).

1.5.2 Mechanisms of miRNA expression deregulation in cancers

As currently understood, the primary mode of miRNA deregulation in cancer is rooted in their altered expression levels which may arise by four main mechanisms.

1. Genomic abnormalities: deletion, amplification and translocation can lead to copy number changes of miRNA genomic loci changing miRNA expression levels e.g. miR-15 and miR-16-1 (Calin et al., 2004; Zhang et al., 2006).
2. Epigenetic factors: Aberrant CpG hypermethylation of miRNA promoters in cancer cells relative to normal tissue leading to silencing to miRNA expression e.g. miR-9-1, miR-124a and miR-127 (Lehmann et al., 2008; Lujambio et al., 2007; Saito et al., 2006).

3. Transcriptional regulation: Dysregulation of transcription factors can lead to aberrant miRNA expression. This is especially true for tissue-specific miRNAs or those with roles in differentiation and development e.g. miR-17-92 cluster (transactivated by MYC) (O'Donnell et al., 2005), let-7 and miR-29 familes (repressed by MYC) (Chang et al., 2008) and miR-34 family (induced by p53) (Raver-Shapira et al., 2007).
4. miRNA processing defects: Aberrant processing of pri-miRNAs can lead to changes in mature miRNA levels. In tumor samples, no correlation was observed between pri-miRNA and mature miRNA expression while in normal tissues there was a positive correlation, suggesting aberrant post-trancriptional regulation of miRNAs in cancers, especially at Drosha processing step (Thomson et al., 2006). Dicer expression is altered in some lung cancers and correlated with poor prognosis (Karube et al., 2005).

1.5.3 Mutations and polymorphisms in miRNAs

Mutations and polymorphisms located in mature miRNAs, precursor stem-loop or the primary miRNA sequence can potentially also contribute to miRNA dysfunction in cancer. Given the sequence-based determination of miRNA function, a change in mature miRNA sequence composition, presents tremendous opportunities for cancer cells to exploit for their growth advantage. Notably however, tumor-specific mutations and polymorphisms in mature miRNAs, especially the seed region, are rare (Diederichs and Haber, 2006; Landgraf et al., 2007; Ryan et al., 2010; Shen et al., 2009). In fact, genetic changes in the effective sequence of mature miRNAs have rarely been documented both in general populations and in cancers (Saunders et al., 2007; Slaby et al., 2011). Germline mutations in the primary transcripts of miR-15 and miR-16-1 in chronic lymphocytic leukemia and familial breast cancer were reported to be responsible for their low expression in these cancers (Calin et al., 2005). In general, when miRNA gene sequence variations are functional, they have

been shown to influence miRNA biogenesis, ultimately contributing to the abnormal abundance component of miRNA dysfunction (Duan et al., 2007; Hu et al., 2008; Jazdzewski et al., 2008; Sun et al., 2009; Sun et al., 2010; Wu et al., 2008; Xu et al., 2008).

1.5.4 Mutations and polymorphisms in miRNA target sites

Sequence variations in miRNA target sites can play a parallel role in influencing miRNA function through altered miRNA-mRNA interaction. Computational analyses of SNPs located in the miRNA binding sites in 3'UTRs of various human genes indicate that variant allele frequencies for some miRNA targeting sites are significantly different between cancer and normal tissues (Yu et al., 2007). In a recent study, known genetic variants of breast cancer susceptibility were analyzed for potential influence on miRNA targeting and were shown to create or abrogate targeting sites, potentially accounting for their altered expression (Nicoloso et al., 2010). Specific examples of target SNPs are known for *KRAS* 3'UTR which disrupts targeting by let-7 in lung cancer (Chin et al., 2008) and for *CD86* targeting by miR-582 (Landi et al., 2008).

Besides SNPs, gain or loss of segments of 3'UTRs with attendant miRNA targeting sites can influence the expression of target genes, as is seen for *HMGA2*, which escapes targeting by let-7 by a chromosomal rearrangements which separates its ORF form its 3'UTR (Mayr et al., 2007), or by alternative splicing for TrkC which creates isoforms with or without 3'UTR targeting sites for miR-9, miR-125a and miR-125b (Laneve et al., 2007).

1.6 miRNAs in gliomas

Gliomas arise from cells of glial origin and are the most common primary brain tumors. Morphological similarity of tumor cells to normal glial cells- astrocytes or oligodendrocytes- is a major criteria for classification of gliomas as astrocytomas,

oligodendrogliomas or mixed oligoastrocytomas (Louis, 2006). Four degrees of malignancies of gliomas are defined by World Health Organization (WHO): grade I, grade II, grade III (anaplastic) and grade IV. Grade I tumors are biologically benign, grades II and III display increasing malignancy and grade IV classification is reserved for glioblastomas (GBM), the most malignant form of astrocytomas (Furnari et al., 2007; Louis, 2006). The median survival of patients with GBMs is significantly shorter (12-18 months) compared to patients with grade III tumors (3 years). Several common molecular lesions in GBMs have previously been implicated in oncogenic activation and recently been analyzed on a large scale in efforts such as TCGA studies (The Cancer Genome Atlas Network, 2008). Among others, mutations in TP53, PTEN, EGFR, RB1, and NF1 have frequently been detected in GBM tumors.

1.7 Pathophysiological features of glioblastomas

Proliferation, invasion and angiogenesis are the hallmark biological processes that underlie GBM pathogenesis (Furnari et al., 2007). Uncontrolled proliferation occurs in GBMs due to cell cycle dysregulation and aberrant mitogenic signaling through receptor tyrosine kinases (EGFR, PDGFR), which typically activate PI3K and MAPK signaling. Invasion is a multi-step process that is driven by cellular motility, cell-cell adhesion, interaction with the extracellular matrix (ECM) and its proteolytic degradation. Glioma cells express proteases, such as metalloproteinases (especially MMP2 and MMP9), that degrade the ECM, and integrins that allow interaction of the glioma cells with components of the ECM. Such interactions lead to altered cytoskeleton configuration promoting cellular migration. Overlapping with proliferative effects, growth factor signaling through EGF, FGF and VEGF which are overexpressed in GBMs also promote cell migration (Louis, 2006). Robust angiogenesis is also present in GBMs and is characterized by microvascular proliferation of glomeruloid vessels. The common angiogenic pathways in GBMs involve angiogenic growth factors such as VEGF and PDGF which are expressed by

tumor cells, for which the receptors are expressed on endothelial cells. The presence of necrosis is a feature that distinguishes GBMs from grade III tumors and is thought to arise from rapidly increasing metabolic demands of the growing tumor mass or due to vascular thrombosis. Necrotic foci are surrounded by hypercellular zones known as pseudopalisades which consist of hypoxic cells that secrete high levels of pro-angiogenic factors such as VEGF (Brat et al., 2004). Furthermore, pseudopalisading cells acquire migratory and invasive properties in response to hypoxia (Louis, 2006).

1.7.1 Functions of specific miRNAs in glioblastomas

Key miRNAs that are over- or under-expressed in GBMs have been shown to regulate the above-mentioned tumor characteristics and will be briefly discussed here.

miR-21 is highly expressed in GBMs and is an anti-apoptotic miRNA that directly inhibits tumor suppressors PTEN, PDCD4 and TPM1 (Moore and Zhang, 2010). Knockdown of miR-21 by locked nucleic acid (LNA) or 2'O-Me-miR-21 antagomir was shown to increase caspase-3-dependent apoptosis (Chan et al., 2005b), and its antagonism represses glioma formation in vivo (Corsten et al., 2007). miR-21 also promotes invasion by targeting inhibitors of MMPs (Gabriely et al., 2008). Thus, miR-21 has been considered an oncogene in GBMs.

miR-296 is upregulated in tumor-associated endothelial cells, and its antagonization reduces angiogenesis in tumor xenografts (Wurdinger et al., 2008). The targeting of hepatocyte growth factor-regulated tyrosine kinase substrate by miR-296 leads to the increased expression of receptors of pro-angiogenic factors VEGFR2 and PDGFR2.

miR-26a is overexpressed in a subset of high-grade gliomas due to genomic amplification of the pri-miR-26a-2 locus, and directly targets the tumor suppressor PTEN facilitating glioma formation in a mouse model (Huse et al., 2009).

miR-10b is one of the most highly up-regulated miRNAs in high- and low-grade gliomas. Inhibition of miR-10b induces cell cycle arrest and apoptosis and also suppresses xenograft tumor growth in vivo (Gabriely et al., 2011).

Specific miRNAs have been shown to promote tumor growth due their effect on angiogenesis. For example, in an orthotopic U87 glioma model, **miR-378** promotes tumor growth and angiogenesis and was shown to target tumor suppressors SuFu and Fus-1 (Lee et al., 2007a). Similarly, **miR-93** from the oncogenic miR-106b~25 cluster, promotes endothelial cell spreading in vitro and tumor growth and angiogenesis in vivo by targeting an integrin, ITGB8 (Fang et al., 2010). Figure 1.4 gives an overview of some of the key oncogenic pathways under the control of miRNAs characterized in GBMs.

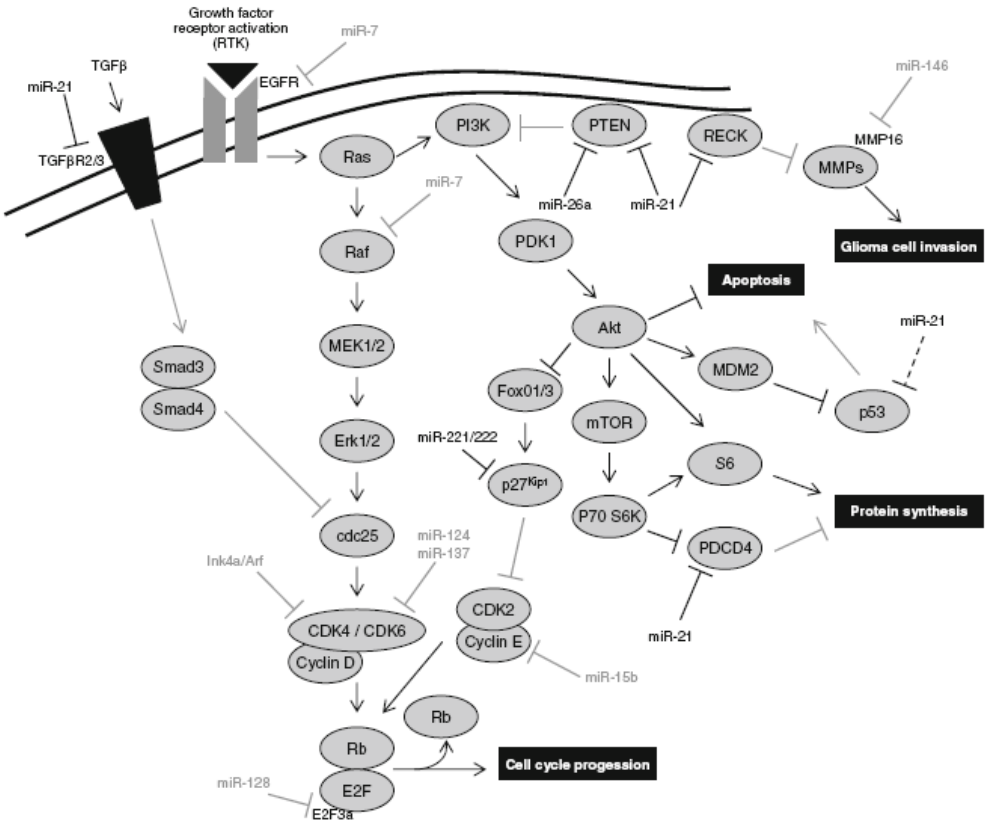

Figure 1.4 miRNA-mediated regulation of key oncogenic pathways in gliomas. Over-expressed miRNAs are shown in black and down-regulated miRNAs are shown in gray. Invasion, apoptosis, cell cycle progression and protein synthesis are major functions affected. Image from (Silber et al., 2009).

1.8 Adenosine-to-Inosine RNA editing

Adenosine-to-inosine (A-to-I) RNA editing is the best-characterized of post-transcriptional events that modify RNA molecules by altering their sequence. It involves the conversion of specific adenosines (A) to inosines (I) in the RNA sequence by the action of adenosine deaminases acting on RNA (ADAR) enzymes (Bass, 2002). In eukaryotes, A-to-I editing generates transcriptome and proteome diversity by expanding the repertoire of gene products to beyond those encoded by the genome (Farajollahi and Maas, 2010).

A-to-I editing can modify protein coding genes, 5'UTR and 3'UTR sequences, intronic retransposon elements (*Alu* and LINEs) and miRNAs. In contrast to other forms of post transcriptional regulation, such as splicing and polyadenylation that alter a large portion of nucleotide sequences, A-to-I editing is site-specific in nature (Gott and Emeson, 2000). In fact, for most substrates that are specifically edited at one or two positions, editing leads to a "recoding" of the substrate (Heale et al., 2011). A-to-I modification is also irreversible.

Editing involves the hydrolytic deamination of the adenine base of adenosine leading to its conversion to inosine (Figure 1.5A) (Nishikura, 2010). As a result the base-pairing specificities are altered from Watson-Crick adenosine-uracil pair to an inosine-cytidine pair (Figure 1.5B).

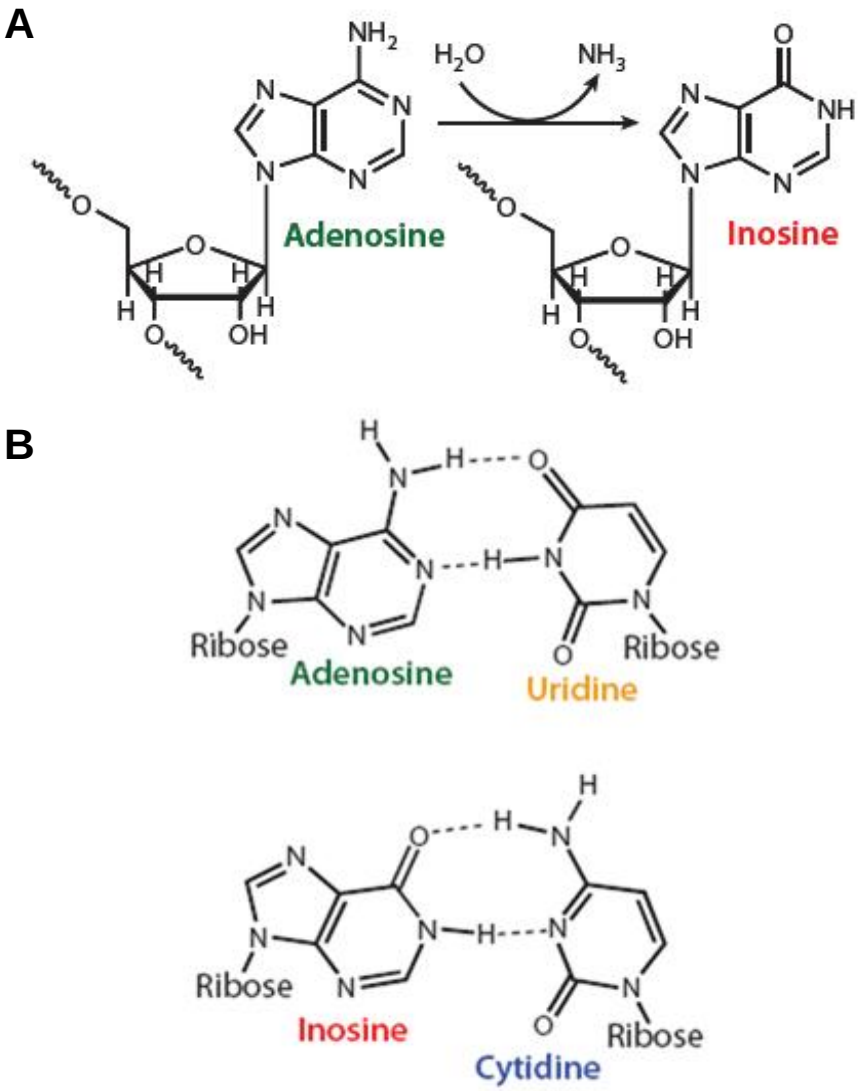

Figure 1.5 Adenosine deamination to inosine by ADAR. ***A.*** Hydrolytic deamination converts adenosine to inosine ***B.*** Base-pairing of adenosine to uridine (top), base-pairing of inosine to cytidine (bottom). Image from (Nishikura, 2010).

1.8.1 A-to-I editing enzymes ADARs

In humans, the ADAR family consists of ADAR1, ADAR2 and ADAR3. These are also known as ADAR, ADARB1 and ADARB2, respectively. Two isoforms of ADAR1, full-length ADAR1 p150 and the shorter N-terminal truncated ADAR1 p110 are known (Patterson and Samuel, 1995). Structurally, all ADARs contain a catalytic deaminase domain at the C-terminal (Figure 1.6). They also possess one to three repeats of dsRNA-binding domain (dsRBD). This domain is required for ADAR interaction and binding to dsRNA (Valente and Nishikura, 2007).

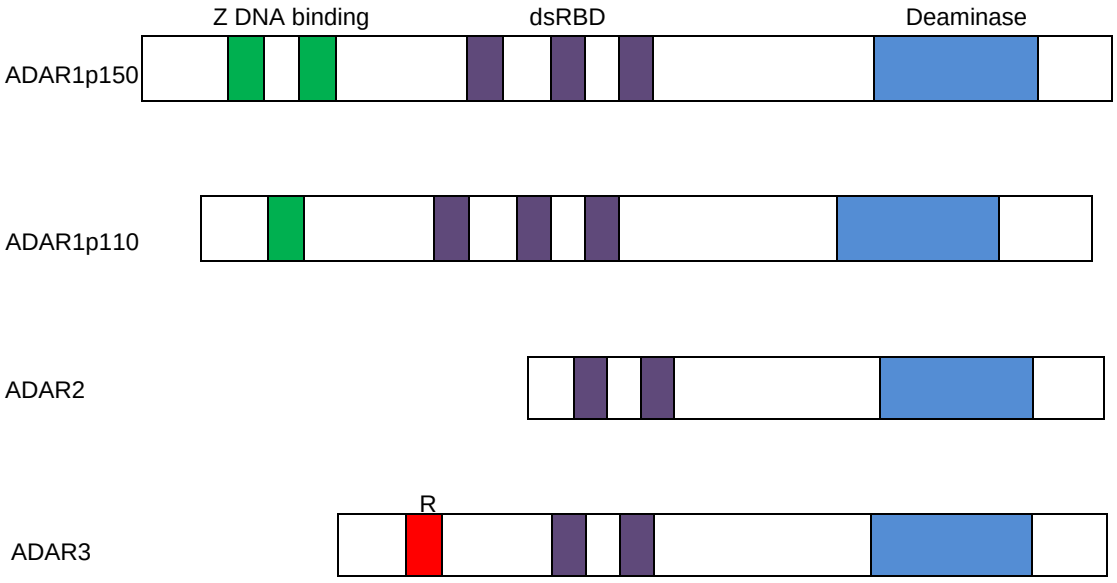

Figure 1.6 Structural organization of ADAR enzymes. Four ADAR enzymes are shown. ADAR1p150 and ADAR1p110 are isoforms of ADAR1. Functional domains common to ADARs are the double-stranded RNA binding domain (dsRBD) and the catalytic deaminase domain. Z DNA binding domains are unique to ADAR1 and R domain is unique to ADAR3. Adapted from (Nishikura, 2010).

The cellular distribution of the different ADARs is unique. ADARp150 is mainly cytoplasmic, whereas ADARp110 is mainly nuclear (Valente and Nishikura, 2005). ADAR2 and ADAR3 are localized to the nucleus by nuclear import by the importin α family (Nishikura, 2010). Evidence suggests that nucleolar accumulation of ADARp110 and ADAR2 also occurs, and is proposed to be a mechanism to sequester enzymatic activity from potential RNA targets until appropriate substrates are present in the nucleus (Nishikura, 2010).

Only ADAR1 and ADAR2 have editing activity in vivo and also appear to undergo homodimerization (Nishikura, 2010). ADAR3 is catalytically invactive and does not undergo homodimerization. ADARs are essential for normal development, as ADAR1$^{-/-}$ mouse embryos die at embryonic day 11.5 (Wang et al., 2004) while ADAR2$^{-/-}$ mice are prone to seizures and die young (Higuchi et al., 2000).

1.8.2 Features of substrates of ADARs

Structural requirements constrain the selectivity of RNA molecules undergoing editing by ADARs. A dsRNA structure rather than any specific RNA sequence is required for editing by ADARs (Heale et al., 2011). Inter- and intramolecular dsRNAs of >20 bp, which represents two turns of the dsRNA helix, can serve as substrate for ADARs. Short duplexes are therefore not edited. Stretches of double-stranded RNA of more than 100 bp length are subject to promiscuous editing by both ADAR1 and ADAR2 with about 50% adenosines present being edited in a non-selective manner (Valente and Nishikura, 2005). On the other hand, dsRNA with extensive secondary structures such as hairpins containing mismatches, bulges and loops are subject to more site-selective editing. Based on the number of dsRBDs, it has been speculated that ADAR2 is mainly responsible for site-selective editing whereas ADAR1 is more prone to promiscuous editing. Nonetheless, ADAR1 and ADAR2 show overlapping but unique site specificities (Bass, 2002).

The editing efficiency of a particular site in a substrate is determined by a combination of factors, including the identity of the nucleotides neighbouring the edited sites, the nucleotide opposing the edited site, and the length and thermodynamic stability of the RNA duplex (Wahlstedt and Öhman, 2011). In general, editing efficiency at individual sites within hyper-edited substrates tends to be lower than in site-selective substrates, but even the specificity and efficiency of editing shows limited variation among healthy individuals, suggesting a non-random editing pattern even for hyper-edited substrates (Kleinberger and Eisenberg, 2010).

1.8.3 A-to-I editing of coding and non-coding substrates

Although, ADAR1 and ADAR2 are expressed in many tissues, A-to-I editing is particularly active in the central nervous system (Mehler and Mattick, 2007). Most site-specific editing substrates are expressed in the brain and include ion channels and neurotransmitter receptors. In general, majority of pre-mRNA editing are localized to non-coding regions of transcripts including introns (73%) and UTRs (25%), specifically within *Alu* repeats (Athanasiadis et al., 2004; Kiran and Baranov, 2010; Levanon et al., 2004).

A-to-I editing within coding sequences of mRNAs can give rise to alternate codons and can change primary protein structure/sequence, given that the translational machinery interprets inosine as guanosine. For coding sequence editing substrates, the requisite dsRNA structure is usually formed by base-pairing between the exon sequence harbouring the editing site and complementary intronic sequence (Valente and Nishikura, 2005). The best characterized substrate undergoing sequence change due to editing is the GluR-B subunit of the AMPA glutamate receptor. Within exon 11 of the GluR-B subunit, a single adenosine undergoes editing in 99% of transcripts changing the genomically encoded Gln (Q) codon to Arg (R) codon (Sommer et al., 1991). Whereas AMPA receptors assembled from GluR-B(Q) subunit are highly Ca^{2+}-permeable, those assembled from GluR-B(R) are Ca^{2+}-impermeable, altering the kinetic properties of the receptor (Lomeli et al., 1994; Sommer et al., 1991).

Inosine is also interpreted as guanosine by the splicing machinery (Valente and Nishikura, 2005). A-to-I editing therefore can regulate splicing by creating or abolishing consensus splice site recognition sequences (AG-GG change or AU-GU change) in the pre-mRNA. The ADAR2 pre-mRNA transcript is an example of an editing substrate affected by splice site alteration (Rueter et al., 1999). Due to the self-editing of ADAR2 pre-mRNA by ADAR2 protein, an alternative splice site is

created in an intron, which leads to the production of a non-functional protein lacking the dsRBD and deaminase domains (Feng et al., 2006).

Despite the prevalence of A-to-I editing in non-coding RNAs, its biological significance is generally poorly understood but is speculated to play a role in gene expression regulation (Nishikura, 2010). For example, as discussed for coding sequences, the creation or destruction of splice recognition sites can lead to alternatively spliced Alu-containing exons, generating variant proteins with distinct functions (Nishikura, 2010). Alternatively, structural changes in Alu hairpin due to editing creating RNA base-pair matches or mismatches may alter the stability of the dsRNA (Valente and Nishikura, 2005).

1.8.4 A-to-I editing of miRNAs

During the processing steps of miRNA biogenesis, primary and precursor miRNAs possess several features of A-to-I editing substrates. The short, dsRNA stem-loop structures within primary miRNAs (pri-miRNAs) with bulges and loops are prototypical of site-specific substrates of ADARs (Wahlstedt and Öhman, 2011). The primarily nuclear localization of ADARs and of pri-miRNAs led to the hypothesis that pri-miRNAs may be subject to A-to-I RNA editing. The hypothesis was validated by the editing, although to low levels, of positions within the pri-miR-22 sequence in samples isolated from human and mouse brain (Luciano et al., 2004). Subsequently, in a survey of editing of 99 primary miRNAs in various tissues carried out by sequencing cDNAs corresponding to each pri-miRs, it was estimated that at least 6% of all human miRNAs may be edited (Blow et al., 2006). All detected editing sites were localized to the predicted stem-loop structures and some were within the 22-nucleotide mature miRNA sequences. Editing frequencies varied from 10 to 70% and displayed tissue-specificity. Additionally, some pri-miRNAs were edited at more than one site and editing frequencies varied for the same pri-miRNAs in different tissues.

It was clear that some pri-miRNAs are highly edited and others are not, suggesting selectivity of editing for specific miRNAs.

A-to-I editing of pri-miRNAs has been shown to affect several aspects of miRNA biology: expression, localization and targeting. First, editing of pri-miR-142 (highly expressed in hematopoietic cells) by ADAR1 and ADAR2 was detected to high-levels in an vitro editing assay (Yang et al., 2006). Subsequently, it was shown that 'pre-edited' pri-miRNAs with 'G' substituted at identified editing sites were unable to generate corresponding pre-edited mature miRNAs or pre-miRNAs. Using in vitro processing assays it was determined that processing was most affected by editing of sites in the stem-loop structure close to Drosha cleavage site, i.e. positions +4 and +5 of the dsRNA fold-back stem, presumably due to disruption of cleavage by Drosha (Lee et al., 2003; Zeng and Cullen, 2003). Furthermore, the failure to detect highly edited pri-miR-142 in vivo was attributed to degradation of highly edited inosine-containing dsRNAs by Tudor-SN, a ribonuclease specific to inosine-containing dsRNA., although this is not a general outcome of miRNA editing.

In addition to inhibiting Drosha processing, editing of pri-miRNAs can also affect downstream processing by Dicer. This was shown for pri-miR-151 for which Dicer cleavage was inhibited by editing of two sites near the terminal loop close to Dicer cleavage site (Kawahara et al., 2007a). The pre-miR-151 was found 100% edited in the brain but no edited mature miR-151 was detected and this was attributed to the inhibition of Dicer cleavage.

For majority of pri-miRNAs that undergo editing in the human brain, the consequence of editing appears to be alteration of their processing by Drosha or Dicer and it has been suggested that 16% of pri-miRNAs are edited in the human brain (Kawahara et al., 2008). Although these studies biochemically characterized the consequences of editing of specific pri-miRNAs, its functional implication in physiological or disease

settings, in terms of miRNA function regulation has not been explored. It is possible that normally editing of pri-miR-142 and pri-miR-151 serve to regulate expression levels of mature miRNAs in certain tissues under specific conditions – regulating downstream targets. However, these possibilities remain unexplored.

1.8.4.1 A-to-I editing of primary miRNAs from miR-376 cluster

To date, the most direct consequence of miRNA editing on downstream miRNA activity has only been reported for miRNAs from the miR-376 cluster (Kawahara et al., 2007b). This cluster encodes four pri-miRNAs which undergo high-level and site-specific editing in the human and mouse brain tissue, with detectable levels of editing in mouse kidney and heart. The major editing sites are located near the 5'-end of either stem arm in the stem-loop structure, a location corresponding to the seed sequence of encoded mature miRNAs. The stem-loop structure and location of editing site within pri-miR-376 resemble that of site-specifially edited coding sequences (Figure 1.7).

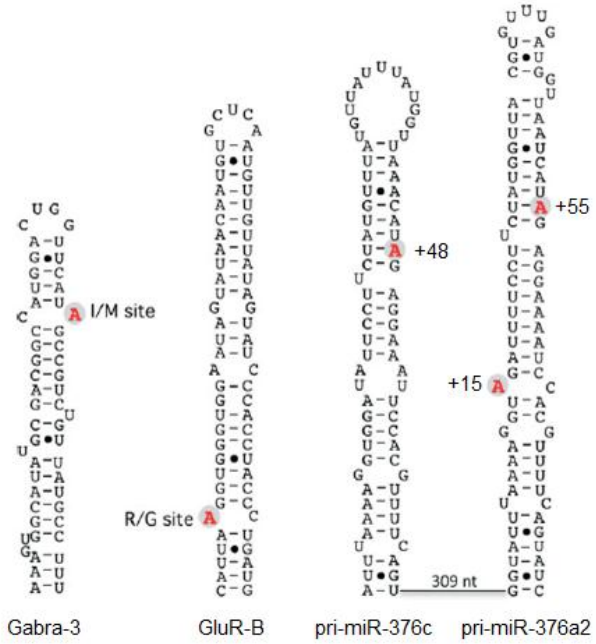

Figure 1.7 Stem-loop configuration of dsRNA structures undergoing site-specific editing. Similarity of structures and location of editing sites in coding sequences of Gabra-3 and GluR-B, and non-coding sequences of pri-miR-376c and pri-miR-376a2. Adapted from (Wahlstedt and Öhman, 2011).

Editing of pri-miRNAs from the miR-376 cluster produces edited mature miRNAs at similarly high frequencies, suggesting that editing of pri-miR-376 transcripts does not affect Drosha or Dicer cleavage. In support of this, in tissues from ADAR2$^{-/-}$ mice, the total expression of one of the mature miRNAs, miR-376a-5p was similar to that in tissue from wild-type mice. This is in contrast to the increase in abundance of mature miR-142 (the primary precursor of which undergoes editing) in spleen from ADAR2$^{-/-}$ mice compared to wild-type mice (Yang et al., 2006).

Given the critical role of miRNA seed sequence in target gene recognition, the altered target gene specificity of edited mature miRNAs was predicted and confirmed. First, it was demonstrated that due to the single base modification of seed sequence (A-to-I, for computational purposes A-to-G), the computationally predicted target gene repertoire of edited miR-376a-5p and unedited miR-376a-5p, were widely different with limited overlap. Conclusively, editing of miR-376a-5p redirected its silencing activity, by rendering it unable to regulate targets of unedited miR-376a-5p, while acquiring the ability to regulate a new set of target genes. One of the target genes of edited miR-376a-5p, PRPS1, was shown to accumulate in ADAR2$^{-/-}$ mouse cortex, because of the lack of expression of edited miR-376a-5p in this tissue. It was also shown that in terms of base-pairing specificity for miRNA target gene selection, a guanosine was equivalent to inosine, as both G-containing and I-containing edited miR-376a-5p showed similar 3'UTR targeting affinities, confirming functional equivalencies of inosine and guanosine in miRNAs by base-pairing to cytosine (Yoshida et al., 1968).

Thus, A-to-I editing of miR-376 represents a post-transcriptional mechanism by which miRNA sequence and targeting ability and function is altered. The edited and unedited miR-376-5p sequence variants are representative of mature miRNA sequence diversity that can be generated through A-to-I. In general, depending on the frequency of editing, mature miRNAs may be "recoded" (by 100% editing) or

expressed as a mixture of edited and unedited transcripts (by <100% editing), in a particular cell type or tissue.

So far, in the human brain, editing of only four other pri-miRNAs is known to lead to the generation of mature miRNAs with edited seed sequence, including miR-379-5p, miR-411-5p, miR-607-3p and miR-99-3p (Kawahara et al., 2008). In mice, by deep sequencing, the expression of 16 edited mature miRNAs in the brain has been identified, with 8 miRNAs edited in the seed (Chiang et al., 2010). Overall, in humans, the generation of variant mature miRNAs by A-to-I editing is relatively rare (de Hoon et al., 2010) although many (~16%) pri-miRNAs undergo editing (Kawahara et al., 2008). The major impact of epigenetic miRNA sequence variation by editing appears to be on the abundance of mature miRNA. The possible outcomes of ADAR-mediated regulation by A-to-I editing of miRNAs on the overall miRNA pathway are summarized in Figure 1.8.

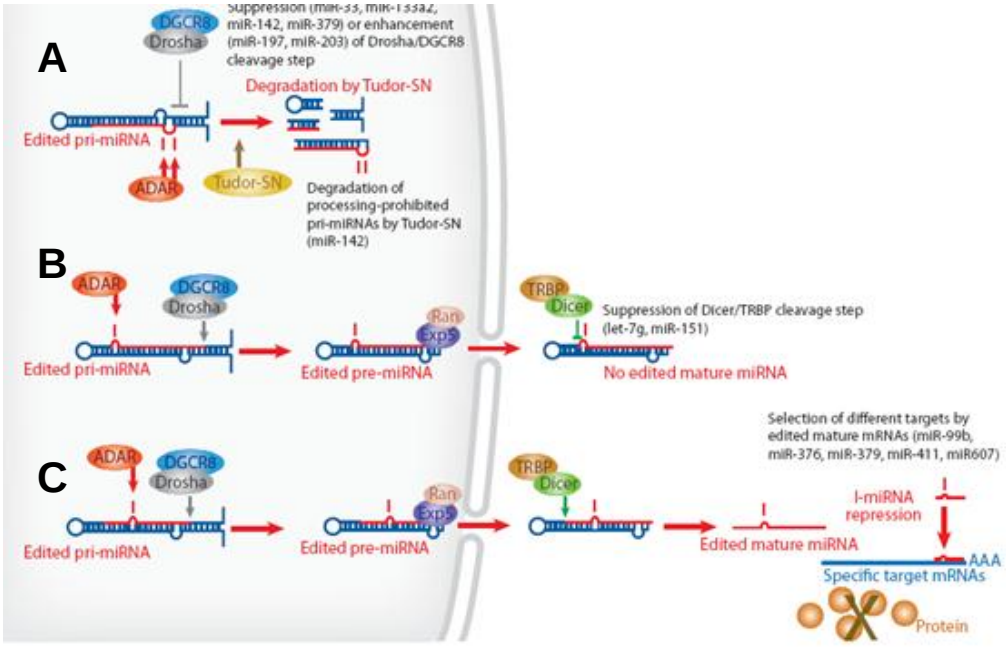

Figure 1.8 Consequences of A-to-I editing of miRNAs. A-to-I editing of pri-miRNA can lead to ***A.*** inhibition of Drosha cleavage and degradation, ***B.*** inhibition of Dicer cleavage or ***C.*** generation of edited mature miRNAs. Image from (Nishikura, 2010).

1.8.5 Regulation of A-to-I editing

Substrates of ADARs, including miRNAs, demonstrate a tissue-specific pattern of editing (Athanasiadis et al., 2004; Blow et al., 2006). Despite the nearly ubiquitous expression of ADARs in various tissues (Nishikura, 2010), and the simultaneous expression of a substrate with potential editing sites, similar levels or even presence of editing for a given substrate is not observed in all tissues (He et al., 2011). This suggests that while tissue-specific editing patterns play a role in tissue-specific functions, editing may be regulated by factors other than ADARs themselves. This is line with findings that editing levels can increase or decrease even ADAR protein levels remain constant (Osenberg et al., 2010; Wahlstedt et al., 2009).

Editing of particular substrates, especially protein-coding genes like glutamate receptors in the brain, has been investigated during the course of rat brain development (Bernard et al., 1999; Lomeli et al., 1994; Paschen et al., 1994; Schmitt et al., 1996; Wahlstedt et al., 2009). For these site-selective edited substrates, the consensus was that editing is low during embryogenesis and increases through the course of development, although in a substrate-specific pattern of increase. Generally, although expression of ADARs does not substantially change, ADAR activity increases during brain development (Wahlstedt et al., 2009). The seeming departure of correlation between ADAR expression levels and editing activity that is generally observed is proposed to be due to the action of regulatory factors (Wahlstedt et al., 2009). However, as ADARs are enzymatically competent without requiring any other proteins, as demonstrated through in vitro studies (Jacobs et al., 2009), few factors that can regulate ADAR activity function have been identified. ADAR1 can be modified by SUMoylation that reduces its editing activity presumably by interfering with dsRNA binding and dimerization (Desterro et al., 2005). The binding of co-factors such as zinc ion or IP_6, an inositol polyphosphate has also been proposed to regulate ADAR acitivity (Macbeth et al., 2005).

1.8.6 A-to-I RNA editing and cancer

The widespread impact of editing on a variety of substrates, at tightly controlled levels under normal circumstances, suggests that perturbation of A-to-I editing will have profound consequences in disease settings. Especially in cancer, the consequence of altering the finely controlled spectrum of post-transcriptional regulation by A-to-I editing can be particularly deleterious.

The first evidence of altered A-to-I editing in cancer came from a study in acute myeloid leukemia. mRNA transcripts of the tumor suppressor, protein tyrosine phosphatase (PTPN), from patients was aberrantly edited creating a novel splice site that would hypothetically produce non-functional protein (Beghini et al., 2000).

ADARs have particularly high level activity in the brain, and also a disproportionately high abundance of highly-edited site-specific substrates compared to other tissues (Mehler and Mattick, 2007). Perhaps due to this or due to the specific nature of post-transcriptional gene regulation in the brain, altered A-to-I editing has most frequently been observed in brain tumors, gliomas. The Q/R site of GluR-B subunit was found to be edited to lower levels (69-88%) in seven glioblastomas (GBMs, grade IV gliomas) down from its 100% editing in normal brain cortex and white matter (Maas et al., 2001). However, ADAR2 expression was normal in tumors. Underediting of various sites in GluR-B and GluR-6 subunits was detected in ten pediatric astrocytomas of WHO grades I-IV (Cenci et al., 2008). Surprisingly, in tumors ADAR2 expression was unchanged while expression of ADAR1 was highly increased. It was shown that in HEK293 cells, high levels of ADAR1 can inhibit ADAR2 site-specific editing activity by heterodimerizing with it, although formal evidence for heterodimerization among different ADARs is lacking (Cho et al., 2003).

A computational analysis of expressed sequence tags (EST) derived from normal and cancer tissues determined that editing within ESTs was significantly lower in brain tumors compared to normal brain tissue, although tumor grade-wise analysis

was not reported (Paz et al., 2007). This was the first demonstration of altered A-to-I editing of Alu sequences (non-coding RNA) in GBMs. Furthermore, it was determined by analysis of RNA sequencing data that global hypoediting also occurs in prostate, lung, kidney and testis tumors, but is most significant in GBMs. To account for the general reduction in editing, ADAR mRNA levels were measured and contrary to previous studies were found to be significantly lower in GBMs and grade III anaplastic astrocytomas.

These studies have laid the backdrop for speculating a crucial role of altered A-to-I editing in cancers, especially in GBMs. However, specific editing substrates playing a role in GBM pathophysiology have not been identified. Two posttranscriptional regulatory mechanisms – A-to-I editing and miRNA-mediated regulation- are particularly active in the brain (Christensen and Schratt, 2009; Mehler and Mattick, 2007). In GBMs, dysregulation of either mechanism has been identified separately; it is a viable notion that a mechanism linking these two critical processes underlies development and progression of GBMs.

1.9 Aims of thesis

Due to the potent multi-gene targeting ability of miRNAs, specified by their sequence, it has been speculated that an alteration to miRNA sequence can be highly deleterious. However, no disease- or tumor-specific functional miRNA sequence variants have thus far been identified. Some miRNAs, such as the miR-376 cluster, are subject to regulated “seed” sequence modification by A-to-I editing in the normal human brain. Evidence suggests that global A-to-I editing is misregulated in gliomas, especially glioblastomas (GBMs) due to dysfunction of the editing machinery, the ADAR enzymes. Thus, it is a possibility that as substrates of ADARs, miRNAs might also be the subject of editing dysfunction in gliomas. The aim of this thesis was therefore, to investigate if A-to-I editing of miRNAs is altered in gliomas, in particular GBMs, and to identify miRNAs that due to a change in their sequence by altered A-

to-I editing, can potentially regulate malignant properties of GBMs, such as growth and invasiveness.

The current study is based on the hypothesis that altered editing activity in GBMs leads to altered editing of some miRNAs changing their sequence and function in tumors. The miR-376 cluster was selected to address this hypothesis as editing of primary miRNAs from this cluster generates highly edited mature miRNAs in the normal brain, and thus likely to be prominently affected by altered A-to-I editing. Three lines of investigation were pursued in this study:

1. Editing analysis was carried out to determine editing status of miR-376 cluster in gliomas and identify candidate miRNAs for characterization of altered A-to-I miRNA editing
2. Analysis of functional consequences of aberrant editing of candidate miRNAs in gliomas, including effects on tumor growth and invasiveness
3. Identification of target genes subject to regulation by candidate miRNAs in cancer cells to understand the mechanism of action of aberrantly edited miRNAs in gliomas

Findings from this investigation identify for the first time, tumor-specific miRNA sequence variants generated due to altered A-to-I editing, and uncover novel modes of deregulation of miRNA function in GBMs. Furthermore, candidate miRNAs subject to aberrant editing, identified in this study, represent potential therapeutic targets for countering the malignancy of GBMs.

2 CHAPTER 2. Materials and methods

2.1 Tumor tissues and cells

Twenty four human brain tumor samples were used in this study. Seventeen samples were obtained from National Neuroscience Institute, Singapore in compliance with a study protocol approved by the institutional review board (CIRB# 2010/337/A). The remaining samples (GBMs 1-4 and AAs 17, 19, 20) were purchased (Asterand and Capital Biosciences). Patient information, where available, are reported in Table 2.1. Five human brain total RNA samples were purchased from Ambion, Clontech and Stratagene to serve as normal brain tissue controls. Human glioma cell lines, U87, U251, SW1088, and SW1783, and human cervical cancer cell line HeLa were from American Type Culture Collection. Frozen normal human astrocytes pellet was purchased from Cell Systems.

Sample ID	Histopathological Classification	Age	Sex	Treatment	Tumor Site
1	GBM	—	—	—	—
2	GBM	—	—	—	—
3	GBM	—	—	—	—
4	GBM	—	—	—	—
5	GBM	48	F	S+Rt+Ct	Left Anterior Temporal
6	GBM	60	M	S+Rt+Ct	Left Temporal lobe
7	GBM	75	F	S+Rt	Left Frontal lobe
8	GBM	59	F	S+Rt+Ct	Right Temporal lobe
9	GBM	51	F	S+Rt+Ct	Left Temporal lobe
10	GBM	46	M	S+Rt+Ct	Left Parietal tumor
11	GBM	80	F	S+Rt	Right Occipital lobe
12	GBM	51	M	S+Rt+Ct	Left Frontal lobe
13	GBM	46	M	S	Right Temporal lobe
14	GBM	75	F	S+Rt+Ct	Left Frontal lobe
15	GBM/GS	52	F	Biopsy+Rt	Cerebellar & Brain Stem tumor
16	GBM/GS	52	M	S	Left Frontal lobe
17	AA	—	—	—	—
18	AA	56	F	S+Rt	Left frontal Parietal tumor
19	AA	—	—	—	—
20	AA	—	—	—	—
21	AOA	44	F	S+Rt+Ct	Left Frontal lobe
22	AOA	42	F	S+Rt+Ct	Left Frontal Temporal lobes
23	AOA	33	M	S+EVD	Left Frontal lobe
24	AOG	27	M	S+Rt	Left Frontal lobe

Table 2.1 Clinicopathological details of primary human tumor samples used in this study. WHO classification of gliomas, AOA: anaplastic oligoastrocytoma (WHO grade III), AOG: anaplastic oligodendroglioma (WHO grade III), AA: anaplastic astrocytoma (WHO grade III), GBM: glioblastoma multiforme (WHO grade IV), GS: gliosarcoma. Treatment regime, S: surgery, Rt: radiotherapy, Ct: chemotherapy, EVD: external ventricular drainage. "—" details not available.

2.2 RNA extraction

Total RNA from cultured cells, cell pellets or tissue samples was prepared using TRIzol (Invitrogen). For frozen tumor samples, tissues were rapidly homogenized in appropriate volume of TRIzol using an ultrasonic processor (Vibra-Cell, Sonics & Materials). For xenograft tumors, tumor tissue in paraformaldehyde-fixed, OCT-embedded cryosections was separated from normal brain tissue and processed using FFPE RNA Isolation Kit (SA Bioscience) to remove paraformaldehyde cross-links and isolate RNA. Enrichment of small RNA fraction from total RNA was done using RNeasy Mini Kit (Qiagen) with a modified RNA cleanup protocol to retain small RNA species.

2.3 DNAse treatment of RNA samples

Total RNA was DNAse-treated to remove traces of genomic DNA contamination. Typically, two micrograms of total RNA was treated with 1 µl (2 units) of Turbo DNAse (Ambion) in 20 µl for 30 min at 37°C, followed by addition of another 1 µl of Turbo DNAse to the sample for further 30 min incubation at 37°C.

2.4 Primary miRNA editing analysis

For editing analysis of primary miRNAs the protocol described previously by Kawahara et al was adopted with slight modifications (Kawahara et al., 2007b).

cDNA synthesis One microgram of DNAse-treated total RNA was used for cDNA synthesis with random hexamer primers (instead of gene-specific priming) and SuperScript III reverse transcriptase (SS III RT) (Invitrogen) to generate a cDNA pool.

PCR amplification Primary miRNAs were PCR-amplified using miRNA-specific primer pairs (Table 2.2). Subsequently, amplification products were gel-purified.

Primary miRNA	Size (bp)	Forward	Reverse
pri-miR-376a1	159	ACAGGTGCACGCTTTCCT	TCCATGGCGACTTCACGT
pri-miR-376a2	159	GGATTGTACTTAGGTTCGTGC	TGGCTTCAGTCCAGCCAT
pri-miR-376b	166	CCATGAACTGTGTTCAGATTTG	CTACGGTCTCTTCCAGAAAC
pri-miR-376c	154	GATAGATTGTGCTTAGGTTCATGC	GTCCAGGAATGTTTCCAAGC

Table 2.2 Primers used for amplification of primary miRNAs. The expected size of the PCR product for each primary miRNA amplified from random hexamer cDNA is specified.

Sequencing analysis Purified RT-PCR products were directly sequenced by dideoxy Sanger sequencing at AITBiotech, Singapore. For each primary miRNA, both forward and reverse sequencing primers were used for sequencing (Table 2.2). Sequencing chromatograms (.ab1 files) generated from the forward and reverse primers were exported to Vector NTI's Contig Express (Informax) and aligned with the expected genomic sequence for each primary miRNA. During cDNA synthesis of primary miRNA transcripts, inosine (I) bases present in the RNA are interpreted as guanosine (G) by reverse transcriptase enzyme and subsequently represented by 'G' in the RT-PCR product (Nishikura, 2006). For known editing sites, the 'G' peak height (represented by the 'G' trace quantification at the specific site) and the 'A' peak height at the same site were noted. A-to-I editing frequency was determined as the % ratio of 'G' peak at the editing site over the sum of 'A' and 'G' peaks at the same site. Sequencing chromatograms used for direct quantification were of high quality with minimal background 'noise' throughout the sequence. This method of editing frequency analysis has been reported to be sensitive enough to accurately quantify frequency of editing as low at 5% (Nakae et al., 2008).

2.5 Mature miRNA editing analysis

A library of small RNA molecules was constructed by addition of 5’ and 3’ adapter sequence and mature miRNA editing analysis was subsequently done by sequencing of miRNA clones.

Small RNA purification Fifty micrograms of total RNA was first purified to enrich the small RNA fraction using the method described for purification of small RNA fraction from total RNA (Section 2.2).

Poly (A) tailing of small RNAs The Poly(A) tailing kit (Ambion) was used to add poly(A) tails to 1.5 µg of the purified small RNA fraction with 2 µl poly(A) polymerase (PAP) enzyme in a 50 µl reaction which were subsequently purified using the RNeasy Mini Kit (Qiagen) using a modified cleanup protocol.

Ligation of 5’ RNA adapter A 5’ RNA adapter was ligated to poly(A)-tailed RNA molecules using T4 RNA ligase (Promega) :
5'-CGACUGGAGCACGAGGACACUGACAUGGACUGAAGGAGUAGAAA-3'.
The ligation reaction consisted of 1.5 µg donor RNA (poly(A)-tailed small RNA) and 0.75 µg acceptor RNA (5’ adapter). Unligated 5’ RNA adapters and other constituents from the ligation reaction were removed using RNeasy Mini Kit.

cDNA synthesis of small RNA library 5’-adapter-ligated, poly(A)-tailed RNA was then used in a cDNA synthesis reaction using the following 3’ oligo(dT) adapter sequence: 5'-ATTCTAGAGGCCGAGGCGGCCGACATG-d(T)30 VN-3' V: A/G/C and N: A/G/C/T

PCR amplification of mature miRNAs Two-step amplification protocol was adopted for amplifying specific mature miRNAs. For the first step, common forward (cFW) and reverse primers (cRV) corresponding to the 5’- and 3’- adapters respectively were used to amplify the pool of mature miRNA species present in the cDNA library constructed. The resultant range of amplification products between 70 and 120 bp

were purified using the QIAEX II Gel Extraction Kit (Qiagen) to ensure recovery of DNA molecules less than 100 bp in size (Figure 2.1A). Subsequently, specific miRNAs were amplified in a second step using the purified amplified mature miRNA library as template. For each mature miRNA, miRNA-specific reverse primer and cFW forward primer was used (Table 2.3). Specific PCR products of ~50 bp size were purified using the QIAEX II Gel Extraction Kit (Figure 2.1B).

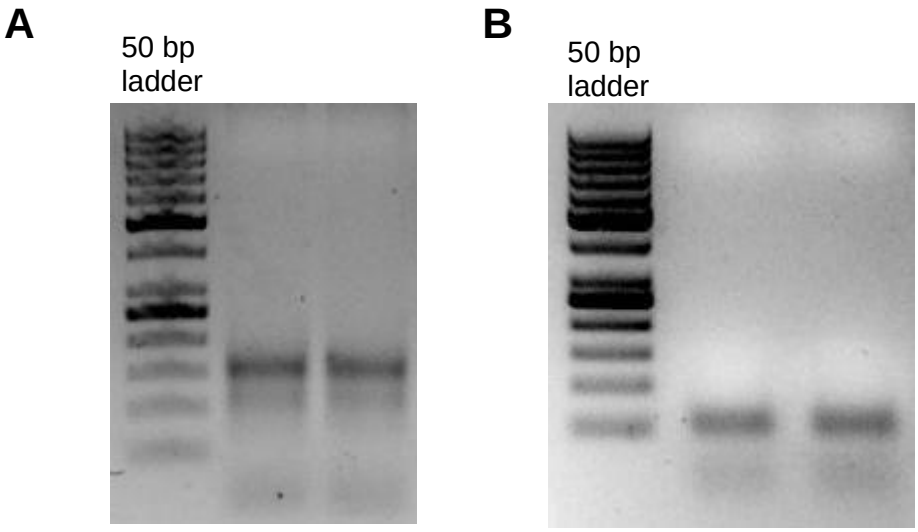

Figure 2.1 PCR amplification of mature miRNAs for sequencing. ***A.*** cFW and cRV primers used to amplify total miRNA pool from small RNA cDNA library. ***B.*** cFW and miRNA-specific primer used to amplify specific mature miRNAs from the PCR product purified from ***A.***

Primer	Sequence
cFW	5'-CTGACATGGACTGAAGGA-3'
cRV	5'-ATTCTAGAGGCCGAGGCGGCCGACATGT-3'
miR-376c RV	5'-TAAACGTGGAATTTCCTC-3'
miR-376a1-5p RV	5'-CAGCACTCATAGAAGGA-3'
miR-376a/b RV	5'-TTTTWACRTGGATTTTCCTC-3'
miR-376a2-5p RV	5'- CACGTAACCATAGAAGG-3'

Table 2.3 Primers used for amplifying mature miRNAs from small RNA cDNA library. W: A or T; R: A or G.

Sequencing of mature miRNAs TOPO TA cloning (Invitrogen) of individual PCR products, corresponding to single mature miRNA. Fifty clones or more were sequenced for each mature miRNAs. Sequences were aligned to expected mature miRNA sequences to identify clones containing 'G' at editing sites for each mature

miRNA. Frequency of editing was determined as the % of clones containing an A-to-G change at editing site among the total number (>50) of clones sequenced.

2.6 Plasmids and contructs

For expression of ADAR2, pCMV-SPORT6-ADAR2 was purchased from Open Biosystem. pCMV-SPORT6-EGFP was constructed by amplifying the 720 bp EGFP coding sequence from pcDNA6.2-GW/EmGFP vector (Invitrogen), which was inserted between EcoRV and NotI sites of pCMV-SPORT6. The miR-376 cluster expression vector was constructed using the Block-iT Pol II miR RNAi system (Invitrogen). The genomic region corresponding to the 1570 bp miR-376 cluster was amplified from human genomic DNA (Biochain Institute) and inserted between SalI and BglII sites of pcDNA6.2-GW/EmGFP. Primers are listed in Table 2.4.

Primer	Sequence
EGFP FP	5'- ATCGGATATCATGGTGAGCAAGGG -3'
EGFP RP	5'- TAGTGCGGCCGCTTACTTGTA -3'
miR-376 cluster FP	5'- ATGTCGACGAGAGTGATGGAAGGT-3'
miR-376 cluster RP	5'- ATAGATCTATACTGAGAACACAGCCTTG-3'

Table 2.4 PCR primers used for expression vector construction. Underlined sequence: restriction enzyme site used for cloning.

2.7 miRNA duplexes and miRNA expression vectors

All miRNA duplexes corresponding to mature miRNAs were synthesized by Dharmacon. The sequences of mature miRNAs used in this study were as follows:

miR-376a*A: GU**A**GAUUCUCCUUCUAUGAGUA
miR-376a*G: GU**G**GAUUCUCCUUCUAUGAGUA
miR-376a*I: GU**I**GAUUCUCCUUCUAUGAGUA I : inosine
miR-376a2-5p(A): GU**A**GAUUUUCCUUCUAUGGUU
miR-376a2-5p(G): GU**G**GAUUUUCCUUCUAUGGUU
miR-376a(A): AUCAU**A**GAGGAAAAUCCACGU
miR-376a(G): AUCAU**G**GAGGAAAAUCCACGU
cel-miR-239b (control): UUUGUACUACACAAAAGUACUG

mIRIDIAN microRNA Mimic Negative Control #2, corresponding to *C. elegans* miRNA cel-miR-239b was also purchased from Dharmacon.

For stable (non-transient) expression of miR-376a*, the expression vector was designed using Block-iT Pol II miR RNAi expression system (Invitrogen). In the stem-loop design, only miR-376a* guide strand is active and the inactive passenger strand does not correspond to miR-376a. The top strand of the duplex encoded miR-376a* with 'A' or 'G' at position 3 of the mature miRNA. The bottom strand sequence design followed from the top strand. The two strands were annealed and ligated to the linearized pcDNA™6.2-GW/EmGFP-miR vectors to generate pmiR-376a* plasmids or pmiR-control plasmids (Table 2.5). EGFP is co-cistronically expressed with the miRNA under the control of CMV promoter.

Strand	Sequence
pmiR-376a*A top	5'TGCTGGTAGATTCTCCTTCTATGAGTAGTTTTGGCCACTGACTG ACTACTCATAAGGAGAATCTAC3'
pmiR-376a*A bottom	5'CCTGGTAGATTCTCCTTATGAGTAGTCAGTCAGTGGCCAAAACT ACTCATAGAAGGAGAATCTACC3'
pmiR-376a*G top	5'TGCTGGTGGATTCTCCTTCTATGAGTAGTTTTGGCCACTGACTG ACTACTCATAAGGAGAATCCAC3'
pmiR-376a*G bottom	5'CCTGGTGGATTCTCCTTATGAGTAGTCAGTCAGTGGCCAAAACT ACTCATAGAAGGAGAATCCACC3'
pmiR-control top	5'TGCTGTTGTACTACACAAAAGTACTGGTTTTGGCCACTGACTGA CCAGTACTTGTGTAGTACAA3'
pmiR-control bottom	5'CCTGTTGTACTACACAAGTACTGGTCAGTCAGTGGCCAAAACCA GTACTTTTGTGTAGTACAAC 3'

Table 2.5 Design of top and bottom strands for constructing miRNA expression vectors encoding stem-loop precursors. Red: sequence of mature miRNA of interest; blue: sequence complementary to the mature miRNA in the fold-back structure of pre-miRNA; underlined sequence: recommended overhands for ligation to linearized vector.

For generation of stable U87 cell lines, pmiR-376a*A or G plasmids were transfected using Lipofecatmine 2000. Stable clones were selected over 2 weeks using 6 μg/ml blasticidin (Invitrogen). Four clones were selected and characterized for each construct.

2.8 siRNAs

The sequence of siRNA against STAT3 has been previously described (Konnikova et al., 2003), and was synthesized at Dharmacon.

STAT3 siRNA 5'-AAC AUC UGC CUA GAU CGG CUA dTdT-3'
5'- U AGC CGA UCU AGG CAG AUG dTdT-3'

siRNA against AMFR was a predesigned HP GenomeWide siRNA (Qiagen) of product ID: SI00022533. siGENOME Non-Targeting siRNA #5 from Dharmacon was used as control siRNA for all experiments.

2.9 Locked nucleic acids

Locked nucleic acid oligonucleotide (LNA) inhibitors against miR-376a*A were custom-designed and purchased from Exiqon. LNA against a scrambled sequence (LNA-scr) was used a control in all experiments.

2.10 Chemicals

Specific STAT3 inhibitor, Stattic was purchased from Merck and dissolved in 100% DMSO to prepare a 100 mM stock and stored at 4°C.

2.11 Quantitative RT-PCR of mRNAs

For mRNAs, total RNA was reverse transcribed using random hexamers by Superscript III RT-PCR kit (Invitrogen). Resulting cDNA was used for PCR using SYBR-Green PCR Mix. PCR and data collection was done on Bio-Rad iCycler Bio-Rad. Expression levels were normalized to 18S rRNA. For quantification of ADAR2 and ADAR1, pre-designed primer sets were purchased from SA Biosciences. All primer sequences are listed in Table 2.6. RT-PCR for primary miRNAs was done using random hexamer cDNAs and primers used in primary miRNA editing analysis.

Gene	Forward	Reverse
STAT3	ACCTGCAGCAATACCATTGAC	AAGGTGAGGGACTCAAACTGC
AMFR	TTCCTACACAGCGGTCAGATAGC	GCCGAAGTCCAGCGTCTCC
PDGFRα	CCACCGTCAAAGGAAAGAAG	CCAATTTGATGGATGGGACT

PDGFRβ	CAGGAGAGACAGCAACAGCA	AACTGTGCCCACACCAGAAG
PDGFα	GATACCTCGCCCATGTTCTG	CAGGCTGGTGTCCAAAGAAT
PDGFβ	TCGAGTGGTCACTCAGCATC	GCGCTCTTCCTGTCTCTCTG
VEGFA	AGCCTTGCCTTGCTGCTCTA	GTGCTGGCCTTGGTGAGG
TGFβR1	TTGTCTTTTGTACAGAGGTGGC	GCTGCTCCTCCTCGTGCT
TGFβR2	GGAAACTTGACTGCACCGTT	CTGCACATCGTCCTGTGG
TGFα	GGGCAGTCATTAAAATGGGA	GCTCTGGGTATTGTGTTGGC
TGFβ1	CTTCCAGCCGAGGTCCTT	CCCTGGACACCAACTATTGC
TGFβ2	CTCCATTGCTGAGACGTCAA	ATAGACATGCCGCCCTTCTT
EGFR	TCCTCTGGAGGCTGAGAAAA	GGGCTCTGGAGGAAAAGAAA
ANGPT1	CCGACTTCATGTTTTCCACA	ACCGGATTTCTCTTCCCAGA
ANGPTL2	GGTAGATGGAGCTGGTGTCG	CACTATGCCCACTCTCACCA
ANGPTL4	TAGTCCACTCTGCCTCTCCC	GAGATGGCCCAGCCAGTT
CXCL12	TGGGCTCCTACTGTAAGGGTT	TTGACCCGAAGCTAAAGTGG
ITGB3	TCATCAGAGCACCAGGCA	TCTGGGCGACTGTGCTG
FN1	ACCTCGGTGTTGTAAGGTGG	CCATAAAGGGCAACCAAGAG
HIF1α	TGGCTGCATCTCGAGACTTT	GAAGACATCGCGGGGAC
NTNG1	GGGTACTCGCATCACACTCA	AAGTGAAACTCGATCCTCCG
TNXB	TCTCAGCTTCATTTCCGTGA	TCTACGGGAGCACAGTGGAC
MMP2	GGAAAGCCAGGATCCATTTT	ATGCCGCCTTTAACTGGAG
PLAU	CCAGCTCACAATTCCAGTCA	TGACCCACAGTGGAAAACAG
HGF	CCCTGTAGCCTTCTCCTTGA	CGCTGGGAGTACTGTGCAAT
NRP2	TGCTCCAGTCCACCTCGTAT	AACTGCATGGAACCCATCTC
RRAS2	CGGGCTGCTCTGTCATCTAT	TCACCATCCAGTTCATCCAG
PEX19	ATTCCCGATGACTCTGCAAC	TGCAGAACCTACTCTCCAAGG
FAM55C	TGGGAGGAAACAAACTGTCC	TGGTGCTGGTCATCAATGTT
ELOVL5	GTATCTCGAGGGCCTAGCAA	TGCTGCTCAAAGCTGCTG
ACVR1	GGAACCACATCGTAGAACGG	TATTTGGGCCTTTGGACTTG
TCF7	AGAGAGAGAGTTGGGGGACA	TCTGCTCATGCATTACCCAC
18S rRNA	AACTTTCGATGGTAGTCGCCG	CCTTGGATGTGGTAGCCGTTT

Table 2.6 Sequences of primers used for qRT-PCR of genes.

2.12 Quantitative RT-PCR of miRNAs

Real-time PCR quantification of mature miRNAs was done as described previously (Wu et al., 2009) except the sequence of the poly (T) adaptor used for cDNA synthesis was modified to 5'-CGATAGCGACGATACAGACTTGTCACTATAGG(T)12VN*-3' and sequence of reverse primer was: 5'-CGATAGCGACGATACAGACTTG-3'. The forward primers corresponded to the full length mature miRNA sequence and were as follows:

miR-376a*A: 5’- GT**A**GATTCTCCTTCTATGAGTAAA
miR-376a*G: 5’- GT**G**GATTCTCCTTCTATGAGTAAA
miR-376a: 5’- ATCAT**A**GAGGAAAATCCACGTAAA
miR-376b: 5’- ATCATAGAGGAAAATCCATGTTAAA
miR-376a2-5p: 5’- GTAGATTTTCCTTCTATGGTTAAA
miR-376c: 5’-ACATAGAGGAAATTCCACGTAAA
miR-127: 5’- TCGGATCCGTCTGAGCTTGGCTAAA
miR-154: 5’- TAGGTTATCCGTGTTGCCTTCGAAA
miR-432: 5’- TCTTGGAGTAGGTCATTGGGTTGGAAA
miR-654: 5’- TGGTGGGCCGCAGAACATGTGCAAA
miR-16: 5’-TAGCAGCACGTAAATATTGGCGAAA
miR-21: 5’-TAGCTTATCAGACTGATGTTGAAA
miR-221: 5’-AGCTACATTGTCTGCTGGGTTTCAAA
miR-106: 5’-AAAAGTGCTTACAGTGCAGGTAGAAA
miR-10b: 5’-TACCCTGTAGAACCGAATTTGTGAAA
5S rRNA: 5'-CCGCCTGGGAATACCGGGTGCTGTAGGCTTT-3' (internal control)

2.13 Cell invasion assay

For in vitro invasion assay, the Boyden chamber assay with Matrigel-coated inserts with 8-µm pores was used (BD Falcon). Three days after transfection with 10 nM miRNA or with 2.5 nM siRNA using Lipofectamine LTX (Invitrogen), glioma cells were starved overnight in unsupplemented OPTI-MEM (Invitrogen). On the day of the assay, cells were stained with Calcein-AM (Invitrogen), trypsinized and seeded onto the upper chamber ($1X10^5$ cells in 200 µl of unsupplemented OPTI-MEM media). Lower chambers were filled with 700 µl of supplemented OPTI-MEM (10% FBS). After 24 hours of incubation at 37ºC, fluorescence readings of invaded cells at the bottom of inserts were measured with Victor3 1420 Multilabel Counter (Perkin Elmer) or number of labeled invading cells was manually counted from 4-5 imaged fields.

2.14 Wound healing assay

For wound healing assay, cells were cultured in 6-well plates, transfected and allowed to reach confluence. The following concentrations were used for

transfections: miRNA: 10 nM, siRNA: 0.625 nM, LNA miRNA inhibitor: 50 nM. An artificial homogenous wound was made using a sterile p200 tip. Cell debris was removed by washing cells with DPBS and medium was replaced with 1% FBS-containing DMEM. The wound borders were imaged just after wounding (t = 0 h) and again after 24 or 36 hours to measure the wound gap distance. Wound coverage was determined as percentage of the gap width covered during incubation from 4-6 measurements for each treatment condition.

2.15 Cell viability, proliferation, and cell cycle assays

Cell viability was measured in 96-well plates using the Cell-Titer Glo Assay (Promega). For growth rate assessment of stable U87 cells or parental and ELM-selected cells, 3000 cells were seeded per well of 96-well plates. Viability was measured from day 0 (day of seeding) until day 7. Cell proliferation was quantified using the colorimetric BrdU cell proliferation assay (Roche). Briefly, at indicated times after transfection, cells were labeled with BrdU for 12 hrs. Labeled cells were fixed and BrdU incorporation was measured as per the protocol using the anti-BrdU-peroxidase immunodetection. Absorbance of the colored product was measured at 370 nm (reference wavelength 492 nm) in a microplate reader (Bio-Rad). For cell cycle analysis, cells treated as indicated were trypsinized and fixed in ice-cold 70% ethanol. Fixed cells were resuspended in PBS containing 0.1% Triton X-100, 20 µg/ml propidium iodide and 200 µg/ml RNase A and incubated in the dark for 30 minutes before analysis by flow cytometry (Beckman Coulter).

2.16 Morphological assessment by flow cytometry

Flow cytometry was used to assess cell morphology of transfected glioma cells. Cells were transfected in 6-well plates as per standard methods. Seventy-two hours after transfection, cells were trypsinized, washed once in PBS and resuspended in 500 µl

of PBS containing 5% FBS. Unfixed cells were assessed for side and front-scatter profiles by flow cytometry (Beckman Coulter).

2.17 Luciferase reporter assays

Plasmid encoding firefly luciferase under CMV promoter, pMIR-Report Luciferase, was purchased from Ambion. Reporter plasmids for STAT3 and AMFR were constructed by cloning the corresponding 3'UTR fragments downstream of the luciferase coding sequence in the MCS of pMIR-Report. All 3'UTR fragments were amplified from human genomic DNA (BioChain Institute) (Table 2.7). pMir-Report ß-galactosidase control plasmid, encoding ß-galactosidase under the control of CMV promoter was also purchased from Ambion and was used as a transfection control.

3' UTR fragment	Size (bp)	Restriction enzymes	Forward primer	Reverse primer
STAT3 full length	2449	SpeI/MluI	AGTCACTAGTCCTCG GAGTGCG	AGTCACGCGTACGGTT CCTATATAACG
STAT3-1002	1002	SpeI /HindIII	ATCGACTAGTACAGTC TGAGACTCTGT	GTCTAAGCTTTCTTAGA GAAGGTCGTC
AMFR full length	1411	SpeI/MluI	TCGTACTAGTCGCTCC CTTGCCTTCCT	ATGCACGCGTTAGCTA TGCTCTCAGCA
AMFR-417	417	SpeI/MluI	TGCTACTAGTGTGTGA ACCTACCTGCC	ATGCACGCGTTAGCTA TGCTCTCAGCA

Table 2.7 Primers used for amplifying 3'UTR regions of target genes. Underlined sequence: restriction enzyme site used for cloning.

For luciferase reporter assay, HeLa cells in 96-well plates were transfected with 30 ng of reporter plasmid, 30 ng of CMV-ß-galactosidase and 20 nM miRNA mimics using Lipofectamine 2000. After 48 hours, luciferase activity was measured using the Luciferase Assay system (Promega). Luciferase readings were normalized to ß-galactosidase activity in the same lysate, quantified by the ß-galactosidase Enzyme Assay System (Promega). For each group, data was collected from at least 4 replicate wells. Data was presented as mean ± SD.

2.18 Gene expression microarray analysis

Total RNA from U87 and SW1783 cell lines transfected as indicated was isolated using Trizol. For each cohort, three independent RNA samples were isolated. Following clean-up with Qiagen RNeasy column, amplification and labeling was done by Kreatech ULS labeling kit as per protocol. Fifteen µg of each labeled RNA sample was hybridized to Affymetrix Human Genome U133 Plus 2.0 arrays. CEL files were imported into GeneSpring GX 11 (Agilent) and signal intensities normalized using MAS5 algorithm and processed to remove 'absent' probesets and those in the lowest 20th percentile from analysis. Genes were filtered based on 1.5- or 2-fold change and $P < 0.05$, with respect to their respective control experiments. Enrichment of specific GO biological functions among the differentially expressed genes was evaluated by NCBI DAVID bioinformatics analysis (http://david.abcc.ncifcrf.gov/) using default settings. For miRNA binding site prediction, RNA 22 analysis (http://cbcsrv.watson.ibm.com/rna22.html) (Miranda et al., 2006) was done on whole 3'UTR sequences and miR-376a* sequence with "A" or "G".

2.19 Western blot and Immunocytochemitstry

Protein was extracted from cells using Cellytic M buffer (Sigma). Protease inhibitor (Fermentas) and phosphatase inhibitor cocktails (Santa Cruz) were added to the lysis buffer at appropriate concentrations. For all transfection experiments, protein extraction was done 72 hrs after transfection. For cells treated with Stattic, protein extraction was done 5 hrs after treatment with Stattic. Protein was quantified by DC protein assay (Bio-Rad). Twenty to forty micrograms of protein was separated on SDS-PAGE and transferred to nitrocellulose membrane using the iBlot system (Invitrogen). Membrane was blocked with 5% BSA and incubated overnight with mouse anti-STAT3 (1:2000, Cell Signaling), rabbit anti-AMFR (1:5000, Novus Biologicals) and mouse anti-ß-actin (1:2000, Abcam). Horseradish peroxidase (HRP)-conjugated anti-mouse secondary antibody (Abcam) was used at 1:2000

dilution and HRP-conjugated anti- rabbit secondary antibody (Amersham) was used at 1:5000 dilution. Chemiluminescent detection of protein was done using Amersham ECL Plus (GE Healthcare) and band intensities were quantified using ImageJ. Immunostaining of actin cytoskeleton in methanol-acetone fixed cells was done using FITC-conjugated anti-actin antibody (1:500, Abcam).

2.20 Xenotransplantation and immunohistochemistry

All handling and care of animals was carried out according to the Guidelines on the Care and Use of Animals for Scientific Purposes issued by the National Advisory Committee for Laboratory Animal Research, Singapore. For xenograft experiments, adult male and female athymic Balb/c nude mice (weight 20 g; aged 6-8 weeks) were used. Brain tumor inoculation was done in the right side of striatum of anesthetized mice, by injecting 0.1 X 10^6 glioma cells, as indicated. On day 21 after tumor inoculation, animals were sacrificed by cardiac perfusion with PBS, followed by 4% paraformaldehyde in PBS. Harvested mouse brains were kept overnight in 30% sucrose, and embedded in Tissue-Tek OCT and cryosectioned. Hematoxylin and eosin staining of sections was done by standard methods. Stained sections were imaged using Olympus microscope. For survival experiments, xenografted animals were monitored until all animals were dead. Animal handling, sectioning and H&E staining were done by Lam Dang Hoang (IBN, A*STAR, Dr. Wang's lab).

Immunohistochemical detection was done on paraformaldehyde-fixed, OCT-embedded cryosections. Following heat-induced antigen retrieval in citrate buffer, sections were incubated with mouse anti-Ki-67 antibody (1:100 dilution, Dako) and rabbit anti-vWF antibody (prediluted, Abcam). Where fluorescent detection was done, Alex-Fluor 568 conjugated secondary antibodies (1:200 dilution, Molecular Probes) were used. For immunoperoxidase staining, biotin-conjugated secondary antibodies (1:200 dilution, BD Biosciences) were used in a three-step detection protocol (Millipore). DAB substrate was from BD Biosciences. Quantification of fluorescent Ki-

67 signal was done using NIH ImageJ, by first converting images to 8-bit, subtracting background and adjusting threshold range to 17-255 (Feuer et al., 2005). Signal intensities were enumerated from similar-size fields (5-6 fields for each tumor core or tumor edge) of different images and compared.

2.21 Selection of invasive U87 cells by experimental lung metastasis (ELM) assay

The ELM assay was performed for U87 cells as essentially done as previously described (Xie et al., 2008). Briefly, 1 X 10^6 U87 cells in 200 µl of PBS were injected intravenously through tail vein of nude mice. After 3 to 4 months, when signs of moribundity appeared, animals were euthanized and lung lesions were collected. Propagation of lesions was done subcutaneously in vivo for four weeks. Establishment of primary ELM-selected cell lines from subcutaneous tumors was done as previously described (Xie et al., 2008). This was done by Lam Dang Hoang. Three independent ELM lines were established and cultured in complete DMEM medium. Early passages (5-7 passages after first plating in vitro) were used for RNA isolation, intracranial injection and transfection.

2.22 Statistical analysis

Statistical significance was determined by paired or unpaired Student's t-test and a two-tailed p value of < 0.05 was considered to be statistically significant. Survival analysis of tumor-bearing mice was carried out using the log-rank test in SigmaStat 3.5 (Systat Software).

3 CHAPTER 3. Analysis of Adenosine-to-Inosine editing of miR-376 cluster in gliomas.

3.1 Introduction and aims

The miR-376 cluster encodes four primary miRNAs (pri-miRs) of related sequence, pri-miR-376a1, 376a2, 376b and 376c which are processed to generate five distinct mature miRNAs- miR-376a*, 376a, 376a2-5p, 376b and 376c (Figure 3.1). In the human brain, nine adenosines within this miRNA cluster are subject to specific and high-level adenosine-to-inosine (A-to-I) RNA editing (Kawahara et al., 2007b). The genomic organization of miR-376 cluster and location of editing sites are illustrated in Figure 3.1. The A-to-I editing enzymes ADAR1 (also known as ADAR) and ADAR2 (also known as ADARB1) are responsible for all editing events within the cluster and demonstrate site-specific preference for activity (Kawahara et al., 2008). For miR-376 cluster, editing of sites in regions of primary miRNA stem-loops comprising mature miRNAs leads to the generation of “edited” mature miRNAs (Kawahara et al., 2007b). Thus far miR-376 cluster members remain the only mature miRNAs found to be abundantly edited in a tissue-specific manner.

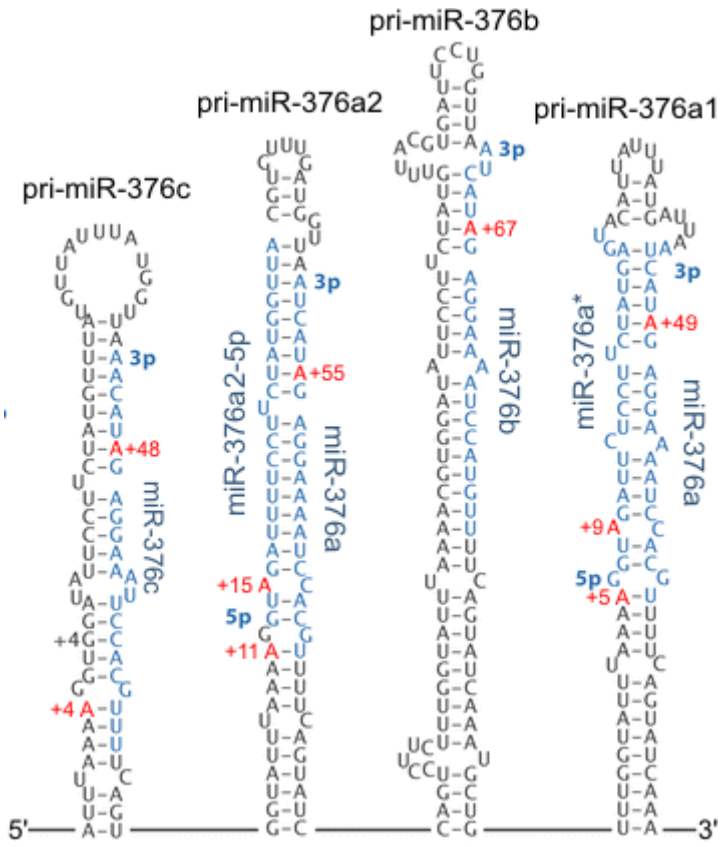

Figure 3.1 Human miR-376 cluster. Schematic representation of the four primary miRNAs, pri-miR-376c, 376a2, 376b, 376c that undergo site-specific A-to-I editing. The processed mature miRNAs are highlighted in blue and labeled. Known editing sites are shown in red. The 5' end of the stem-loop sequences annotated the Sanger miRBase database is counted as +1. Adapted from (Nishikura, 2010).

Altered editing of several substrates in gliomas and related cell lines have previously been identified and are listed in Table 3.1. Reduced expression of *ADAR1* and *ADAR2* (Paz et al., 2007) or reduced activity of the enzymes without any change in expression (Cenci et al., 2008; Maas et al., 2001) has been demonstrated for cancers, especially gliomas. Here only editing events and substrates from the nervous system are discussed, as they are most frequently observed. This is possibly because A-to-I editing is particularly prevalent in the brain as ADARs are preferentially expressed and exhibit high activity in the brain (Mehler and Mattick, 2007).

Substrate	Enzyme responsible	Status of ADAR	Reference
GluR-B	ADAR2	Reduced activity	(Maas et al., 2001)
GluR-B GluR-6	ADAR2	Reduced activity	(Cenci et al., 2008)
Alu repeats within MED13 *Alu* repeats within BRCA1	likely ADAR1 (Wahlstedt and Öhman, 2011)	Reduced expression	(Paz et al., 2007)
CYFIP2	ADAR2		
FLNA	ADAR1, ADAR2		
BLCAP	ADAR2, ADAR1	nd	(Galeano et al., 2010)

Table 3.1 Altered A-to-I editing in gliomas of known substrates. Summary of reduced A-to-I RNA editing events in various protein-coding and non-coding substrates in gliomas and related cell lines.nd: not determined.

The general loss of editing in human brain tumors, manifest as underediting of a handful of known substrates, suggests a fundamental change in the function of the editing machinery. As miRNAs are also substrates of the same editing machinery, it is likely miRNAs also suffer abnormal editing levels in these tumors. Therefore, the aim of this chapter was to investigate A-to-I editing of miR-376 cluster in glioma tissues and cell lines to identify: a) patterns of miRNA editing in tumors and b) specific miRNAs that might be aberrantly edited.

3.2 Editing analysis of primary miRNAs in gliomas

Since transcription of the miR-376 cluster produces a long single primary transcript with pri-miR-376a1, 376a2, 376c and 376b and A-to-I editing occurs on the primary transcript (Kawahara et al., 2007b), direct sequencing of RT-PCR products corresponding to pri-miRNAs was done to determine the frequency of A-to-I editing (hereafter ‘editing’). Editing analysis was done for a set of 24 high-grade gliomas which included: 16 glioblastomas (GBM; grade IV), 4 anaplastic astrocytomas (AA; grade III), 3 anaplastic oligoastrocytoma (AOA; grade III) and 1 anaplastic oligodendroglioma (AOG; grade III). Total RNA was isolated from all samples. Five RNA samples obtained from normal brain tissues were included in the analysis to

serve as normal controls and as a reference for normal editing in the human brain. Direct sequencing of RT-PCR products corresponding to pri-miR-376a1, 376a2, 376b and 376c was performed (Figure 3.2) and from sequencing chromatograms, the frequency of editing was determined as the % ratio of 'G' peak to the sum of 'A' and 'G' peaks at editing sites.

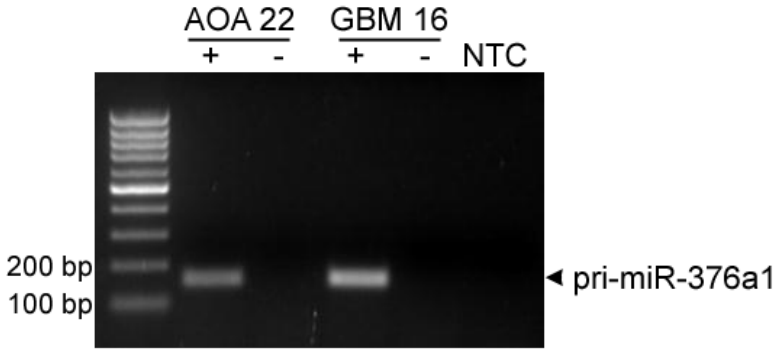

Figure 3.2 RT-PCR of pri-miRNAs from miR-376 cluster. Representative gel image of RT-PCR of pri-miR-376a1 from two glioma samples, AOA 22 and GBM 16. cDNA prepared with reverse transcriptase (+) and without reverse transcriptase (-) for each sample were subjected to the same PCR amplification. Absence of PCR product in (-) lane indicates absence of genomic DNA contamination. PCR products from (+) lanes were extracted for sequencing. NTC: no-template control.

Sequencing of 5 normal human brain tissue samples confirmed that editing at the sites was high and to the same extents as described previously (Kawahara et al., 2007b) and with low variance among samples (Table 3.2). Compared to normal brain, in glioma samples variable extents of altered editing were observed, appearing as reduced or absent 'G' peaks at the editing sites in sequence chromatograms (Figure 3.3). Quantification of editing frequencies for all sites revealed that overall editing of miR-376 cluster was significantly reduced in human gliomas compared to normal brain, as summarized in Table 3.2. Baseline editing frequencies of 0-4% were observed for some sites in several glioma samples, representative of negligible editing.

For some sites, tumor samples displayed great variability in editing levels (+48 site for pri-miR-376c) whereas for others, editing levels were consistently low across all samples (+5 site of pri-miR-376a1). Within individual tumors, there was some correlation between degree of reduction in editing at various sites i.e. tumors with low-level editing of one site tended to have low-level editing for other sites (GBM 1, GBM 2 and AA 17) and vice-versa (AOG 24). This is line with a common editing machinery, and its dysfunction as the underlying mechanism for altered editing of substrates, with the degree of dysfunction reflected commonly in the factor of reduction of editing at distinct sites. Interestingly, some sites with normally high-editing levels mostly remained highly edited in tumor tissues e.g. site +55 of pri-miR-376a2.

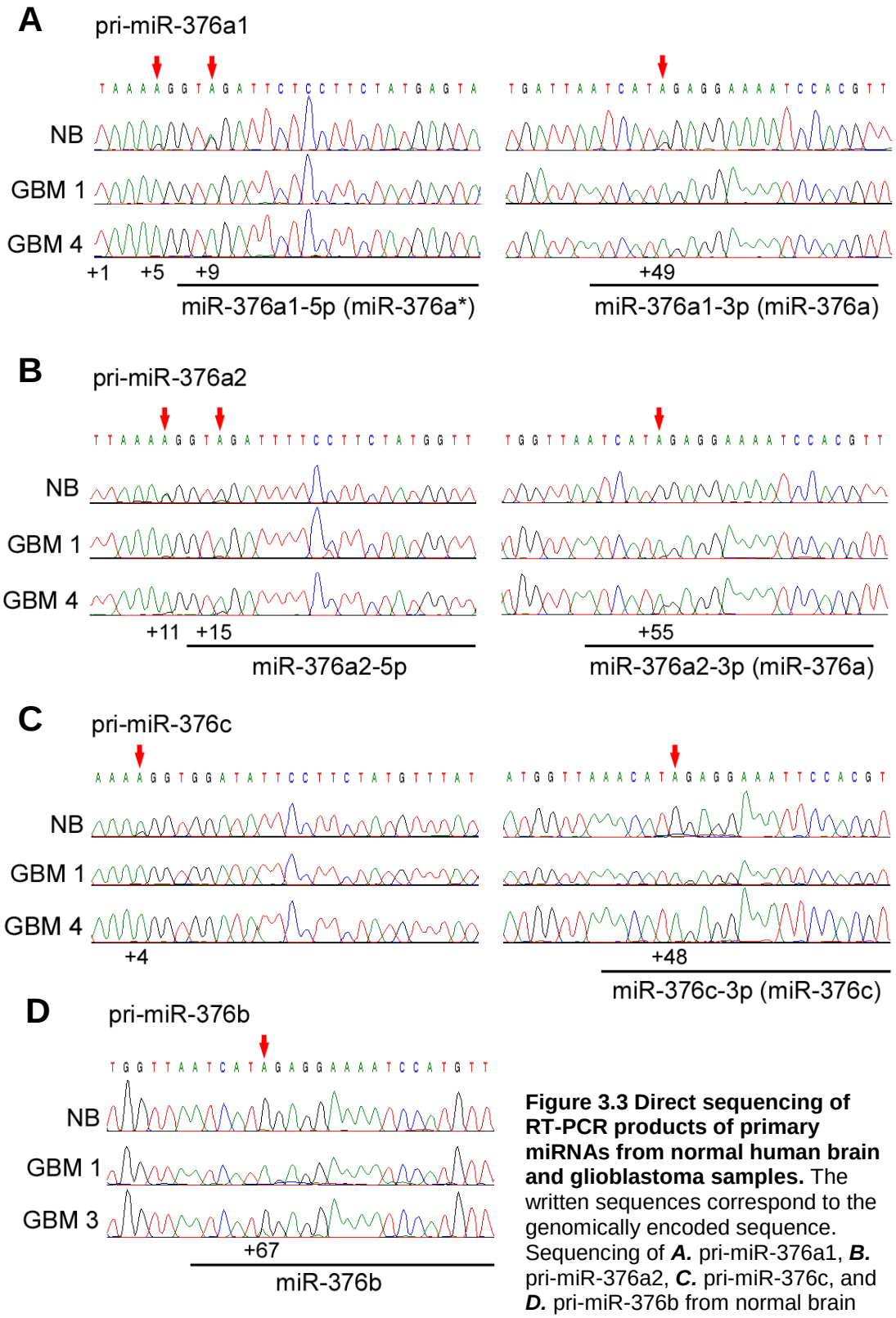

Figure 3.3 Direct sequencing of RT-PCR products of primary miRNAs from normal human brain and glioblastoma samples. The written sequences correspond to the genomically encoded sequence. Sequencing of ***A.*** pri-miR-376a1, ***B.*** pri-miR-376a2, ***C.*** pri-miR-376c, and ***D.*** pri-miR-376b from normal brain (NB) and glioblastomas (GBMs).

Regions underlined correspond to mature miRNAs: miR-376a1-5p (miR-376a*) and miR-376a1-3p (miR-376a) processed from pri-miR-376a1, miR-376a2-5p and miR-376a from pri-miR-376a2, miR-376c from pri-miR-376c, and miR-376b from pri-miR-376b. For each primary miRNA the 5' end of stem-loop sequence annotated in the Sanger miRBase site is counted as +1. Editing sites are indicated by red arrows, at which A-to-I editing is detected as black guanosine (G) trace, either substituting the genomically encoded A trace or appearing together with the A trace. Note the reduction or absence of a 'G' peak at editing sites in GBM samples.

Sample ID (Tumors)	Histopathological Classification	Frequency of Editing (%)								
		pri-miR-376a1			pri-miR-376a2			pri-miR-376c		pri-miR-376b
		[a]site +5	+9 ‡	+49 †	+11	+15 †	+55 †	+4	+48 †	+67 †
	Normal Brain (n = 5)	15.74 ± 4.32	46.56 ± 2.17	25.21 ± 3.50	52.6 ± 5.25	90.74 ± 6.58	98.52 ±1.26	24.34 ± 0.77	93.63 ± 2.02	94.40 ±1.87
1	GBM	2.02	0.93	0	7.5	8.9	5.06	3.03	4.86	3.58
2	GBM	2.3	2.85	2.5	5.35	7.17	13.65	4.36	6.64	2.7
3	GBM	2.94	3.56	9.31	15.99	30.66	97.8	5.56	76.14	89.1
4	GBM	3.57	2.4	0	10.08	16.47	36.57	1.44	3.58	–
5	GBM	2.24	1.64	1.7	20.17	38.21	95.92	–	–	66.75
6	GBM	2.31	1.33	41.97	16.58	21.24	91.29	1.28	72.09	92.9
7	GBM	2.35	1.55	3.68	2.64	0	92.57	–	–	–
8	GBM	2.06	2.98	0	11.94	49.03	92.55	0	61.21	–
9	GBM	0.87	3.2	0	22.86	70.02	52.25	1.79	95.43	98.47
10	GBM	2.13	1.89	97.3	21.27	52.16	97.45	0.52	94.78	
11	GBM	2.42	2.46	2.18	6.18	3.48	69.73	1.27	71.04	63.4
12	GBM	0.21	13.64	0	9.04	39.15	83.41	10.58	75.29	81.31
13	GBM	–	–	–	5.64	0.46	91.83	–	–	–
14	GBM	–	–	–	11.31	8.62	0.38	–	–	–
15	GBM/GS	1.67	24.14	1.39	12.82	45.03	95.04	2.43	91.21	65.86
16	GBM/GS	3.58	12.07	9	23.4	29.16	90.13	0.39	66.97	74.93
17	AA	2.51	1.54	3.13	10.42	13.01	26.61	3.39	4.06	
18	AA	1.49	5.27	0	10.31	58.31	98.72	1.93	97.76	91.21
19	AA	2.73	1.88	0	3.31	96.75	98.48	–	–	–
20	AA	2.65	32.99	16.69	19.83	42.93	98.22	32.82	97.11	–
21	AOA	9.16	16.28	14.64	16.29	16.42	92.61	3.73	72.22	88.75
22	AOA	0.29	58.71	2.23	33.8	49.73	95.51	0.52	19.51	90.76
23	AOA	2.46	96.71	0	7.47	36.79	97.07	40.08	64.53	66.89
24	AOG	2.5	19.39	32.65	25.46	50.33	93.74	1.3	93.11	94.41

Table 3.2 Quantification of A-to-I RNA editing of primary miRNAs from miR-376 cluster in normal human brain and primary gliomas. Direct sequencing of RT-PCR products corresponding to each pri-miRNA was done and frequency of editing was determined as the % ratio of 'G' peak to the sum of 'A' and 'G' peaks at indicated editing sites.

GBM, glioblastoma multiforme; AA, anaplastic astrocytoma; AOA, anaplastic oligoastrocytoma; AOG, anaplastic oligodendroglioma; GS, gliosarcoma.

[a] Position of editing site within each pri-miRNA. The 5' end of the stem-loop annotated in Sanger miRBase registry is counted as +1.

† Editing site in seed sequence of processed mature miRNA; ‡ Seed sequence of mature miR-376a*; '–' PCR product could not be amplified.

Of the nine editing sites within the miR-376 cluster, six lie within the seed sequences of processed mature miRNAs. The remaining three sites lie within the stem-loop sequence of pri-miRNAs just outside of mature miRNA sequence, i.e. +5 site of pri-miR-376a1, +9 site of pri-miR-376a2 and +4 site of pri-miR-367c (Figure 3.1). Changes to editing frequencies of mature miRNA seed sites are expected to have greater consequence on miRNA function, as the seed sequence determines miRNA function through target selection (Bartel, 2009). Hence, altered editing at mature miRNA sites was considered of greater significance.

The editing frequencies for mature miRNA seed sequence sites in grade IV glioma samples (GBMs) and normal brain was further compared (Figure 3.4). Overall, there was a broad disparity in the reduction of editing levels among the mature miRNA seed editing sites. The +9 site of pri-miR-376a1 and +15 site of pri-miR-376a2 appeared most affected in terms of extent of editing loss suffered. Although +49 site of pri-miR-376a1, corresponding to mature miR-376a, appears to be negligibly edited in most GBMs, it is only moderately edited in the normal brain (~25%). Additionally, miR-376a is also encoded by pri-miR-376a2, site +55 of which lies within this mature miRNA. Cumulatively, mature miR-376a derived from pri-miR-376a1 and pri-miR-376a2 would retain relatively high levels of editing in GBMs.

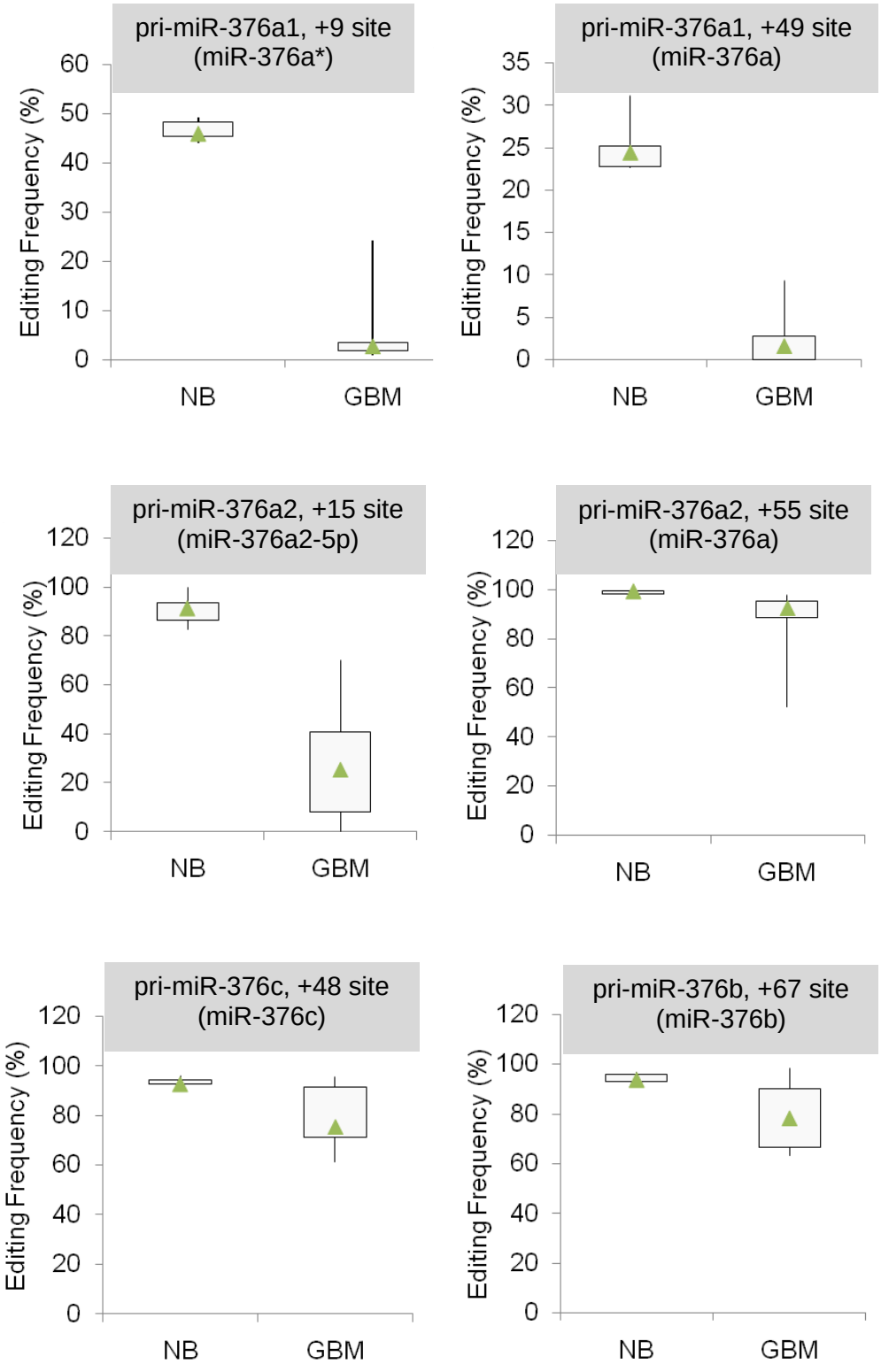

Figure 3.4 Editing frequency of sites in miR-376 cluster corresponding to mature miRNA seed sequences. Position of edited sites within indicated primary miRNAs are shown and the mature miRNA to which they correspond are specified in brackets. Editing levels for each site are compared between normal brain (NB) and glioblastoma samples (GBM). Boxplots show the median (▲), first and third quartile boxes, minimum and maximum data points. Outliers are not shown.

Interestingly, when tumors were grouped by histopathology, a correlation between editing of +9 site of pri-miR-376a1 and tumor type was revealed. Among all GBMs, two tumors classified as gliosarcomas (GBMs 15 and16) retained substantial editing of +9 site of pri-miR-376a1 (12-24%; Table 3.2). This was also observed in gliomas classified as anaplastic oligoastrocytomas (AOA) and anaplastic oligodendrogliomas (AOG) (16-97% in 4/4 tumors). However, most anaplastic astrocytomas (AAs) and GBMs (14/16 tumors, excluding known gliosarcomas) consistently displayed <5% editing at +9 site of pri-miR-376a1 (Figure 3.5A). Although site +15 or pri-miR-376a2 is highly edited (~90%) in the normal brain, its degree of editing reduction demonstrated great variability among glioma grades and samples (Figure 3.5B). These results suggest that extent of altered editing is combinatorially dependent on the tumor type and the editing site itself and that reduced editing of some sites may be of greater significance than others in GBMs. Specifically, the +9 site of pri-miR-376a1 displayed a tumor-type dependent editing aberration and is particularly lowly edited in GBMs. This site corresponds to the seed sequence of the encoded mature miR-376a1-5p, also known as miR-376a*. Accordingly, mature miR-376a* consistently displays negligible levels of editing in GBMs, in contrast to its relatively highly edited status in the normal brain tissue.

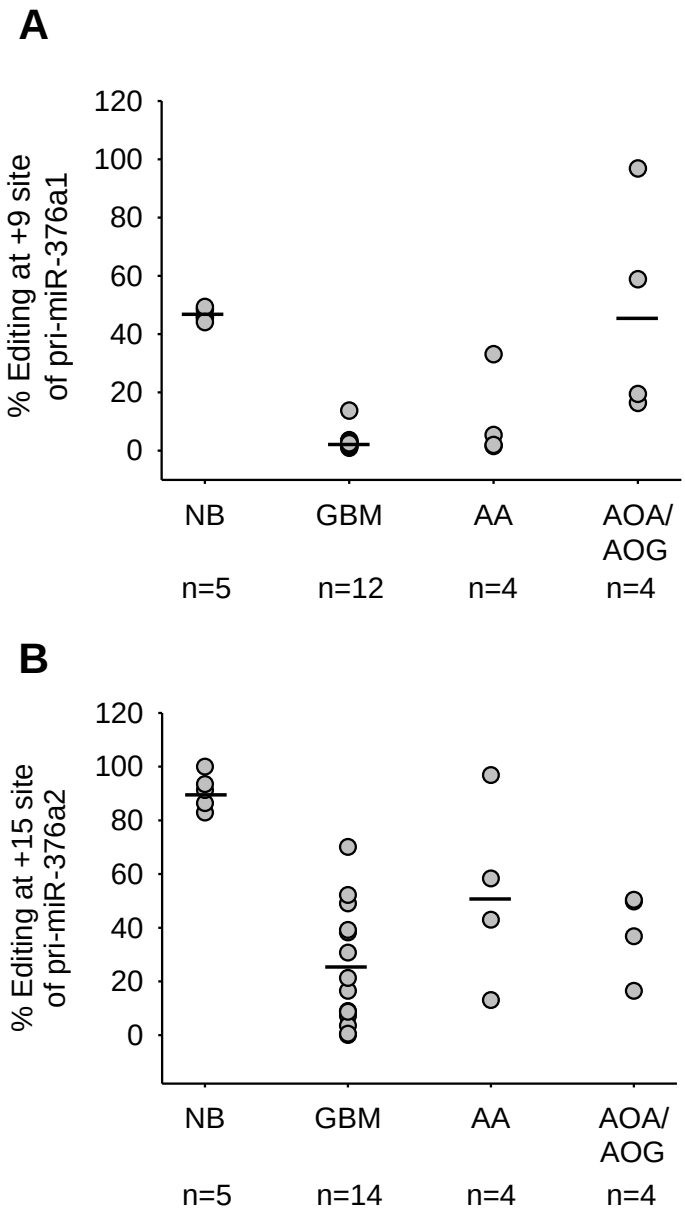

Figure 3.5 Editing frequencies based on tumor histopathological classification. ***A.*** Editing frequency of +9 site of pri-miR-376a1 (corresponding to mature miR-376a*). ***B.*** Editing frequency of +15 site of pri-miR-376a2 (corresponding to mature miR-376a2-5p). NB: normal brain; GBM: glioblastoma multiforme; AA: anaplastic astrocytoma; AOA: anaplastic oligoastrocytoma; AOG: anaplastic oligodendroglioma. Horizontal bars designate mean values. Among GBMs, gliosarcomas are not displayed.

3.3 Editing analysis of primary miRNAs in glioma cell lines and astrocyte cells

To evaluate editing of miR-376 cluster at a cellular level, rather than in tumor tissue with mixed cell populations, a similar analysis of primary miRNA editing was carried out in four glioma cell lines (U87, U251, SW1783 and SW1088) (Table 3.3). In glioma cell lines, editing frequencies for all sites were reduced, as in tumor samples, but demonstrated far more consistency across cell lines. The results are in agreement with the low level of editing observed for GluR-B Q/R site in A172, U118 and U87 glioma cell lines (Cenci et al., 2008) and reduced editing that characterizes transformed cell lines (Levanon et al., 2005).

As the brain is a complex tissue composed of multiple cell types, editing frequencies obtained using the normal brain as control represents an “average”. Thus, the use of normal brain limits attribution of observed editing to any particular cell type in the brain. As gliomas, particularly astrocytomas and glioblastomas, potentially arise from transformed astrocytes (Huse and Holland, 2010), editing frequencies were investigated in normal human astrocytes isolated from adult brain cortex (Table 3.3). In normal astrocytes editing of all sites corresponding to mature miRNAs, was remarkably high at ~95%, except site +49 of pri-miR-376a1. Interestingly, for non-mature miRNA sites even within the same pri-miRNA, editing was limited to very low levels in astrocytes suggesting that other cell types -neurons or oligodendrocytes- contribute to the detectable editing frequencies observed at these sites for the whole brain. Importantly, it was confirmed that in normal astrocytes as in normal brain, site +9 of pri-miR-376a1 (corresponding to miR-376a*) is highly edited to ~95%. The contrastingly low, nearly negligible, level of editing of this site in GBMs is therefore striking and suggests its functional importance in GBMs. Therefore, from among several highly edited mature miRNAs from miR-376 cluster in brain and astrocytes, miR-376a* is disparately more affected by reduced editing in GBMs.

Cell Type	Frequency of Editing (%)								
	pri-miR-376a1			pri-miR-376a2			pri-miR-376c		pri-miR-376b
	[a]site +5	+9 [‡]	+49 [†]	+11	+15 [†]	+55 [†]	+4	+48 [†]	+67 [†]
Normal Astrocytes	3.65	95.13	1.56	1.13	94.59	91.44	1.9	94.14	97.96
U87	1.71	1.51	2.35	11.23	13.87	75.74	0.96	42.7	52.61
SW1783	0	1.46	6.98	7.93	12.56	81.81	1.89	38.32	57.31
SW1088	0	2.02	1.39	4.68	5.46	62.67	1.21	17.9	32.98
U251	2.59	3.04	6.29	8.66	13.57	82.53	2.19	37.94	55.39

Table 3.3 Quantification of A-to-I RNA editing of primary miRNAs from miR-376 cluster in normal astrocytes and glioma cell lines. Direct sequencing of RT-PCR products corresponding to each pri-miRNA was done and frequency of editing was determined as the % ratio of 'G' peak to the sum of 'A' and 'G' peaks at indicated editing sites.

[a] Position of editing site within each pri-miRNA. The 5' end of stem-loop transcript annotated in Sanger miRBase registry is counted as +1.

[†] Editing site in seed sequence of processed mature miRNA; [‡] Seed sequence of mature miR-376a*.

3.4 Editing analysis of mature miRNAs

Mature miRNA editing frequency was measured in glioma cell lines using the targeted cloning strategy developed previously by (Kawahara et al., 2007b), to correlate their editing frequency to that of pri-miRNAs from which they are derived. For each mature miRNA, the % of cDNA clones of mature miRNA RT-PCR products with A-to-G change at editing sites indicate the editing frequency of mature miRNAs. The trend of mature miRNA editing frequency corresponded to that for pri-miRNAs for U251, SW1088 and SW1783 cells (Figure 3.6 and Table 3.3). Indeed, the mature miR-376a* was negligibly edited to 0-5% in glioma cell lines, matching well with the editing frequency of +9 site of pri-miR-376a1, the site corresponding to seed sequence of this miRNA.

A

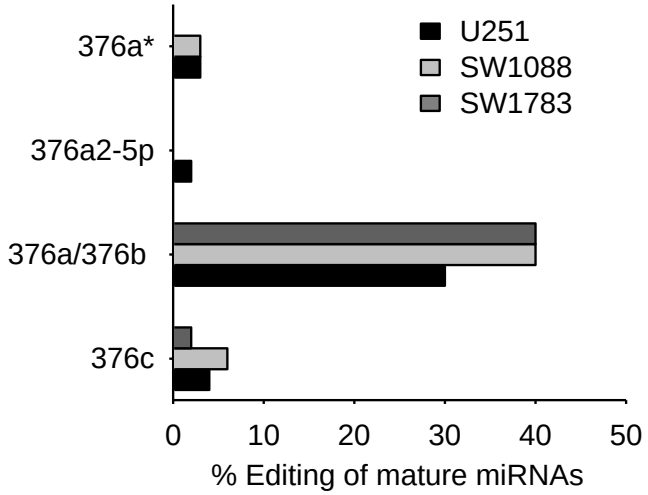

B

	Mature miRNA			
	miR-376a*	miR-376a2-5p	miR-376a/376b	miR-376c
U251	1/36	1/44	13/44	2/48
SW1088	1/44	0/39	7/17	3/49
SW1783	0/48	0/44	8/20	1/48

Figure 3.6 Editing frequency of mature miRNAs. Using a targeted cloning strategy, editing of mature miRNAs from miR-376 cluster was measured in U251, SW1088 and SW1783 glioma cells ***A.*** cDNA clones (n > 50) for each miRNA were sequenced and frequency of editing was determined as the % of clones containing A-to-G change. miR-376a and miR-376b cannot be distinguished by this sequencing strategy. ***B.*** For each mature miRNA, number of clones with A-to-G change/total number of clones containing positive sequences of acceptable quality is shown. This was used to calculate editing frequency shown in ***A.***

Although the trends of mature miRNA and primary editing frequencies were correlated, the editing frequency was in general lower than expected for mature miRNAs - assuming that edited mature miRNAs are produced at frequencies similar to edited pri-miRNAs. The underestimation was attributed to cloning bias, as editing frequencies of mature miRNAs from normal brain samples, as measured by us, were also measurably lower than primary miRNA editing. For miR-376a*, 13 of 47 clones contained A-to-G change for an estimated editing frequency of 27% in normal brain, compared to the 50% editing determined by Kawahara et al (Kawahara et al., 2007b). Nonetheless, for pri-miRNAs from normal brain, the editing frequency determined in this study, was completely corresponding to published data, verifying the methodology used for quantifying pri-miRNA editing.The discrepancy between editing levels of mature and primary miRNAs is deemed not to be of significant concern as:

1. Equivalency of editing frequencies between primary and mature miRNAs from miR-376 cluster has been conclusively demonstrated previously (Kawahara et al., 2007b).
2. In the scenario of interest in this study where primary miRNAs are unedited or underedited as in GBMs especially for miR-376a*, mature miRNAs will necessarily remain unedited, as they cannot be independently edited. Hence, a cloning bias which underestimates editing of mature miRNAs cannot lead to any further underestimation of editing of ‘unedited’ miRNAs.

Hence, based on previous findings and the current analysis, editing frequency of sites in primary miRNAs corresponding to mature miRNA sequences are good estimates of editing frequency of mature miRNAs. Therefore, among mature miRNAs from miR-376 cluster, miR-376a* is present almost exclusively in the unedited form in GBMs as judged from the negligible editing frequency of its seed site in pri-miR-376a1.

3.5 Expression of mature miRNAs in gliomas

Transcriptional and post-transcriptional mechanisms can both regulate miRNA abundance which is commonly altered in cancers. In this chapter, one of the aims was to investigate the expression levels of mature miRNAs from miR-376 cluster. In the context of GBMs, where mature miRNA editing, especially for miR-376a*, is reduced it is important to determine if mature miRNA abundance is also affected, possibly due to altered editing. Therefore, quantification of mature miRNA abundance was done by qRT-PCR using miRNA-specific primers. It was demonstrated that 'A' and 'G' containing primers are equally efficient in amplifying mature miRNAs. Both GBMs and AAs expressed miR-376a* at variable levels (with no apparent correlation to editing frequency), although the tendency was for miR-376a* to be expressed lower than in normal brain (Figure 3.7). Measurement of levels of other mature miRNAs from miR-376 cluster also revealed a general variability of expression, although miR-376a appeared significantly down-regulated in tumors (Figure 3.8).

.

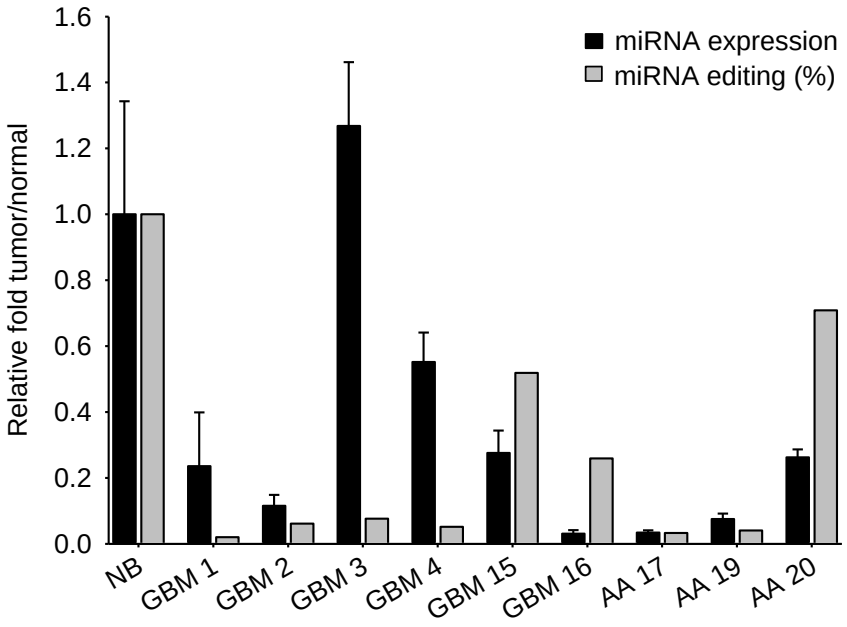

Figure 3.7 Expression and editing of miR-376a* in a panel of tumor samples. Expression of miR-376a* was measured by qRT-PCR and values were normalized to 5S rRNA from the same sample. Editing frequency (%) was obtained from the frequency of editing of site +9 of pri-miR-376a1 (corresponding to miR-376a*), and was normalized to the % editing in normal brain (NB) for the same site. Both expression and editing data are plotted on the same scale normalized to NB. Bars represent mean ± SD for expression data.

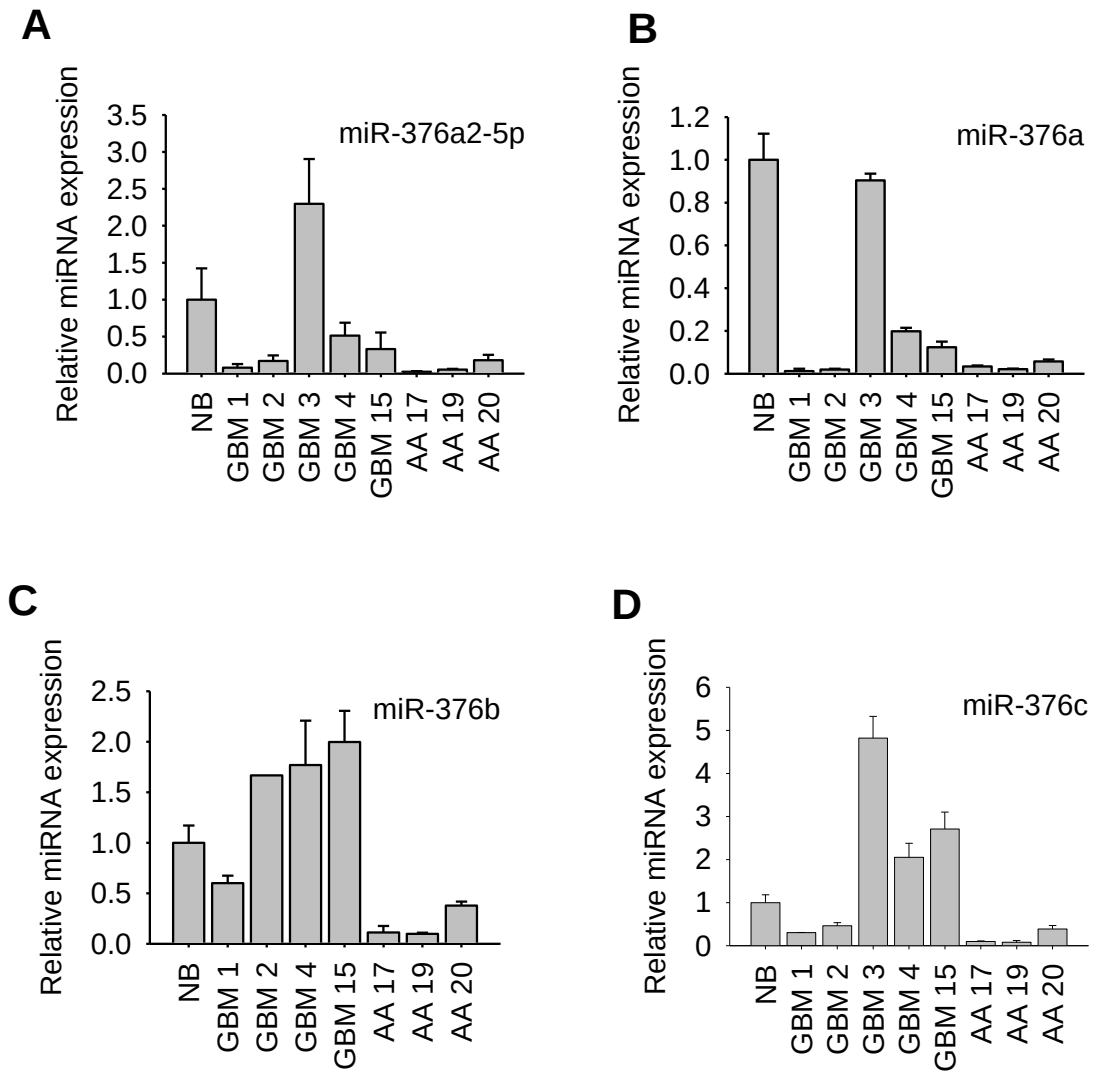

Figure 3.8 Expression of mature miRNAs from miR-376 cluster in a panel of tumor samples. ***A.*** miR-376a2-5p, ***B.*** miR-376a, ***C.*** miR-376b, ***D.*** miR-376c. Expression of miRNAs was measured by qRT-PCR and values were normalized to 5S rRNA from the same sample. NB: Normal brain. Data represents mean ± SD.

In order to conclusively establish the expression of miRNAs in a large panel of tumors, the Cancer Genome Atlas (TCGA) dataset on miRNA expression in GBMs was interrogated (The Cancer Genome Atlas Network, 2008). The Anduril framework was used for analysis of microarray-derived miRNA expression data from 251 GBM and 10 normal brain samples which is available in the TCGA dataset (Ovaska et al., 2010). Table 3.4 summarizes these results for mature miRNAs from miR-376 cluster for which TCGA data is available. Mature miR-376a2-5p is currently not annotated in

Sanger miRBase, hence expression information on this miRNA from public databases is unavailable.

Overall, expression of mature miRNAs from miR-376 cluster in GBMs is similar to that in the normal brain, except for miR-376a which is expressed at half the abundance of normal brain, in agreement with earlier qRT-PCR analysis (Figure 3.8B). Significantly, the total abundance of miR-376a* (comprising both unedited and edited transcripts) in GBMs is highly similar to that in normal brain tissue (0.853-fold). Microarray and qRT-PCR-based miRNA detection methods are unable to distinguish between mature miRNA isoforms differing by a single-base and hence expression data represents cumulative levels of both edited and unedited miRNAs. Together, expression and editing data suggests that miR-376a* is expressed almost exclusively in the unedited form in GBMs, at abundance largely similar to that of the edited transcript in the normal brain.

miRNA	Fold-change in GBM	p-value
miR-376a*	0.853	2.49E-05
miR-376a	0.517	1.18E-09
miR-376b	0.941	0.0422
miR-376c	0.789	8.54E-05

Table 3.4 Expression of miR-376 cluster members in TCGA dataset. Summary of analysis of TCGA data using Anduril framework for miRNA expression. Samples included in the analysis include 251 GBMs and fold-change is relative to miRNA expression in 10 normal brain samples. p-value associated to fold change is also reported and obtained from the same analysis.

The cumulative data from editing and expression analysis suggests that from miR-376 cluster, only mature miR-376a* displays a strong tumor-type specific editing aberration and accumulates almost entirely as the unedited variant in GBMs. Thus, unedited miR-376a* is a tumor-specific miRNA sequence variant, aberrantly produced due to the loss of regulated A-to-I editing in GBMs.

3.6 Expression of mature miRNAs in glioma cell lines

The expression of mature miRNAs was also measured in glioma cell lines and compared to normal astrocytes. In contrast to GBMs, expression of all miRNAs from miR-376 cluster was consistently reduced several-fold in glioma cell lines (Figure 3.9A-E). miR-376a* and miR-376a2-5p especially were negligibly expressed in U87, U118 and SW1783 cell lines. This data suggests that in addition to low level of editing, glioma cells also have low expression of miRNAs from miR-376 cluster. This effectively amounts to neither the edited nor the unedited mature miRNA being expressed in glioma cell lines in vitro, especially for miR-376a*. Interestingly, it was noted that normal astrocytes have highly-enriched expression of mature miRNAs compared even to normal brain tissue (Figure 3.9F), suggesting that from among cell types of the brain, astrocytes specifically express high levels of miRNAs from miR-376 cluster. Coupled with high-level (nearly 100%) editing of mature miRNA seed sites in astrocytes (Table 3.3), this suggests a pertinent role for edited mature miRNAs in the normal function of astrocytes.

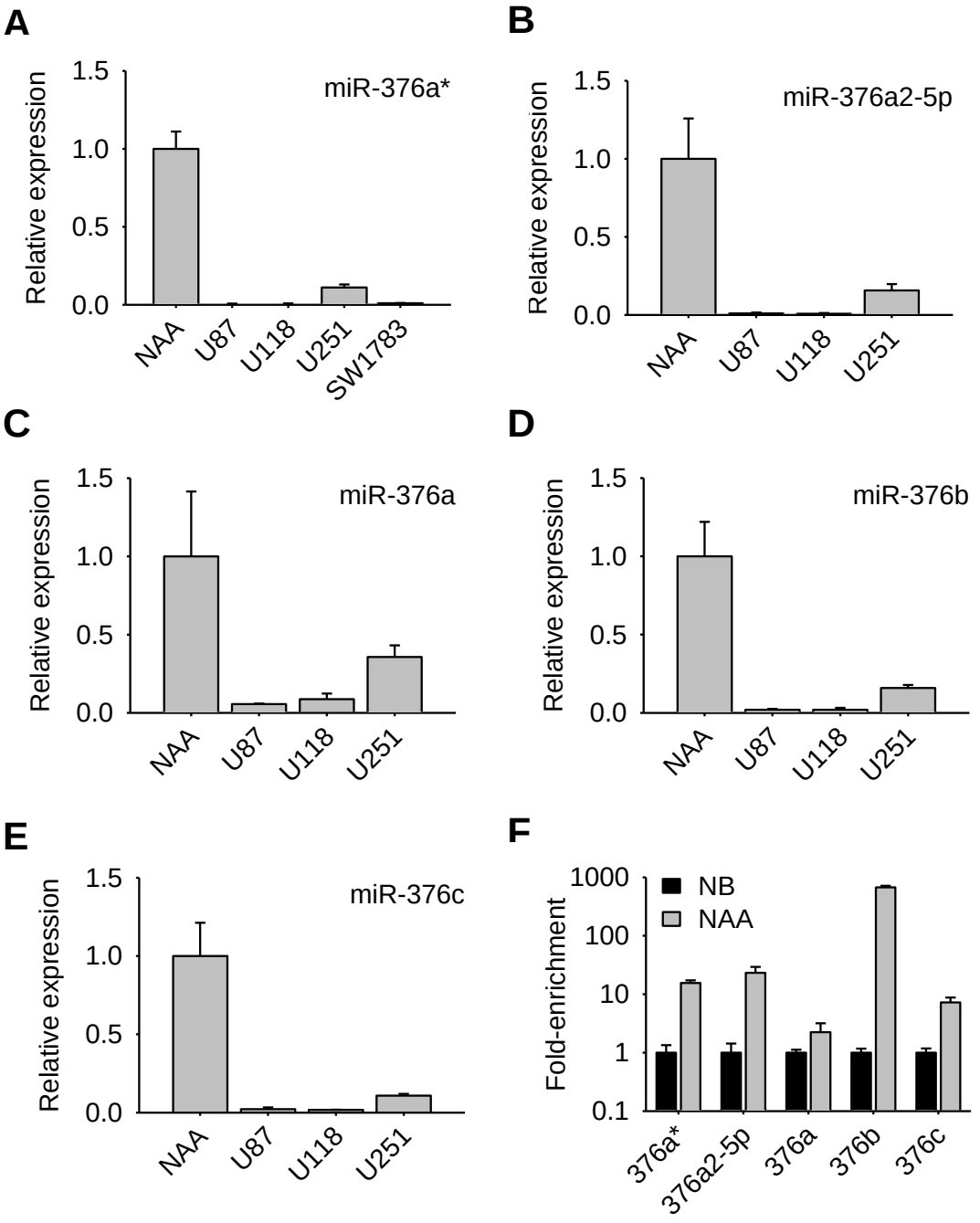

Figure 3.9 Expression of mature miRNAs from miR-376 cluster in glioma cell lines and normal astrocytes. Expression of miRNAs was measured by qRT-PCR and values were normalized to 5S rRNA from the same sample ***A.*** miR-376a*, ***B.*** miR-376a2-5p, ***C.*** miR-376a, ***D.*** miR-376b, ***E.*** miR-376c. Values are relative to normal astrocytes (NAA) ***F.*** Fold-enrichment of mature miRNA expression in NAA compared to normal brain (NB). Data represents mean ± SD.

3.7 Underediting of miR-376a* is due to ADAR2 dysfunction

The A-to-I editing enzymes, ADAR1 and ADAR2 edit all sites within the miR-376 cluster with varying specificities for each site. As it happens for other editing substrates reported in GBMs, the reduction in editing levels of miR-376 cluster sites necessarily stems from attenuated ADAR function either due to low expression or reduced activity without change in expression. Therefore to account for the changes in editing frequencies of miR-376 cluster sites in gliomas, mRNA levels of *ADAR1* and *ADAR2* were quantified in tumors by qRT-PCR.

ADAR1 was found to be generally underexpressed in gliomas, independent of tumor type, and did not show any correlation with frequency of editing at any particular site from miR-376 cluster (Figure 3.10A). Most GBMs showed markedly diminished levels (<20% of normal levels) of *ADAR2* expression (Figure 3.10B). In contrast, most grade III gliomas (7/8 AA, AOA and AOG) retained significantly higher levels of *ADAR2* (nearly 50% of normal levels). ADAR2 exclusively edits the +9 site of pri-miR-376a1, which displays negligibly low-level editing specifically in GBMs, while retaining significant editing in AOA and AOG. Accordingly, the low expression of *ADAR2* in GBMs is likely to be the underlying reason for underediting of site +9 of pri-miR-376a1 (miR-376a*) in GBM tumors. Interestingly, in GBMs 12, 15 and 16, despite the high-level editing of miR-376a* measured (Table 3.2), *ADAR2* expression was low similar to other GBMs. This suggests that loss of *ADAR2* expression is a common event in GBMs and exceptional accumulation of edited miR-376a* in some GBMs may depend on factors other than *ADAR2* mRNA levels.

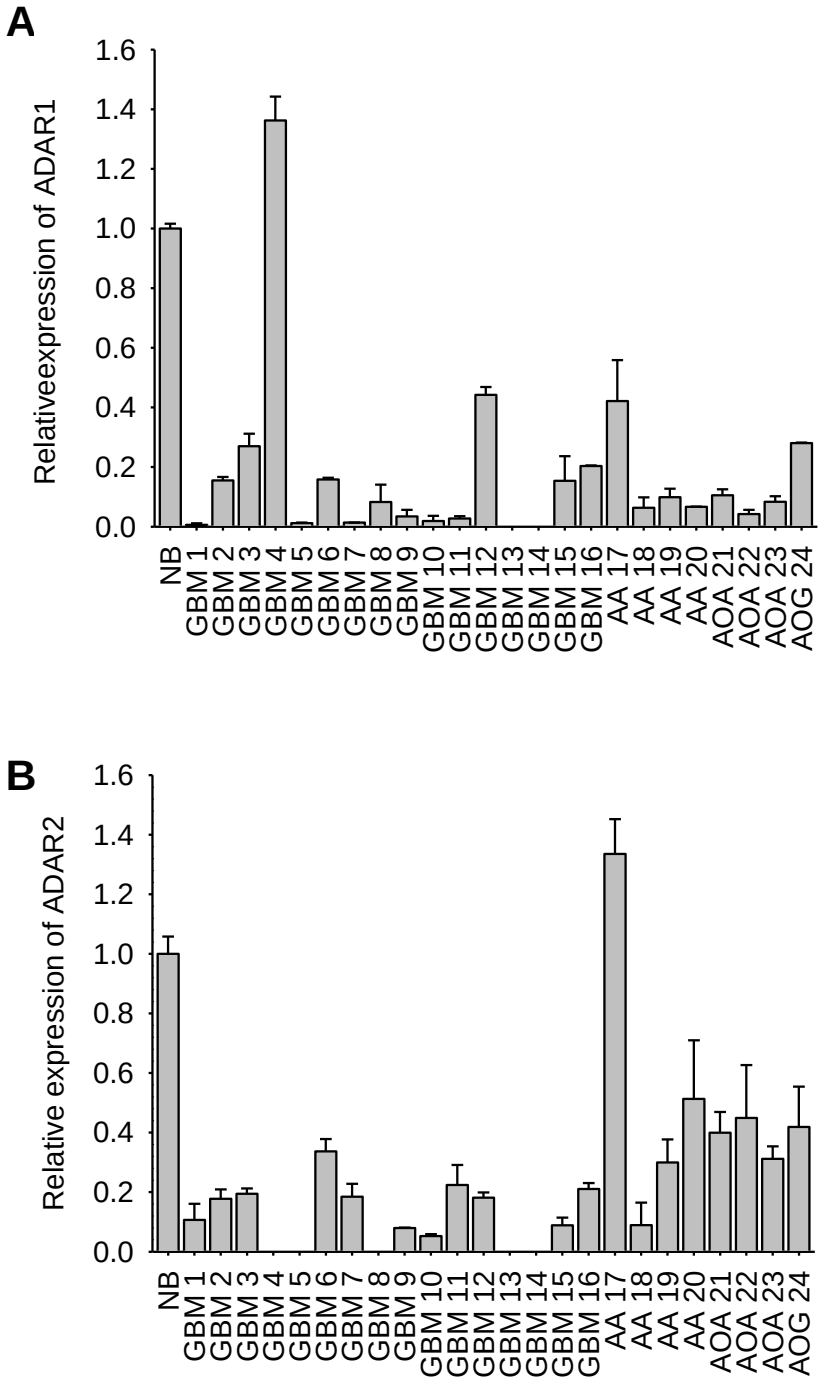

Figure 3.10 Expression of ADAR1 and ADAR2 in gliomas. ***A.*** Relative quantification of *ADAR1* mRNA in normal brain (NB) and 24 glioma samples (GBM, AA, AOA, AOG). ***B.*** Relative quantification of *ADAR2* mRNA by qRT-PCR. 18S rRNA was used for normalization. Data represents mean ± SD.

To establish a causal link between ADAR2 function and editing of miR-376a*, ADAR2 was ectopically expressed in glioma cells by transfecting an expression vector encoding ADAR2. The cells were co-transfected with an expression vector encoding miR-376 cluster and editing analysis was carried out. It was necessary to ectopically introduce the miR-376 cluster as substrate for editing, given that this miRNA cluster is generally lowly expressed in glioma cells (Figure 3.9). Direct sequencing of RT-PCR products corresponding to pri-miR-376a1, 376a2, 376b and 376c, from U87 glioma cells over-expressing ADAR2 was done (Figure 3.11). As controls, U87 cells were transfected with EGFP expression plasmid instead of ADAR2.

Form the sequencing chromatograms, it was seen that editing at site +9 of pri-miR-376a1 was restored to ~95% in U87 cells in the presence of ectopic ADAR2 (Figure 3.11), corresponding with established specificity of ADAR2 for editing this site (Nishikura, 2010). Within pri-miR-376a1, +49 site was edited to ~60% in the presence of ADAR2, compared to 5-10% in control cells. It is known that this site is preferentially edited by ADAR1, potentially accounting for its relatively lower editing levels than +9 site of pri-miR-376a1. Of note, editing remained highly specific to known editing sites. No spurious editing events represented by presence of ‘G’ peaks at non-editing ‘A’ sites were detected when ADAR2 was overexpressed. Furthermore, ADAR2 also edited to high levels (nearly 100%), +5 site of pri-miR-376a1, +11 and +15 sites of pri-miR-376a2, and +4 site of pri-miR-376c (Figure 3.11). It is known that pri-miR-376b is exclusively edited by ADAR1 and accordingly, no change was detected in editing levels when ADAR2 was overexpressed.

Surprisingly however, editing of +55 site of pri-miR-376a2 and +48 site of pri-miR-376c was lesser in the presence of ADAR2 than in control cells. Similar to +49 site of pri-miR-376a1, the +55 site of pri-miR-376a2 is preferentially edited by ADAR1. It is still not clear which enzyme edits +48 site of pri-miR-376c. Both these sites remain

normally highly edited even in glioma cells (Table 3.3). The diminished editing levels in the presence of ADAR2 could potentially be due to the degradation of hyper-edited transcripts. Degradation of edited pri-miRNA transcripts has previously been reported for pri-miR-142 (Yang et al., 2006). Thus, although editing occurs to high levels, the RT-PCR product derived from cDNA pools contains an over-representation of unedited transcripts, as edited transcripts undergo degradation. Alternatively, the ectopic ADAR2 could compete with factors responsible for editing these sites in glioma cells, while itself being unable to carry out editing at these sites.

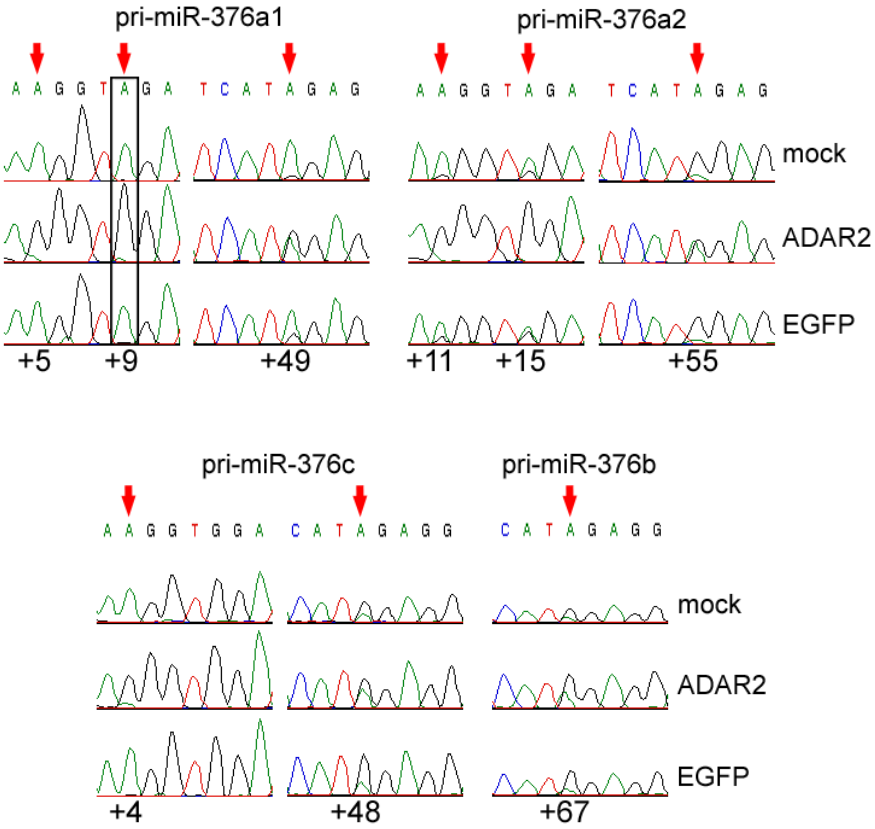

Figure 3.11 ADAR2 expression restores editing of pri-miR-376a1 in U87 cells. Direct sequencing of RT-PCR products of primary miRNAs from U87 cells overexpressing ADAR2. Expression vector encoding miR-376 cluster was co-transfected for higher expression of the editing substrates, the pri-miRNA transcripts. Editing sites are indicated by arrows, at which A-to-I editing is detected as black (G) trace. The 5' end of stem-loop sequence annotated in the Sanger miRBase site is counted as +1 and site corresponding to mature miR-376a*, +9 site of pri-miR-376a1-5p is boxed. EGFP transfection served as a control. In ADAR2 transfectants, note the presence or greater height of 'G' peak at editing sites in contrast to controls and absence of 'G' trace at non-editing 'A' sites.

Finally, the expression of mature miRNAs was measured under conditions of ADAR2 overexpression to confirm that editing of pri-miRNAs from miR-376 cluster does not impact their processing. It was confirmed that endogenous levels of mature miRNAs were similar to mock-transected and EGFP-transfected cells (Figure 3.12). Thus, editing by ADAR2 does not affect miRNA abundance but generates edited mature miRNAs.

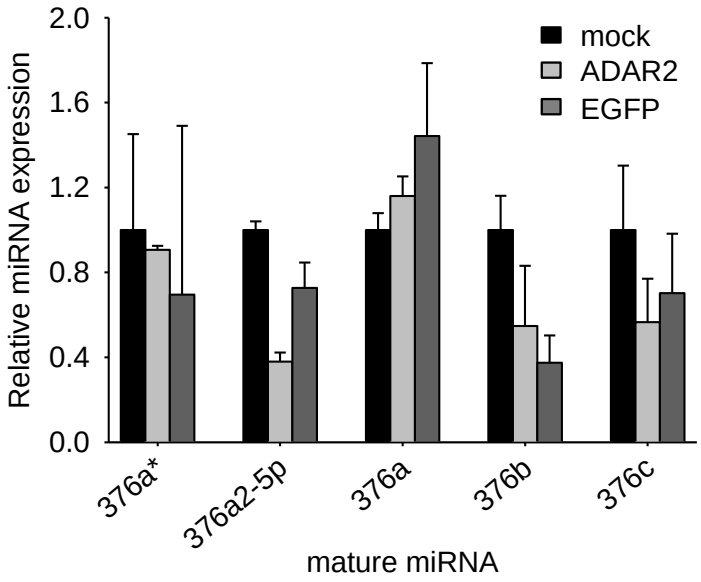

Figure 3.12 Abundance of mature miRNAs in ADAR2-transfected U87 cells. Endogenous mature miRNA levels were measured after transfection of ADAR2 expression plasmid in U87 cells. Untransfected and EGFP-transfected cells were used as controls. Measurement was done by qRT-PCR and values were normalized to 5S rRNA. Data represents mean ± SD.

3.8 Discussion

By direct sequencing of primary miRNAs from miR-376 cluster it was determined that A-to-I editing of sites in this cluster is altered in gliomas. From high-level editing in normal brain and astrocyte cells, editing was measurably reduced for several editing sites in high-grade gliomas and glioma cell lines. Processing of unedited primary transcripts therefore leads to an increased abundance of unedited mature miRNA at the expense of edited miRNA transcripts. In this chapter it was established that due to loss of editing of +9 site of pri-miR-376a1, miR-376a* harboured in this primary miRNA, displays a consistently negligible level of editing in most GBMs, accumulating entirely as unedited miR-376a*.

The seed sequences of all mature miRNAs from the miR-376 cluster are edited from 50-100% when studying the whole brain and to nearly 100% in astrocytes. The high-level editing is reminiscent of 100% recoding of the GluR-B receptor at Q/R site, the only site-selective editing substrate in the brain (among ion channels and neurotransmitter receptors) to undergo such extensive modification (Higuchi et al., 2000), implying an important role for A-to-I editing-mediated “recoding” of miR-376 cluster miRNAs in normal cells.

In agreement with previous findings made in a large cohort of gliomas (Paz et al., 2007), a widespread reduction in *ADAR1* and *ADAR2* mRNA levels in high-grade gliomas, especially GBMs, was uncovered. However, the results were contrary to findings in ten pediatric astrocytomas and limited panel of seven GBMs, where *ADAR2* mRNA levels were not changed (Cenci et al., 2008; Maas et al., 2001). This discrepancy is likely to be due to the difference in tumor types (GBMs vs. pediatric astrocytomas) or the limited number of samples examined in these previous studies. Interestingly, from miR-376 cluster in gliomas, the +9 site of pri-miR-376a1 (corresponding to mature miR-376a*) suffers disparately greater loss of editing than any other site. This is surprising as a common editing machinery, comprising ADAR1

and ADAR2, is responsible for editing all sites within the cluster. This outcome could possibly arise due to the differential sensitivity of each site to attenuated enzyme function, stemming from variable editing efficiencies of ADARs for different sites depending on RNA sequence and structure (Valente and Nishikura, 2005). Thus, despite limited ADAR amounts, sites such as +55 site of pri-miR-376a2 may still be highly edited in tumors, as it was observed through sequencing analysis. Additionally, the involvement of other factors that regulate ADAR activity for each site cannot be ruled out (Wahlstedt et al., 2009).

As the substrates of ADARs are numerous, ADAR dysfunction will undoubtedly have pleiotropic effects. Notably however, even the most well-studied target of A-to-I editing, the GluR-B subunit of the glutamate receptor, suffered a modest loss of editing from 100% to 69-88% in GBMs (Maas et al., 2001), in contrast to the nearly complete abolishment of editing for miR-376a* in GBMs, as reported here. The global effects of A-to-I editing loss in GBMs are speculated to manifest through a variety of substrates, each contributing to the disease phenotype, but the elucidation of these effects need be studied for each substrate individually in the relevant context. For example, overexpression of ADAR1 and ADAR2 in U87 and U118 glioma cell lines has been shown to suppress their proliferation rates (Cenci et al., 2008; Paz et al., 2007), but this can be ruled out as a consequence of restored editing of miRNAs from miR-376 cluster given their low endogenous expression in these cell lines.

miRNAs from miR-376 cluster have never before been implicated in gliomas. While a relative over-abundance of unedited miR-376a* (at the expense of edited miR-376a*) in glioma tissue compared to normal brain is uncovered in this study, this “differential” expression has not been detected using either microarray or qRT-PCR techniques in previous miRNA profiling studies in gliomas (Ciafre et al., 2005; Godlewski et al., 2008; Silber et al., 2008). This is attributable to the limited discriminatory power of PCR and microarray probes, which detect equally efficiently both the unedited and

edited forms of miR-376a*. This limitation was also observed in other studies reporting inability to discriminate miRNA sequence variants by Taqman miRNA qPCR assays (Christensen et al., 2010; Hoffman et al., 2009). As such, barring any change at the transcriptional or stability levels, which would affect overall abundance, many variant miRNA sequences will escape detection by traditional quantification methods. Importantly, precisely due to these limitations the conclusion could be drawn that the absolute amounts of miR-376a* are nearly unchanged in GBMs compared to normal brain (0.853-fold) as gathered from the analysis of TCGA miRNA data on GBMs. Therefore, the only component of miRNA function subject to change in context of altered A-to-I editing was the sequence of miR-376a*.

Previous efforts on uncovering miRNA-sequence based changes in cancers have included high-throughput sequencing methods, including next-generation sequencing, for detection of editing of mature miRNAs. In neuroblastomas (NBs), miR-376a and miR-376c were found be edited but no differential editing was found between NBs with favorable and unfavorable outcomes (Schulte et al., 2010). In a study in breast cancers comparing normal and carcinoma tissues (both invasive and in situ), the same two miRNAs had nucleotide variations at the edited sites but no difference in editing levels between normal and tumor tissue was reported (Farazi et al., 2011). In hepatitis B-related hepatocellular carcinomas, 31% and 50% of miR-376c was edited in the HCC and normal liver tissue respectively and for miR-376a, 86% was edited in HCC compared to 50% in normal tissue (Mizuguchi et al., 2011). Whether this is considered a significant difference in editing frequency and sequence composition was not discussed. The lack of substantial change to miRNA sequence by editing in non-CNS tumors suggests that ADAR function is largely maintained in these tumors.

For miR-376a*, a glioma-type dependent suppression of editing was observed. For grade III oligoastrocytomas (OAO) and oligodendrogliomas (OAG), and exceptionally for two variant GBMs (gliosarcomas) (Nicholas et al., 2011), relatively high editing

frequencies were detectable corresponding with relatively higher *ADAR2* mRNA levels (50% of normal brain). These results are partially in line with the finding that in mice with one functional *ADAR2* allele, 99% of Q/R site of GluR-B mRNA was still edited, suggesting sufficiency of ADAR enzyme activity even at 50% of normal ADAR quantities (Higuchi et al., 2000). OAGs and OAOs generally have better prognosis than AAs and GBMs (Louis, 2006); whether this is related to the presence of edited miR-376a* transcripts is an interesting question. From the tumor-type dependent editing pattern, a diagnostic value for glioma classification, and GBM subclassification, based on miR-376a* editing frequency is also conceivable. Due to limited availability of lower-grade patient gliomas (Grade II OAO, OAG, astrocytoma), it was not possible to investigate grade-wise changes in editing frequencies of miR-376 cluster. Nonetheless, overall editing levels are predicted to be higher in lower-grade tumors as supported by relatively higher ADAR activity and levels in these tumors compared to GBMs (Paz et al., 2007).

Changes in transcript editing levels due to ADAR dysfunction most likely play a role in progression rather than initiation of malignant growth, given that mouse models of ADAR dysfunction do not have increased cancer incidence (Farajollahi and Maas, 2010), The aggregation of unedited miR-376a*, initiated by loss of A-to-I editing in GBMs, may be one of the cumulative lesions conferring considerable malignant advantage during cancer progression, accounting for its exceptionally low editing levels in GBMs, compared to other editing substrates, including miRNAs from miR-376 cluster. Thus, based on the editing and expression analyses in gliomas, it can be concluded that unedited miR-376a* is GBM-specific miRNA sequence variant that accumulates in tumors due to aberrant A-to-I editing. This accumulation potentially presents malignant advantage to GBM cells during tumor progression.

4 CHAPTER 4. Regulation of growth and invasion of glioblastomas by miR-376a*

4.1 Introduction and aims

In the previous chapter it was established that A-to-I editing of miR-376a* is attenuated in glioblastomas (GBM), and this was associated with low expression of ADAR2 enzyme. As a result, the unedited miR-376a* aberrantly accumulates in GBMs. Furthermore, this effect was observed specifically in GBMs as grade III tumors (astrocytomas, oligoastrocytomas and oligodendrogliomas) retained significantly higher levels of editing of miR-376a*. The unedited miR-376a* seed sequence contains an 'A' at +3 position of the mature miRNA and hence differs from the normally occurring edited miR-376a* (in brain- astrocytes and potentially other cell types), which contains an 'I' at the same position (Figure 4.1). miRNAs are characterized by their ability to modulate multiple genes simulatenously and play crucial roles in several processes related to cancer development. A change to the miRNA sequence can disrupt or create target mRNA-miRNA interactions, and is predicted to cause widespread effects on gene regulation. The aim of this chapter was to understand if the aberrant accumulation of unedited miR-376a* has any functional significance related to GBM growth or invasion.

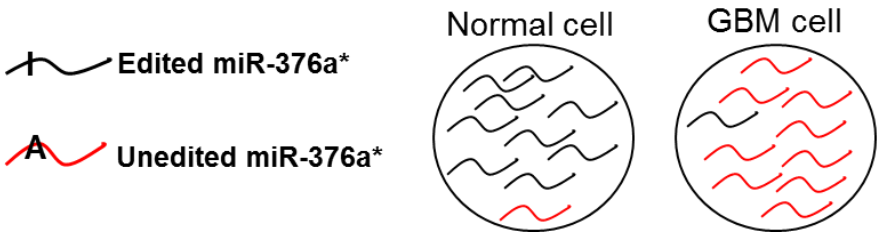

Figure 4.1 Accumulation of unedited miR-376a* in glioblastomas. Schematic representation of the differential expression of edited and unedited miR-376a* in normal cells and glioblastoma (GBM) cells, as a result of attenuated A-to-I editing in GBMs. A: adenosine in miRNA seed, I: inosine in miRNA seed.

While all high-grade gliomas (grade III and IV) are highly proliferative, GBMs are especially aggressive and are characterized by extensive invasiveness into surrounding normal tissues (Furnari et al., 2007). Studies have linked the expression of molecular markers related to invasion and angiogenesis, MMP2 and VEGF, specifically in GBMs (in contrast to AAs) in line with their highly invasive nature (Dreyfuss et al., 2009; Du et al., 2008; Mayes et al., 2006; Zhou et al., 2005). Importantly, based on transcriptional profiling of a cohort of high-grade gliomas linking tumor development to neuroglial development, grade III tumors (oligodendrogliomas and astrocytomas) were classified as 'proneural' which generally have a tendency towards longer survival (Phillips et al., 2006; Verhaak et al., 2010). On the other hand, primary GBMs are mostly classified as 'mesenchymal' with worse prognosis. These findings point to increasing aggressiveness of GBM tumors compared to grade III counterparts due to increased invasion, which can modulate other features such as angiogenesis. Therefore, given the GBM-specific accumulation of unedited miR-376a*, the nature of its involvement in regulation of GBM malignancy, was first investigated with regards to invasiveness.

4.2 Establishment of highly invasive glioma cell line

Although high-grade gliomas, especially GBMs, are highly invasive (Furnari et al., 2007), human glioma-derived cell lines, such as U87 cells, often lose this property over in vitro culture time, and form non-invasive tumors in vivo in orthotopic models (Gladson et al., 2010; Radaelli et al., 2009; Xie et al., 2008). Past efforts to develop more representative models for human GBMs have involved the selection/enrichment of invasive glioma cell population from non-invasive parental cell population.

Human GBMs xenografted subcutaneously are able to metastasize to the lung and liver (Huang et al., 1995). This observation alludes to the intrinsic metastatic potential of glioma cells. The experimental lung metastasis (ELM) assay can be used to enrich metastatic and invasive cells from cancer cells (Clark et al., 2000). This assay is

generally used to study the metastatic ability of cancer cells and involves the injection of cells into the tail-vein of immunodeficient mice. A small proportion of the injected cells are able to survive in circulation and over a period of time, are able to form lung metastases, from which the metastatic cell sub-population can be isolated. The ELM assay was first applied by Xie et al to enrich metastatic glioma cells from parental U87 cells (Xie et al., 2008). The metastatic sub-population glioma cells displayed greater invasiveness and aggressive tumor growth upon orthotopic injection (Xie et al., 2008). Therefore in this study, to enrich highly invasive cells from U87 glioma cell line, an in vivo ELM assay was performed by injecting U87 cells through the tail vein and selecting metastatic cell populations from the lung, followed by expanding them in vitro (Clark et al., 2000; Xie et al., 2008). The strategy and time-lines of this assay are summarized in Figure 4.2A. Three independent ELM lines were established. The morphology of ELM derived cells was distinct from the parental U87 cells and exhibited different degrees of adherence to the culture dishes. In general, whereas parental U87 were spindle-shaped, ELM cells were flatter (Figure 4.2B). The established ELM cell lines were characterized for invasive properties and miRNA editing analsysis was subsequently carried out.

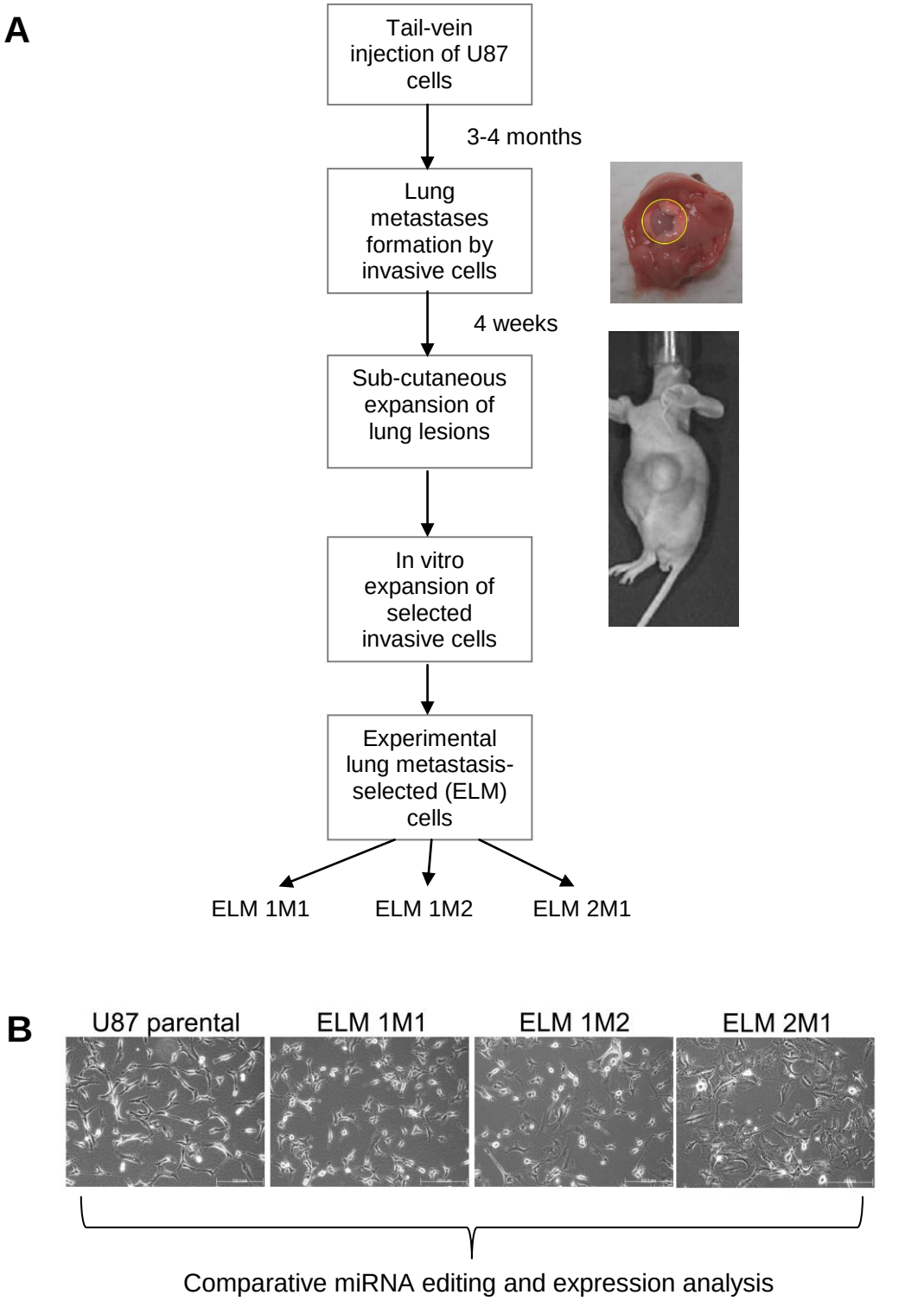

Figure 4.2 Selection of invasive glioma cells using experimental lung metastasis assay. ***A.*** Schematic of the ELM assay applied to enrich a population of highly invasive cells from U87 parental cells. Three independent ELM lines were established and named ELM 1M1, ELM 1M2 and ELM 2M1. Details of this procedure are described in Materials and Methods section. ***B.*** Comparison of morphology of U87 cells and the ELM-derived cells ELM 1M1, ELM 1M2 and ELM 2M1. miRNA editing and expression analysis was carried out.

Next, ELM cells were injected intracranially into nude mice brain to assess orthotopic tumor formation. Histological analysis of tumors formed 21 days after glioma cell injection was done by H&E staining (Figure 4.3A). In agreement with previous studies, tumors formed by parental U87 cells appeared well-circumscribed, non-invasive and were confined near the injection site (Piao et al., 2009; Radaelli et al., 2009). In contrast, ELM 1M1 cells formed multiple tumors, including in the left hemisphere, despite single site of injection in the right striatum. ELM 2M1 cells formed large aggressive tumors which extended along multiple fronts to form highly non-uniform tumor mass with extensive vascularization (Figure 4.3A). At higher magnification, it was observed that the boundary of the U87 tumor was well-delineated from the normal brain tissue and lacked infiltrative projections (Figure 4.3B). On the other hand for ELM 1M1 cells, invasive cell foci were observable separate from the main tumor mass (black arrowheads, Figure 4.B). Necrosis and pseudopalisading glioma cells were present in ELM 2M1 tumors. This suggested that ELM-selected U87 cells are able to form more aggressive tumors with several features of GBMs such as invasion, necrosis and angiogenesis.

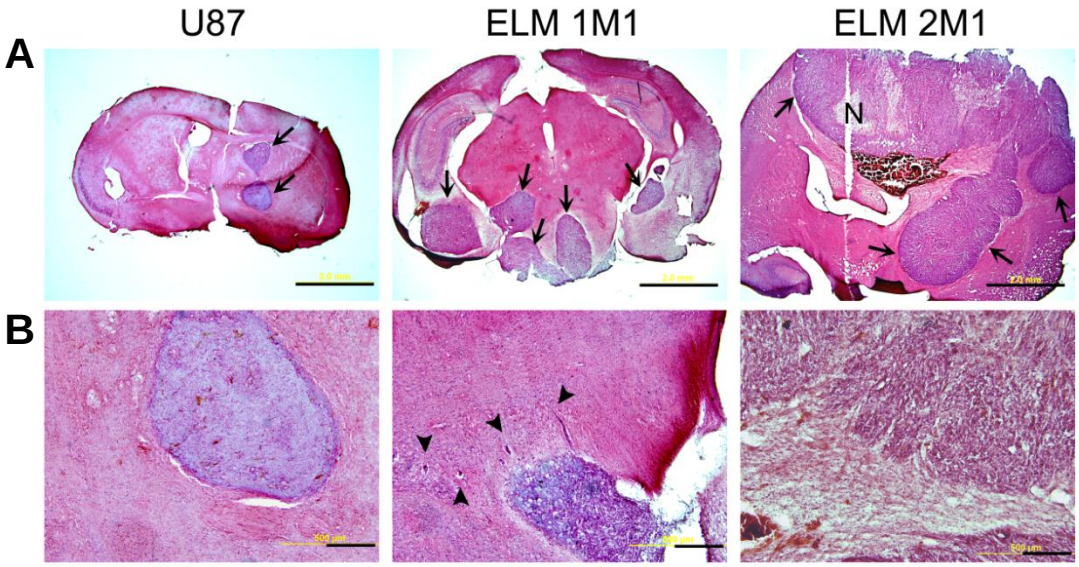

Figure 4.3 In vivo tumor formation by U87 and ELM cells. H&E staining of tumors formed at day 21 after brain inoculation of U87 cells, ELM 1M1 and ELM 2M1. Cells were injected in the right striatum. ***A.*** Whole brain section showing aggressive tumor growth for ELM cells. Arrows indicate the tumor region after H&E staining. N: necrosis Scale bar = 2 mm. ***B.*** H&E-stained tumor sections shown at higher magnification, highlighting disseminated tumors (black arrowheads) for ELM 1M1 and pseudopalisading glioma cells at necrotic region for ELM 2M1. Scale bar: 250 µm.

The cellular property selected for through the ELM assay is invasion, suggesting that the differences in orthotopic tumor formation between parental U87 and ELM cells could be due to changes to the invasive capacity of the tumor cells. Matrigel invasion assay was carried out to assess invasiveness of ELM cells in vitro. Both ELM 1M1 and 2M1 cells displayed a significantly greater invasive capacity compared to U87 cells (Figure 4.4A)**.** ELM 2M1 cells had a 2-fold greater (p=0.0002) invasive capacity and ELM 1M1 cells were 1.5-fold more invasive (p=0.0076) compared to parental U87 cells. Interestingly, the difference in degree of invasion between ELM 1M1 and ELM 2M1 cells was also significant (p=0.013).

Additionally, wound healing scratch assay confirmed the highly migratory nature of ELM cells. Compared to U87 cells, both ELM 1M1 and ELM 2M1 migrated significantly faster, covering a greater distance of the wound gap in 24 hours (p=0.002 for 2M1 and p=0.013 for 1M1) (Figure 4.4B). ELM 2M1 cells were in fact

more migratory than ELM 1M1 cells (p=0.004), paralleling the observations made in the matrigel invasion assay.

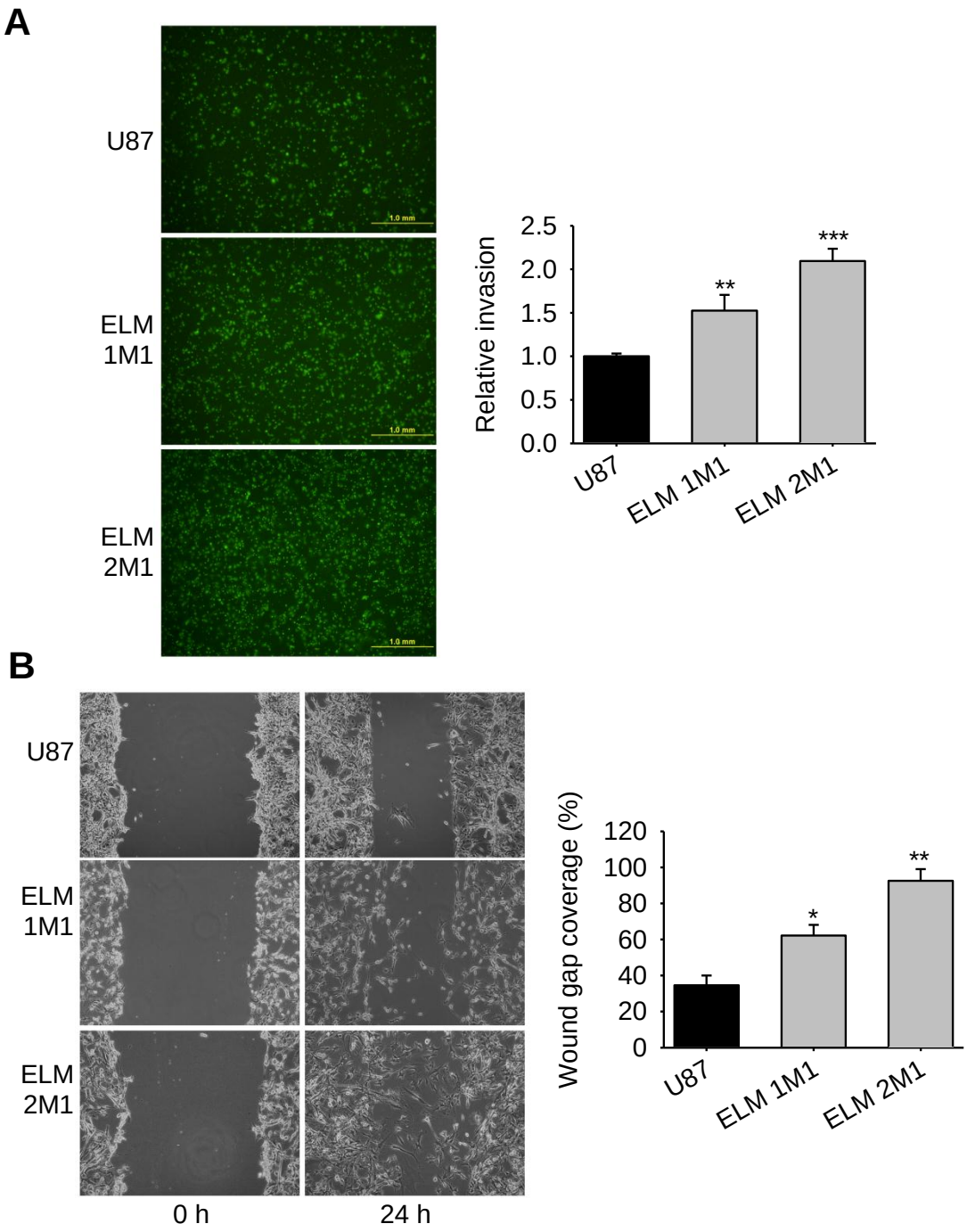

Figure 4.4 Increased in vitro invasion and migration of ELM cells. ***A.*** Matrigel invasion assay of parental U87, ELM 1M1 and ELM 2M1 cells. Photomicrographs showing Calcein-AM labeled cells that invaded through matrigel-coated inserts. Graph shows the number of invading cells quantified by fluorescence relative to U87 cells. ***B.*** Wound healing assay showing increased migration ability of ELM 1M1 and 2M1 compared to parental U87 cells. Images were taken at indicated time-points and wound gap closure was assessed, for which representative images are shown. Graph shows the quantification of percentage wound gap closure (relative to t=0h) at end-point of observation. Data are presented as mean ± SD. *p<0.05, **p<0.01, ***p<0.001 by t-test vs. U87.

Interestingly, in vitro proliferation rates of ELM cells in serum-containing media was several-fold lower than U87 cells (Figure 4.5), in agreement with the inverse correlation between glioma cell proliferation and motility (Giese et al., 2003; McDonough et al., 1998; Molina et al., 2010). Together the in vivo and in vitro assessment supports that ELM selection is effective in enriching glioma cells that are more migratory and invasive.

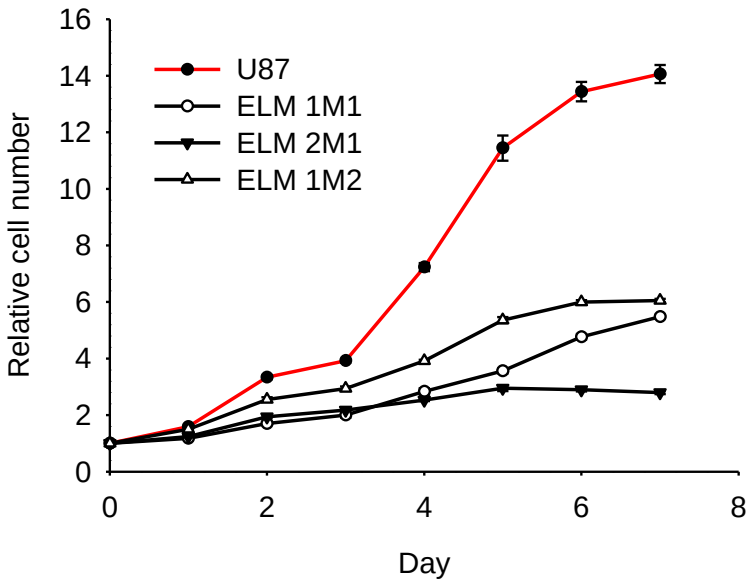

Figure 4.5 Reduced in vitro proliferation rates of ELM cells. In vitro growth curves for parental U87 and ELM cells. For each cohort, number of cells in five wells was counted for 7 days as indicated and plotted relative to cell number on day 0. Data are presented as mean ± SD.

4.3 Editing analysis of miR-376 cluster in ELM cells

To investigate if extent of A-to-I editing of miRNAs from the miR-376 cluster, especially miR-376a*, correlate with tumor cell invasiveness, editing analysis of pri-miRNAs from miR-376 cluster was performed for ELM-selected U87 cells. By direct sequencing of pri-miRNAs it was determined that overall editing levels for all sites within miR-376 cluster in 3 ELM cell lines were similar to U87 cells (Figure 4.6A). Negligible 'G' trace at +9 site of pri-miR-376a1, confirmed that miR-376a* remained unedited in ELM cells, as in parental U87 cells. Similar ratio of 'G' peak heights to 'A' and 'G' peaks at editing sites were observed for all sites, the quantification for which is presented in Figure 4.6B. Furthermore, the mRNA levels of editing enzymes, *ADAR1* and *ADAR2,* in ELM cells did not differ significantly from that in U87 cells (Figure 4.6C), accounting for the lack of any significant changes to overall A-to-I editing in ELMs cells. Specifically, *ADAR2* which is responsible for editing of +9 site of pri-miR-376a1, corresponding to miR-376a*, remained unchanged between U87 cells and 3 independent ELM cell lines.

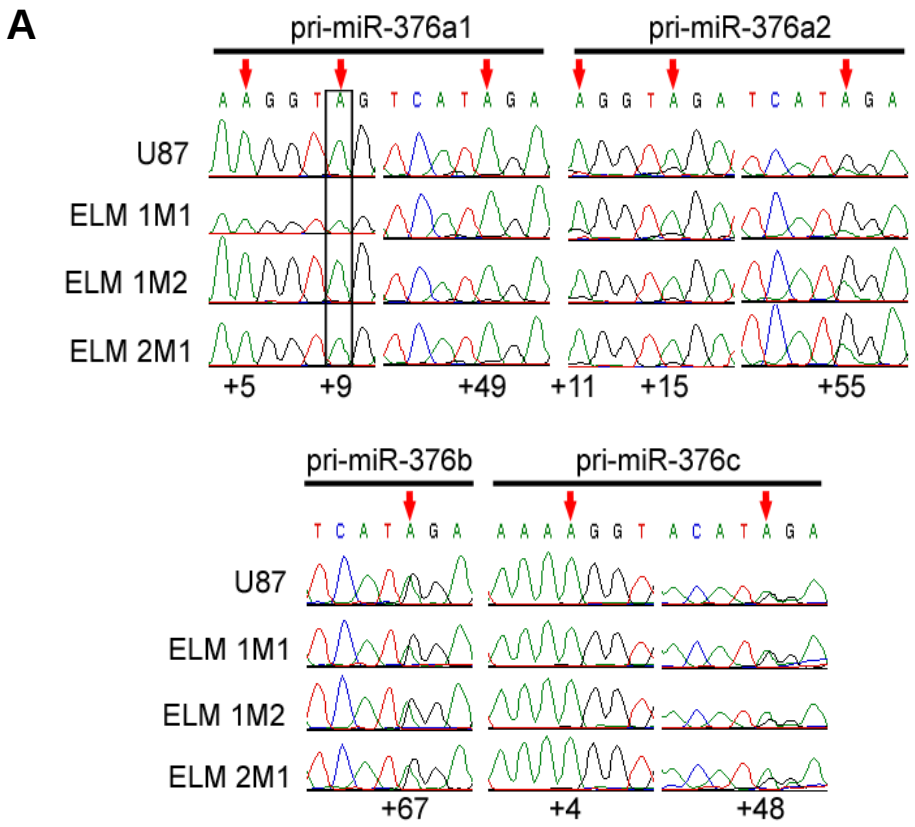

B

Cell line	Frequency of Editing (%)								
	pri-miR-376a1			pri-miR-376a2			pri-miR-376b	pri-miR-376c	
	site +5	+9 ‡	+49	+11	+15	+55	+67	+4	+48
U87	1.61	3.6	4.69	11.23	14.62	75.74	52.61	0.96	42.69
ELM 1M1	1.68	5.82	5.02	20.5	19.82	78.55	61.72	1.02	42.78
ELM 1M2	2.11	3.89	7.02	14.91	13.89	69	55.75	3.95	30.69
ELM 2M1	2.28	2.85	7.31	10.54	15.93	74.66	56.14	1.7	36.73

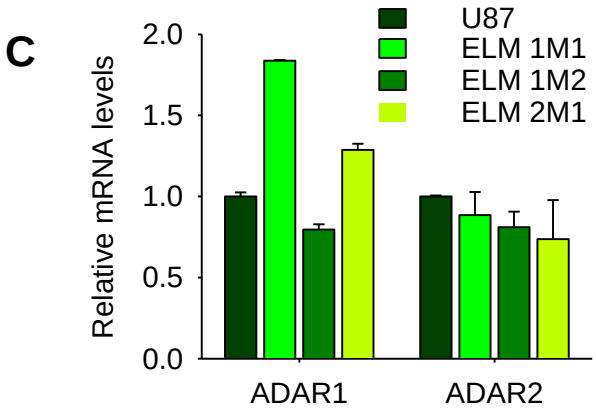

Figure 4.6 Editing analysis of pri-miRNAs from miR-376 cluster in ELM cells. *A.* Chromatograms of direct sequencing of RT-PCR products from parental U87 and three ELM cell lines. All editing sites are highlighted by arrows. For each pri-miRNA, the 5' end of stem-loop sequence annotated in the Sanger miRBase site is counted as +1 and +9 site of pri-miR-376a1 corresponding to miR-376a* is boxed. ***B.*** Quantification of editing frequencies of pri-miRNAs. Editing frequency is calculated as the % ratio of 'G' peak over the sum of 'A' and 'G' peaks for the editing site. ‡ Editing site corresponding to miR-376a* ***C.*** Relative mRNA levels of editing enzymes, *ADAR1* and *ADAR2*, in parental U87 and ELM cells measured by qRT-PCR. All values were normalized to 18S rRNA.

4.4 Unedited miR-376a* accumulates in invasive glioma cells

Although editing levels were unchanged for miR-376 cluster in ELM cells, the expression of miRNAs from this cluster could potentially be related to the invasiveness of the cells. Therefore, the expression of pri-miRNAs and mature miRNAs from miR-376 cluster was measured in ELM cells to assess changes in transcript abundance. Transcripts corresponding to pri-miR-376a1, 376a2, 376b and 376c were amplified by RT-PCR and expression was compared between parental U87 and ELM cells. All pri-miRNAs were moderately but not consistently increased in ELM cells (Figure 4.7A). Quantification of pri-miR-376a1 showed that it was increased 1.5 to 1.8-fold in ELM cells and the other pri-miRNAs were variably increased between 1.5 to 4-fold (Figure 4.7B).

Significantly, when mature miRNA levels were quantified by qRT-PCR, miR-376a* was found to be enriched 7-fold in ELM 1M1 and 1M2 cells and was increased 75-fold in ELM 2M1 cells (Figure 4.7C). Surprisingly, none of the other mature miRNAs from miR-376 cluster, which are co-transcribed with miR-376a*, were significantly enriched in ELM cells (Figure 4.7C). Furthermore, the fold-increase of miR-376a* correlated with the increase in invasion and migration capacity of ELM 1M1 and 1M2 cells, determined earlier (Figure 4.4). Also, the relative expression of selected miRNAs from chromosome 14q32.31 miRNA locus (where miR-376 cluster lies), those ubiquitously expressed (miR-16) and those with known functions in gliomas (miR-21, miR-221, miR-10b, miR-206), did not show significant changes in ELM cells (Figure 4.7C). Given that editing of miR-376a* does not change in ELM cells and it remains unedited, the miRNA expression data indicates that it is the unedited miR-376a* that is significantly increased in ELM cells. Collectively, this study suggests a mechanism for highly specific enrichment of unedited miR-376a* in invasive glioma cells.

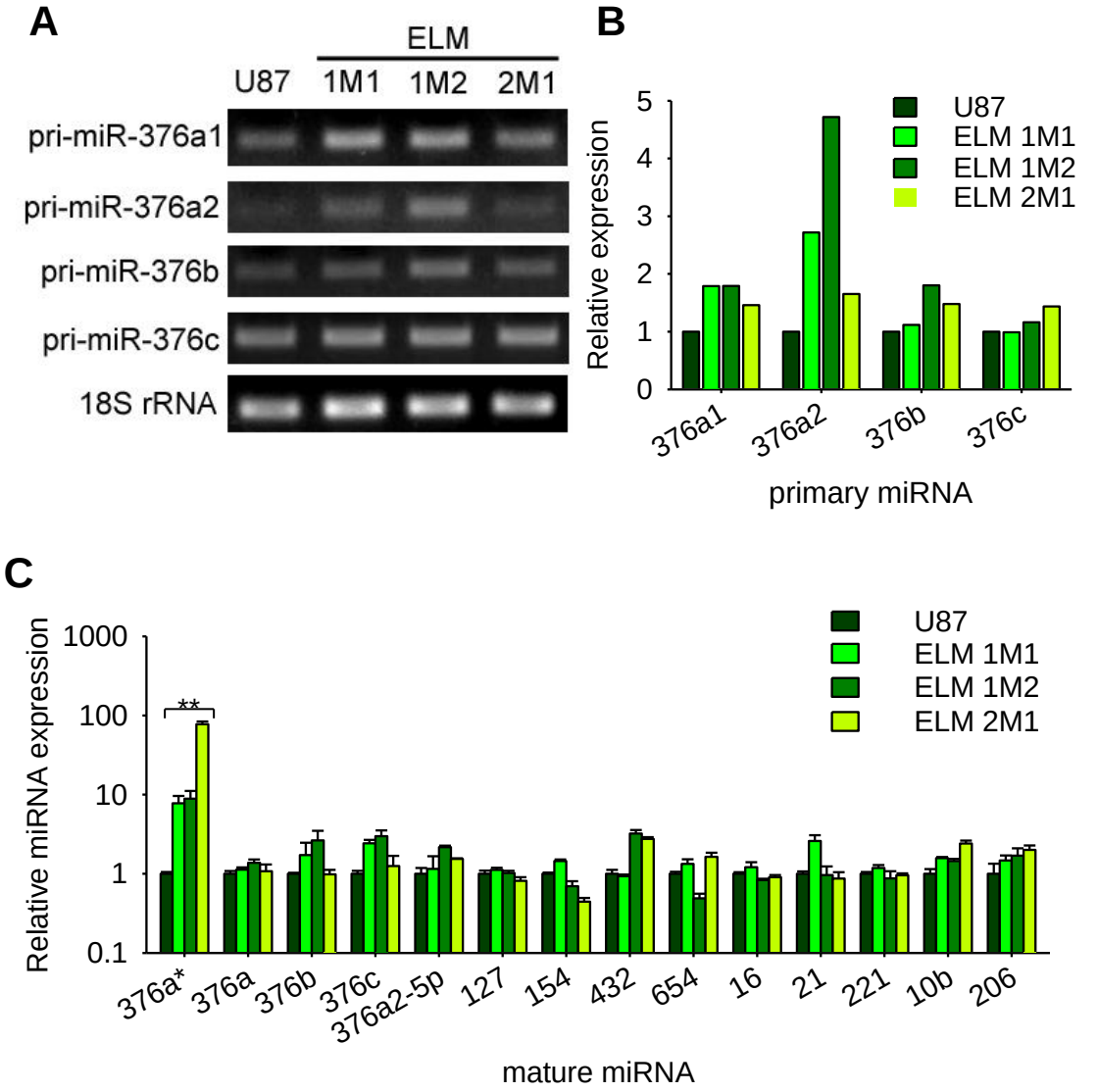

Figure 4.7 Expression of miR-376 cluster members in ELM cells. ***A.*** RT-PCR analysis of transcripts corresponding to indicated primary miRNAs from miR-376 cluster in U87 and ELM cells. ***B.*** Semi-quantitative expression analysis of RT-PCR products of pri-miRNAs from ***A.***. Densitometric analysis was done using ImageJ and values were normalized to 18S rRNA.***C.*** Relative abundance of various mature miRNAs in U87 and ELM cells measured by qRT-PCR. miR-376a*, 376a, 376b, 376c and 376a2-5p are from miR-376 cluster. miR-127, 154, 432, 654 are from chromosome 14q32.31 miRNA cluster- the larger cluster of miRNAs including miR-376 sub-cluster. miR-16 is ubiquitously expressed in several cell types. miR-21, 221, 10b, 206 are implicated in gliomas. Expression was normalized to 5S rRNA. Data represents mean ± SD. **p<0.01 by t-test for ELM 1M1, 1M2 vs. U87 and p<0.001 for ELM 2M1 vs. U87.

It was surprising to note that among mature miR-376 miRNAs, only miR-376a* was specifically up-regulated, especially considering that miR-376a is processed from the same pri-miRNA as miR-376a*(pri-miR-376a1) and together they constitute a mature miRNA duplex. As such, it is expected that miR-376a would be similarly affected by regulatory processes affecting miR-376a*. In U87 cells, the absolute abundance of miR-376a is several-fold higher than that of miR-376a* as evidenced by its significantly lower threshold detection cycle (Ct) during qRT-PCR compared to Ct of miR-376a* (Figure 4.8). A more negative delta Ct indicates lower miRNA abundance. During selection of ELM cells, delta Ct of miR-376a* becomes less negative (as it becomes more abundant) but that of miR-376a remains unchanged. The relative ratios of miR-376a* to miR-376a increases in ELM cells as the difference in their delta Cts becomes smaller (Figure 4.8), approaching that of normal astrocytes which have the highest expression of both miRNAs and also nearly similar expression levels of miR-376a* and miR-376a (although miR-376a* is nearly 100% edited in normal astrocytes). As miR-376a* and miR-376a are processed from the same precursor and the expression of pri-miR-376a1 is changed only 1-5-1.8-fold in ELM cells, this suggests that the miR-376a* expression increases in ELM cells due to increased stability of the mature miRNA, while there is no change in stability of miR-376a strand. Together, this suggests a highly-specific stabilizing mechanism for enrichment of miR-376a* during the selection of ELM cells, independent of transcription of the long miR-376 cluster or its own primary transcript, pri-miR-376a1. Cumulatively, editing and expression analyses show that abundance of unedited miR-376a* is increased in invasive ELM cells. Although by a distinct mechanism, this increase in unedited miR-376a* expression parallels the accumulation of unedited miR-376a* in primary human GBMs due to attenuated A-to-I editing.

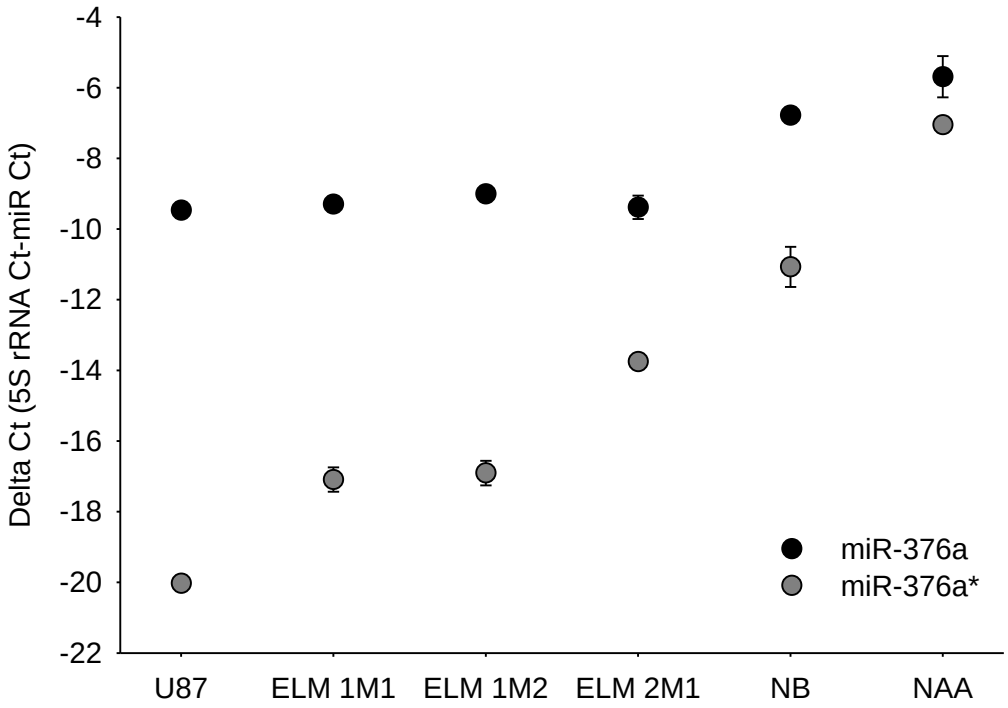

Figure 4.8 Relative abundance of mature miR-376a and miR-376a* in normal and glioma cells. qRT-PCR quantification of miRNAs in U87 and ELM cells. Delta Ct represents the difference between the threshold detection cycle (Ct) of 5S rRNA (endogenous normalization control) and Ct of miRNA. A less negative delta Ct value indicates higher abundance. All miRNAs are expressed at lower abundance than 5S rRNA. The accumulation of miR-376a* in ELM cells is indicated by the increasing delta Ct values. There is no change in the abundance of miR-376a in ELM cells compared to parental U87 cells. Normal astrocytes (NAA) have higher delta Ct for both miR-376a* and miR-376a and also the most similar expression for the two miRNAs. NB: normal brain. Data represents mean ± SD.

4.5 Unedited miR-376a* promotes glioma cell invasion and migration in vitro

The specific accumulation of unedited miR-376a* in high-grade invasive GBMs and in selected invasive glioma cells, suggested that this miRNA may modulate the invasive behaviour of glioma cells. As glioma cell lines have low endogenous levels of either variant of miR-376a*, ectopic expression of miRNAs in glioma cells was first employed to study its cellular effects. The pri-miR-376a1 encodes two mature miRNAs: miR-376a* and miR-376a (Figure 4.9A). Although both undergo editing in the brain, editing of miR-376a is negligibly altered in GBMs and thus unlikely to be of functional significance in this context. To delineate the function of miR-376a* in GBMs, the native precursor-based expression could not be used as both mature miRNAs would be processed from this precursor.

Hence, synthesized miRNA mimics were employed. In the miR-376a* mimic duplex, the passenger strand is not equivalent to miR-376a and will not act as miR-376a. Cellularly, editing of miR-376a* substitutes a single adenosine (A) for inosine (I), and previous works have shown equivalency of inosine and guanosine (G) in preferential base-pairing with cytosine (Borchert et al., 2009; Maas, 2010). Mimics for miR-376a* in the unedited form, hereafter “miR-376a*A”, and in edited forms, hereafter “miR-376a*G” and “miR-376a*I” were designed (Figure 4.9B). For stable expression of miR-376a*, a stem-loop construct was engineered such that the passenger strand of the processed duplex is not equivalent to miR-376a, and was incorporated downstream of EGFP reporter which is polycistronally expressed (Figure 4.9C). In this construct, at the appropriate position “A” or “G” was substituted so that the processed mature miRNA is miR-376a*A or miR-376a*G, respectively. As it is not possible to encode the incorporation of inosine in DNA, for stable expression of edited miR-376a* it was technically possible to express only the G-form of miR-376a*,

i.e. miR-376a*G using plasmid-based expression. For overexpression experiments, a miRNA mimic corresponding to *C. elegans* miRNA, cel-miR-293b was used as a control. The corresponding control mature miRNA sequence was incorporated into the stem-loop construct described in Figure 4.9C for stable expression of control miRNA. Expression of miR-376a* in glioma cells by miRNA mimics and in cells stably expressing miR-376a* was verified by qRT-PCR (Figure 4.9D and E).

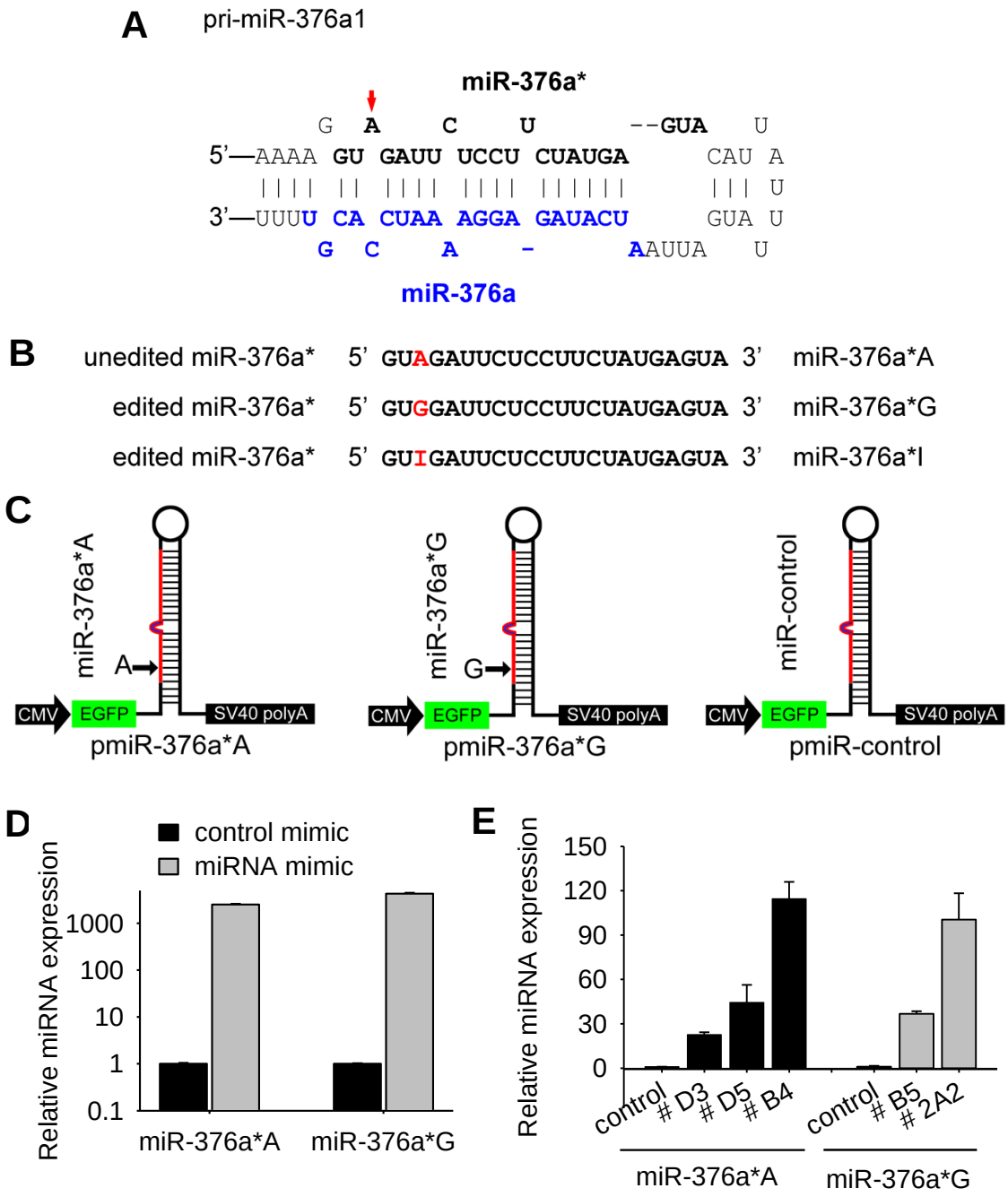

Figure 4.9 Strategy for ectopic expression of miR-376a*. *A.* Schematic diagram of stem-loop of precursor-miR-376a1. miR-376a* is highlighted in black bold and the site undergoing A-to-I editing is indicated by red arrow. miR-376a is highlighted in blue. ***B.*** Three versions of miR-376a* miRNA mimics used in subsequent experiments are indicated with A, G or I at the site of editing. ***C.*** Schematic of design of stem-loop constructs for stable expression of 376a*A, miR-376a*G and miR-control (cel-miR-293b). The position of mature miRNA in the engineered precursor is shown in red. For prmiR-376a* the opposing precursor arm does not encode miR-376a. Constructs were used to generate U87 cells stably expressing miR-376a* or control mIRNA. ***D.*** Confirmation of expression of miR-376a*A or miR-376a*G in U87 cells transiently transfected with 10 nM miRNA mimics. Measurement was done by qRT-PCR using forward primers corresponding to A- or G- version of miR-376a*. Results are displayed on the same scale for miR-376a*A and miR-376a*G. U87 cells transfected with control miRNA serve as baseline of expression of miR-376a*. ***E.*** Expression of miR-376a*A or miR-376a*G in stably transfected U87 cell lines. Values are relative to miRNA expression in U87 cells stably transfected with control miRNA. For ***D.*** and ***E.*** expression was normalized to 5S rRNA. Data represents mean ± SD.

Upon transfection of different forms of miR-376a*, dramatic and distinct morphological changes in U87 and SW1783 glioma cells were observed. miR-376a*A caused cells to adopt a flatter morphology with a highly organized actin cytoskeleton, visualized by actin-FITC immunostaining (Figure 4.10A). In contrast, both miR-376a*G and miR-376a*I caused cells to become more spindle-shaped, retract membrane projections and lose actin cytoskeleton organization (Figure 4.10A). In terms of cell morphology, miR-376a*G and miR-376a*I were indistinguishable (Figure 4.10A). These changes were highly specific to the properties of miR-376a*A and miR-376a*G and not due to the mere presence of ‘G’ or ‘I’ in the seed sequence as other miRNAs, miR-376a and miR-376a2-5p which also undergo seed sequence editing, did not induce distinct morphological changes when transfected in U87 cells as unedited (with ‘A’ in seed sequence) or edited (with ‘G’ in seed sequence) miRNAs (Figure 4.10B). Flow cytometry was used to confirm these morphological changes in six glioma cell lines, as from the side-scatter profile of cells, changes to intracellular density and complexity (a measure of cytoskeletal organization) can be measured. The forward-scatter profile in flow cytometry indicates the size or volume of cells. Compared to control- transfected cells, an increase in side-scatter distribution was consistently seen for all miR-376a*A-transfected glioma cells whereas a decrease in side-scatter was seen for miR-376a*G-transfected cells, while the forward-scatter profiles remained unchanged (Figure 4.11). This shows that the morphological phenotypes induced by miR-376a*A and miR-376a*G are not restricted to U87 or SW1783 cells but are reproducible in a larger panel of glioma cell lines, suggesting a general effect of miR-376a* on the morphology of glioma cells.

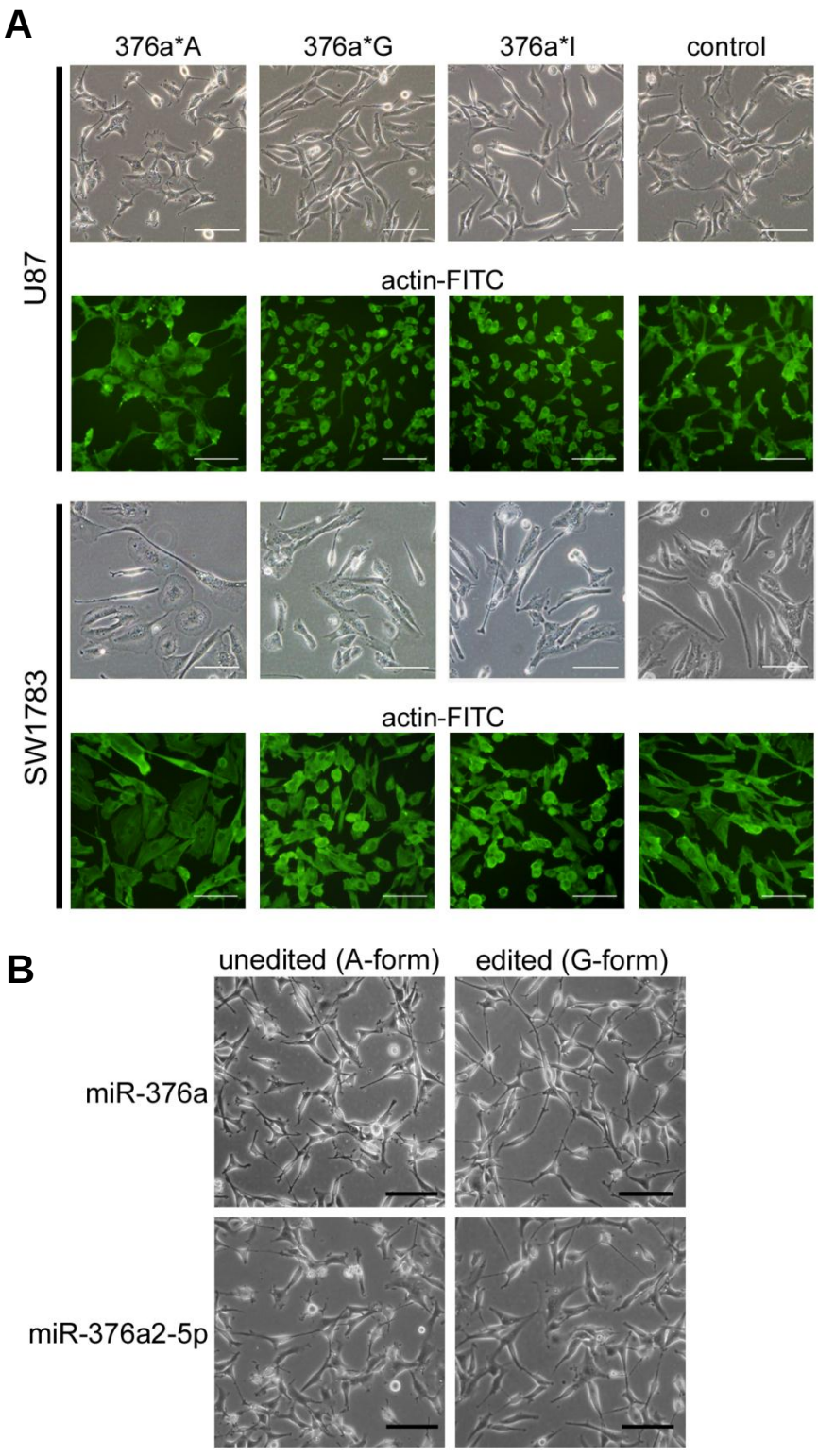

Figure 4.10 Morphological changes induced by miR-376a*. ***A.*** Morphology of U87 and SW1783 glioma cells transiently transfected with miRNA mimics corresponding to miR-376a*A/G/I or control miRNA. Actin-FITC labeling highlights the organized actin cytoskeleton in miR-376a*A transfected cells. Loss of cytoskeletal organization is observed in both miR-376a*G and miR-376a*I transfected cells. Scale bar = 60 µm. ***B.*** Morphology of U87 cells transfected with miR-376a or miR-376a2-5p with 'A' or 'G' in seed sequence, the unedited and edited forms respcectively. Scale bar = 100 µm.

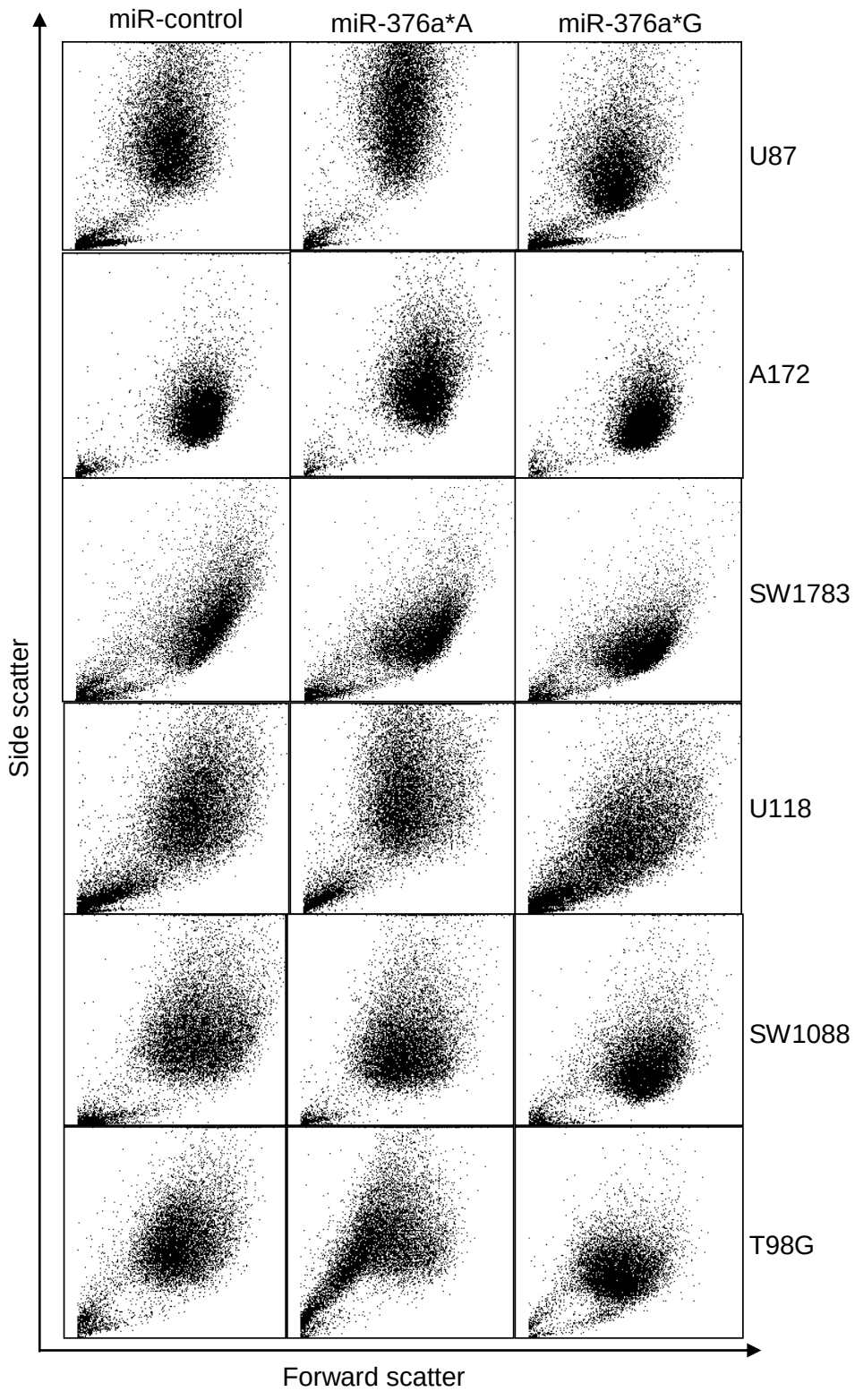

Figure 4.11 Characterization of morphology of transfected glioma cells by flow cytometry. Side scatter and forward scatter data was collected for six glioma cell lines. Note the opposite shifts in side scatter profiles for cells transfected with miR-376a*A and miR-376a*G. Side scatter is proportional to intracellular complexity and granularity while forward scatter is proportional to cell size.

Changes in cell morphology and actin cytoskeleton organization are well-documented to be intimately linked with migration of glioma cells (Bigarella et al., 2009; Chan et al., 2005a; Chandrasekar et al., 2003; Chintala et al., 1999). As migration is a prerequisite for cancer cell invasion, a matrigel invasion assay was used to assess the invasiveness of glioma cells ectopically expressing miR-376a*. Transient or stable ectopic expression of miR-376a*A significantly enhanced the invasiveness of three glioma cell lines by 1.5-1.8-fold (Figure 4.12). In contrast, under the same experimental conditions, miR-376a*G suppressed glioma cell invasion to below basal levels.

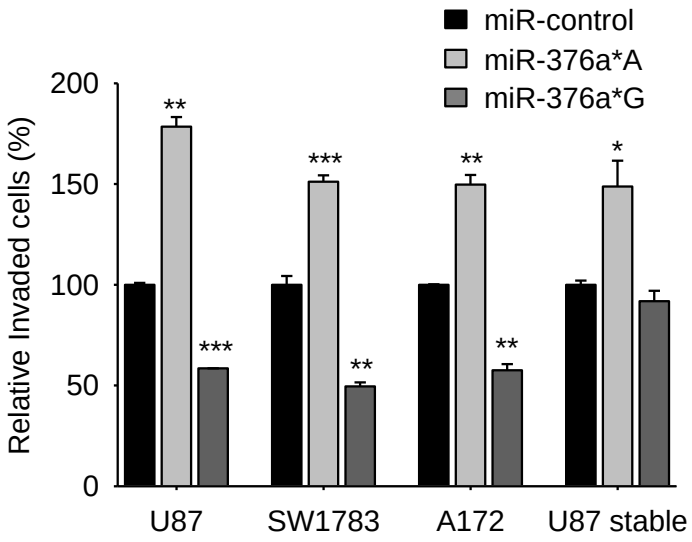

Figure 4.12 Modulation of glioma cell invasion by miR-376a*. Matrigel invasion assay of glioma cells transfected with miR-376a* or control miRNA. U87, SW1783 and A172 cells were transiently transfected with miRNA mimics. U87 stable cells represent U87 cells that stably express miR-376a*A or miR-376a*G. Number of seeded cells that invaded the matrigel were quantified by measurement of fluorescence of labeled cells. Values are normalized to control for each cell line. Data are presented as mean ± SD. *p<0.05, **p<0.01, ***p<0.001 by t-test relative to control.

Wound-healing assay was carried out to assess the effect of miR-376a* on cell migration. Similar to changes in the invasive capacity, miR-376a*A promoted the migration of glioma cells whereas miR-376a*G potently suppressed the ability to migrate (Figure 4.13).

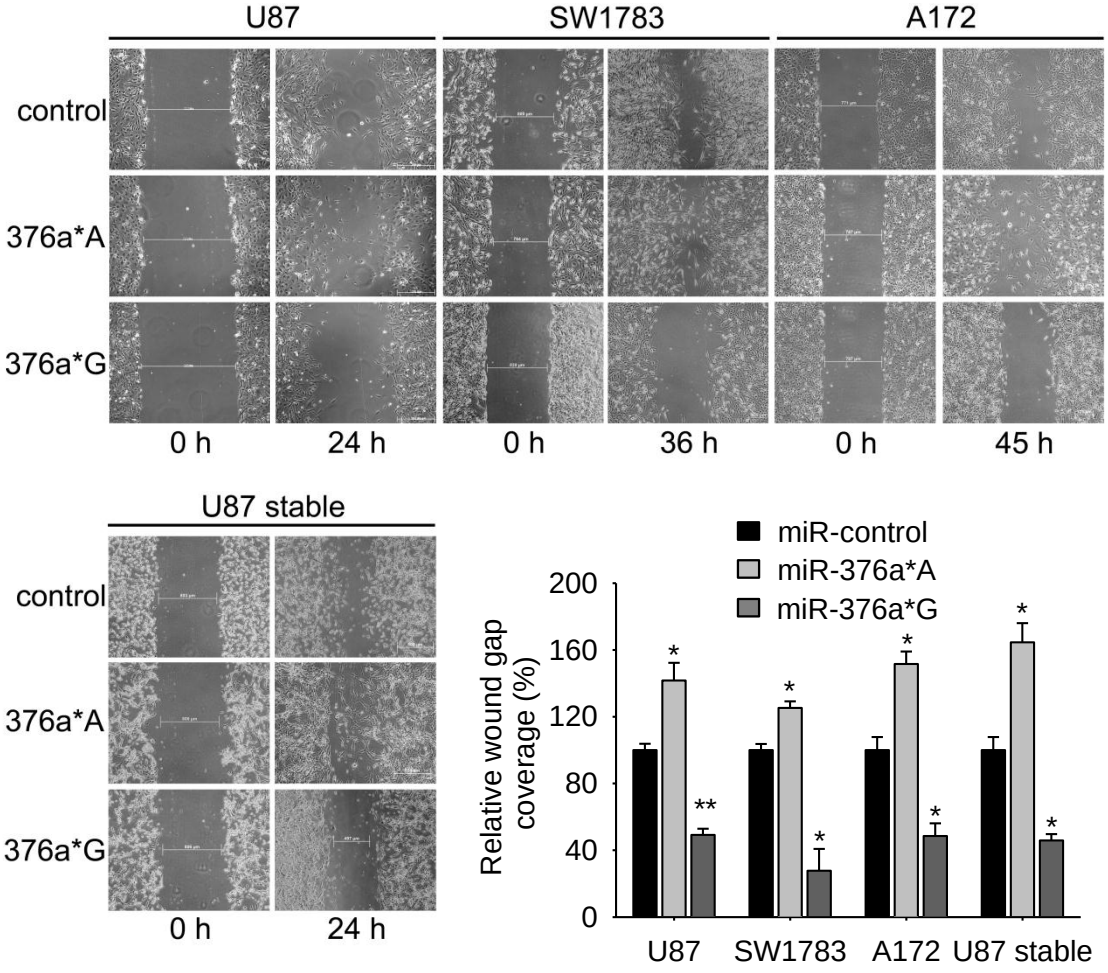

Figure 4.13 Modulation of glioma cell migration by miR-376a*. Wound-healing assay of glioma cells expressing miR-376a*. U87, SW1783 and A172 cells were transiently transfected with miRNA mimics. U87 stable cells represent U87 cells that stably express miR-376a*A or miR-376a*G. Scratches were made to confluent monolayers of transfected cells and photographs taken at indicated time-points. Graph shows the relative percentage wound gap closure (relative to t=0h) at end-point of observation. Data are presented as mean ± SD. *p<0.05, **p<0.01by t-test relative to control.

Additionally, when miR-376a*A was specifically knocked down in ELM 2M1 cells (which have the highest expression of miR-376a* among glioma cell lines) by transfecting lock-nucleic acid (LNA)-modified oligonucleotides against miR-376a*A (LNA-376a*A), their ability to migrate in a wound-healing assay was significantly abrogated, reversing their inherent highly migratory phenotype (Figure 4.14). This effect was confirmed to be not non-specific due to the introduction of LNA oligos, as LNA-376a*A did not affect motility of U87 cells, which have negligible expression of miR-376a* (Figure 4.14). Thus, the over-expression and knockdown experiments show that miR-376a*A has a pro-invasive and pro-migratory function in glioma cell in vitro.

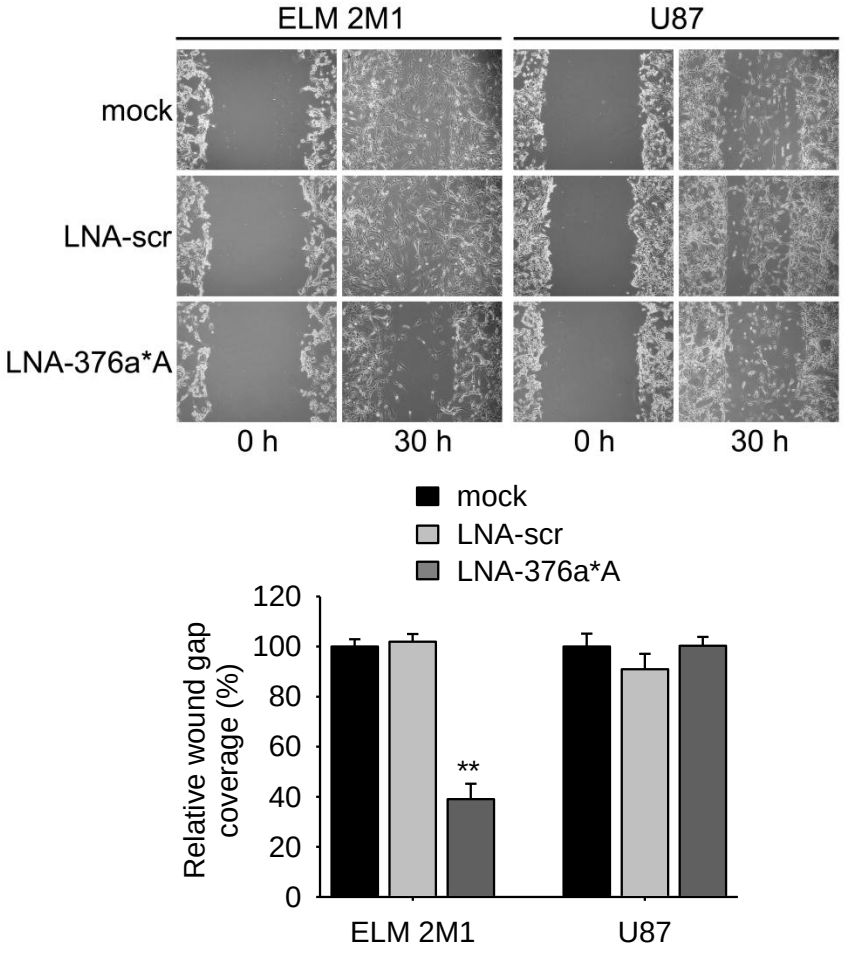

Figure 4.14 Knockdown of miR-376a*A suppresses migration of ELM cells. Wound healing migration assay of ELM 2M1 and U87 cells after LNA-mediated knockdown of miR-376a*A. scr, scrambled control. Graph shows the relative % wound gap coverage. Data are presented as mean ± SD, **p<0.01 by t-test.

4.6 Effects of miR-376a* on cell proliferation

The effects of miR-376a* on cell proliferation were investigated in order to assess if changes in proliferation contribute to the increased migration and invasion of glioma cells. By BrdU incorporation assay it was determined that miR-376a*A in fact suppressed proliferation rates of U87 and A172 glioma cells, while miR-376a*G exerted the opposite effect (Figure 4.15A), limiting the possibility that the observed increase or decrease in invasion or migration was due to a similar change in cell proliferation. Cell cycle analysis supported these effects on proliferation as miR-376a*A caused an accumulation of cells in the G1-phase of cell cycle, while miR-376a*G exerted the opposite effect on proliferation and caused a shift towards S and G2/M phases, suggestive of hastened cell cycle progression (Figure 4.15B). Collectively, these results suggest that miR-376a*A and 376a*G have distinct and opposing functions in glioma cells. Significantly, introduction of miR-376a*A in glioma cells, recapitulating the presence of unedited miR-376a* in GBMs, is able to promote their invasive behaviour.

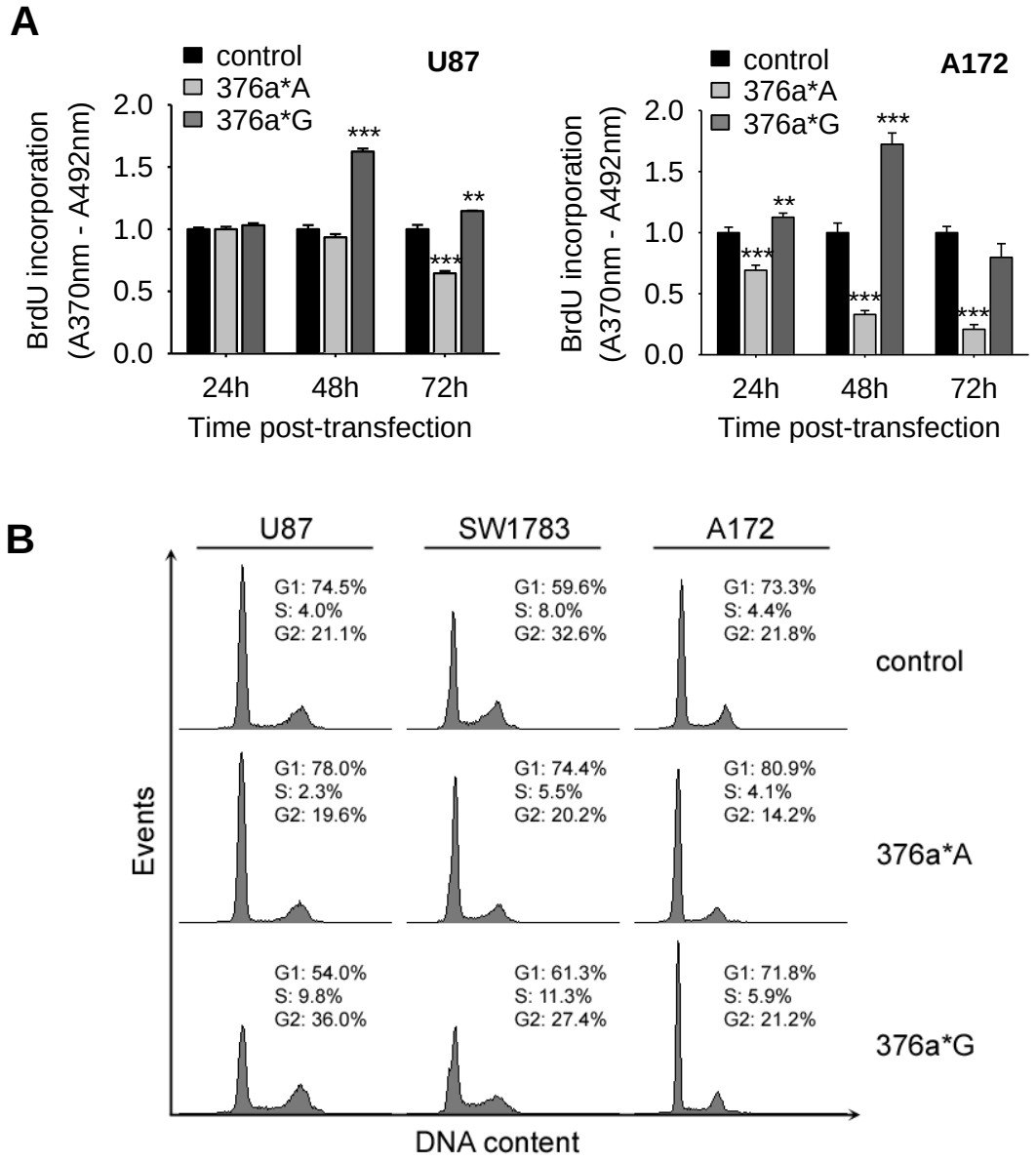

Figure 4.15 Effects of miR-376a* on cell proliferation. ***A.*** Measurement of cell proliferation of transiently transfected U87 and A172 glioma cells, using the BrdU incorporation assay. BrdU incorporation was measured at indicated time-points after transfection and five wells were used for each group. miR-376a*A decreases proliferation based on decreased BrdU incorporation (at 48 and 72 h), while miR-376a*G promotes proliferation (at 48 h). Data is shown relative to control cells at each time point and represents mean ± SD. **p<0.01 and ***p<0.001 by t-test relative to control. ***B.*** Flow cytometry of propidium iodide-stained cells to assess cell cycle distribution of transfected U87, SW1783 and A172 glioma cells. While miR-376a*A causes an increase in cells in G1 phase, miR-376a*G results in an increase in cells in S- and G2-phases.

4.7 Overexpression of unedited miR-376a* promotes aggressive growth of orthotopic gliomas

Having established that in vitro migration and invasion is regulated by miR-376a*, the potential for in vivo modulation of tumor growth by miR-376a* was investigated next. For this purpose, the orthotopic U87 cell glioma mouse model was employed as these cells are tumorigenic but non-invasive in the brain and would help address if unedited miR-376a* promotes tumor aggressiveness. U87 cells stably expressing miR-376a*A, hereafter U87/376a*A, or miR-376a*G, hereafter U87/376a*G or control miRNA were injected into the brains of nude mice. Measurement of in vitro proliferation rates of stable cell lines confirmed that U87/376a*A cells grew slower in vitro than control cells, while U87/376a*G cells were more proliferative similar to observations made for transiently transfected glioma cells (Figure 4.16A). At day 21 after tumor inoculation, brains were collected and sectioned for histological analysis.The formation of tumors U87/376a*A and U87/376a*G and the expression of miRNAs at this time-point was confirmed by fluorescent imaging of sections which showed tumors expressing abundant EGFP from the EGFP-miRNA polycistron (Figure 4.16B).

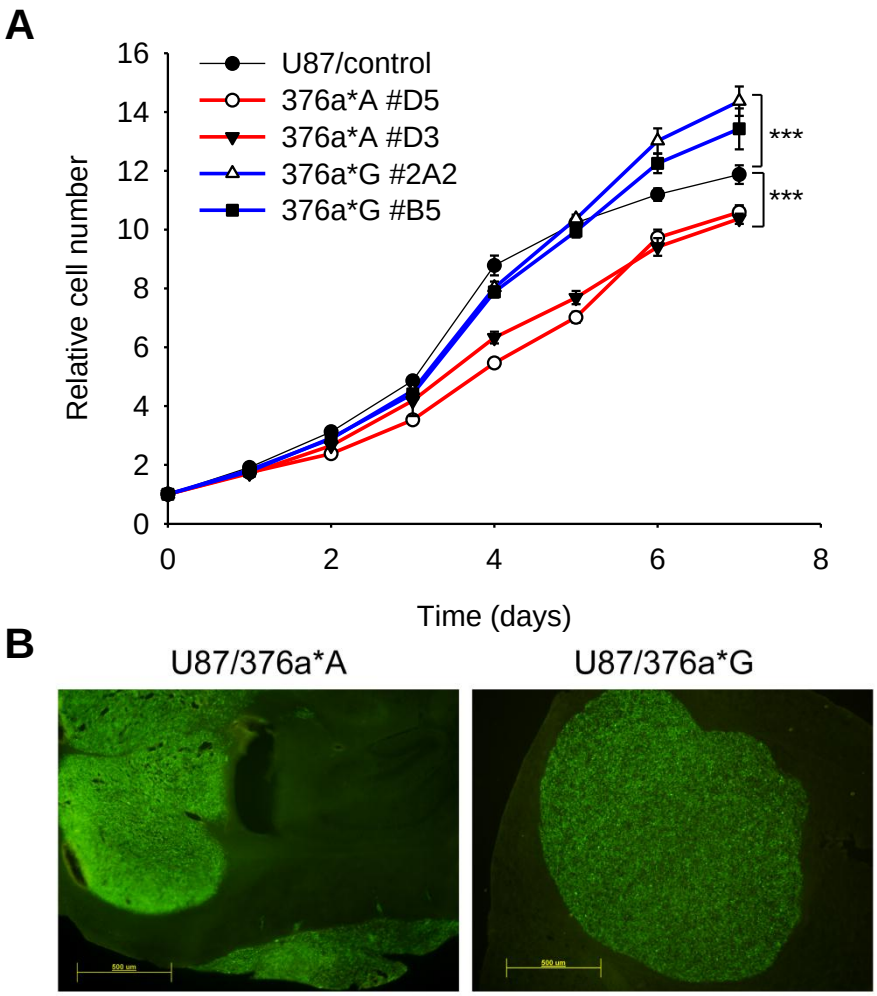

Figure 4.16 In vitro and in vivo growth of U87 cells expressing miR-376a*. *A.* In vitro growth curves of U87 cells stably transfected with miR-376a*A, miR-376a*G or control miRNA. Growth curves in red correspond to U87/376a*A stable clones, those in blue are for U87/376a*G stable clones and growth curve in black is for control U87 cells. For each cohort, number of cells in five wells was counted for 7 days as indicated and plotted relative to cell number on day 0. Data represents mean ± SD. ***p<0.001 by t-test compared to control U87 cells. ***B.*** Representative fluorescent images of sections from U87/376a*A or U87/376a*G tumors showing EGFP from EGFP-miRNA polycistronic expression cassette detectable at day 21 after orthotopic injection of stably transfected U87 cells.

Histological analysis of the tumors formed at day 21 after injection of U87/376a*A or U87/376a*G cells was done by H&E staining. U87/376a*A cells caused the formation of large aggressive tumors of irregular shape, with extensive intratumoral necrosis (Figure 4.17A(i)). In contrast, tumors formed by U87/376a*G cells were highly uniform and well-circumscribed, characteristic of expansile growth of non-invasive tumors like U87 tumors (Radaelli et al., 2009). Boundaries of U87/376a*A tumors were marked by infiltrative projections associated with vascular structures and satellite tumors, while U87/376a*G tumors were well-delineated from the normal brain (Figure 4.17A(ii)).

U87/376a*A tumors stained for Ki-67 proliferation marker showed high but non-uniform distribution of Ki-67+ cells which especially colonized regions around blood vessels (Figure 4.17A(iii)), indicating perivascular invasion (Winkler et al., 2009). A roughly two-fold enrichment of Ki-67 signal at the invasion fronts of U87/376a*A tumors in relation to the core was noted, while U87 and U87/376a*G tumors showed uniform distribution of Ki-67+ cells consistent with expansile growth (Figure 4.17B). As the in vitro proliferation rates of all stable cell lines were similar (Figure 4.16A), the aggressive tumor growth caused by U87/376a*A cells was not due to higher intrinsic proliferation, necessitating the involvement of the microenvironment such as angiogenesis for supporting this growth. In line with the ability of invasive glioma cells to induce vascular remodeling and angiogenesis (Nowacki and Kojder, 2001; Vajkoczy et al., 1999; Winkler et al., 2009), staining for von Willebrand factor (vWF), an angiogenesis marker, revealed the presence of abundant blood vessels in and surrounding U87/376a*A tumors, in contrast to U87/376a*G tumors (Figure 4.17A(iv)).

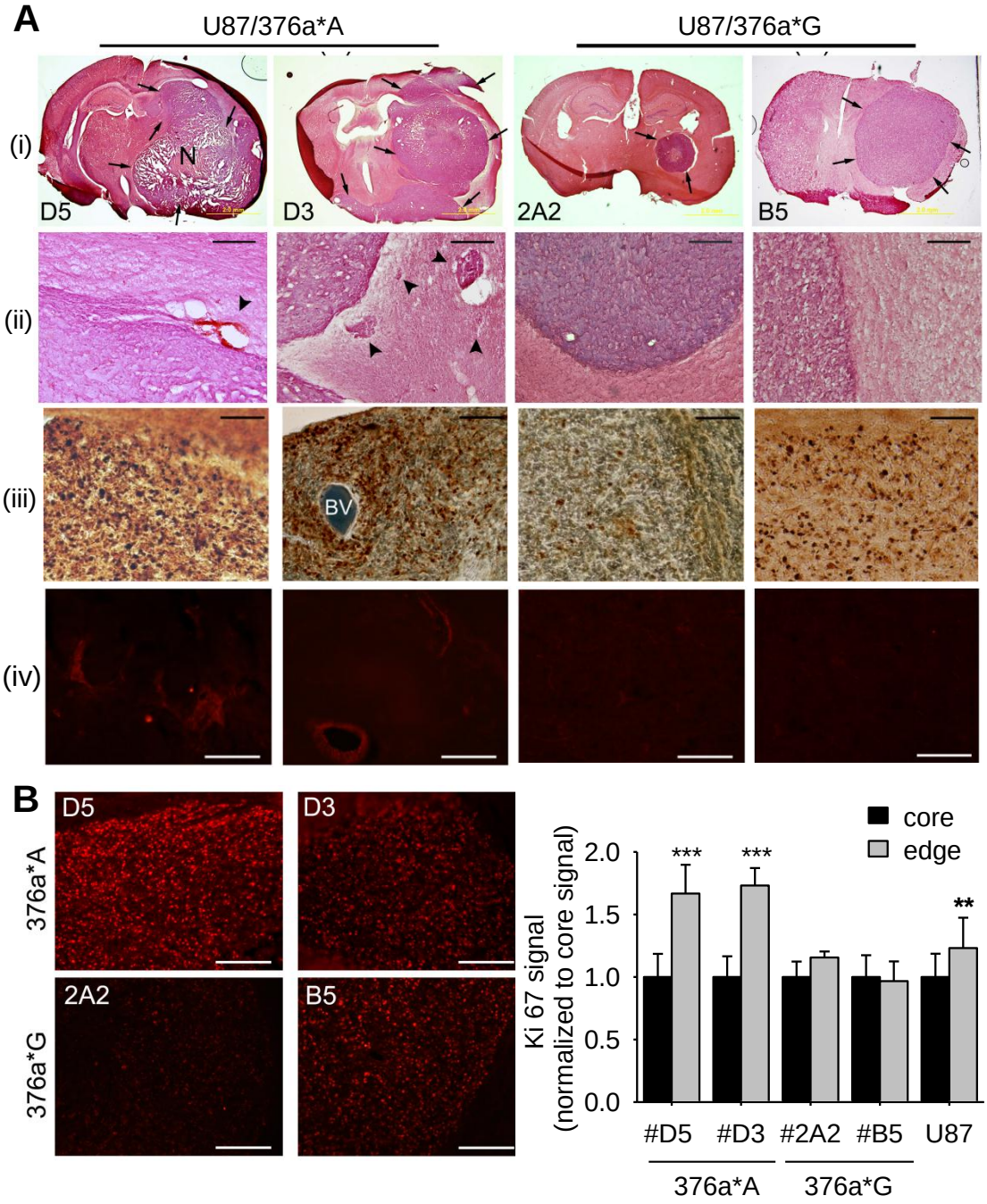

Figure 4.17 Histological and immunostaining analysis of orthotopic tumors formed on day 21 after injection of stably transfected U87 cells – U87/376a*A and U87/376a*G. ***A.*** **(i)** H&E staining of tumor sections. Three individual stable cell lines were injected for each miRNA; representative images from two are shown. Arrows indicate tumors after H&E staining; N: necrosis in U87/376a*A #D5. **(ii)** H&E staining showing tumor boundaries at higher magnification. Black arrowheads indicate peritumoral vascular structures (capillaries and blood vessels) (# D5) and disseminated tumors in the brain adjacent to the invading edge of tumor (# D3) for U87/376a*A tumors. Scale bar: 200 µm. **(iii)** Immunostaining of tumor sections for Ki-67. BV: blood vessel. Scale bar: 100 µm. **(iv)** Immunostaining of tumor sections for vWF. Distinct vascular structures are observed for U87/miR-376a*A. Using similar detection methods no staining for vWF was observed in U87/miR-376a*G. Scale bar: 100 µm. ***B.*** Fluorescent detection of Ki-67 in tumor sections. Scale bar: 200 µm. Right: Quantification of fluorescent Ki-67 signals using ImageJ. Bar graphs show relative Ki-67 signals at tumor edge (invasive front) and core. Data represents mean ± SD. **p<0.01 and ***p<0.001 by t-test.

Conclusive evidence of the ability of miR-376a*A to promote aggressive tumor growth came from the survival rates of mice bearing tumors formed by U87 cells with higher expression of miR-376a*A. Indeed, both U87/376a*A and U87/ELM cells, with enrichment of miR-376a*A, caused a significantly shortened survival time of animals compared to control U87 cells (Figure 4.18A). Importantly, as invasiveness was the only property selected for by the ELM assay, the observed differences in survival are chiefly attributable to enhanced tumor burden through invasive dissemination of tumor cells. Furthermore, there was an inverse correlation between the fold-enrichment of miR-376a*A in ELM cells and survival rates of tumor-bearing mice. ELM 2M1 with a 75-fold increase in miR-376a*A, had a median survival time of 21 days, whereas ELM 1M1 with a 7-fold increase, had a significantly higher median survival time of 28 days (p=0.8E6), although survival times for both ELM 1M1 and ELM 2M1 were shorter than the control group (Figure 4.18B). Although, miR-376a*G suppresses cell invasion in vitro, tumors formed in vivo by U87/376a*G and the associated survival rates were similar to control tumors (Figure 4.18), probably due to the inherently non-invasive nature of the U87 glioma model.

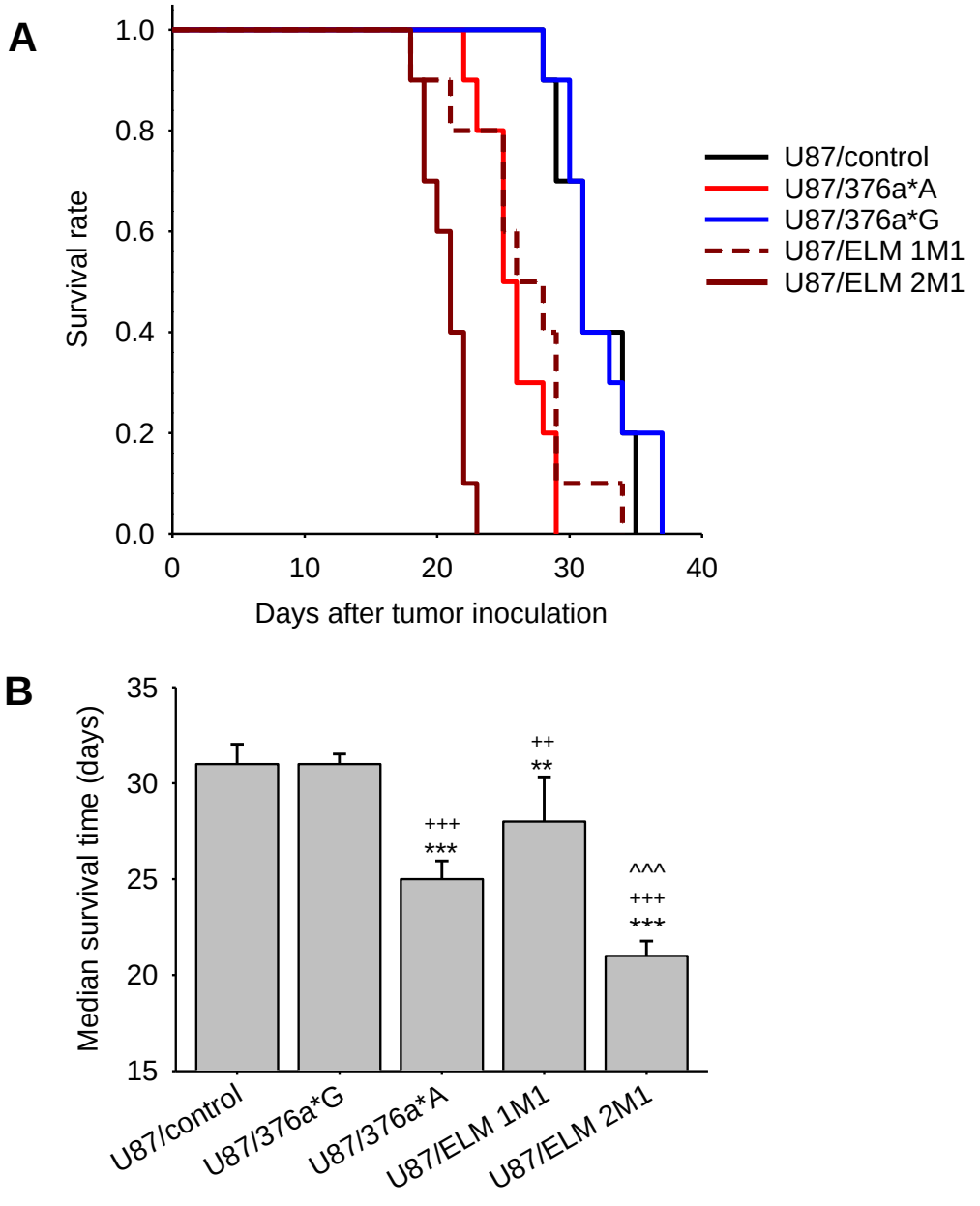

Figure 4.18 Survival of tumor-bearing mice in orthotopic glioma model. *A.* Kaplan-Meier survival analysis after intracranial implantation of various glioma cell lines. Cells stably expressing miR-376a* are U87/376a*A #D5, and U87/376a*G #2A2. ELM 1M1 and ELM 2M1 cells were enriched from U87 cells by ELM assay. ***B.*** Median survival of animals receiving intracranial injection of glioma cells in ***A.***. Statistical analysis was done using log-rank test (n = 10). Error bars represent SE. ***p<0.001 and **p<0.01 vs. U87/control, +++p<0.001 and ++p<0.01 vs. U87/376a*G, ^^^p<0.001 vs. U87/ELM 1M1.

qRT-PCR analysis of tumor samples collected from mouse brain was carried out to quantify expression of factors known to be involved in glioma growth and invasiveness. RNA was extracted from tumor sections for analysis. Components of growth factor signalling pathways, *PDGF*, *VEGF*, *TGFB* and their receptors were found to be enriched (5- to 45-fold) in U87/376a*A tumors (Figure 4.19A), together with mRNAs of several glioma invasion-promoting factors, which were expressed 5- to 20-fold higher (Figure 4.19B). For example, VEGF is a pro-angiogenic factor in gliomas and was increased nearly 25-fold in U87/376a*A tumors. MMP2, a protease that is involved in the degradation of ECM, is expressed only in GBMs and is absent in grade III astrocytomas (Du et al., 2008) was 2.5-fold enriched in U87/376a*A tumors (Figure 4.20B). Other factors that were expressed at higher levels in U87/376a*A tumors included integrins (*ITGB3*), ECM proteins (*TNXB, FN1*), proteases (*PLAU*) and angiogenic factors (*ANGPTL1*, *ANGPTL4*, *ANGPT1*).

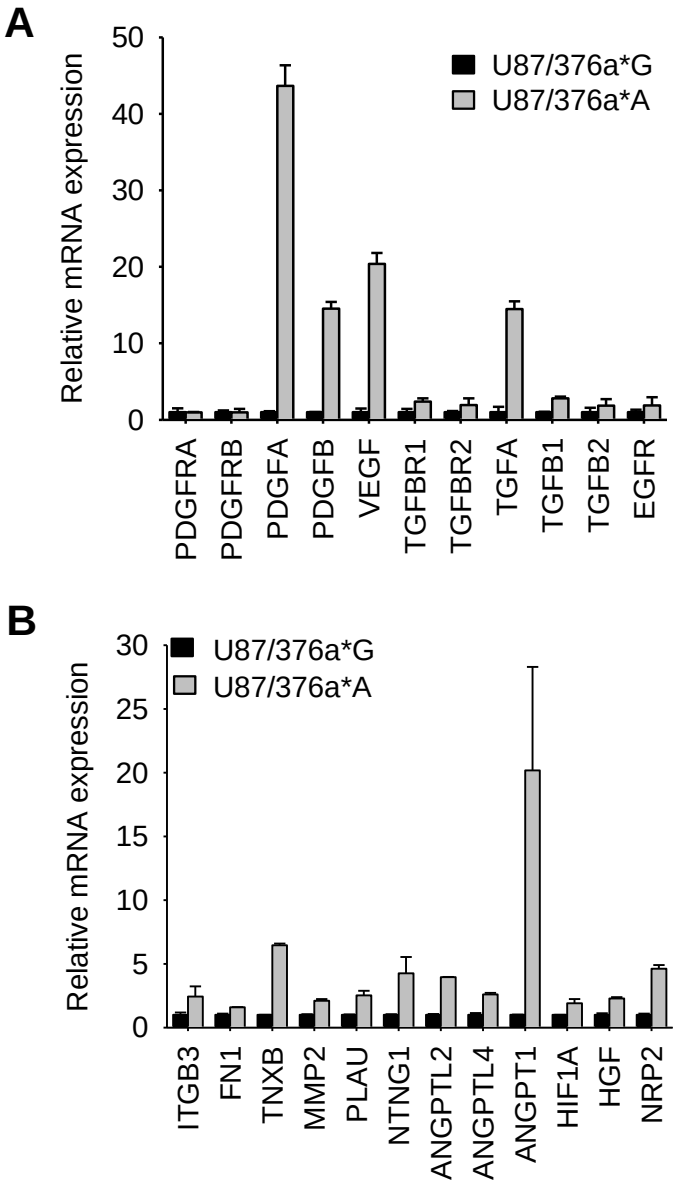

Figure 4.19 Quantification of factors involved in glioma invasion and angiogenesis in orthotopic tumors. qRT-PCR measurement of ***A.*** components of upstream growth factor signaling pathways and ***B.*** factors promoting glioma cell invasion and angiogenesis. RNA was isolated from tumors formed in vivo. 18S rRNA was used for normalization. Data represents mean ± SD.

Collectively, these results show that expression of miR-376a*A (unedited miR-376a*) in otherwise non-invasive U87 cells promotes aggressive tumor growth characterized by invasion, angiogenesis and necrosis, hallmarks of human GBMs. Coincident with the aggregation of unedited miR-376a* in GBMs, the data supports a major pro-invasive role for this miRNA in GBMs.

4.8 Discussion

In the previous chapter, it was established that due to loss of A-to-I editing, unedited miR-376a* accumulates in GBMs. Changes in transcript editing levels due to ADAR dysfunction most likely play a role in progression rather than initiation of malignant growth (Farajollahi and Maas, 2010). As increased aggressivesenes due to invasion and angiogenesis distinguish GBMs from grade III gliomas (Louis, 2006), the impact of aberrant accumulation of unedited miR-376a* with respect to the malignant property of invasion was investigated. In vivo and in vitro analysis showed that unedited miR-376a*, the aberrant tumor-specific variant promotes migration and invasion, in stark contrast to the normal 'edited' variant that suppresses these features.

A role for unedited miR-376a* in malignant progression was supported by its specific enrichment in selected invasive U87 cells (ELM cells), as in GBMs. Undoubtedly, during the selection of ELM cells in vivo, several factors that collectively aid survival and metastatic colonization of glioma cells would accumulate, deriving from a sub-population of surviving cells with the relevant intrinsic properties that aid such behavior in vivo. As such, miR-376a* represents only one of many contributing factors to the phenotypic differences between ELM and parental U87 cells. Nonetheless, the specific knockdown of miR-376a* in ELM cells was able to inhibit their migratory capacity, suggesting among other factors, miR-376a* may play a central role in glioma cell migration.

The miR-376 cluster encodes four primary miRNAs that are polycistronically transcribed and generate five mature miRNAs (Kawahara et al., 2007b). In ELM cells, although expression was increased marginally for all primary miRNAs, mature miR-376a* accumulated disparately more. Mechanistically, this specific accumulation is likely due to a post-transcriptional selective bias for miR-376a*. It has been suggested that strand selection itself is a form of posttranscriptional regulation and

could possibly account for disparity in abundance of mature miR-376a* and miR-376a (Siomi and Siomi, 2010). Additionally, miRNA degradation and stability are also subject to individual control by the target mRNAs themselves and other factors that recognize specific sequence elements of the miRNA. The observation that even in different tissues the ratio of miRNA/miRNA* strands are widely different is in line with the presence of factors that regulate individual miRNA strand stability and hence function (Hu et al., 2009). Importantly, the studies in ELM cells showed that by completely independent means, the abundance of unedited miR-376a* increased in selected invasive gliomas. In GBMs, a parallel increase in unedited miR-376a* also occurs but is mediated by the loss of A-to-I editing, while transcription rates remained unaffected. The convergence of independent study systems on the same phenomenon of increased abundance of unedited miR-376a* points to a crucial role of this miRNA in invasiveness.

Using synthetic mimics and engineered pre-miRNAs the function of miR-376a* in glioma cells was dissected independent from that of miR-376a, which is naturally encoded in pri-miR-376a1. Because of the tumor-type dependent and extensive reduction in editing of miR-376a*, its function is likely to be most impacted due to altered editing and hence this was the primary subject of investigation. Nonetheless, it cannot be ruled out that miR-376a and miR-376a* or other miRNAs from the cluster at their respective editing frequencies have a combinatorial role in glioma pathogenesis.

Ectopic expression of miR-376a*A (unedited) and miR-376a*G (edited) produced obvious but distinct morphological changes which correlated with the in vitro migration and invasion ability of glioma cells. miR-376a*A promoted motility and invasion of glioma cells while miR-376a*G suppressed these to below basal levels. The polarizing effects of the two forms of miR-376a* on glioma cell migration was unexpected but raises the interesting possibility that single-base change by editing is

sufficient to reverse certain functions of miRNAs. The role of edited miR-376a* will need to be more thoroughly investigated in the context of normal cells where it is normally expressed.

The pro-migratory and pro-invasive phenotype induced by miR-376a*A was reproducible in vivo. In contrast to tumors typically produced by orthotopic implantation of U87 glioma cells, the U87/376a*A-expressing tumors bore a far greater resemblance to human malignant gliomas with central necrosis and viable tumor rim (Giese et al., 2003). Also, the distribution of proliferating Ki-67+ cells in miR-376a*A-expressing tumors coincided with characteristics of invasive tumor growth (Ma et al., 2007; Nilsson et al., 2004; Silber et al., 2009). Higher degree of vascularization was concomitantly observed in these tumors, which was attributed to the ability of invasive glioma cells to induce vascular remodeling and angiogenesis for gaining further invasive advantage traversing perivascular spaces (Louis, 2006; Nowacki and Kojder, 2001; Vajkoczy et al., 1999; Winkler et al., 2009). The peritumoral angiogenesis observed in these tumors likely supports both invasive spread and the main tumor growth resulting in the larger main tumor mass formed by the more invasive U87/376*A cells (Winkler et al., 2009). Additionally, several cytokines and growth factors that are known to promote both migration and angiogenesis, e.g. *PDGF*, *VEGF*, *TGFβ* were upregulated in U87/376a*A tumors (Louis, 2006). On the other hand, U87/376a*G and control tumors lacking population of invasive cells were unable to remodel the brain vasculature for a growth advantage and remained confined within well-delineated boundaries. The shortened survival of mice bearing the aggressive tumors is reminiscent of the unfavorable prognosis faced by GBM patients. A correlative analysis between editing frequency of miR-376a* and survival of patients from a large cohort, will provide conclusive evidence on the nature of tumor aggressiveness caused by this miRNA.

Besides increased invasiveness, a common thread that emerged between ELM cells and glioma cells overexpressing miR-376a*A was their suppressed proliferation rate. This is in agreement with previous findings that in glioma cells, positive modulators of migration (miR-376a*A in this thesis) usually inhibit proliferation, and inhibition of migration (as by miR-376a*G) promotes cell proliferation (Godlewski et al., 2010; Lipinski et al., 2005). Among miRNAs, miR-451 in GBMs is known to promote cell proliferation while suppressing cell migration and serves as a switch to balance proliferation and migration in response to metabolic stress (Godlewski et al., 2010). The inverse relation between cell migration and proliferation falls under the hypothesis of “go or grow” that proposes that cell division and cell migration are temporally exclusive events that dictates that proliferating cells cannot migrate and vice-versa (Lipinski et al., 2005). However, the distinction between proliferation and invasion is not clear in vivo as depending on the anatomic sites, invasive cells in human gliomas showed higher or lower proliferation rates (Giese et al., 2003). Evidently, invasive glioma cells also retain the property of proliferation but have temporarily lowered proliferation rate during migration, as they can reestablish recurrent tumor masses (Giese et al., 2003). In addition to the ability of invasive glioma cells to remodel the vasculature, the end-point of tumor formation by invasive glioma cells is the greater overall aggressiveness of tumors formed, as observed with both ELM cells and U87/376a*A cells.

Although miR-376a* is expressed in primary gliomas, glioma cell lines examined here had low endogenous levels of miRNAs from miR-376 cluster. The differences between serum-cultured glioma cells and primary gliomas are well-documented, especially the inability of cultured cells to form invasive orthotopic tumors when xenografted (Lee et al., 2006). It is speculated that during long-term culture, loss of expression of miR-376 cluster occurs due to in vitro selection pressure conferring a proliferative advantage (Fomchenko and Holland, 2006). This is line with the

observations that unedited miR-376a* is expressed in GBMs and has anti-proliferative effect on glioma cells, a property that is likely diluted during long-term culture. Furthermore, from the results obtained in this study it can be speculated that the low levels of unedited miR-376a* is one of the contributing factors for the non-invasive nature of glioma cells cultured in vitro, as by introducing unedited miR-376a* the invasiveness of glioma cells was enhanced.

Significantly, a role for miR-376a* in invasion promotion in GBMs or any other cancer has previously explicitly not been demonstrated. However, using a non-conventional approach to study the role of miRNAs in tumorigenesis, a recent in vitro study showed that the expression of precursor miR-376a (pre-miRNA, encoding both miR-376a and miR-376a*) or the whole miR-376 cluster promoted the migration and invasion of otherwise non-migratory tumor cells derived from in vitro transformation of non-human primate kidney cells (Teferedegne et al., 2010). In this study, increased expression of miR-376a coincided with the acquisition of invasiveness during the process of spontaneous in vitro transformation of cells, although it was not made clear if levels of miR-376a* was measured. It would be interesting to delineate if unedited miR-376a* from the pre-miR-376a is responsible for the enhanced migratory phenotype. It has been reported that in GBMs, glutamate receptors assembled from the unedited (Q-containing) GluR-B subunit, are highly Ca2+-permeable and expression of this form of the receptor can promote glioma cell invasion (Ishiuchi et al., 2002), suggesting a general role of unedited substrates in promoting invasiveness. No other target of A-to-I editing (mRNA or miRNA) has been functionally characterized in gliomas.

Other miRNAs from miR-376 cluster have previously been implicated in various cancers, including miR-376c which promotes ovarian cancer cell survival (Ye et al., 2011) and is also overexpressed in a subset of acute myeloid leukemia (Dixon-McIver et al., 2008). Additionally, miR-376a expression is increased in pancreatic

cancer cells (Lee et al., 2007b) and it also negatively regulates erythroid differentiation (Wang et al., 2011). ADAR1 and ADAR2 expression has been detected in mouse pancreatic islets and ß-cells, where ADAR2 expression was regulated under conditions of metabolic stress in vivo together with 100% editing at the Q/R site of GluR-B RNA (Gan et al., 2006). As the editing machinery is expressed in other cell types with nearly ubiquitous expression of miRNAs from miR-376 cluster in various tissues (kidney, bone marrow, pancreas) the occurrence and consequence of normal and abnormal editing of these miRNAs in other cell types represents an avenue worth investigating.

Finally, a recent study on GBM subclasses and miRNA expression, identified miR-376a and 376a* to be associated with ‘neural’ subtype of GBMs (Kim et al., 2011). This subtype has significantly shorter survival compared to those with ‘oligoneural’ classification, which coincides with the ‘proneural’ classification based on mRNA expression (Phillips et al., 2006; Verhaak et al., 2010). Interestingly, the proneural classification also encompasses most grade III gliomas. Considering that miR-376a* is unedited specifically in GBMs and not in grade III gliomas, the association of miR-376a* with a subtype of GBMs with poorer prognosis, coincides with the poorer prognosis of GBM patients compared to patients with grade III gliomas. Therefore, several lines of evidence presented in this chapter, including the specific accumulation of unedited miR-376a* in selected invasive cells leads to the conclusion that the aberrant accumulation of unedited miR-376a* in GBMs due to attenuated A-to-I editing has functional consequences related to GBM malignancy. Thus, unedited miR-376a* is a GBM-specific functional miRNA sequence variant that promotes glioma cell migration and invasion.

5 CHAPTER 5. Genome-wide transcriptional changes by unedited and edited miR-376a* in cancer-related pathways

5.1 Introduction and aims

As unedited and edited miR-376a* differ only by a single base, their opposing morphological and migratory effects in glioma cells were particularly striking. To investigate their cellular effects in a broader context, a study of genome-wide transcriptional effects was undertaken. miRNAs can establish and maintain transcriptional networks that are highly informative of their cellular function (Lim et al., 2005). Genome-wide analysis is typically performed using microarrays to understand global effects of miRNA function in an environment or cellular context in which the miRNA and its targets are expressed (Li et al., 2009; Sarver et al., 2010; Wei et al., 2008). Overexpression or knockdown of a particular miRNA will respectively exaggerate or relieve the regulation of its direct target genes and associated downstream effectors, translating to a global perturbation of relevant components of the cellular transcriptome constituting networks or pathways. These networks or pathways can be gleaned using genome-wide transcriptional analysis. Thus, in this chapter, the aim was to identify genome-wide changes effected by miR-376a* in edited and unedited forms using microarray analysis.

5.2 Distinct global gene expression profiles regulated by edited and unedited miR-376a* in cancer cells

The overexpression strategy was used to investigate the genome-wide expression profiles of miR-376a*. U87 glioma cells were used as these cells have low level of expression of both forms of miR-376a* and provide the appropriate cellular context for study, as they are derived from GBMs and harbour a glioma-relevant transcriptome. Unedited miR-376a* (miR-376a*A) and edited miR-376a* (miR-

376a*G) were transfected into U87 glioma cells.Transfection was carried out for 72 hours, to allow transcriptional changes to accumulate, as these would be more informative from a global perspective and more representative of the cellular transcriptome maintained by miRNA in their natural context. Using Affymetrix microarrays, genome-wide transcriptional changes in U87 cells transfected with miR-376a*A or miR-376a*G compared to control miRNA were identified.

In line with broad regulatory functions of miRNAs, expression of several transcript probesets were found to be substantially changed when miR-376a*A or miR-376*G was introduced in U87 cells. A fold-change of 2-fold, statistical significance of $p < 0.05$, and Benjamini-Hochberg multiple testing correction was imposed to identify the most significantly affected transcripts. Differentially expressed probesets corresponded to the following number of differentially expressed genes: for miR-376a*A- 686 up-regulated and 894 down-regulated, and for miR-376a*G-1220 up-regulated and 1237 down-regulated genes. The range of differential expression was very wide for both miR-376a*A and miR-376a*G, and reached up to 40 to 50-fold differential expression for some transcripts. When the differentially expressed genes (compared to control miRNA) were clustered by unsupervised hierarchical clustering, the overall gene expression pattern rendered by miR-376a*A and miR-376a*G were found be dramatically different. Clusters of genes that were up-regulated by miR-376a*A were found be unchanged or oppositely regulated by miR-376a*G (Figure 5.1). Similarly, genes down-regulated by miR-376a*A were up-regulated or unchanged by miR-376a*G. In effect, very limited groups of transcripts were similarly regulated by miR-376a*A and miR-376a*G. This shows that in U87 cells, miR-376a*A and miR-376a*G differing only by a single base in their seed sequence have very distinct and non-overlapping overall effects on the cellular transcriptome.

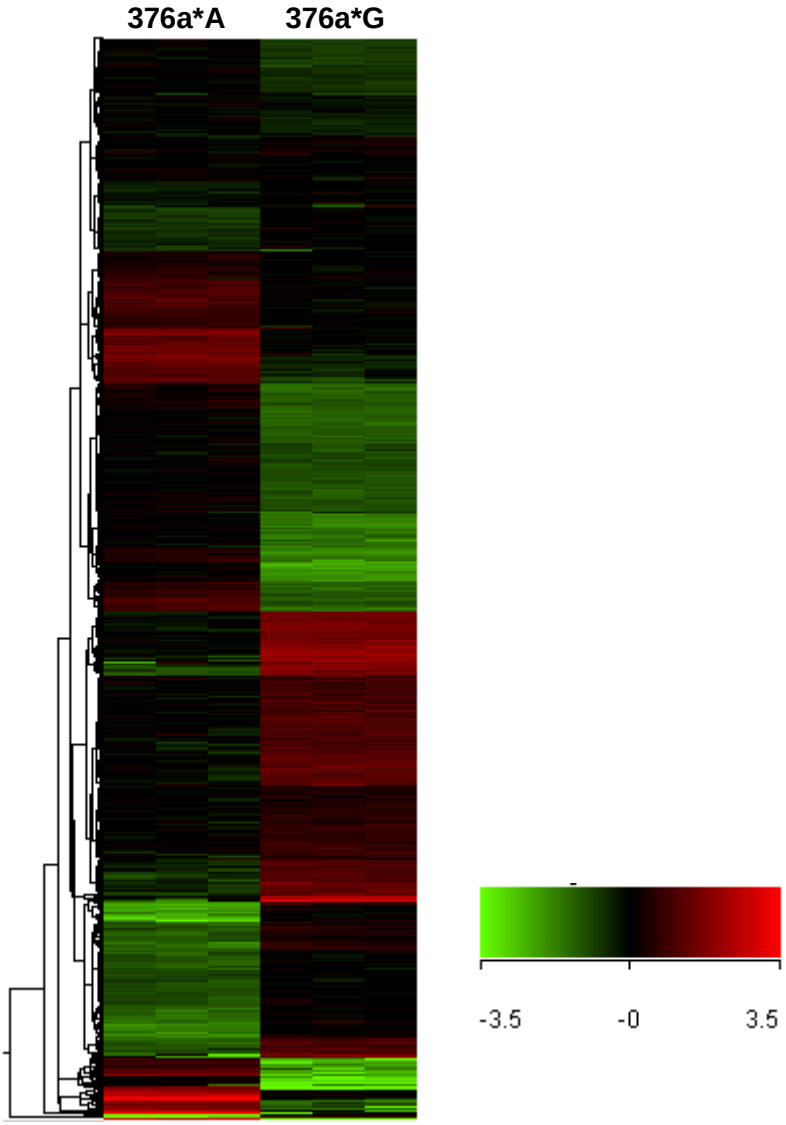

Figure 5.1 Global transcriptional changes caused by miR-376a* in U87 cells.Hierarchical clustering of normalized expression levels of transcripts that are significantly differentially expressed in miR-376a*A or miR-376a*G-transfected cells compared to control miRNA. The list of differentially genes for each miRNA was filtered based on fold-change > |2|, $p < 0.05$ and Benjamini-Hochberg multiple testing correction. Scale bar on the right depicts the zero-centred log-scale normalized expression values.

To gain a deeper understanding of the nature of gene expression modulation by miR-376a*, the functions of differentially expressed genes were probed. DAVID bioinformatics resources is an online data analysis tool that can identify enriched associated gene annotation terms (such as Gene Ontology) and therefore functions or pathways among gene lists generated from high-throughput analysis such as microarrays (Huang da et al., 2009a; Huang da et al., 2009b). The results of DAVID analysis of up- and down-regulated genes from miR-376a*A and miR-376a*G are summarized in Table 5.1, listing the 'representative' cluster annotation term, enrichment scores (which ranks importance of annotation groups), p-value of enrichment and false-discovery rate (FDR) to control discovery of false-positives. In strong agreement with cellular changes related to migration and invasion, "cell adhesion" and "cell motion" functions were significantly enriched in genes up-regulated by miR-376a*A (Table 5.1). In contrast, a very significant proportion of genes up-regulated by miR-376a*G were involved in "cell cycle", confirming earlier results that miR-376a*G increased proliferation rate and cell cycle progression. Reciprocally, genes down-regulated by miR-376a*A were related to "cell cycle", and those down-regulated by miR-376a*G were involved in "cell migration".

Interestingly, by DAVID analysis the functional enrichment of "development", both multicellular organsimal and vasculature, and "cell differentiation", were also identified among genes up-regulated by miR-376a*A and those down-regulated by miR-376a*G. Developmental pathways are often exploited by malignant cells for gaining advantages for tumor growth and invasion (Ma and Weinberg, 2008). In gliomas, these include the neurodevelopment-related PDGF and TGF signaling pathways (Golestaneh and Mishra, 2005; Hoelzinger et al., 2007; Louis, 2006). Heat map clustering of genes involved in the processes of development, vasculature,cell motion and cell cycle highlight the particularly contrasting pattern of transcript-level changes induced by miR-376a*A and miR-376a*G (Figure 5.2).

Annotated Biological Process	Enrichment Score	p-value	FDR	Gene Count	%
Genes up-regulated by miR-376a*A					
GO:0007275~multicellular organismal development	15.20	3.8E-21	6.9E-18	199	29.3
GO:0001944~vasculature development	8.50	6.3E-11	1.1E-07	35	5.2
GO:0007155~cell adhesion	8.17	2.0E-11	3.6E-08	65	9.6
GO:0001501~skeletal system development	6.44	2.9E-09	5.3E-06	37	5.4
GO:0030154~cell differentiation	5.82	2.8E-12	5.0E-09	117	17.2
GO:0006928~cell motion	5.29	4.9E-07	8.8E-04	42	6.2
GO:0009605~response to external stimulus	4.81	9.5E-10	1.7E-06	73	10.8
Genes down-regulated by miR-376a*A					
GO:0022403~cell cycle phase	4.06	1.5E-06	2.7E-03	42	4.7
GO:0044248~cellular catabolic process	2.22	3.8E-04	6.7E-01	70	7.9
Genes up-regulated by miR-376a*G					
GO:0007049~cell cycle	35.13	1.6E-47	2.8E-44	166	13.7
GO:0006259~DNA metabolic process	10.54	2.1E-28	3.8E-25	105	8.7
GO:0000226~microtubule cytoskeleton organization	8.64	1.8E-11	3.2E-08	35	2.9
GO:0051726~regulation of cell cycle	7.81	9.5E-16	1.8E-12	64	5.3
GO:0007059~chromosome segregation	7.68	2.9E-17	5.2E-14	32	2.6
Genes down-regulated by miR-376a*G					
GO:0001944~vasculature development	6.59	4.4E-09	7.9E-06	44	3.6
GO:0009653~anatomical structure morphogenesis	4.47	1.6E-07	2.9E-04	124	10.1
GO:0009966~regulation of signal transduction	4.15	8.9E-07	1.6E-03	95	7.8
GO:0030154~cell differentiation	2.73	5.2E-05	9.4E-02	146	11.9
GO:0016477~cell migration	2.37	5.2E-04	9.5E-01	34	2.8

Table 5.1 Functional enrichment analysis of genes differentially regulated by miR-376a*. Genes differentially expressed after treatment of U87 cells with miR-376a*A or miR-376a*G relative to control miRNA were identified by Affymetrix microarray. Gene lists were analyzed by DAVID Bioinformatics Resources. The most significantly enriched GO Biological Process annotation terms in the gene lists, are presented with enrichment score, p-value, false discovery rate, the number and % of total genes falling in each annotation cluster.

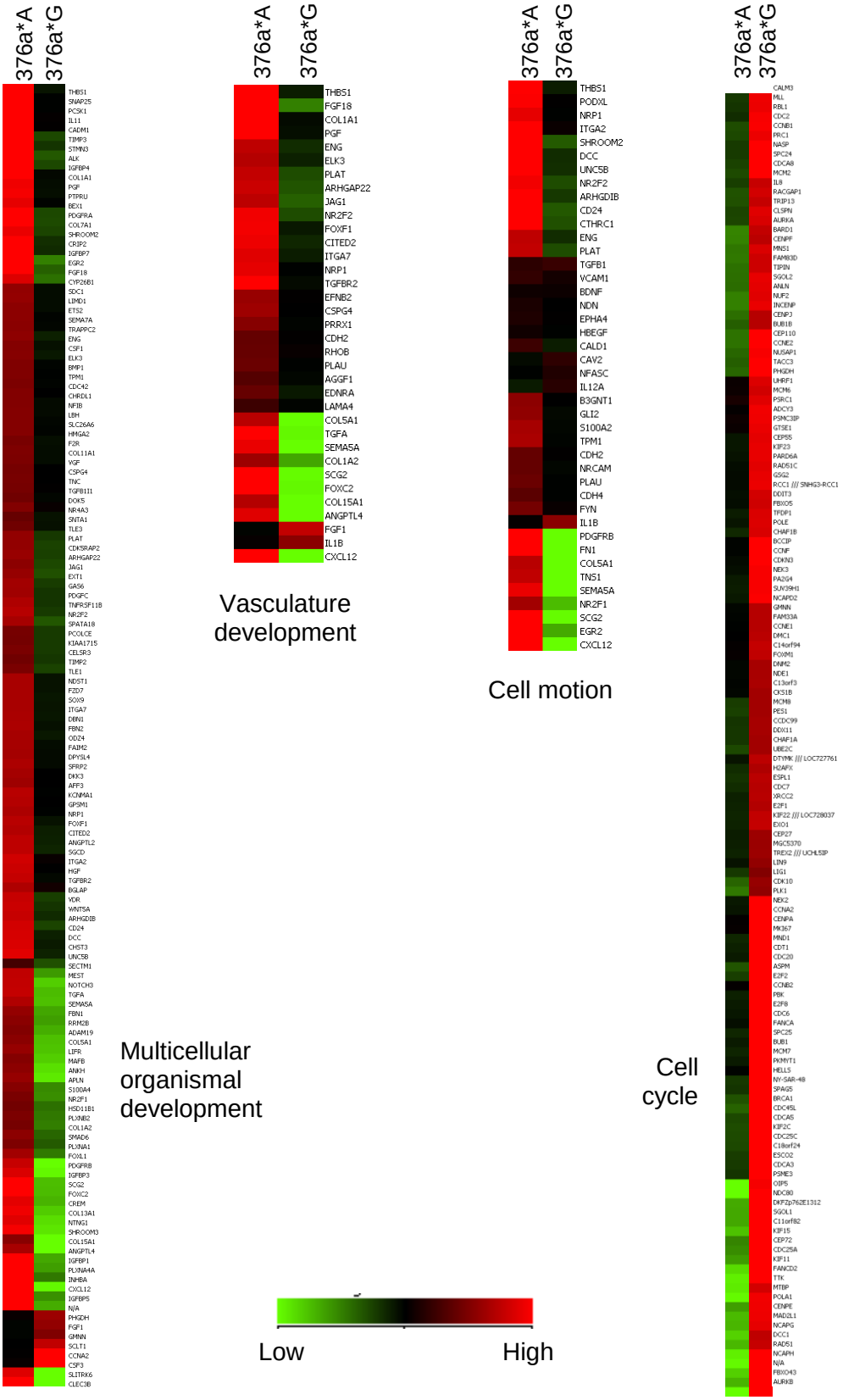

Figure 5.2 Heat maps of expression of differentially regulated genes in miR-376*A- and miR-376a*G-transfected cells. Subsets of genes falling in GO Biological Process enrichment clusters from **Table 5.1** were used to generate heat maps. Genes related to development, cell motion and vasculature were selected to emphasize the opposite effects on expression elicited by miR-376a*A and miR-376a*G. Heat map is coloured by normalized gene expression.

Using a similar method applying DAVID analysis, associated KEGG pathway annotations of differentially expressed genes were also interrogated. This analysis revealed that miR-376a*A had a significant effect on the ECM-receptor and focal adhesion pathways, while miR-376a*G affected the cell cyle and DNA replication pathways (Figure 5.3). ECM-receptor interaction is critical to the motility and invasion of cells and its enrichment among genes regulated by miR-376a*A further strengthened a role for this miRNA in cell invasion. The distinct effect of miR-376a*G on cell cycle suggests that its role is related to controlling cell cycle progression. Overall, the functions of miR-376a*A and miR-376a*G are highly distinct and inclined to being opposing.

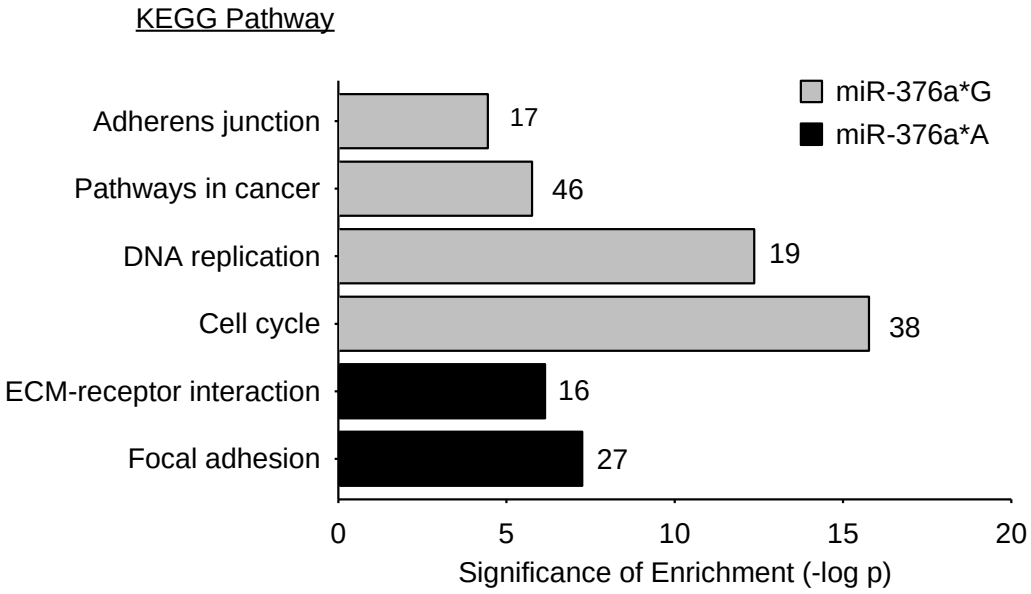

Figure 5.3 Summary of pathway enrichment analysis of differentially expressed genes. Lists of transcripts regulated by miR-376a*A or miR-376a*G were analyzed for enrichment of KEGG pathway terms. Significance of enrichment (-log10 [p-value]) and the number of differentially expressed genes mapping to the pathway are shown next to the bar.

From among the genes that are differentially regulated by miR-376a*A, a set of genes which are known to pleiotropically regulate glioma cell invasion, migration and angiogenesis (Hoelzinger et al., 2007; Louis, 2006) were used to validate the microarray results by qRT-PCR (Figure 5.4). Almost consistently, miR-376*A increased while miR-376a*G decreased the expression of selected growth factors receptors, angiogenesis regulators, chemokines and ECM-receptor genes (Figure 5.4A). Additionally, the similar transcript-level changes brought about by miR-376a*G and miR-376a*I for these key regulatory mRNAs (Figure 5.4B) strengthened the equivalency of their cellular effects.

We are limited by the use of “G”-containing miR-376a* as edited miRNA, for stable expression required for long-term in vivo studies, as inosine cannot be encoded in the DNA, but is only introduced posttranscriptionally. For valid comparison between transient and stable expression experiments, miR-376a*G was used consistently for experiments. The fact that miR-376a*G and miR-376a*I produced similar cellular effects in glioma cells as well as transcriptional level changes suggests a strong consistency in their function as miRNAs. This equivalency of “I” and “G” in miRNA base-pairing has been demonstrated before (Borchert et al., 2009; Kawahara et al., 2007b) and is also furthered in this thesis.

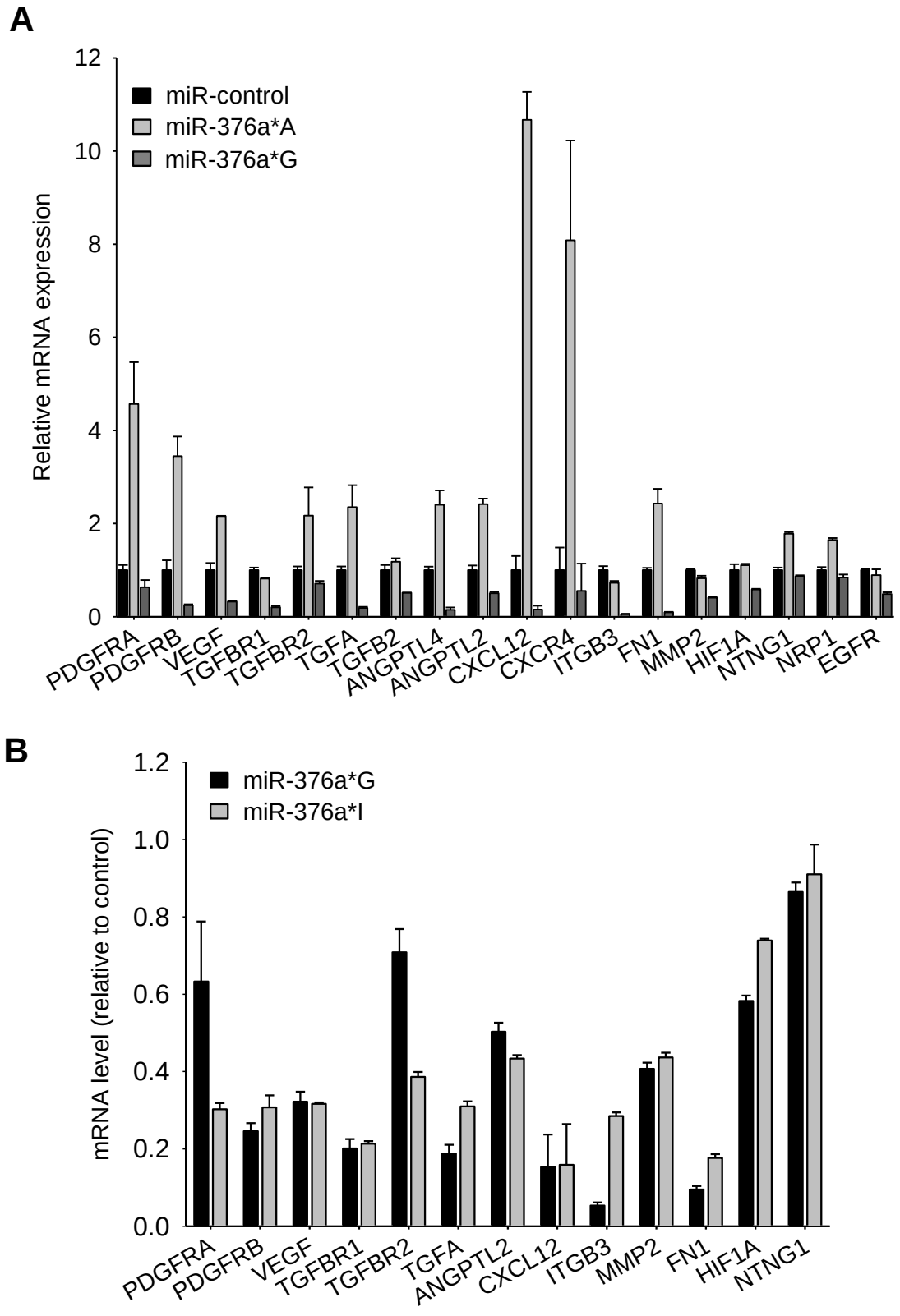

Figure 5.4 Verification of expression of genes involved in glioma migration, invasion and angiogenesis. *A.* Relative mRNA expression quantified by qRT-PCR in U87 cells transfected with miR-376a*A or 376a*G. *B.* Comparison of expression levels of a set of genes in U87 cells transfected with miR-376a*G and miR-376a*I. Expression was normalized to 18S rRNA. Data represents mean ± SD.

5.3 Discussion

In addition to the validated effects of unedited and edited miR-376a* on cell migration and invasion described in previous chapter, the global effects of these miRNAs on the transcriptome of glioma cells was investigated. The opposing effects of miR-376a*A and miR-376a*G on transcripts relevant to cell migration, invasion and growth factor signaling pathways were readily apparent from the global transcriptome changes effected by each miRNA. Apart from these, transcripts involved in vasculature development, potentially relevant to angiogenesis during glioma development, were also upregulated by miR-376a*A. Such broad effects on cancer-related pathways is in support of the ability of a single miRNA to pleiotropically impact cancer-related pathways (Valastyan et al., 2009). The regulation of miR-376a*G on cell cycle was obvious from the gene expression changes and deserves further investigation into its impact on the modulation of cell migration. As edited and unedited miR-376a* differ by a single base, the nearly opposing regulatory effects of the two miRNAs are a unique phenomenon that possibly ties into a regulatory switch that is normally imposed during development. It is conceivable that such a switch would cause a migratory cell to become non-migratory due to editing-mediated single base-change of a regulatory miRNA.

Indeed, a role for unedited transcripts in early development and edited transcripts in functional adult brain has been suggested previously (Wahlstedt et al., 2009). Interestingly, a neural progenitor cell (NPC) origin for primary human gliomas has been proposed (Louis, 2006). Also, A-to-I editing is a developmentally regulated process in the brain that progressively increases over developmental time, as measured by the increasing editing frequency of editing substrates, and is highly restricted during early development (Wahlstedt et al., 2009). Interestingly, a study in human NPCs found that the GluR-B Q/R site is unedited in NPCs but upon differentiation to neurons and astrocytes, the site undergoes high-level editing

(Whitney et al., 2008). During embryonic development and also during NPC differentiation, levels of ADAR2 are upregulated (Paupard et al., 2000; Whitney et al., 2008). Perturbation of this developmentally regulated phenomenon by altered function of editing enzymes, ADARs, possibly represents a mechanism of gliomagenesis. From a cancer development view-point a change to ADARs presents a greater opportunity for tumor cells to collectively manipulate the function of several targets. The link between A-to-I editing and development and differentiation and the presence of unedited transcripts in GBMs supports a reversal to a developmentally earlier stage by glioma cells due to lowered ADAR function or levels, and acquisition of embryonic features of migration.

6 CHAPTER 6. Identification of target genes of unedited and edited miR-376a*

6.1 Introduction and aims

The aim of this chapter was to investigate the mechanism by which miR-376a*A is able to promote glioma cell migration and invasion by identifying its direct target genes. Notably as shown in the Chapters 4 and 5, miR-376a*G, the edited counterpart, suppresses glioma cell migration and invasion and is associated with global transcription changes supporting suppressed invasion characteristics. As shown in Chapter 3, due to altered editing in GBMs, a switch from miR-376a*G in normal cells to miR-376a*A in glioma cells occurs. Given this switch and its opposing effects (manifest as effects of miR-376a*A and miR-376a*G), it was hypothesized that the function of miR-376a*A in glioma cells is dependent on two simultaneous aspects of miRNA targeting: gained accessibility to certain target genes (represented by targets of miR-376a*A) and lost accessibility to other target genes (represented by targets of miR-376a*G). The pro-invasive property of miR-376a*A in GBMs would therefore be the sum of these two aspects. Evidently, this would exclude targets common to both miR-376a*A and 376a*G from playing a role in their unique functions. Thus, in this section, the aim was to identify unique target genes of both miR-376a*A and miR-376a*G that could account for the observed cellular effects in glioma cells related to migration and invasion.

6.2 Distinct potential target gene sets of miR-376a*A and miR-376a*G

To identify potential target genes of the two miRNA forms, miR-376a*A and 376a*G were separately transfected in U87 and SW1783 glioma cells and by microarray, genes differentially regulated by each of them compared to control, at early time-points ($P < 0.05$; fold-change > 1.5 at 24 hours) were identified. Among these, the down-regulated transcripts potentially represent direct targets of miRNAs (Lim et al., 2005). This analysis depends on the ability of miRNAs to affect the stability of target transcripts which in previous studies have been shown to be highly enriched within their 3'UTRs for motifs corresponding to complementary miRNA seed sequence (He et al., 2007; Lim et al., 2005; Linsley et al., 2007). This strategy has been successfully applied for identification of targets of let-7 (Johnson et al., 2007), miR-372 and miR-373 (Voorhoeve et al., 2006) and miR-24 (Lal et al., 2009).

The 24 hours-post transfection time-point was selected as this allows a higher possibility of detection of transcripts directly down-regulated by miRNAs when mRNA silencing is maximal, as compared to indirect targets whose mRNA levels may be secondarily affected due to protein depletion of upstream regulatory factors (Jackson et al., 2003). The 1.5-fold change (compared to control miRNA) cut-off was imposed as large changes in transcript abundances are not expected due to miRNA regulation (Baek et al., 2008; Selbach et al., 2008). Although this method has the advantage of being high-throughput, miRNA targets that are exclusively regulated by translational repression and whose mRNA transcript abundance is not affected by miRNA regulation will not be identified by this method. Nonetheless, recent studies indicate that the predominant mode of action of miRNAs is reduction of target mRNA levels and that the fraction of targets that are exclusively regulated by translational repression is very small (Baek et al., 2008; Guo et al., 2010), so the potential utility of microarray-based target identification is justified.

Based on this analysis, a number of array probesets were found down-regulated by miR-376a*A and miR-376a*G, compared to control miRNA, in both U87 and SW1783 cells (Figure 6.1). Interestingly, a number of probesets were also up-regulated in miR-376a*A and miR-376a*G-transfected cells compared to control miRNA-transfected cells at the same 24-hour time-point (Figure 6.1). Although, potentially functionally relevant, the up-regulated genes are unlikely to be direct target genes of miRNAs and were not considered experimentally.

	Down-regulated genes		Up-regulated genes	
	miR-376a*A	**miR-376a*G**	miR-376a*A	miR-376a*G
U87	**315**	**491**	241	360
SW1783	**239**	**354**	191	258

Figure 6.1 Microarray analysis of genes differentially regulated by miR-376a*A and miR-376a*G. Number of genes down-regulated or up-regulated by miR-376a*A or miR-376a*G in U87 and SW1783 cells, 24 hours after transfection. Comparison was done against cells transfected with control miRNA and a 1.5-fold-change cutoff was applied.

As a first step, transcripts that were commonly down-regulated by both miR-376a*A and miR-376a*G were isolated in each cell line, U87 and SW1783. In agreement with the redirection of target gene specificity by editing of miRNAs, the proportion of commonly down-regulated transcripts among total down-regulated transcripts was small (~10%) (Figure 6.2A). These transcripts were removed from consideration as targets. The remaining genes down-regulated exclusively by miR-376a*A or by miR-376a*G, potentially represent unique target genes for each miRNA. By overlapping these gene lists from U87 and SW1783 experiments, the list of candidate target genes was further narrowed down. Using this strategy 116 genes uniquely down-regulated by miR-376a*A and 142 genes for miR-376a*G were identified (Figure 6.2B). Transcripts representing candidate target genes are listed in Appendix Tables A1 and A2.

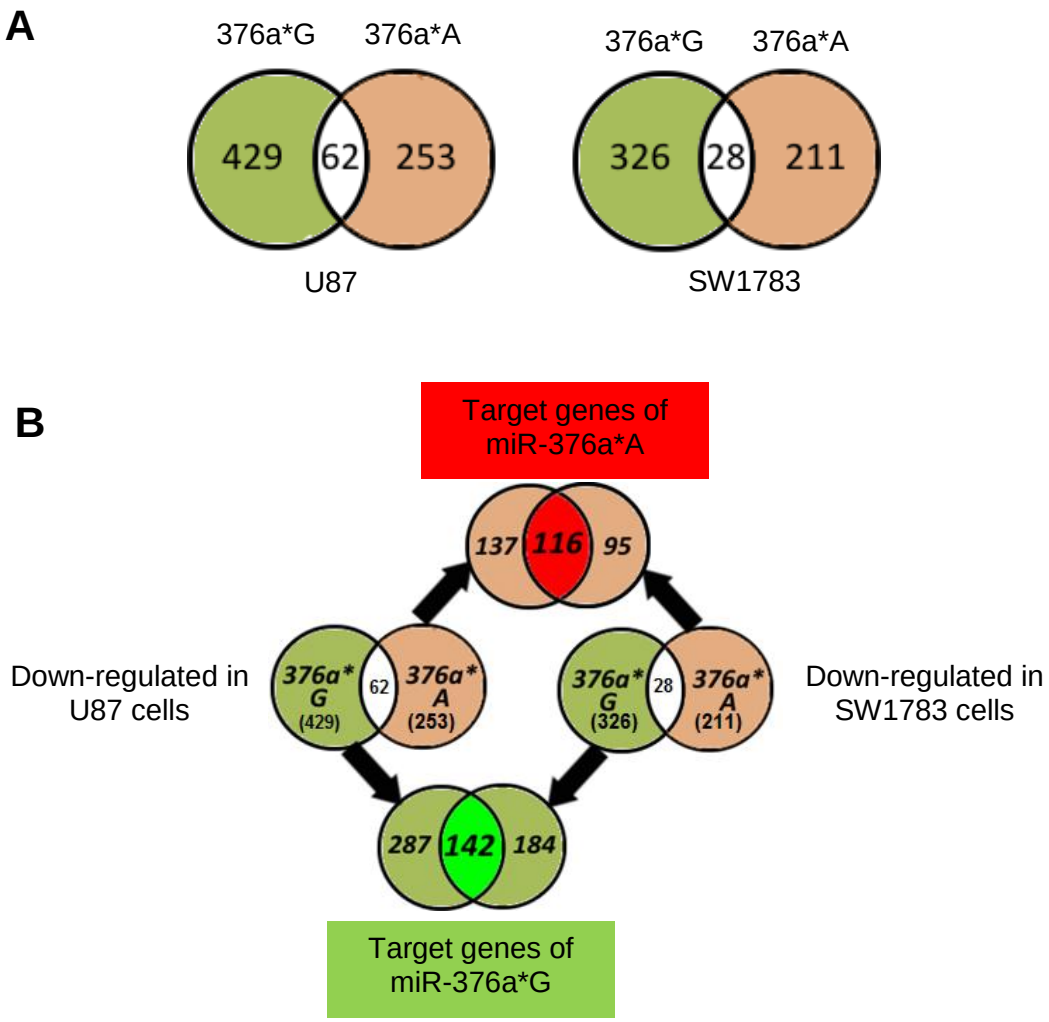

Figure 6.2 Potential target genes of miR-376a*A and miR-376a*G identified by microarray. *A.* Overlap of genes down-regulated by miR-376a*A and miR-376a*G to isolate those that are commonly or uniquely down-regulated by each miRNA in U87 and SW1783 cells lines. ***B.*** Candidate target genes of miR-376a*A and miR-376a*G identified by overlap of gene lists from ***A.*** derived for both U87 and SW1783 cells. 116 potential candidate genes for miR-376a*A and 142 potential candidates for miR-376a*G were narrowed down by this analysis.

It is to be noted that the degree of down-regulation of transcripts does not directly represent the targeting efficacy and is likely also determined by the half-life of transcripts, as long-lived transcripts will undergo relatively more destabilization than relatively short-lived ones (Gu et al., 2009), therefore the degree of down-regulation was not considered a significant factor and all genes that were significantly down-regulated >1.5-fold were equally considered as potential targets.

The microarray results were verified for selected genes that were highly down-regulated for each miRNA. U87 cells transfected with miR-376a*A or miR-376a*G were analyzed for mRNA levels of *RRAS2*, *PEX19*, *FAM55C* and *ELOVL5* (down-regulated by miR-376a*A) and for *TCF7* and *ACVR1* (down-regulated by miR-376a*G) using qRT-PCR (Figure 6.3A). In accordance with microarray data, only one of the two miRNAs suppressed mRNA levels of each of the genes, in the expected pattern (Figure 6.3A). Furthermore, the fold-change determined by qRT-PCR was similar to that determined by microarray for U87 and SW1783 cells (Figure 6.3B).

A

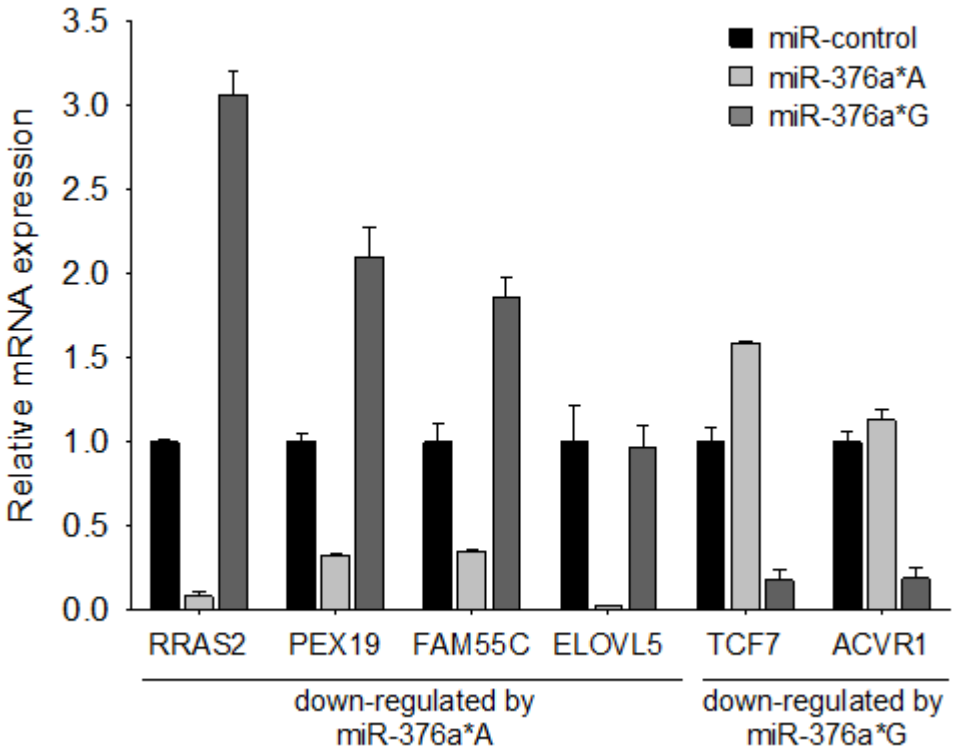

B

		Down-regulation fold-change determined by microarray	
		U87	SW1783
miR-376a*A targets	RRAS2	6.26	5.37
	PEX19	5.12	3.34
	FAM55C	3.16	2.38
	ELOVL5	4.8	2.3
miR-376a*G targets	TCF7	4.58	3.16
	ACVR1	4.85	4.42

Figure 6.3 Verification of microarray results by qRT-PCR for top down-regulated genes. ***A.*** Relative levels of mRNAs indicated genes measured by qRT-PCR. 18S rRNA was used for normalization. Data represents mean ± SD. ***B.*** Down-regulation fold-change determined by microarray for U87 and SW1783 cells.

6.3 Prediction of miRNA-binding sites in candidate target genes

For the potential candidate target genes of each of miR-376a*A and miR-376a*G that were identified from the microarray analysis, it was important to demonstrate the presence of specific miRNA-binding sites in their 3'UTRs. At the same time, it would be expected that potential targets of miR-376a*A would only harbour binding sites for miR-376a*A, and not for miR-376a*G, although the two miRNAs differ only by a single base. Similarly, the opposite would apply for miR-376a*G target genes.

The 3'UTR sequences for each potential target gene were retrieved and miRNA-binding sites for both miR-376a*A and miR-376a*G in 3'UTRs were searched for using the online program RNA22 (Miranda et al., 2006). This program allows flexibility of inputting "custom" miRNA sequences necessary to distinguish miR-376a*A and miR-376a*G. This option is not available in other popular prediction softwares such as PicTar or miRanda (Betel et al., 2008; Krek et al., 2005), which predict target genes only for currently known miRNAs annotated in Sanger miRBase – precluding predictions for edited miR-376a* (miR-376a*G).

The program RNA22 identifies regions of 3'UTR (or any other input mRNA sequence) that have the potential to form thermodynamically favorable duplex with a miRNA sequence of interest. RNA22 does not use cross-species conservation of target site as a criteria for prediction and is resilient to noise (Brodersen and Voinnet, 2009; Miranda et al., 2006). Also, this program allows the presence of G:U pairs in the miRNA seed region, which broadens the scope of potential binding sites (Brodersen and Voinnet, 2009; Miranda et al., 2006).

Using RNA22, for majority of genes down-regulated by miR-376a*A, at least one miR-376a*A-binding site was found in their 3'UTRs. Similarly, most genes down-regulated by miR-376a*G had predicted sites in their 3'UTRs for miR-376a*G. For a

proportion of candidate targets of miR-376a*A, equivalent numbers of miR-376a*G sites were also predicted either distinct or overlapping with miR-376a*A sites. The same was reciprocally applicable to miR-376a*G targets. As miR-376a*A and 376a*G differ only by a single-base, this was not surprising for computational prediction. Nonetheless, those targets with *nearly equal* numbers and strengths of target site predictions for both miR-376a*A and 376a*G were not further investigated as targets, in order to increase the likelihood of identifying genuine specific targets of each. The presence of a putative miRNA-binding site in the 3'UTR, although the given miRNA was unable to down-regulate the mRNA of target gene, raises the possibility that under certain other experimental conditions these sites may be functional. Additionally, although the miRNA may not be able to induce the degradation of mRNA of a target gene, it may still be able to inhibit protein translation, not detectable by microarray analysis. To streamline the process of target validation, an additional criterion of significantly higher numbers and strengths of miRNA-targeting sites only for the miRNA that was identified to initially down-regulate target mRNAs was imposed. This further led to the elimination of several genes, leaving those targets which are only down-regulated at mRNA level by either miR-376a*A or miR-376a*G and have predicted sites for the appropriate miRNA in their 3'UTR. The overall strategy used for candidate gene identification is summarized in Figure 6.4. Furthermore, combined with the *a priori* knowledge of the role of miR-376a* in cell migration and invasion, the focus was on candidate targets that are known to be potentially involved in these functions.

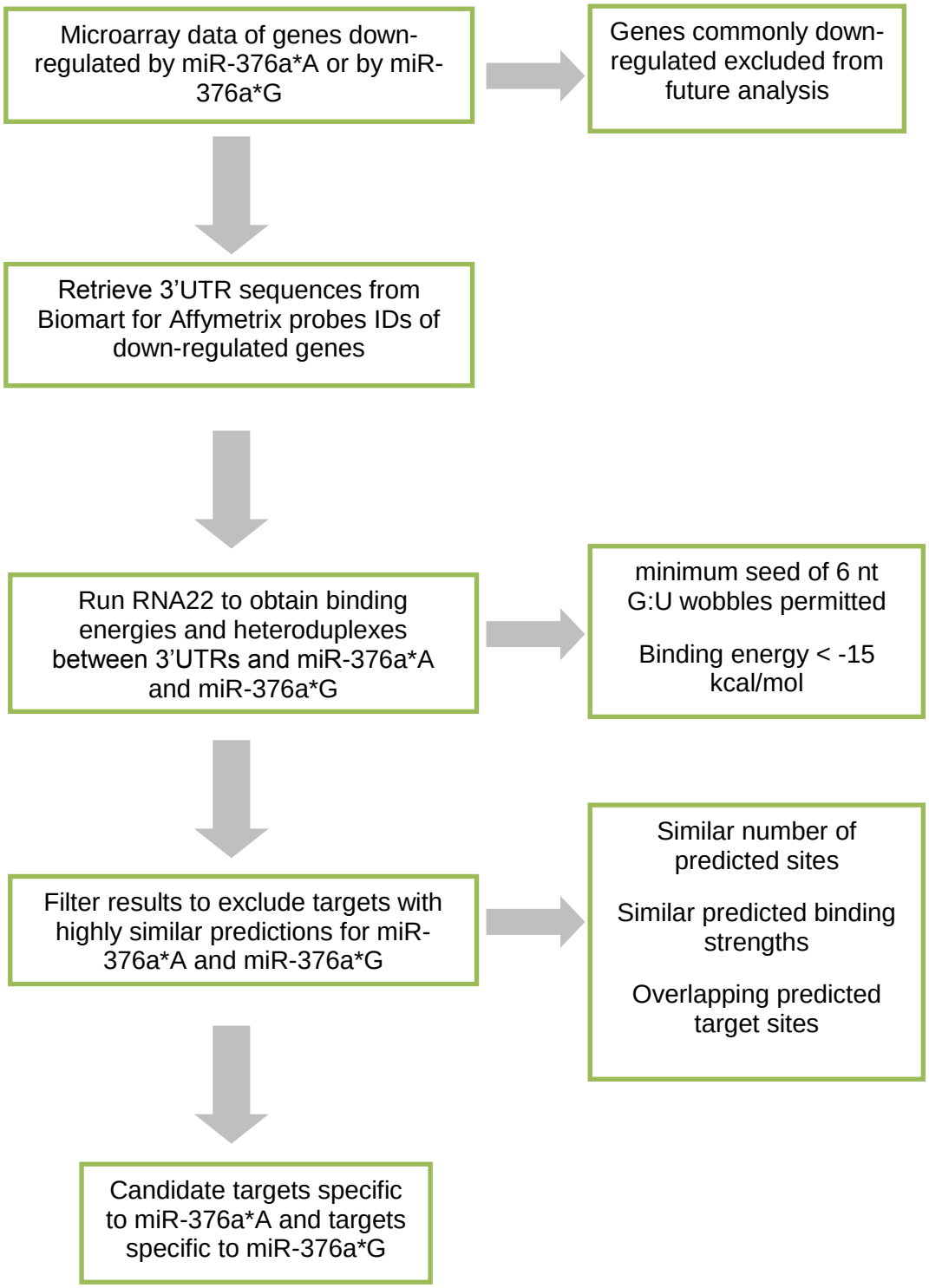

Figure 6.4 Strategy for identification of potential candidate genes specific to miR-376a*A and miR-376a*G. Genes identified to be down-regulated either by miR-376a*A or by miR-376a*G but not by both were selected for analysis of their 3'UTRs for miRNA binding sites using RNA22. Genes with similar prediction for miR-376a*A and miR-376a*G binding were removed leaving a list of candidate genes that are both regulated uniquely by either miR-376a*A or miR-376a*G and have 3"UTR binding sites for one of the two appropriate miRNAs.

6.4 STAT3 is specifically targeted by unedited miR-376a*

Based on the microarray and target site prediction analysis, STAT3 from the signal transducer and activators of transcription (STAT) family was identified as a potential target with functions relevant to cancer cell migration. Four binding sites for miR-376a*A were identified in *STAT3* 3'UTR, which failed to be predicted as miR-376a*G-binding sites, although an independent site for miR-376a*G was also predicted downstream (nucleotides 1877-1898 of 3'UTR) (Figure 6.5A). Folding energies of the predicted heteroduplexes are shown in Figure 6.5B. It was noted that the predicted heteroduplexes formed contained one or more G:U wobbles in the miRNA seed region. It has been previously demonstrated that despite the presence of multiple G:U pairs in the seed region, miRNA binding can still be functionally productive and be able to mediate target repression (Brodersen and Voinnet, 2009; Miranda et al., 2006), especially when present multiply miRNA (Brennecke et al., 2005), as in STAT3 3'UTR. Furthermore, additional Watson-Crick base-pairing at the 3' end of the miRNA from positions 12, 13 or 14, as seen for most sites predicted for miR-376a*A binding (Figure 6.5B), is known to enhance miRNA targeting (Grimson et al., 2007). Overall, the predictions for miR-376a*A-binding sites in *STAT3* 3'UTR suggest multiplicity of action of at least four miRNA binding sites. Conservation of target sites was found but was restricted to primate species (Figure 6.5C).

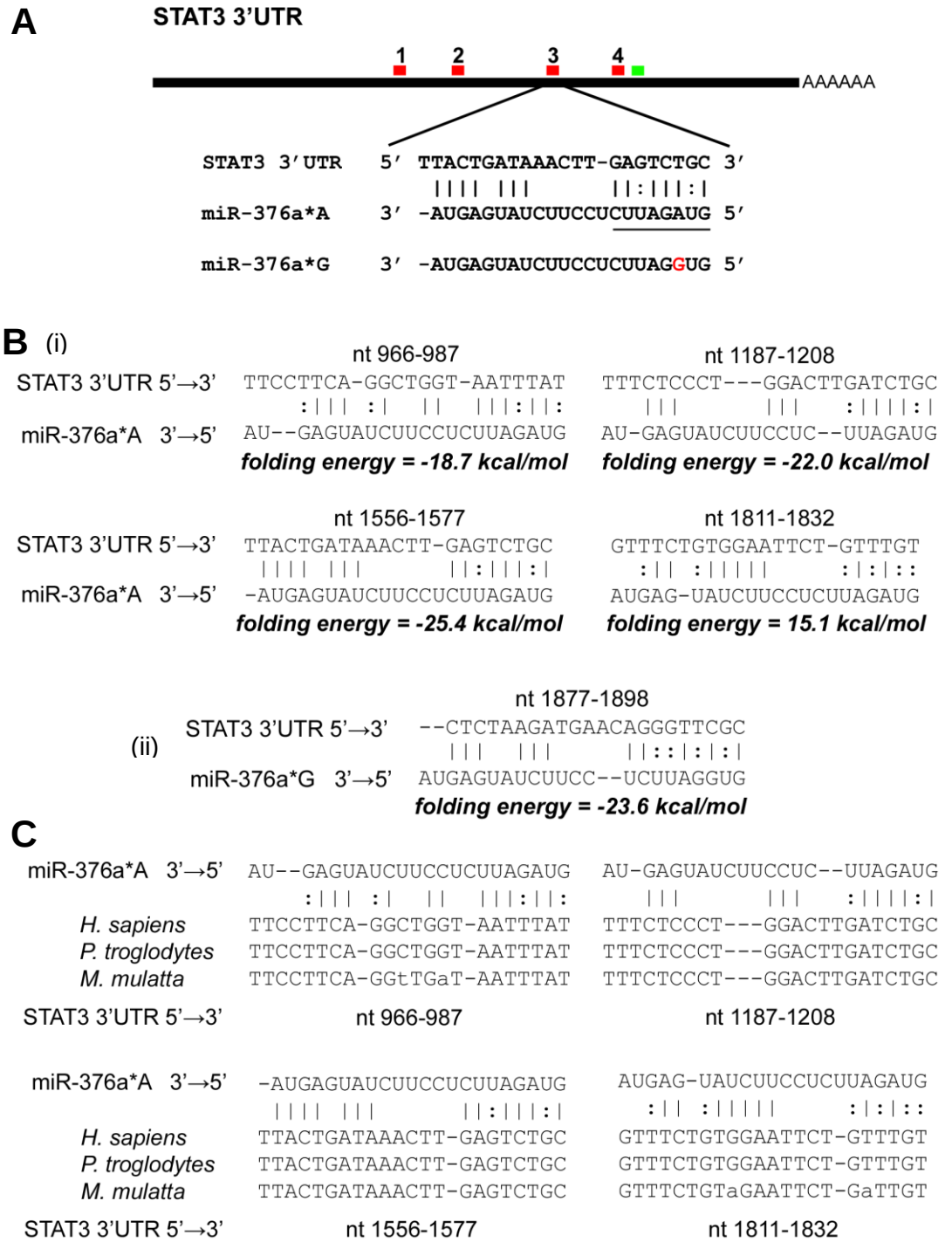

Figure 6.5 Conserved miR-376a*A binding sites in STAT3 3'UTR. ***A.*** Schematic representation of *STAT3* 3'UTR. Red bars show predicted miR-376a*A-binding sites. Green bar shows predicted miR-376a*G-binding site. Sequence of binding site 3 is shown aligned to miR-376a*A and seed region in underlined. Single base difference between miR-376a*A and 376a*G is highlighted. ***B.*** Folding energies of predicted miRNA:mRNA heteroduplexes between **(i)** miR-376a*A and *STAT3* 3'UTR and **(ii)** miR-376a*G and *STAT3* 3'UTR ***C.*** Alignment of potential miR-376a*A binding sites in *STAT3* 3'UTRs of different species indicating evolutionary conservation. Non-conserved residues within binding region are written in lowercase. nt: nucleotide position in 3'UTR.

To validate the specificity of miRNA targeting, luciferase-reporter assays were performed. In the luciferase-reporter asay, the 3'UTR of the gene of interest encompassing the miRNA target sites is cloned downstream of the luciferase coding sequence in a luciferase reporter vector (pmiR-Report) (Figure 6.6A). Binding of miRNA to the target sites reduces the luciferase activity which is measurable in a luciferase assay. A plasmid encoding ß-galactosidase, was co-transfected to serve as a control for transfection efficiency. For STAT3, two luciferase reporter vectors were constructed: first, containing a 1002 bp *STAT3* 3'UTR region encompassing four miR-376a*A sites but excluding the miR-376a*G site; second, containing the entire 2449 bp *STAT3* 3'UTR (Figure 6.6B).

The luciferase assays were performed in HeLa cells as they have low expression of miR-376a* (Kawahara et al., 2007b) and avoids intereference from endogenous miRNA expression. Glioma cells were not used for the luciferase assays given the extensive changes mediated by both miR-376a*A and miR-376a*G in glioma cell lines, which may produce secondary effects on expression from the luciferase reporter constructs.

Only miR-376a*A decreased luciferase activity by 70% for both reporter constructs while both miR-376a*G and miR-376a*I were ineffective in suppressing luciferase expression below control levels (Figure 6.6C). This indicates that the single base difference between miR-376a*A and miR-376a*G/I determines in an "on/off" manner the ability of miR-376a* to target *STAT3* 3'UTR as there were no incremental changes to the luciferase targeting ability when miRNA sequence was changed from having an 'A' in the seed sequence to having a 'G' or 'I' in the seed sequence. The full-length *STAT3* 3'UTR luciferase reporter, containing the predicted miR-376a*G binding site failed to respond to both forms of edited miRNA, miR-376a*G and miR-376a*I (Figure 6.6C), suggesting that this predicted site is non-functional, at least under these experimental conditions.

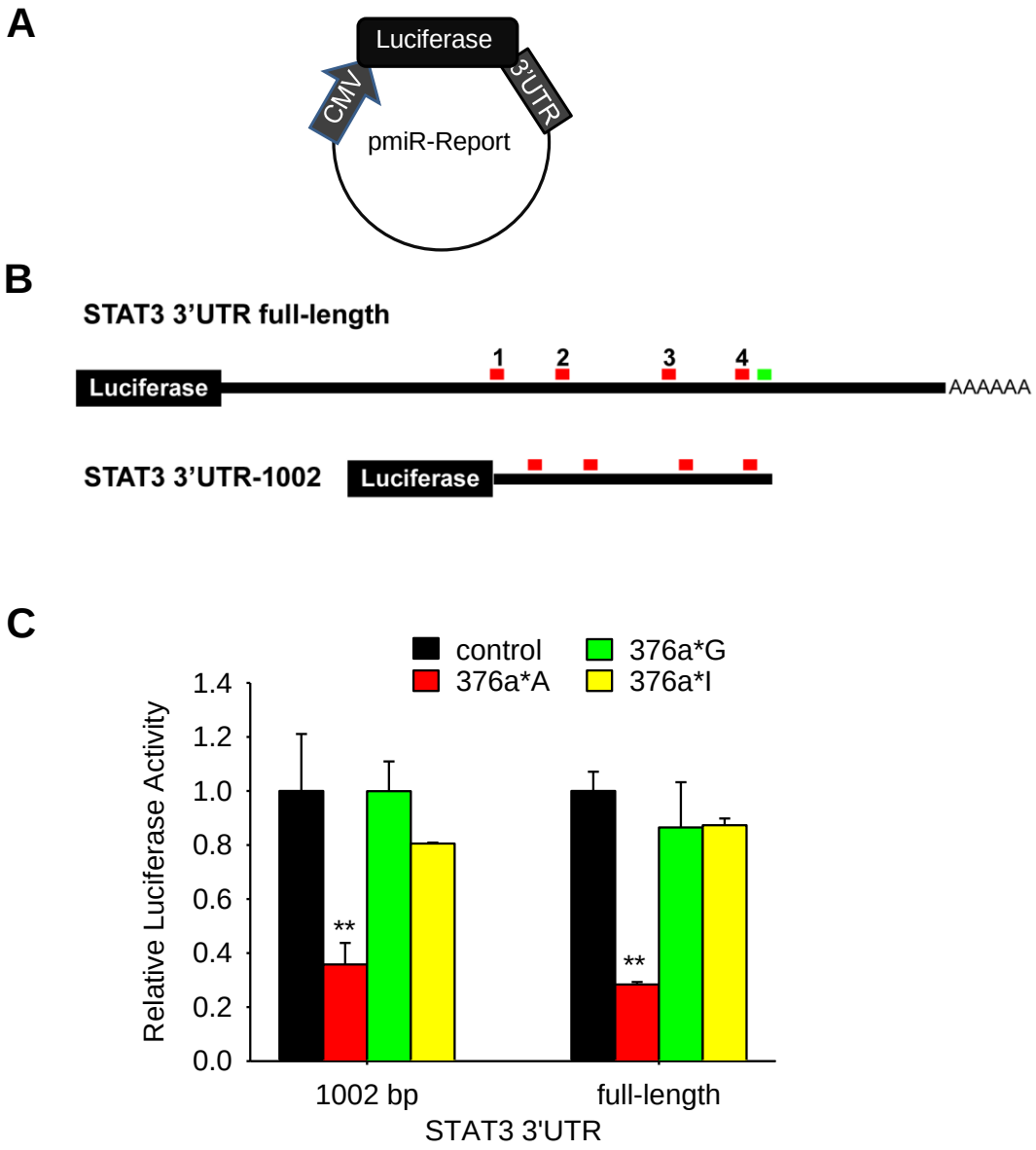

Figure 6.6 Specific targeting of STAT3 3'UTR by miR-376a*A. ***A.*** The pmiR-Report vector used for constructing luciferase reporter vectors. CMV promoter drives the expression of firefly luciferase, downstream of which appropriate 3'UTR sequence is cloned. ***B.*** Two luciferase reporter constructs used for verification of STAT3 targeting by miR-376a*A. Red bars show predicted miR-376a*A binding sites. Green bar shows predicted miR-376a*G binding site within 3'UTR. STAT3 3'UTR full-length includes the entire 2449 bp *STAT3* 3'UTR. STAT3 3'UTR-1002 represents the fragment of the 3'UTR which includes all predicted miR-376a*A binding sites but excludes the predicted miR-376a*G binding site. ***C.*** Targeting of *STAT3* 3'UTR by miR-376a*A. Luciferase reporter constructs for partial or full-length STAT3 3'UTR were cotransfected with miR-376a* or control miRNA in HeLa cells. Luciferase readings were normalized to ß-galactosidase activity and for each construct, expressed relative to readings for control miRNA. Data represents mean ± SD. **p<0.01 by t-test vs. control.

In U87 and SW1783 cells, it was verified that *STAT3* mRNA levels were subject to extensive down-regulation by 50-70% by miR-376a*A, but not by miR-376a*G as validated by qRT-PCR (Figure 6.7A). Similarly, STAT3 protein was reduced specifically by 60-70% by miR-376a*A (Figure 6.7B). These results confirmed the direct and specific regulation of *STAT3* by miR-376a*A via the predicted miRNA binding sites. Thus, STAT3 represents a direct specific target of miR-376a*A, subject to downregulation only by this miRNA.

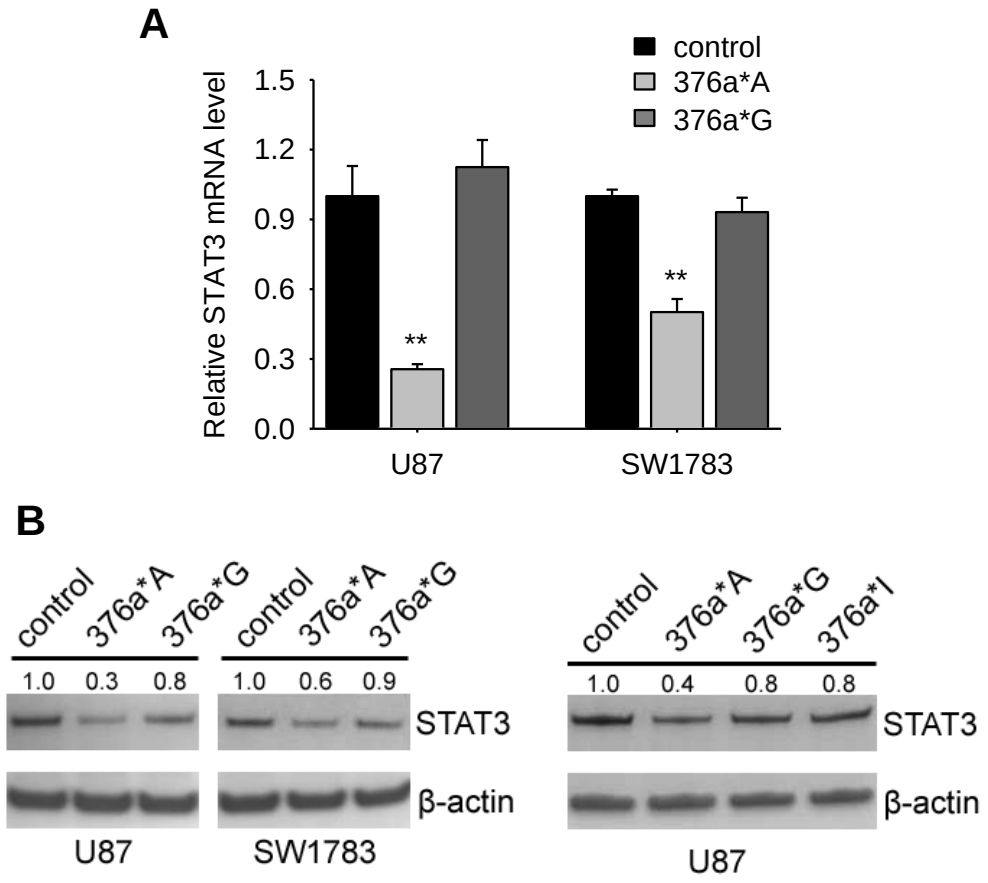

Figure 6.7 Specific mRNA and protein down-regulation of STAT3 by miR-376a*A. ***A.*** Quantification of STAT3 expression by qRT-PCR in transfected glioma cells. 18S rRNA was used for normalization. Data represents mean ± SD. **p<0.01 by t-test vs. control. ***B.*** Immunoblotting for total STAT3 levels in transfected glioma cells. ß-actin was used as loading control. Densitometric analysis was done by Image J software and protein amounts are shown relative to control miRNA.

To investigate if in primary glioma samples, there was a correlation between STAT3 expression and miR-376a*A expression, *STAT3* mRNA levels were quantified by qRT-PCR. Gliomas were stratified according to the frequency of editing of miR-376a* determined from the direct sequencing of pri-miR-376a1. “Low” and “high” frequency editing distinguished tumors with base-line editing of 0-5% and those with measurably substantial editing of >12% for +9 site of pri-miR-376a1. Under the premise that total expression of miR-376a* in human GBMs is not subject to major deregulation (0.853-fold of normal brain), editing frequency of miR-376a* is a surrogate measure for miR-376a*A expression. Based on this, a correlation was found between *STAT3* mRNA levels and the editing frequency of miR-376a* (Figure 6.8). In most tumors with low % editing of miR-376a*, miR-376a*A accumulates down-regulating *STAT3* mRNAs. Conversely, tumors with relatively high-level editing have more miR-376a*G which does not target STAT3, allowing the accumulation of *STAT3* mRNA.

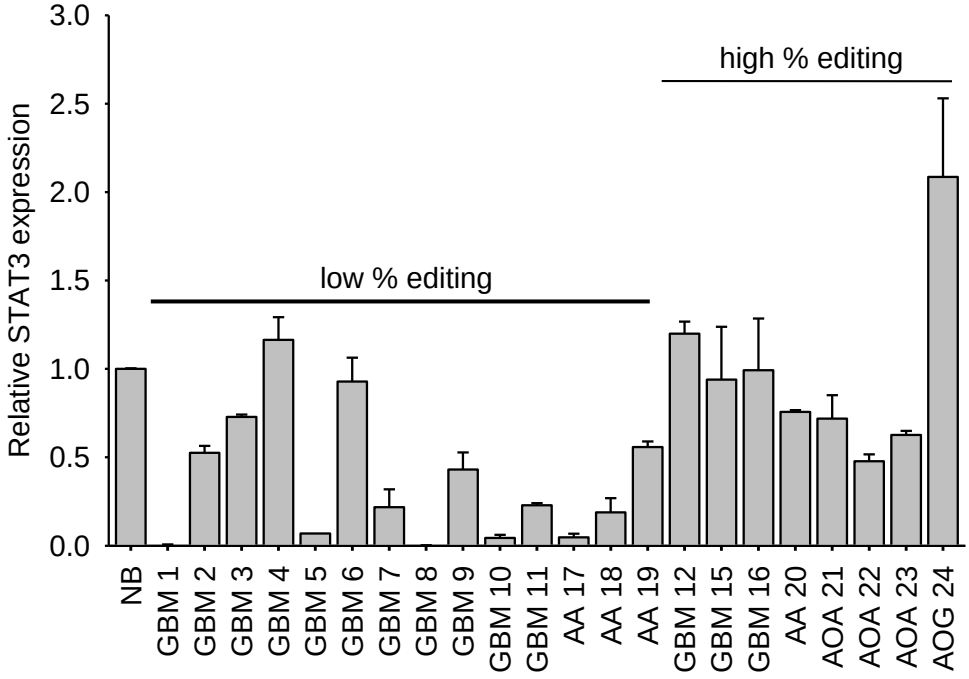

Figure 6.8 Correlation between STAT3 mRNA and miR-376a* editing frequency in glioma samples. Quantification of *STAT3* mRNA levels by qRT-PCR in normal brain (NB) and 22 tumor samples. Samples were grouped by % editing of miR-376a*. high % editing: >12% editing. In samples with low % editing it is inferred that levels of miR-376*A are higher compared to samples with high % editing. Data represents mean ± SD.

6.5 Inhibition of STAT3 function promotes cell migration

STAT3 has been reported to function as a tumor suppressor in PTEN-deficient glioblastomas (de la Iglesia et al., 2009). U87 and SW1783 glioma cells both exhibit PTEN-deficiency as noted from the Catalogue of Somatic Mutations In Cancer database (Bamford et al., 2004; de la Iglesia et al., 2008a). In the context of the findings reported in this thesis, as miR-376a*A promotes glioma cell migration and negatively regulates STAT3, STAT3 should assume an inhibitory role in cell migration. As such, attempts were made to silence *STAT3* using siRNA to assess its effects on migration, a prerequisite for invasion. However, *STAT3* knockdown by siRNA even at low doses (0.625 nM) resulted in cell death, making any effects on cell migration secondary to the effects on cell viability and hence not a reliable measurement. Additionally by Western blot it was determined that siRNA-mediated knockdown of STAT3 caused significantly more depletion of STAT3 protein than did miR-376a*A treatment, and it was difficult to observe a dose-dependence even when the dose was varied 80-fold, suggesting limits to the ability to adjust dose (Figure 6.9). As such, this imposed limitations on the use of STAT3 siRNA to phenocopy the effects of miR-376a*A expression.

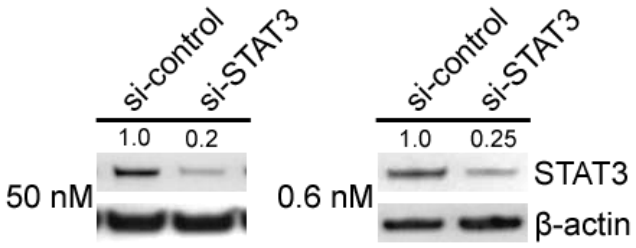

Figure 6.9 siRNA-mediated knockdown of STAT3. U87 cells were transfected with high (50 nM) or low (0.625 nM) dose of siRNA and STAT3 protein knockdown was assessed by Western blot. ß-actin was used as loading control. Densitometric analysis was done by Image J software and protein amounts are shown relative to control siRNA (si-control).

To overcome these issues, we took advantage of a small-molecule inhibitor of STAT3 function, Stattic for blocking STAT3 function (Schust et al., 2006). At a relatively low dose (0.05-0.5 μM) where cell viability was not adversely affected, Stattic treatment significantly increased migration in both U87 and SW1783 cells (Figure 6.10A). As Stattic does not reduce the levels of total STAT3 protein but inhibits phosphorylation at tyrosine 705 and subsequent dimerization (and nuclear translocation), the levels of phosphorylated STAT3 (p-STAT3) was quantified in treated cells. In U87 and SW1783 cells, the levels of p-STAT3 were reduced to similar levels (70%) in both conditions that promote cell migration, miR-376a*A transfection and 0.05-0.5 μM Stattic treatment (Figure 6.10B). These data suggest that partial but not total inhibition of STAT3 function promotes glioma cell migration. In summary, STAT3 is a target specific to the unedited miR-376a* which accumulates in GBMs and partial inhibition of STAT3 function by miR-376a*A or by specific STAT3 inhibitor promotes glioma cell migration in vitro.

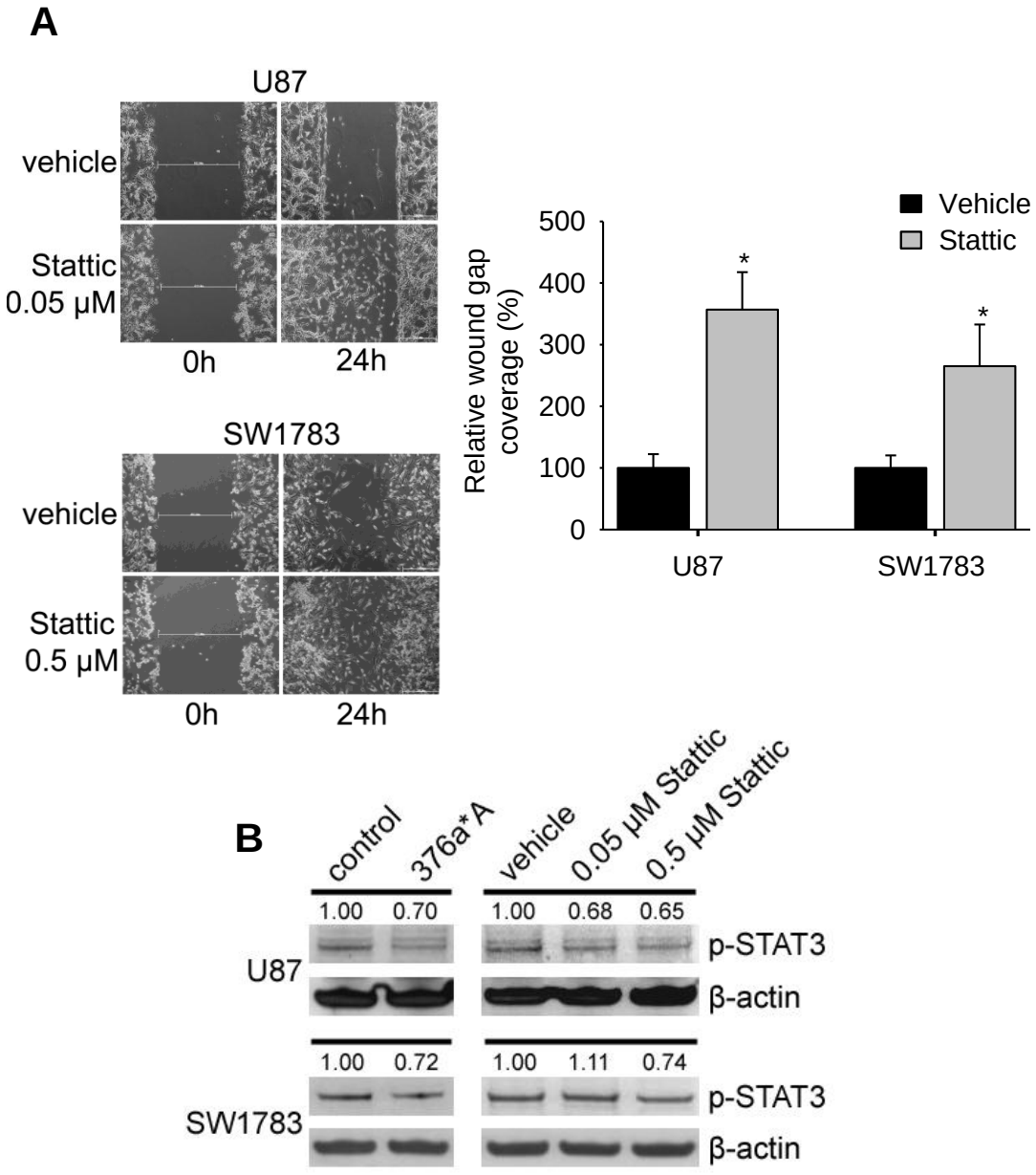

Figure 6.10 Inhibition of STAT3 activity promotes glioma cell migration. ***A.*** Inhibition of STAT3 activity by small molecule inhibitor Stattic promotes migration of U87and SW1783 cells in a wound-healing assay. Images were taken at indicated time-points after wound was made to a confluent cell monolayer and indicated concentrations of Stattic were added to the replacement medium. Graph shows relative % wound gap closure. Data represents mean ± SD. *p<0.05 by t-test. ***B.*** Immunoblotting of phosphorylated STAT3 (p-STAT3) in miR-376a*A-transfected and Stattic-treated cells. ß-actin was used as loading control. Densitometric analysis was done by ImageJ. p-STAT3 amounts are shown relative to control miRNA or to vehicle (DMSO)-treated cells.

6.6 AMFR is specifically targeted by edited miR-376a*

Using the strategy described previously, a specific target of miR-376a*G was identified next. The autocrine motility factor receptor (AMFR) represents a potential specific target of miR-376a*G, 'untargetable' to miR-376a*A .The 3'UTR of *AMFR* harbours two predicted conserved binding sites for miR-376a*G, while none were predicted for miR-376a*A (Figure 6.11A). The folding energies for the predicted heteroduplex are shown in Figure 6.11B. Conservation of one of the two predicted sites is high across mammalian species, but a single mismatch (C-to-T) in the seed region for the second binding site is present in all species except *H. sapiens* (Figure 6.11C). As a consequence of this mismatch, this binding site is no longer accessible (by computational prediction) to miR-376a*G but interestingly, becomes' accessible' to miR-376a*A.

Also, the two predicted sites for miR-376a*G overlap one another. It is possible that only one of the two sites is functional as it is unlikely that both predicted sites can be simultaneously occupied by miRNA; binding of miRNA to one site will occupy a portion of the binding region of the second site preventing its binding.

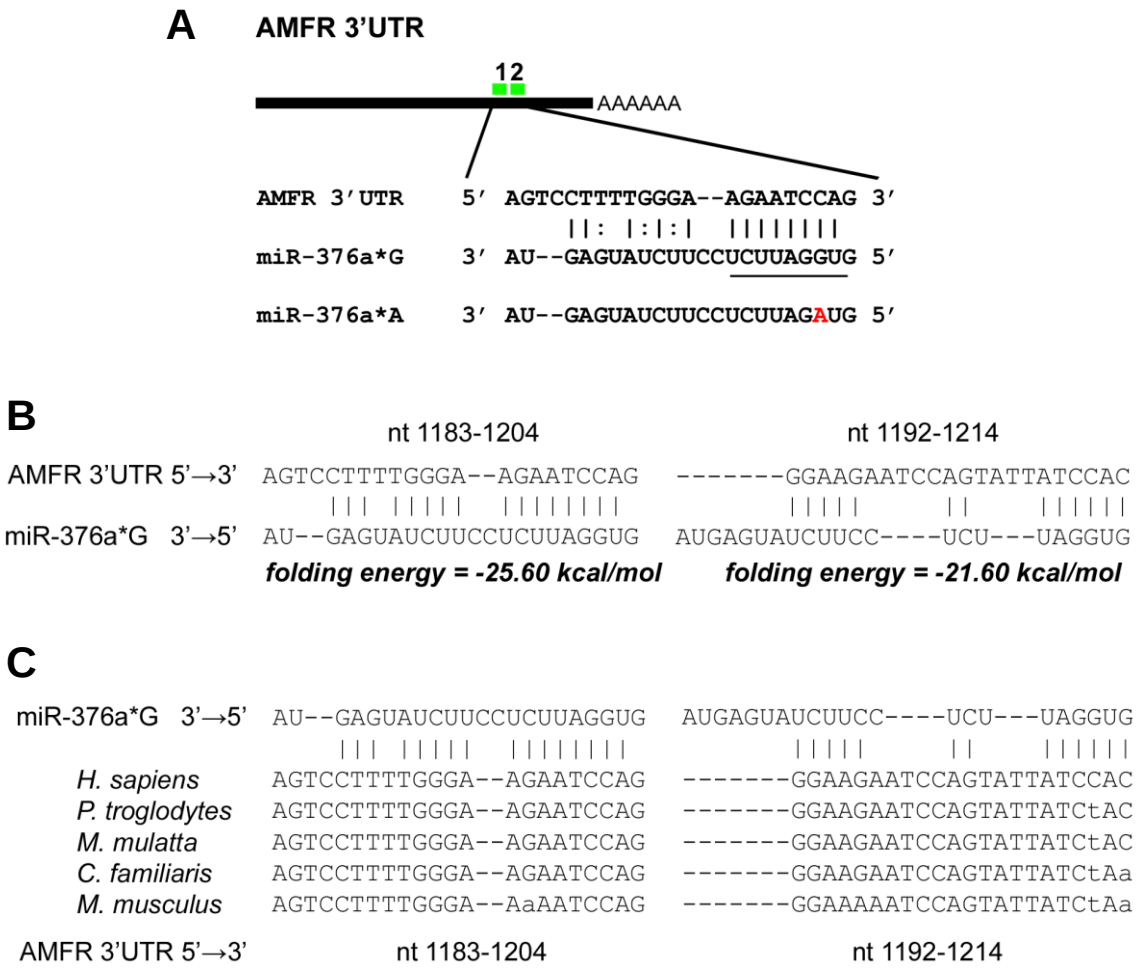

Figure 6.11 Conserved miR-376a*G binding sites in AMFR 3'UTR. ***A.*** Schematic representation of *AMFR* 3'UTR. Green bars show predicted miR-376a*G-binding sites. No binding sites for miR-376a*A were predicted, Sequence of binding site 1 is shown aligned to miR-376a*G and seed region in underlined. Single base difference between miR-376a*G and 376a*A is highlighted. ***B.*** Folding energies of predicted miRNA:mRNA heteroduplexes between miR-376a*G and *AMFR* 3'UTR ***C.*** Alignment of potential miR-376a*G binding sites in *AMFR* 3'UTRs of different species indicating evolutionary conservation. Non-conserved residues within binding region are written in lowercase. nt: nucleotide position in 3'UTR.

To validate targeting of *AMFR* 3'UTR by miR-376a*G, luciferase reporter assays were carried out. Two luciferase reporter vectors were constructed for AMFR, first, fused to full-length 1411 bp AMFR *3'UTR* and second, containing or partial 417 bp *AMFR* 3'UTR (Figure 6.12A). In the luciferase reporter assay, only miR-376a*G was able to suppress luciferase expression by 50% for both reporter constructs, compared to control miRNA and miR-376a*A (Figure 6.12B). There was no

measurable difference between the degree of luciferase suppression by miR-376a*G when using the partial or full-length constructs, suggesting that extending the 3'UTR to include potential endogenous miRNA bindings sites did not mask the suppressive effect of miR-376a*G. As expected with redirection of targeting specificity, miR-376a*A was unable to target the 3'UTR of *AMFR*. This confirms that the single base difference between miR-376a*G and miR-376a*A determines the specificity of targeting of *AMFR* in an "on/off" manner.

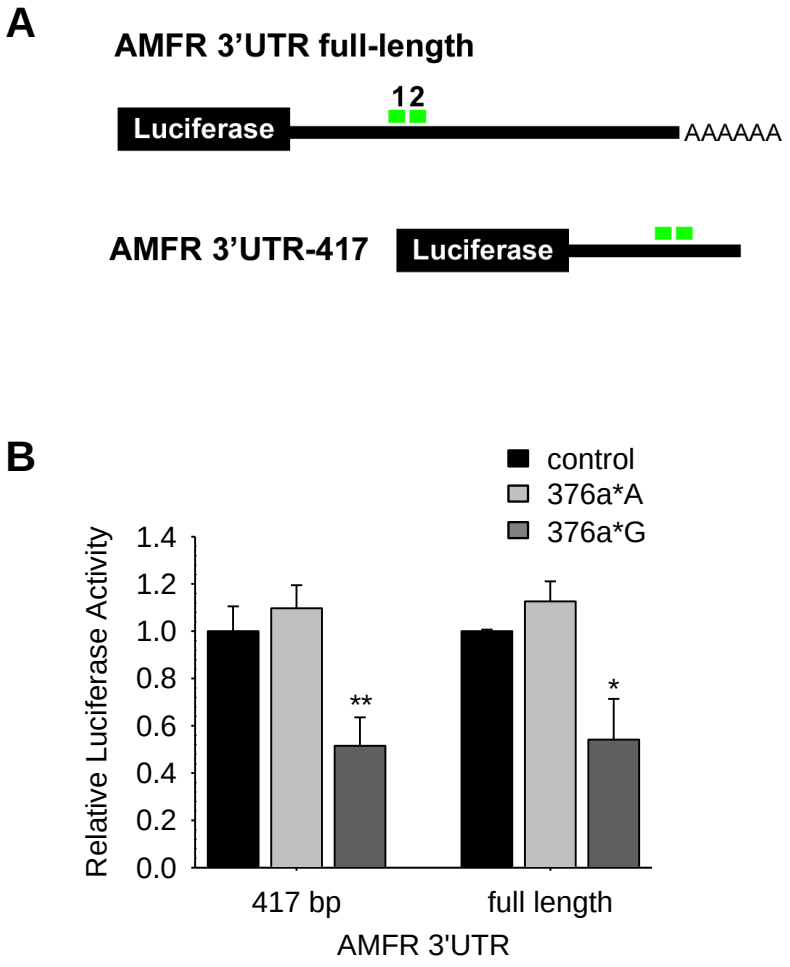

Figure 6.12 Specific targeting of AMFR 3'UTR by miR-376a*G*. *A.* Two luciferase reporter constructs used for verification of *AMFR* targeting by miR-376a*G. Green bar shows predicted miR-376a*G binding site within 3'UTR. AMFR 3'UTR full-length indicates the whole 1411 bp AMFR 3'UTR. AMFR 3'UTR-417 represents a 417 bp fragment of the AMFR 3'UTR. ***B.*** Targeting of *AMFR* 3'UTR by miR-376a*G. Luciferase reporter constructs for partial or full-length AMFR 3'UTR were cotransfected with miR-376a* or control miRNA in HeLa cells. Luciferase readings were normalized to ß-galactosidase activity and for each construct, expressed relative to readings for control miRNA. Data represents mean ± SD. *p<0.05 and **p<0.01 by t-test vs. control.

At the mRNA level it was confirmed that both miR-376a*G and miR-376a*I were able to down-regulate AMFR mRNA by ~50% (Figure 6.13A). Accordingly, protein levels of AMFR were robustly suppressed (40-70%) by miR-376a*G but not by miR-376a*A (Figure 6.13B). However, in tumor samples, a direct correlation between editing frequency of miR-376a* and absolute *AMFR* mRNA levels could not be found, suggesting in tumors protein accumulation of AMFR may be more sensitive to miR-376a*G regulation (not shown).

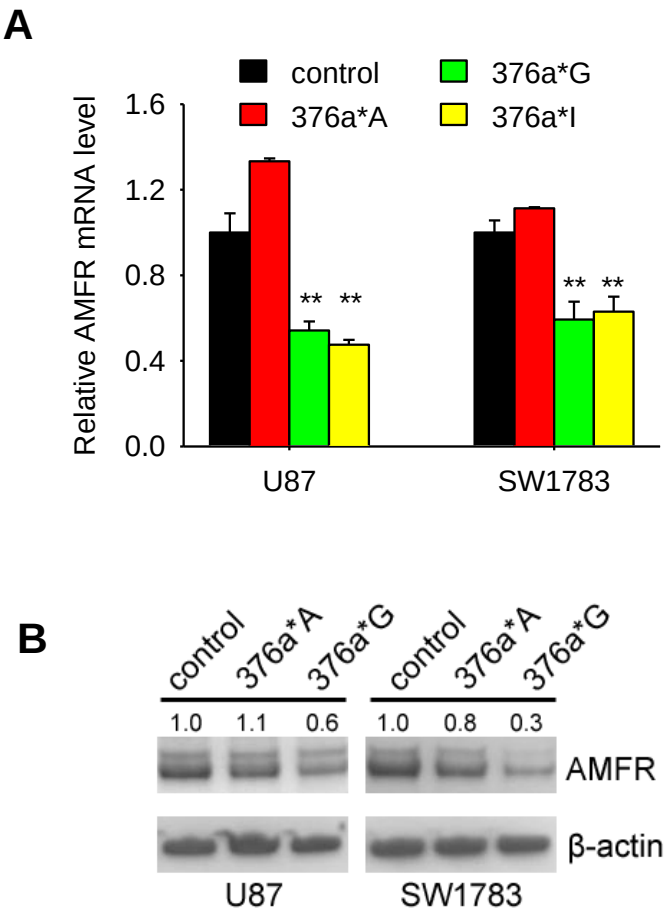

Figure 6.13 Specific mRNA and protein down-regulation of AMFR by miR-376a*G*. *A.* Quantification of AMFR expression by qRT-PCR in transfected glioma cells. 18S rRNA was used for normalization. Data represents mean ± SD. **p<0.01 by t-test vs. control. ***B.*** Immunoblotting for total AMFR levels in transfected glioma cells. ß-actin was used as loading control. Densitometric analysis was done by Image J software and protein amounts are shown relative to control miRNA.

6.7 Knockdown of AMFR inhibits glioma cell migration

As a receptor for the tumor autocrine motility factor, AMFR has been shown to promote sarcoma metastasis (Tsai et al., 2007) and is present in high-grade astrocytomas (Tanizaki et al., 2006). Given that AMFR is a specific target of miR-376a*G and miR-376a*G is able to reduce migration ability of glioma cells, blocking the function of AMFR is expected to produce a similar phenotype of suppressed migration.

Knockdown of AMFR by low concentration of siRNA (0.625 nM) was done in U87 and SW1783 cells. This suppressed migratory ability of U87 and SW1783 cells to nearly half of control siRNA-transfected cells, as assessed in a wound-healing assay (Figure 6.14A). Knockdown of AMFR protein by siRNA even at 0.625 nM concentration of siRNA was highly effective as confirmed by Western blotting (Figure 6.14B). As it is technically challenging to lower the dose of siRNA further because of limitations of transfection reagents and as this dose did not affect cell viability, attempts were not made to further lower the dose of siRNA used to achieve a more moderate knockdown of AMFR.

Thus, reduction in AMFR protein by siRNA, as by miR-376a*G, is able to inhibit glioma cell migration. In summary, AMFR is a target specific to the edited miR-376a*, which is normally present in the brain but due to altered A-to-I editing is not present in GBMs. Due to this, the regulation of AMFR by miR-376a*G is lost, enhancing the migration of glioma cells.

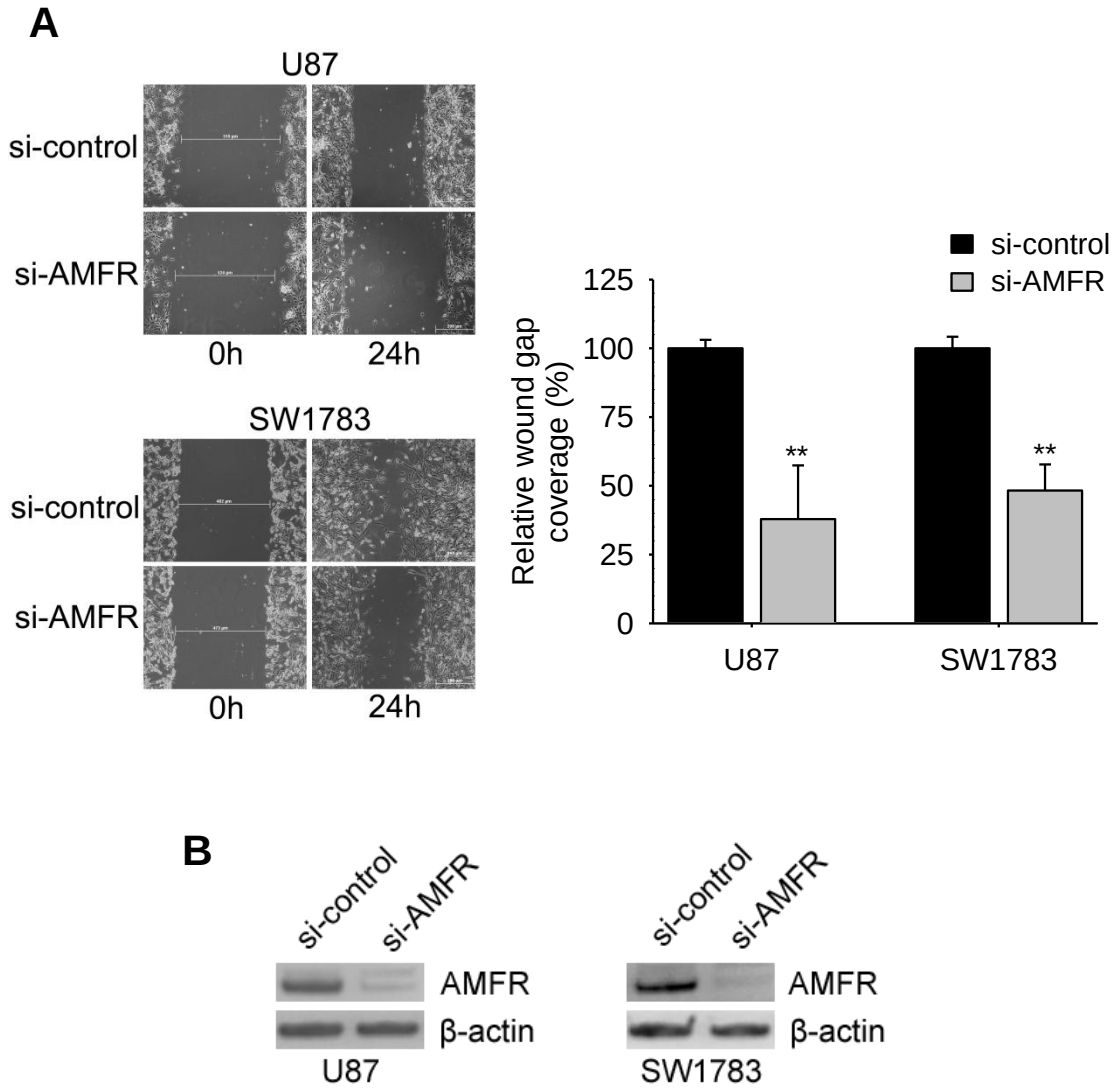

Figure 6.14 Inhibition of AMFR inhibits glioma cell migration. ***A.*** Knockdown of AMFR by siRNA (si-AMFR) suppresses migration of U87and SW1783 cells in a wound-healing assay. Images were taken at indicated time-points after wound was made to a confluent monolayer of trasfected cells. si-control: control siRNA. Graph shows relative % wound gap closure. Data represents mean ± SD. **p<0.01 vs. control. ***B.*** Immunoblotting of AMFR protein in glioma cells transfected with 0.625 nM AMFR siRNA or control siRNA (si-control).

In order to demonstrate in vivo specificity of targeting by miRNAs, *AMFR* and *STAT3* mRNA levels were measured in xenograft tumors formed by U87 cells expressing miR-376a*A or miR-376a*G. The target of edited miR-376a*, *AMFR* was relatively lower in U87/376a*G tumors, and the target of unedited miR-376a*, *STAT3* was lower in U87/376a*A tumors, confirming the expected specificity of targeting in vivo (Figure 6.15). The expression data coincides with the observed features of U87/376a*A tumors formed in vivo which displayed overall greater aggressiveness and invasion, as would be expected of tumors formed by highly migratory and invasive cells. Together, these results suggest that blocking the migration-promoting effect of AMFR by miR-376a*G accounts for its anti-migratory property. More importantly, the data suggests that in addition to its ability to target STAT3, the inability of miR-376a*A to target AMFR may further contribute to its pro-migratory and pro-invasive property.

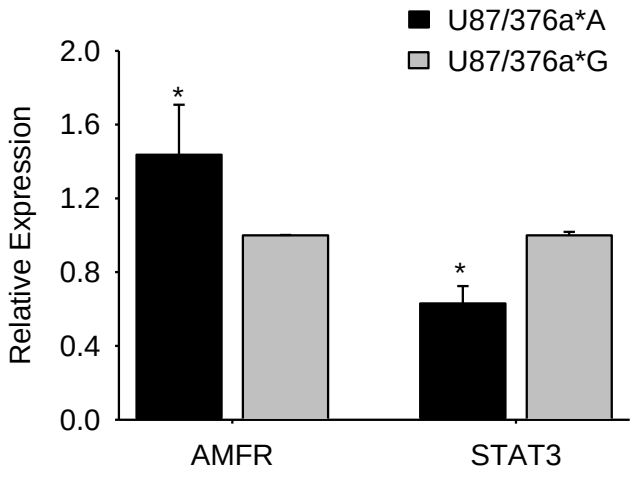

Figure 6.15 Relative expression of AMFR and STAT3 mRNA in xenograft tumors formed by U87 cells stably expressing miR-376a*. U87/376a*A cells stably express miR-376a*A and U87/376a*G cells stably express miR-376a*G. (Section 4.7). RNA was isolated from tumor sections. 18S rRNA was used for normalization. Values are relative to gene expression in U87/376a*G. Data represents mean ± SD. *p<0.05 by t-test vs. U87/376a*G.

Attenuated A-to-I editing in glioma may exert a dual effect: increased inhibition to the migration-restraining effect of STAT3 by the accumulation of unedited miR-376a* (miR-376a*A) coupled with failure in blocking AMFR function of promoting cell migration due to the decrease of edited miR-376a* (miR-376a*G/I) level, as summarized in Figure 6.16. These effects may collectively contribute to the migratory and invasive properties of GBMs.

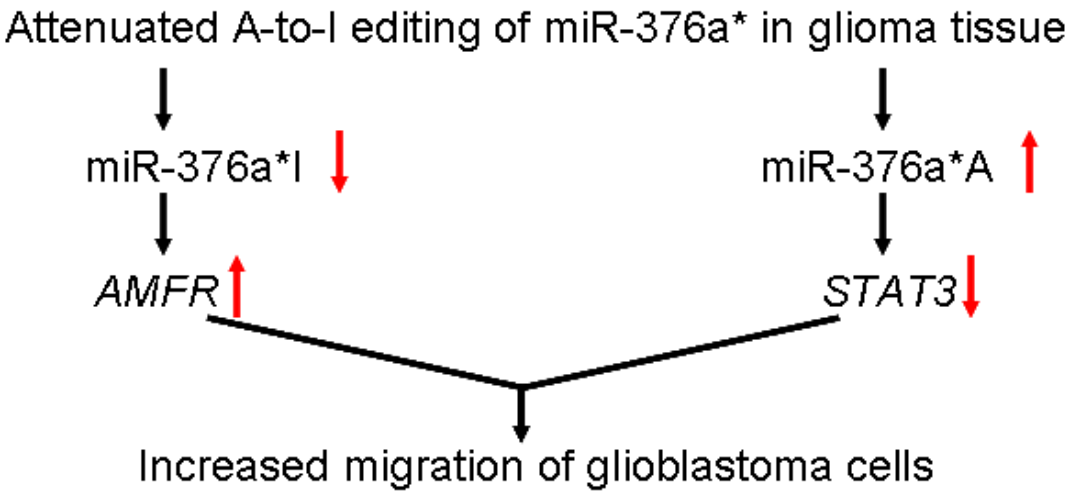

Figure 6.16 Schematic diagram summarizing the roles of AMFR and STAT3 in glioblastoma migration. Summary of findings indicating opposite roles of AMFR and STAT3 in regulating glioma cell migration, being subject to regulation by miR-376a*. When A-to-I editing of miR-376a* is attenuated in glioblastoma, the accumulation of unedited miR-376a* (miR-376a*A) down-regulate STAT3 while a decreased level of edited miR-376a* (miR-376a*I) leads to up-regulation of AMFR, collectively resulting in increased migration of glioblastoma cells.

6.8 Discussion

The presence of unedited and edited variants of miR-376a* in diseased and normal states respectively suggest that each form establishes a distinct cell-type specific transcriptome, subject to alteration with miRNA sequence alteration. Using enforced miRNA expression in glioma cell lines, genes that are down-regulated by miR-376a*A and miR-376a*G respectively were identified, representing elements of the transcriptome subject to regulation by each miRNA. In agreement with redirection of target gene specificity by miRNA seed sequence editing, few genes were found to be under common regulation by miR-376a*A and miR-376a*G (Kawahara et al., 2007b). Using a combination of microarray-based target gene analysis and computational prediction of miRNA-binding sites, specific target genes for each miRNA form were identified to account for their function in glioma cells.

STAT3 was identified as a specific target of unedited miR-376a*, through down-regulation of which, the pro-migratory program of this miRNA is enacted. STAT3 is a member of the STAT (Signal Transducers and Activators of Transcription) family of transcription factors that serve as signaling hubs downstream of extracellular signaling molecules including cytokines (Levy and Darnell, 2002). As a transcription factor mediating growth factor and cytokine signaling, STAT3 regulates cell growth, differentiation and survival (Hirano et al., 2000; Takeda and Akira, 2000) and has been linked to oncogenesis (Bromberg, 2002; Calo et al., 2003). Critically, STAT3 plays a crucial role in the differentiation of neural stem cells (NSCs) to astrocytes (Bonni et al., 1997; Rajan and McKay, 1998).

The role of STAT3 in GBM pathology is controversial as it can act as either an oncogene or a tumor suppressor depending on the genetic context of tumors (de la Iglesia et al., 2008b; de la Iglesia et al., 2009). In PTEN-deficient tumors STAT3 acts as a tumor suppressor but in tumors with EGFR mutation (EGFRvIII), STAT3 acts as an oncogene.

As reported in this thesis, at least in the context of cellular migration, suppression of STAT3 function has a pro-migratory effect. It has been shown that STAT3 knockout transforms normal mouse astrocytes, increasing their proliferation rate, invasiveness and tumor-forming ability (de la Iglesia et al., 2008b). Furthermore, in glioma cells, introduction of constitutively active STAT3 suppressed cellular proliferation and invasiveness (de la Iglesia et al., 2008a). While a basal level of endogenous phospho-STAT3 (Tyr 705), presumably still signaling-competent, was detected for PTEN-deficient U87 and A172 glioma cells, the effects of suppression of endogenous STAT3 in these cells was left unexplored (de la Iglesia et al., 2008a). This thesis extends these findings by showing that partial inhibition of the endogenous level of phospho-STAT3 using a small-molecule inhibitor promotes migration of U87 and SW1783 cells. It is noteworthy that both U87 and SW1783 cells are PTEN-negative. Further investigation into these observations will need to be carried out in a larger panel of glioma cell lines.

In contradiction to the findings presented here, studies have shown that inhibition of STAT3 by siRNA, curcumin and small-molecule inhibitors AG490 and JSI-124 can inhibit proliferation, migration and invasion of glioma cells (Chen et al., 2010; Liu et al., 2010; Senft et al., 2011; Weissenberger et al., 2010). For these studies, it cannot be ruled out that the observed effect on migration/invasion were partly due to cell death induced by the treatment. Further, curcumin, JSI-124 (cucurbitacin I) and AG490 have pleiotropic effects on several signaling pathways and are not specific inhibitors of STAT3, as demonstrated by their successful application in the inhibition of other signaling pathways (Aggarwal et al., 2003; Caceres-Cortes, 2008; Sun et al., 2005). Thus, although these compounds have potent anti-cancer effects, it is difficult to attribute the observed reduction in glioma cell migration and invasion solely to STAT3 suppression. On the other hand, in this study, small-molecule STAT3 inhibitor, Stattic was used as it is highly specific for STAT3. Stattic binds to the SH2 domain of

STAT3, required for both tyrosine phosphorylation and dimerization for nuclear translocation, and does not affect activation or levels of other members of the Jak/STAT pathway (Schust et al., 2006). Thus, the use of inhibition methods with varying specificities, and the low concentration of Stattic used to achieve partial STAT3 inhibition are likely the reasons the results diverge from some of the previous studies.

Evidence for a cytostatic effect in contrast to the oncogenic role assumed for STAT3 in gliomas comes from differentiation studies. Activation of STAT3 is required for differentiation of glioblastoma-initiating cells (GICs) to both astrocytes and oligodendrocytes following exposure to LIF or IFN-ß, respectively (Lee et al., 2008b; Yuki et al., 2009). By effectively reducing the pool of tumor-initiating cells due to differentiation, animals receiving injection of GICs primed for differentiation had much better survival compared to those injected with GICs unable to undergo differentiation – translating to a role for STAT3 in reducing tumorigenecity of GICs. In terms of mechanism of cancer cell migration and invasion, STAT3 dominant negative mutant, which cannot be phosphorylated, was shown to induce a constitutive pro-invasive activity in human colonic and kidney cancer cells, while the constitutively active form of STAT3 was permissive to invasion through HGF/c-Met signaling (Rivat et al., 2004). It is interesting to note that in the absence of any external signaling, cells in which STAT3 function was abrogated had a much higher migration rate than those with wild-type STAT3. It was reasoned that STAT3 regulates both positive and negative regulators of invasion in tumor cells, maintaining a balance between the two. Whether this applies to glioma cells will need to investigated in the future and can potentially address the dichotomous role of STAT3 in gliomas. The narrow range of phosphorylated STAT3 reduction by miR-376a*A or by Stattic, necessary to promote migration in glioma cells in the curent study, is in line with the hypothesis of a balance of positive and negative factors under the common control of STAT3.

Due to the change in miRNA sequence by altered editing, target genes that would normally be accessible to the edited miR-376a*, become ‘untargetable’ in GBMs, further contributing to disruption of miRNA function. One such target identified here is the autocrine motility factor receptor (AMFR), a target specific to edited miR-376a* in gliomas. A mechanistic role for AMFR in promotion of glioma cell migration and invasion has not yet been demonstrated. Nonetheless, it has been shown that in normal brain tissue, there is no expression of AMFR or AMF in glial cells, while abundant mRNA levels of both are found in majority of grade III astrocytomas and GBMs (Tanizaki et al., 2006). The observation that AMFR positivity is particularly abundant in pseudopalisading cells in necrotic region suggests that actively migrating glioma cells express AMFR (Brat et al., 2004). AMFR expression correlates with poor prognosis in several carcinomas due to increased invasion and metastatic predisposition (Hirono et al., 1996; Maruyama et al., 1995; Takanami et al., 2001). The autocrine cytokine AMF is known to produce directional and random motility in tumor cells (Liotta et al., 1986). Significantly, in this thesis, it was demonstrated for the first time that knockdown of AMFR is sufficient to inhibit migration of glioma cells. At the mRNA level a direct correlation of editing frequency of miR-376a* and AMFR expression in human gliomas could not be established. It cannot be ruled out that there exists such a correlation at the protein level. This will need to be further investigated. Nonetheless, the abolishment of edited miR-376a* function due to loss of editing could be additionally responsible for promotion of migration of glioma cells.

In summary, based on miRNA targeting of STAT3 and AMFR, the redirection of target gene specificity of miR-376a* was confirmed in glioma cells. Significantly, this redirection mediated by a single base change in miRNA seed sequence was shown to have functional consequences in promoting glioma cell migration. The consequence of altered editing of miR-376a* is based on the dual effect of aberrantly garnered ability to target STAT3 and the inability to target AMFR.

7 CHAPTER 7. General discussion

The aim of this thesis was to establish a link between post-transcriptional regulation of miRNAs by A-to-I editing and tumorigenesis. It is known that in the normal adult brain, miRNAs from miR-376 cluster undergo regulated high-level seed sequence editing that specifically replaces an adenosine with inosine, which possesses the same base-pairing affinities as guanosine. As A-to-I editing is generally misregulated in GBMs, it was hypothesized that among several substrates of ADAR enzymes, miRNAs are critical mediators of ADAR dysfunction that regulate tumor growth and invasiveness. The main findings of this study support a role for altered A-to-I editing of miRNAs in promoting GBM invasiveness.

7.1 Summary and conclusions

In Chapter three, it was first established that in comparison to normal brain, A-to-I editing of miRNAs from miR-376 cluster is significantly reduced in high-grade gliomas, including GBMs due to low expression of ADARs. Consequently, the seed sequence of mature miRNAs are underedited or unedited in gliomas, contributing to a miRNA sequence composition distinct from that in the normal situation. Furthermore, among various cell types of the brain, normal astrocytes were found to have high level (nearly 100%) editing of mature miRNAs. In gliomas, the various editing sites within miR-376 cluster demonstrate variable extents of loss of editing, but some sites are more affected than others. From the analysis of twenty-four human glioma samples, it was observed that specifically, miR-376a* aberrantly accumulates entirely in the unedited form in GBMs.

To investigate the consequences of aberrant accumulation of unedited miR-376a* in GBMs, in Chapter four, functional analysis of this miRNA was carried out. First, it was demonstrated that during the establishment of a highly invasive glioma cell population from parental non-invasive cells using the experimental lung metastasis (ELM) assay, unedited miR-376a* was specifically enriched, paralleling its

accumulation in human GBMs. Furthermore, in glioma cell lines, introduction of unedited miR-376a* (adenosine-containing form) promoted their migration and invasion *in vitro*. Remarkably, edited miR-376a*, differing by a single base in the seed sequence (guanosine-containing form) was able to suppress these features. Additionally, knockdown of unedited miR-376a* in highly invasive ELM cells was sufficient to suppress their highly-migratory property. Using the orthotopic glioma model, it was also established that the expression of unedited miR-376a* promotes invasive tumor growth by otherwise non-invasive U87 glioma cells. These tumors also recapitulated features of human GBMs such as necrosis and high degree of vascularization. Thus, unedited miR-376a* is a functional tumor specific- sequence variant, the aberrant accumulation of which, promotes malignant properties of glioma cells.

In Chapter five, a genome-wide transcriptome analysis was undertaken to delineate the differences in cellular effects of unedited miR-376a* and edited miR-376a* which oppositely regulated glioma cell migration and invasion. This analysis showed that although differing by only a single base unedited and edited miR-376a* produce highly distinct gene expression changes in glioma cells with remarkably limited overlap. Specifically, unedited miR-376a* causes the up-regulation of gene clusters associated with invasion, motility and angiogenesis in agreement with its ability to promote cell invasion and induce aggressive tumor growth.

In Chapter six, the mechanism underlying the invasion-promoting effect of miR-376a* was investigated by identifying its target gene specificity in glioma cells. Based on the redirection of target gene specificity due to seed sequence modification by A-to-I editing, targets genes exclusively targeted by unedited or by edited miR-376a* were identified to account for their cellular effects of respectively, promoting and suppressing glioma cell migration and invasion. STAT3 was identified as a specific target of unedited miR-376a* as *STAT3* 3’UTR could only be targeted by unedited

miR-376a* and mRNA and protein levels of STAT3 were down-regulated only by unedited miR-376a*. Furthermore, specific inhibition of STAT3 by a small-molecule inhibitor, was able to promote cell migration, phenocopying the effects of unedited miR-376a* on cell migration. Thus, STAT3 is a migration-suppressing gene in GBMs, the down-regulation of which, by unedited miR-376a* promotes glioma cell migration.

AMFR was identified as a target gene of edited miR-376a*. *AMFR* 3'UTR was targeted only by edited miR-376a*, remaining 'untargetable' to unedited miR-376a*. Similarly, mRNA and protein levels of AMFR were diminished only by edited miR-376a* while unedited miR-376a* had no effects on these. Furthermore, specific knockdown of AMFR by RNA interference suppressed the migration of glioma cells phenocopying the effects of edited miR-376a* on cell migration. Significantly, these results suggest a dual effect of attenuated A-to-I editing in GBMs: increased inhibition of the migration-restraining effect of STAT3 by the accumulation of unedited miR-376a*coupled with failure in blocking AMFR function of promoting cell migration due to the decrease of edited miR-376a* level. These effects likely collectively contribute to the migratory and invasive properties of GBMs.

In summary, this study demonstrates for the first time that A-to-I editing of miRNAs in gliomas in altered and this has significant functional consequences in promoting malignant properties of glioma cells, mediated through the function of unedited miRNA sequence variants present in glioma cells.

7.2 Significance

7.2.1 miRNA sequence variations in cancer

The sequence of mature miRNAs dictates potent modulation of several target genes simultaneously and thus, harbours enormous potential both for normal regulation and for malignant exploitation. A significant contribution of this study is in the identification of a functional miRNA sequence variant in human cancers. The presence of mature

miRNA sequence variants has long been speculated (Calin and Croce, 2006; Kloosterman and Plasterk, 2006), but specific examples of genome-derived functional miRNA polymorphisms or mutations have thus far not been identified or functionally characterized, possibly due to their rare occurrence (Saunders et al., 2007). In this study, the “epigenetic space” generated by post-transcriptional processes such as A-to-I editing was considered a source of miRNA sequence variation introduced in a regulated and functionally-relevant manner. Accordingly, due to loss of regulated A-to-I editing, one of the miRNAs regulated by editing- miR-376a*- was shown to be present as the unedited variant in glioma cells and as the edited variant in normal cells. Recently, sequencing studies have determined that other than miRNAs from miR-376 cluster editing of mature miRNAs itself is also very rare (de Hoon et al., 2010). Therefore, the example of sequence variation due to aberrant A-to-I editing uncovered in this study may represent an exceptional and important case of tumor specific miRNA sequence variations. It is also noteworthy that even among miRNAs from miR-376 cluster, only miR-376a* demonstrated a consistently negligible level of editing in GBMs. Therefore, specifically, unedited miR-376a* may be a major regulator of GBM progression.

7.2.2 Regulation of miRNA function by single base change

It was also identified in this study that while unedited miR-376a* promotes glioma cell invasion, edited miR-376a* was able to suppress this feature. While it is conceivable that miRNAs differing by a single base would have distinct but overlapping functions or one of the miRNAs may be non-functional, it was remarkable that these miRNAs in fact have opposite regulatory functions in cancer cells. The unedited miR-376a* may have an important function related to migration in undifferentiated cells such as neural stem cells, and by regulated A-to-I editing this function gets “edited out” in edited miR-376a* which then assumes a migration-suppressing function in fully differentiated cells like astrocytes. In glioma cells, the resurrection of the function of

unedited mR-376a* by attenuated A-to-I editing then allows this miRNA to promote migration. This scenario illustrates a potential post-transcriptional mechanism for elegantly switching and appropriating miRNA functions by just a single base change in the miRNA sequence depending on the cellular environment and differentiation state. Such a mechanism would present several advantages over transcriptional changes to regulatory entities and is in support of a functional role for A-to-I editing of specific substrates instead of genomic recoding of these substrates (Nishikura, 2010; Wahlstedt et al., 2009).

7.3 Future work

From the miR-376 cluster, editing of other sites corresponding to mature miRNAs were also highly reduced in gliomas, although not as consistently as miR-376a*. This includes the site corresponding to mature miR-376a2-5p which shares the seed sequence with miR-376a* and differs by 3 nucleotides in total. Thus, together with miR-376a*, unedited miR-376a2-5p may also have a role in tumor growth and invasiveness. This will need to be further investigated. Also, for other sites a fractional reduction in editing frequency that produces an intermediate ratio of edited to unedited mature miRNA forms in the diseased state may also be of functional relevance but are considerably more challenging to investigate experimentally.

Although A-to-I editing is commonly thought to result in I-to-C pairing it has been suggested that in the context of miRNA function I-to-U and I-to-A wobble base pairs may also be involved (Das and Carmichael, 2007). How and if this relevant to base-pairing of edited miR-376a* will need to be further investigated, as this property of the I-base can potentially expand the target gene repertoire beyond that predictable by current computational methods. The presence of I-A wobble base has not been considered during miRNA binding to mRNAs and will inevitably to be overlooked by the traditional methods of miRNA target gene prediction. Nonetheless, results from previous studies and current investigation imply that I and G have equivalent

functions in miRNA base-pairing with target gene (Borchert et al., 2009; Kawahara et al., 2007a) and substituting G for an I should adequately represent the I-containing miRNA.

The identification of unedited miR-376a* as a pro-invasive factor in GBMs, leads to the possibility of inhibiting its function for therapeutically addressing the greatest challenge in treatment of GBMs - infiltration into the normal brain. Inhibition of miRNAs can be achieved by anti-miRNA molecules such as LNAs, 2'-O-methyl antisense oligos or by the vector-based expression of transcripts antisense to target miRNAs (Garzon et al., 2010). However, in the case of edited miR-376a* knockdown in diseased cells in brain tumors presents considerable challenges as normal cells express unedited miR-376a* differing only by a single base from the target of antagonism. Among potential knockdown systems, LNA molecules can discriminate single-base mismatches in RNA and DNA molecules (Johnson et al., 2004; Lee et al., 2008a), however, their utility in specifically knocking down one of two miRNAs differing by a single base has yet to be demonstrated. Alternatively, considering that restoring ADAR2 activity restored editing of miR-376a* in glioma cells, the introduction of the enzyme in diseased cells can also be considered. However, this is most likely to have effects on several editing substrates and the possibility of creating unwanted or deleterious editing events cannot be ruled out. A related but unanswered question includes how and why ADAR dysfunction occurs in gliomas. Investigation into the identity of regulatory factors of ADARs, either transcriptional, or interactional will be the subject of future studies.

8 References

Aggarwal, B. B., Kumar, A., and Bharti, A. C. (2003). Anticancer potential of curcumin: preclinical and clinical studies. Anticancer Res *23*, 363-398.

Aigner, A. (2011). MicroRNAs (miRNAs) in cancer invasion and metastasis: therapeutic approaches based on metastasis-related miRNAs. J Mol Med (Berl) *89*, 445-457.

Athanasiadis, A., Rich, A., and Maas, S. (2004). Widespread A-to-I RNA editing of Alu-containing mRNAs in the human transcriptome. PLoS Biol *2*, e391.

Babak, T., Zhang, W., Morris, Q., Blencowe, B. J., and Hughes, T. R. (2004a). Probing microRNAs with microarrays: tissue specificity and functional inference. RNA *10*, 1813-1819.

Babak, T., Zhang, W., Morris, Q., Blencowe, B. J., and Hughes, T. R. (2004b). Probing microRNAs with microarrays: Tissue specificity and functional inference. RNA *10*, 1813-1819.

Baek, D., Villen, J., Shin, C., Camargo, F. D., Gygi, S. P., and Bartel, D. P. (2008). The impact of microRNAs on protein output. Nature *455*, 64-71.

Bagga, S., Bracht, J., Hunter, S., Massirer, K., Holtz, J., Eachus, R., and Pasquinelli, A. E. (2005). Regulation by let-7 and lin-4 miRNAs results in target mRNA degradation. Cell *122*, 553-563.

Bamford, S., Dawson, E., Forbes, S., Clements, J., Pettett, R., Dogan, A., Flanagan, A., Teague, J., Futreal, P. A., Stratton, M. R., and Wooster, R. (2004). The COSMIC (Catalogue of Somatic Mutations in Cancer) database and website. Br J Cancer *91*, 355-358.

Bartel, D. P. (2004). MicroRNAs: genomics, biogenesis, mechanism, and function. Cell *116*, 281-297.

Bartel, D. P. (2009). MicroRNAs: target recognition and regulatory functions. Cell *136*, 215-233.

Bass, B. L. (2002). RNA editing by adenosine deaminases that act on RNA. Annu Rev Biochem *71*, 817-846.

Beghini, A., Ripamonti, C. B., Peterlongo, P., Roversi, G., Cairoli, R., Morra, E., and Larizza, L. (2000). RNA hyperediting and alternative splicing of hematopoietic cell phosphatase (PTPN6) gene in acute myeloid leukemia. Hum Mol Genet *9*, 2297-2304.

Behm-Ansmant, I., Rehwinkel, J., Doerks, T., Stark, A., Bork, P., and Izaurralde, E. (2006). mRNA degradation by miRNAs and GW182 requires both CCR4:NOT deadenylase and DCP1:DCP2 decapping complexes. Genes Dev *20*, 1885-1898.

Bernard, A., Ferhat, L., Dessi, F., Charton, G., Represa, A., Ben-Ari, Y., and Khrestchatisky, M. (1999). Q/R editing of the rat GluR5 and GluR6 kainate receptors in vivo and in vitro: evidence for independent developmental, pathological and cellular regulation. Eur J Neurosci *11*, 604-616.

Betel, D., Wilson, M., Gabow, A., Marks, D. S., and Sander, C. (2008). The microRNA.org resource: targets and expression. Nucleic Acids Res *36*, D149-153.

Bigarella, C. L., Borges, L., Costa, F. F., and Saad, S. T. (2009). ARHGAP21 modulates FAK activity and impairs glioblastoma cell migration. Biochim Biophys Acta *1793*, 806-816.

Blow, M. J., Grocock, R. J., van Dongen, S., Enright, A. J., Dicks, E., Futreal, P. A., Wooster, R., and Stratton, M. R. (2006). RNA editing of human microRNAs. Genome Biol *7*, R27.

Bonni, A., Sun, Y., Nadal-Vicens, M., Bhatt, A., Frank, D. A., Rozovsky, I., Stahl, N., Yancopoulos, G. D., and Greenberg, M. E. (1997). Regulation of gliogenesis in the central nervous system by the JAK-STAT signaling pathway. Science *278*, 477-483.

Borchert, G. M., Gilmore, B. L., Spengler, R. M., Xing, Y., Lanier, W., Bhattacharya, D., and Davidson, B. L. (2009). Adenosine deamination in human transcripts generates novel microRNA binding sites. Hum Mol Genet *18*, 4801-4807.

Brat, D. J., Castellano-Sanchez, A. A., Hunter, S. B., Pecot, M., Cohen, C., Hammond, E. H., Devi, S. N., Kaur, B., and Van Meir, E. G. (2004). Pseudopalisades in glioblastoma are hypoxic, express extracellular matrix proteases, and are formed by an actively migrating cell population. Cancer Res *64*, 920-927.

Brennecke, J., Stark, A., Russell, R. B., and Cohen, S. M. (2005). Principles of microRNA-target recognition. PLoS Biol *3*, e85.

Brodersen, P., and Voinnet, O. (2009). Revisiting the principles of microRNA target recognition and mode of action. Nat Rev Mol Cell Biol *10*, 141-148.

Bromberg, J. (2002). Stat proteins and oncogenesis. J Clin Invest *109*, 1139-1142.

Caceres-Cortes, J. R. (2008). A potent anti-carcinoma and anti-acute myeloblastic leukemia agent, AG490. Anticancer Agents Med Chem *8*, 717-722.

Calin, G. A., and Croce, C. M. (2006). MicroRNA signatures in human cancers. Nat Rev Cancer *6*, 857-866.

Calin, G. A., Ferracin, M., Cimmino, A., Di Leva, G., Shimizu, M., Wojcik, S. E., Iorio, M. V., Visone, R., Sever, N. I., Fabbri, M.*, et al.* (2005). A MicroRNA signature associated with prognosis and progression in chronic lymphocytic leukemia. N Engl J Med *353*, 1793-1801.

Calin, G. A., Sevignani, C., Dumitru, C. D., Hyslop, T., Noch, E., Yendamuri, S., Shimizu, M., Rattan, S., Bullrich, F., Negrini, M., and Croce, C. M. (2004). Human microRNA genes are frequently located at fragile sites and genomic regions involved in cancers. Proc Natl Acad Sci U S A *101*, 2999-3004.

Calo, V., Migliavacca, M., Bazan, V., Macaluso, M., Buscemi, M., Gebbia, N., and Russo, A. (2003). STAT proteins: from normal control of cellular events to tumorigenesis. J Cell Physiol *197*, 157-168.

The Cancer Genome Atlas Research Network (2008). Comprehensive genomic characterization defines human glioblastoma genes and core pathways. Nature *455*, 1061-1068.

Cenci, C., Barzotti, R., Galeano, F., Corbelli, S., Rota, R., Massimi, L., Di Rocco, C., O'Connell, M. A., and Gallo, A. (2008). Down-regulation of RNA editing in pediatric astrocytomas: ADAR2 editing activity inhibits cell migration and proliferation. J Biol Chem *283*, 7251-7260.

Chan, A. Y., Coniglio, S. J., Chuang, Y. Y., Michaelson, D., Knaus, U. G., Philips, M. R., and Symons, M. (2005a). Roles of the Rac1 and Rac3 GTPases in human tumor cell invasion. Oncogene *24*, 7821-7829.

Chan, J. A., Krichevsky, A. M., and Kosik, K. S. (2005b). MicroRNA-21 is an antiapoptotic factor in human glioblastoma cells. Cancer Res *65*, 6029-6033.

Chandrasekar, N., Mohanam, S., Gujrati, M., Olivero, W. C., Dinh, D. H., and Rao, J. S. (2003). Downregulation of uPA inhibits migration and PI3k/Akt signaling in glioblastoma cells. Oncogene *22*, 392-400.

Chang, T. C., Yu, D., Lee, Y. S., Wentzel, E. A., Arking, D. E., West, K. M., Dang, C. V., Thomas-Tikhonenko, A., and Mendell, J. T. (2008). Widespread microRNA repression by Myc contributes to tumorigenesis. Nat Genet *40*, 43-50.

Chen, F., Xu, Y., Luo, Y., Zheng, D., Song, Y., Yu, K., Li, H., Zhang, L., Zhong, W., and Ji, Y. (2010). Down-regulation of Stat3 decreases invasion activity and induces apoptosis of human glioma cells. J Mol Neurosci *40*, 353-359.

Chendrimada, T. P., Finn, K. J., Ji, X., Baillat, D., Gregory, R. I., Liebhaber, S. A., Pasquinelli, A. E., and Shiekhattar, R. (2007). MicroRNA silencing through RISC recruitment of eIF6. Nature *447*, 823-828.

Chiang, H. R., Schoenfeld, L. W., Ruby, J. G., Auyeung, V. C., Spies, N., Baek, D., Johnston, W. K., Russ, C., Luo, S., Babiarz, J. E.*, et al.* (2010). Mammalian microRNAs: experimental evaluation of novel and previously annotated genes. Genes Dev *24*, 992-1009.

Chin, L. J., Ratner, E., Leng, S., Zhai, R., Nallur, S., Babar, I., Muller, R. U., Straka, E., Su, L., Burki, E. A.*, et al.* (2008). A SNP in a let-7 microRNA complementary site in the KRAS 3' untranslated region increases non-small cell lung cancer risk. Cancer Res *68*, 8535-8540.

Chintala, S. K., Kyritsis, A. P., Mohan, P. M., Mohanam, S., Sawaya, R., Gokslan, Z., Yung, W. K., Steck, P., Uhm, J. H., Aggarwal, B. B., and Rao, J. S. (1999). Altered actin cytoskeleton and inhibition of matrix metalloproteinase expression by vanadate and phenylarsine oxide, inhibitors of phosphotyrosine phosphatases: modulation of migration and invasion of human malignant glioma cells. Mol Carcinog *26*, 274-285.

Cho, D. S., Yang, W., Lee, J. T., Shiekhattar, R., Murray, J. M., and Nishikura, K. (2003). Requirement of dimerization for RNA editing activity of adenosine deaminases acting on RNA. J Biol Chem *278*, 17093-17102.

Christensen, B. C., Avissar-Whiting, M., Ouellet, L. G., Butler, R. A., Nelson, H. H., McClean, M. D., Marsit, C. J., and Kelsey, K. T. (2010). Mature microRNA sequence polymorphism in MIR196A2 is associated with risk and prognosis of head and neck cancer. Clin Cancer Res *16*, 3713-3720.

Christensen, M., and Schratt, G. M. (2009). microRNA involvement in developmental and functional aspects of the nervous system and in neurological diseases. Neurosci Lett *466*, 55-62.

Ciafre, S. A., Galardi, S., Mangiola, A., Ferracin, M., Liu, C. G., Sabatino, G., Negrini, M., Maira, G., Croce, C. M., and Farace, M. G. (2005). Extensive modulation of a set of microRNAs in primary glioblastoma. Biochem Biophys Res Commun *334*, 1351-1358.

Clark, E. A., Golub, T. R., Lander, E. S., and Hynes, R. O. (2000). Genomic analysis of metastasis reveals an essential role for RhoC. Nature *406*, 532-535.

Corsten, M. F., Miranda, R., Kasmieh, R., Krichevsky, A. M., Weissleder, R., and Shah, K. (2007). MicroRNA-21 knockdown disrupts glioma growth in vivo and displays synergistic cytotoxicity with neural precursor cell delivered S-TRAIL in human gliomas. Cancer Res *67*, 8994-9000.

Croce, C. M. (2009). Causes and consequences of microRNA dysregulation in cancer. Nat Rev Genet *10*, 704-714.

Czech, B., Zhou, R., Erlich, Y., Brennecke, J., Binari, R., Villalta, C., Gordon, A., Perrimon, N., and Hannon, G. J. (2009). Hierarchical rules for Argonaute loading in Drosophila. Mol Cell *36*, 445-456.

Das, A. K., and Carmichael, G. G. (2007). ADAR editing wobbles the microRNA world. ACS Chem Biol *2*, 217-220.

Davis, E., Caiment, F., Tordoir, X., Cavaille, J., Ferguson-Smith, A., Cockett, N., Georges, M., and Charlier, C. (2005). RNAi-mediated allelic trans-interaction at the imprinted Rtl1/Peg11 locus. Curr Biol *15*, 743-749.

de Hoon, M. J., Taft, R. J., Hashimoto, T., Kanamori-Katayama, M., Kawaji, H., Kawano, M., Kishima, M., Lassmann, T., Faulkner, G. J., Mattick, J. S.*, et al.* (2010). Cross-mapping and the identification of editing sites in mature microRNAs in high-throughput sequencing libraries. Genome Res *20*, 257-264.

de la Iglesia, N., Konopka, G., Lim, K. L., Nutt, C. L., Bromberg, J. F., Frank, D. A., Mischel, P. S., Louis, D. N., and Bonni, A. (2008a). Deregulation of a STAT3-interleukin 8 signaling pathway promotes human glioblastoma cell proliferation and invasiveness. J Neurosci *28*, 5870-5878.

de la Iglesia, N., Konopka, G., Puram, S. V., Chan, J. A., Bachoo, R. M., You, M. J., Levy, D. E., Depinho, R. A., and Bonni, A. (2008b). Identification of a PTEN-regulated STAT3 brain tumor suppressor pathway. Genes Dev *22*, 449-462.

de la Iglesia, N., Puram, S. V., and Bonni, A. (2009). STAT3 regulation of glioblastoma pathogenesis. Curr Mol Med *9*, 580-590.

Desterro, J. M., Keegan, L. P., Jaffray, E., Hay, R. T., O'Connell, M. A., and Carmo-Fonseca, M. (2005). SUMO-1 modification alters ADAR1 editing activity. Mol Biol Cell *16*, 5115-5126.

Didiano, D., and Hobert, O. (2006). Perfect seed pairing is not a generally reliable predictor for miRNA-target interactions. Nat Struct Mol Biol *13*, 849-851.

Diederichs, S., and Haber, D. A. (2006). Sequence variations of microRNAs in human cancer: alterations in predicted secondary structure do not affect processing. Cancer Res *66*, 6097-6104.

Dixon-McIver, A., East, P., Mein, C. A., Cazier, J. B., Molloy, G., Chaplin, T., Andrew Lister, T., Young, B. D., and Debernardi, S. (2008). Distinctive patterns of microRNA expression associated with karyotype in acute myeloid leukaemia. PLoS One *3*, e2141.

Doench, J. G., and Sharp, P. A. (2004). Specificity of microRNA target selection in translational repression. Genes Dev *18*, 504-511.

Dreyfuss, J. M., Johnson, M. D., and Park, P. J. (2009). Meta-analysis of glioblastoma multiforme versus anaplastic astrocytoma identifies robust gene markers. Mol Cancer *8*, 71.

Du, R., Petritsch, C., Lu, K., Liu, P., Haller, A., Ganss, R., Song, H., Vandenberg, S., and Bergers, G. (2008). Matrix metalloproteinase-2 regulates vascular patterning and growth affecting tumor cell survival and invasion in GBM. Neuro Oncol *10*, 254-264.

Duan, R., Pak, C., and Jin, P. (2007). Single nucleotide polymorphism associated with mature miR-125a alters the processing of pri-miRNA. Hum Mol Genet *16*, 1124-1131.

Duursma, A. M., Kedde, M., Schrier, M., le Sage, C., and Agami, R. (2008). miR-148 targets human DNMT3b protein coding region. RNA *14*, 872-877.

Dykxhoorn, D. M. (2010). MicroRNAs and metastasis: little RNAs go a long way. Cancer Res *70*, 6401-6406.

Eulalio, A., Huntzinger, E., and Izaurralde, E. (2008). Getting to the root of miRNA-mediated gene silencing. Cell *132*, 9-14.

Fang, L., Deng, Z., Shatseva, T., Yang, J., Peng, C., Du, W. W., Yee, A. J., Ang, L. C., He, C., Shan, S. W., and Yang, B. B. (2010). MicroRNA miR-93 promotes tumor growth and angiogenesis by targeting integrin-beta8. Oncogene *30*, 806-821.

Farajollahi, S., and Maas, S. (2010). Molecular diversity through RNA editing: a balancing act. Trends Genet *26*, 221-230.

Farazi, T. A., Horlings, H. M., Ten Hoeve, J. J., Mihailovic, A., Halfwerk, H., Morozov, P., Brown, M., Hafner, M., Reyal, F., van Kouwenhove, M*., et al.* (2011). MicroRNA Sequence and Expression Analysis in Breast Tumors by Deep Sequencing. Cancer Res *71*, 4443-4453.

Feng, Y., Sansam, C. L., Singh, M., and Emeson, R. B. (2006). Altered RNA editing in mice lacking ADAR2 autoregulation. Mol Cell Biol *26*, 480-488.

Feuer, R., Pagarigan, R. R., Harkins, S., Liu, F., Hunziker, I. P., and Whitton, J. L. (2005). Coxsackievirus targets proliferating neuronal progenitor cells in the neonatal CNS. J Neurosci *25*, 2434-2444.

Filipowicz, W., Bhattacharyya, S. N., and Sonenberg, N. (2008). Mechanisms of post-transcriptional regulation by microRNAs: are the answers in sight? Nat Rev Genet *9*, 102-114.

Fomchenko, E. I., and Holland, E. C. (2006). Mouse models of brain tumors and their applications in preclinical trials. Clin Cancer Res *12*, 5288-5297.

Forman, J. J., Legesse-Miller, A., and Coller, H. A. (2008). A search for conserved sequences in coding regions reveals that the let-7 microRNA targets Dicer within its coding sequence. Proc Natl Acad Sci U S A *105*, 14879-14884.

Friedman, R. C., Farh, K. K., Burge, C. B., and Bartel, D. P. (2009). Most mammalian mRNAs are conserved targets of microRNAs. Genome Res *19*, 92-105.

Furnari, F. B., Fenton, T., Bachoo, R. M., Mukasa, A., Stommel, J. M., Stegh, A., Hahn, W. C., Ligon, K. L., Louis, D. N., Brennan, C*., et al.* (2007). Malignant astrocytic glioma: genetics, biology, and paths to treatment. Genes Dev *21*, 2683-2710.

Gabriely, G., Wurdinger, T., Kesari, S., Esau, C. C., Burchard, J., Linsley, P. S., and Krichevsky, A. M. (2008). MicroRNA 21 promotes glioma invasion by targeting matrix metalloproteinase regulators. Mol Cell Biol *28*, 5369-5380.

Gabriely, G., Yi, M., Narayan, R. S., Niers, J. M., Wurdinger, T., Imitola, J., Ligon, K. L., Kesari, S., Esau, C., Stephens, R. M.*, et al.* (2011). Human Glioma Growth Is Controlled by MicroRNA-10b. Cancer Res *71*, 3563-3572.

Galeano, F., Leroy, A., Rossetti, C., Gromova, I., Gautier, P., Keegan, L. P., Massimi, L., Di Rocco, C., O'Connell, M. A., and Gallo, A. (2010). Human BLCAP transcript: new editing events in normal and cancerous tissues. Int J Cancer *127*, 127-137.

Gan, Z., Zhao, L., Yang, L., Huang, P., Zhao, F., Li, W., and Liu, Y. (2006). RNA editing by ADAR2 is metabolically regulated in pancreatic islets and beta-cells. J Biol Chem *281*, 33386-33394.

Gartel, A. L., and Kandel, E. S. (2008). miRNAs: Little known mediators of oncogenesis. Semin Cancer Biol *18*, 103-110.

Garzon, R., Marcucci, G., and Croce, C. M. (2010). Targeting microRNAs in cancer: rationale, strategies and challenges. Nat Rev Drug Discov *9*, 775-789.

Gaur, A., Jewell, D. A., Liang, Y., Ridzon, D., Moore, J. H., Chen, C., Ambros, V. R., and Israel, M. A. (2007). Characterization of microRNA expression levels and their biological correlates in human cancer cell lines. Cancer Res *67*, 2456-2468.

Giese, A., Bjerkvig, R., Berens, M. E., and Westphal, M. (2003). Cost of migration: invasion of malignant gliomas and implications for treatment. J Clin Oncol *21*, 1624-1636.

Gladson, C. L., Prayson, R. A., and Liu, W. M. (2010). The pathobiology of glioma tumors. Annu Rev Pathol *5*, 33-50.

Godlewski, J., Nowicki, M. O., Bronisz, A., Nuovo, G., Palatini, J., De Lay, M., Van Brocklyn, J., Ostrowski, M. C., Chiocca, E. A., and Lawler, S. E. (2010). MicroRNA-451 regulates LKB1/AMPK signaling and allows adaptation to metabolic stress in glioma cells. Mol Cell *37*, 620-632.

Godlewski, J., Nowicki, M. O., Bronisz, A., Williams, S., Otsuki, A., Nuovo, G., Raychaudhury, A., Newton, H. B., Chiocca, E. A., and Lawler, S. (2008). Targeting of the Bmi-1 oncogene/stem cell renewal factor by microRNA-128 inhibits glioma proliferation and self-renewal. Cancer Res *68*, 9125-9130.

Golestaneh, N., and Mishra, B. (2005). TGF-beta, neuronal stem cells and glioblastoma. Oncogene *24*, 5722-5730.

Gott, J. M., and Emeson, R. B. (2000). Functions and mechanisms of RNA editing. Annu Rev Genet *34*, 499-531.

Griffiths-Jones, S., Hui, J. H., Marco, A., and Ronshaugen, M. (2011). MicroRNA evolution by arm switching. EMBO Rep *12*, 172-177.

Griffiths-Jones, S., Saini, H. K., van Dongen, S., and Enright, A. J. (2008). miRBase: tools for microRNA genomics. Nucleic Acids Res *36*, D154-158.

Grimson, A., Farh, K. K., Johnston, W. K., Garrett-Engele, P., Lim, L. P., and Bartel, D. P. (2007). MicroRNA targeting specificity in mammals: determinants beyond seed pairing. Mol Cell *27*, 91-105.

Gu, S., Jin, L., Zhang, F., Sarnow, P., and Kay, M. A. (2009). Biological basis for restriction of microRNA targets to the 3' untranslated region in mammalian mRNAs. Nat Struct Mol Biol *16*, 144-150.

Guil, S., and Caceres, J. F. (2007). The multifunctional RNA-binding protein hnRNP A1 is required for processing of miR-18a. Nat Struct Mol Biol *14*, 591-596.

Guo, H., Ingolia, N. T., Weissman, J. S., and Bartel, D. P. (2010). Mammalian microRNAs predominantly act to decrease target mRNA levels. Nature *466*, 835-840.

Han, J., Lee, Y., Yeom, K. H., Nam, J. W., Heo, I., Rhee, J. K., Sohn, S. Y., Cho, Y., Zhang, B. T., and Kim, V. N. (2006). Molecular basis for the recognition of primary microRNAs by the Drosha-DGCR8 complex. Cell *125*, 887-901.

He, L., He, X., Lim, L. P., de Stanchina, E., Xuan, Z., Liang, Y., Xue, W., Zender, L., Magnus, J., Ridzon, D.*, et al.* (2007). A microRNA component of the p53 tumour suppressor network. Nature *447*, 1130-1134.

He, T., Wang, Q., Feng, G., Hu, Y., Wang, L., and Wang, Y. (2011). Computational detection and functional analysis of human tissue-specific A-to-I RNA editing. PLoS One *6*, e18129.

Heale, B. S., Keegan, L. P., and O'Connell, M. A. (2011). The effect of RNA editing and ADARs on miRNA biogenesis and function. Adv Exp Med Biol *700*, 76-84.

Hendrickson, D. G., Hogan, D. J., McCullough, H. L., Myers, J. W., Herschlag, D., Ferrell, J. E., and Brown, P. O. (2009). Concordant regulation of translation and mRNA abundance for hundreds of targets of a human microRNA. PLoS Biol *7*, e1000238.

Higuchi, M., Maas, S., Single, F. N., Hartner, J., Rozov, A., Burnashev, N., Feldmeyer, D., Sprengel, R., and Seeburg, P. H. (2000). Point mutation in an AMPA receptor gene rescues lethality in mice deficient in the RNA-editing enzyme ADAR2. Nature *406*, 78-81.

Hirano, T., Ishihara, K., and Hibi, M. (2000). Roles of STAT3 in mediating the cell growth, differentiation and survival signals relayed through the IL-6 family of cytokine receptors. Oncogene *19*, 2548-2556.

Hirono, Y., Fushida, S., Yonemura, Y., Yamamoto, H., Watanabe, H., and Raz, A. (1996). Expression of autocrine motility factor receptor correlates with disease progression in human gastric cancer. Br J Cancer *74*, 2003-2007.

Hoelzinger, D. B., Demuth, T., and Berens, M. E. (2007). Autocrine factors that sustain glioma invasion and paracrine biology in the brain microenvironment. J Natl Cancer Inst *99*, 1583-1593.

Hoffman, A. E., Zheng, T., Yi, C., Leaderer, D., Weidhaas, J., Slack, F., Zhang, Y., Paranjape, T., and Zhu, Y. (2009). microRNA miR-196a-2 and breast cancer: a genetic and epigenetic association study and functional analysis. Cancer Res *69*, 5970-5977.

Hu, H. Y., Yan, Z., Xu, Y., Hu, H., Menzel, C., Zhou, Y. H., Chen, W., and Khaitovich, P. (2009). Sequence features associated with microRNA strand selection in humans and flies. BMC Genomics *10*, 413.

Hu, Z., Chen, J., Tian, T., Zhou, X., Gu, H., Xu, L., Zeng, Y., Miao, R., Jin, G., Ma, H.*, et al.* (2008). Genetic variants of miRNA sequences and non-small cell lung cancer survival. J Clin Invest *118*, 2600-2608.

Huang da, W., Sherman, B. T., and Lempicki, R. A. (2009a). Bioinformatics enrichment tools: paths toward the comprehensive functional analysis of large gene lists. Nucleic Acids Res *37*, 1-13.

Huang da, W., Sherman, B. T., and Lempicki, R. A. (2009b). Systematic and integrative analysis of large gene lists using DAVID bioinformatics resources. Nat Protoc *4*, 44-57.

Huang, P., Allam, A., Taghian, A., Freeman, J., Duffy, M., and Suit, H. D. (1995). Growth and metastatic behavior of five human glioblastomas compared with nine other histological types of human tumor xenografts in SCID mice. J Neurosurg *83*, 308-315.

Huntzinger, E., and Izaurralde, E. (2011). Gene silencing by microRNAs: contributions of translational repression and mRNA decay. Nat Rev Genet *12*, 99-110.

Hurst, D. R., Edmonds, M. D., and Welch, D. R. (2009). Metastamir: the field of metastasis-regulatory microRNA is spreading. Cancer Res *69*, 7495-7498.

Huse, J. T., Brennan, C., Hambardzumyan, D., Wee, B., Pena, J., Rouhanifard, S. H., Sohn-Lee, C., le Sage, C., Agami, R., Tuschl, T., and Holland, E. C. (2009). The PTEN-regulating microRNA miR-26a is amplified in high-grade glioma and facilitates gliomagenesis in vivo. Genes Dev *23*, 1327-1337.

Huse, J. T., and Holland, E. C. (2010). Targeting brain cancer: advances in the molecular pathology of malignant glioma and medulloblastoma. Nat Rev Cancer *10*, 319-331.

Hutvagner, G. (2005). Small RNA asymmetry in RNAi: function in RISC assembly and gene regulation. FEBS Lett *579*, 5850-5857.

Ishiuchi, S., Tsuzuki, K., Yoshida, Y., Yamada, N., Hagimura, N., Okado, H., Miwa, A., Kurihara, H., Nakazato, Y., Tamura, M.*, et al.* (2002). Blockage of Ca(2+)-permeable AMPA receptors suppresses migration and induces apoptosis in human glioblastoma cells. Nat Med *8*, 971-978.

Jackson, A. L., Bartz, S. R., Schelter, J., Kobayashi, S. V., Burchard, J., Mao, M., Li, B., Cavet, G., and Linsley, P. S. (2003). Expression profiling reveals off-target gene regulation by RNAi. Nat Biotechnol *21*, 635-637.

Jacobs, M. M., Fogg, R. L., Emeson, R. B., and Stanwood, G. D. (2009). ADAR1 and ADAR2 expression and editing activity during forebrain development. Dev Neurosci *31*, 223-237.

Jazdzewski, K., Murray, E. L., Franssila, K., Jarzab, B., Schoenberg, D. R., and de la Chapelle, A. (2008). Common SNP in pre-miR-146a decreases mature miR expression and predisposes to papillary thyroid carcinoma. Proc Natl Acad Sci U S A *105*, 7269-7274.

Johnson, C. D., Esquela-Kerscher, A., Stefani, G., Byrom, M., Kelnar, K., Ovcharenko, D., Wilson, M., Wang, X., Shelton, J., Shingara, J.*, et al.* (2007). The let-7 microRNA represses cell proliferation pathways in human cells. Cancer Res *67*, 7713-7722.

Johnson, M. P., Haupt, L. M., and Griffiths, L. R. (2004). Locked nucleic acid (LNA) single nucleotide polymorphism (SNP) genotype analysis and validation using real-time PCR. Nucleic Acids Res *32*, e55.

Jones-Rhoades, M. W., Bartel, D. P., and Bartel, B. (2006). MicroRNAS and their regulatory roles in plants. Annu Rev Plant Biol *57*, 19-53.

Karube, Y., Tanaka, H., Osada, H., Tomida, S., Tatematsu, Y., Yanagisawa, K., Yatabe, Y., Takamizawa, J., Miyoshi, S., Mitsudomi, T., and Takahashi, T. (2005). Reduced expression of Dicer associated with poor prognosis in lung cancer patients. Cancer Sci *96*, 111-115.

Kawahara, Y., Megraw, M., Kreider, E., Iizasa, H., Valente, L., Hatzigeorgiou, A. G., and Nishikura, K. (2008). Frequency and fate of microRNA editing in human brain. Nucleic Acids Res *36*, 5270-5280.

Kawahara, Y., Zinshteyn, B., Chendrimada, T. P., Shiekhattar, R., and Nishikura, K. (2007a). RNA editing of the microRNA-151 precursor blocks cleavage by the Dicer-TRBP complex. EMBO Rep *8*, 763-769.

Kawahara, Y., Zinshteyn, B., Sethupathy, P., Iizasa, H., Hatzigeorgiou, A. G., and Nishikura, K. (2007b). Redirection of silencing targets by adenosine-to-inosine editing of miRNAs. Science *315*, 1137-1140.

Kertesz, M., Iovino, N., Unnerstall, U., Gaul, U., and Segal, E. (2007). The role of site accessibility in microRNA target recognition. Nat Genet *39*, 1278-1284.

Khvorova, A., Reynolds, A., and Jayasena, S. D. (2003). Functional siRNAs and miRNAs exhibit strand bias. Cell *115*, 209-216.

Kim, T. M., Huang, W., Park, R., Park, P. J., and Johnson, M. D. (2011). A developmental taxonomy of glioblastoma defined and maintained by MicroRNAs. Cancer Res *71*, 3387-3399.

Kim, V. N., Han, J., and Siomi, M. C. (2009). Biogenesis of small RNAs in animals. Nat Rev Mol Cell Biol *10*, 126-139.

Kim, V. N., and Nam, J. W. (2006). Genomics of microRNA. Trends Genet *22*, 165-173.

Kim, Y. K., and Kim, V. N. (2007). Processing of intronic microRNAs. EMBO J *26*, 775-783.

Kiran, A., and Baranov, P. V. (2010). DARNED: a DAtabase of RNa EDiting in humans. Bioinformatics *26*, 1772-1776.

Kiriakidou, M., Tan, G. S., Lamprinaki, S., De Planell-Saguer, M., Nelson, P. T., and Mourelatos, Z. (2007). An mRNA m7G cap binding-like motif within human Ago2 represses translation. Cell *129*, 1141-1151.

Kleinberger, Y., and Eisenberg, E. (2010). Large-scale analysis of structural, sequence and thermodynamic characteristics of A-to-I RNA editing sites in human Alu repeats. BMC Genomics *11*, 453.

Kloosterman, W. P., and Plasterk, R. H. (2006). The diverse functions of microRNAs in animal development and disease. Dev Cell *11*, 441-450.

Konnikova, L., Kotecki, M., Kruger, M. M., and Cochran, B. H. (2003). Knockdown of STAT3 expression by RNAi induces apoptosis in astrocytoma cells. BMC Cancer *3*, 23.

Krek, A., Grun, D., Poy, M. N., Wolf, R., Rosenberg, L., Epstein, E. J., MacMenamin, P., da Piedade, I., Gunsalus, K. C., Stoffel, M., and Rajewsky, N. (2005). Combinatorial microRNA target predictions. Nat Genet *37*, 495-500.

Krutzfeldt, J., Rajewsky, N., Braich, R., Rajeev, K. G., Tuschl, T., Manoharan, M., and Stoffel, M. (2005). Silencing of microRNAs in vivo with 'antagomirs'. Nature *438*, 685-689.

Kumar, M. S., Lu, J., Mercer, K. L., Golub, T. R., and Jacks, T. (2007). Impaired microRNA processing enhances cellular transformation and tumorigenesis. Nat Genet *39*, 673-677.

Lal, A., Kim, H. H., Abdelmohsen, K., Kuwano, Y., Pullmann, R., Jr., Srikantan, S., Subrahmanyam, R., Martindale, J. L., Yang, X., Ahmed, F.*, et al.* (2008). p16(INK4a) translation suppressed by miR-24. PLoS One *3*, e1864.

Lal, A., Navarro, F., Maher, C. A., Maliszewski, L. E., Yan, N., O'Day, E., Chowdhury, D., Dykxhoorn, D. M., Tsai, P., Hofmann, O.*, et al.* (2009). miR-24 Inhibits cell proliferation by targeting E2F2, MYC, and other cell-cycle genes via binding to "seedless" 3'UTR microRNA recognition elements. Mol Cell *35*, 610-625.

Landgraf, P., Rusu, M., Sheridan, R., Sewer, A., Iovino, N., Aravin, A., Pfeffer, S., Rice, A., Kamphorst, A. O., Landthaler, M.*, et al.* (2007). A mammalian microRNA expression atlas based on small RNA library sequencing. Cell *129*, 1401-1414.

Landi, D., Gemignani, F., Naccarati, A., Pardini, B., Vodicka, P., Vodickova, L., Novotny, J., Forsti, A., Hemminki, K., Canzian, F., and Landi, S. (2008). Polymorphisms within micro-RNA-binding sites and risk of sporadic colorectal cancer. Carcinogenesis *29*, 579-584.

Laneve, P., Di Marcotullio, L., Gioia, U., Fiori, M. E., Ferretti, E., Gulino, A., Bozzoni, I., and Caffarelli, E. (2007). The interplay between microRNAs and the neurotrophin receptor tropomyosin-related kinase C controls proliferation of human neuroblastoma cells. Proc Natl Acad Sci U S A *104*, 7957-7962.

Lau, N. C., Lim, L. P., Weinstein, E. G., and Bartel, D. P. (2001). An abundant class of tiny RNAs with probable regulatory roles in Caenorhabditis elegans. Science *294*, 858-862.

Lee, D. Y., Deng, Z., Wang, C. H., and Yang, B. B. (2007a). MicroRNA-378 promotes cell survival, tumor growth, and angiogenesis by targeting SuFu and Fus-1 expression. Proc Natl Acad Sci U S A *104*, 20350-20355.

Lee, E. J., Gusev, Y., Jiang, J., Nuovo, G. J., Lerner, M. R., Frankel, W. L., Morgan, D. L., Postier, R. G., Brackett, D. J., and Schmittgen, T. D. (2007b). Expression profiling identifies microRNA signature in pancreatic cancer. Int J Cancer *120*, 1046-1054.

Lee, I., Ajay, S. S., Chen, H., Maruyama, A., Wang, N., McInnis, M. G., and Athey, B. D. (2008a). Discriminating single-base difference miRNA expressions using microarray Probe Design Guru (ProDeG). Nucleic Acids Res *36*, e27.

Lee, J., Kotliarova, S., Kotliarov, Y., Li, A., Su, Q., Donin, N. M., Pastorino, S., Purow, B. W., Christopher, N., Zhang, W.*, et al.* (2006). Tumor stem cells derived from glioblastomas cultured in bFGF and EGF more closely mirror the phenotype and genotype of primary tumors than do serum-cultured cell lines. Cancer Cell *9*, 391-403.

Lee, J., Son, M. J., Woolard, K., Donin, N. M., Li, A., Cheng, C. H., Kotliarova, S., Kotliarov, Y., Walling, J., Ahn, S.*, et al.* (2008b). Epigenetic-mediated dysfunction of the bone

morphogenetic protein pathway inhibits differentiation of glioblastoma-initiating cells. Cancer Cell *13*, 69-80.

Lee, Y., Ahn, C., Han, J., Choi, H., Kim, J., Yim, J., Lee, J., Provost, P., Radmark, O., Kim, S., and Kim, V. N. (2003). The nuclear RNase III Drosha initiates microRNA processing. Nature *425*, 415-419.

Lee, Y., Kim, M., Han, J., Yeom, K. H., Lee, S., Baek, S. H., and Kim, V. N. (2004). MicroRNA genes are transcribed by RNA polymerase II. EMBO J *23*, 4051-4060.

Lehmann, U., Hasemeier, B., Christgen, M., Muller, M., Romermann, D., Langer, F., and Kreipe, H. (2008). Epigenetic inactivation of microRNA gene hsa-mir-9-1 in human breast cancer. J Pathol *214*, 17-24.

Levanon, E. Y., Eisenberg, E., Yelin, R., Nemzer, S., Hallegger, M., Shemesh, R., Fligelman, Z. Y., Shoshan, A., Pollock, S. R., Sztybel, D.*, et al.* (2004). Systematic identification of abundant A-to-I editing sites in the human transcriptome. Nat Biotechnol *22*, 1001-1005.

Levanon, K., Eisenberg, E., Rechavi, G., and Levanon, E. Y. (2005). Letter from the editor: Adenosine-to-inosine RNA editing in Alu repeats in the human genome. EMBO Rep *6*, 831-835.

Levy, D. E., and Darnell, J. E., Jr. (2002). Stats: transcriptional control and biological impact. Nat Rev Mol Cell Biol *3*, 651-662.

Lewis, B. P., Burge, C. B., and Bartel, D. P. (2005). Conserved seed pairing, often flanked by adenosines, indicates that thousands of human genes are microRNA targets. Cell *120*, 15-20.

Li, M., Lee, K. F., Lu, Y., Clarke, I., Shih, D., Eberhart, C., Collins, V. P., Van Meter, T., Picard, D., Zhou, L.*, et al.* (2009). Frequent amplification of a chr19q13.41 microRNA polycistron in aggressive primitive neuroectodermal brain tumors. Cancer Cell *16*, 533-546.

Lim, L. P., Lau, N. C., Garrett-Engele, P., Grimson, A., Schelter, J. M., Castle, J., Bartel, D. P., Linsley, P. S., and Johnson, J. M. (2005). Microarray analysis shows that some microRNAs downregulate large numbers of target mRNAs. Nature *433*, 769-773.

Linsley, P. S., Schelter, J., Burchard, J., Kibukawa, M., Martin, M. M., Bartz, S. R., Johnson, J. M., Cummins, J. M., Raymond, C. K., Dai, H.*, et al.* (2007). Transcripts targeted by the microRNA-16 family cooperatively regulate cell cycle progression. Mol Cell Biol *27*, 2240-2252.

Liotta, L. A., Mandler, R., Murano, G., Katz, D. A., Gordon, R. K., Chiang, P. K., and Schiffmann, E. (1986). Tumor cell autocrine motility factor. Proc Natl Acad Sci U S A *83*, 3302-3306.

Lipinski, C. A., Tran, N. L., Menashi, E., Rohl, C., Kloss, J., Bay, R. C., Berens, M. E., and Loftus, J. C. (2005). The tyrosine kinase pyk2 promotes migration and invasion of glioma cells. Neoplasia *7*, 435-445.

Liu, Q., Li, G., Li, R., Shen, J., He, Q., Deng, L., Zhang, C., and Zhang, J. (2010). IL-6 promotion of glioblastoma cell invasion and angiogenesis in U251 and T98G cell lines. J Neurooncol *100*, 165-176.

Lomeli, H., Mosbacher, J., Melcher, T., Hoger, T., Geiger, J. R., Kuner, T., Monyer, H., Higuchi, M., Bach, A., and Seeburg, P. H. (1994). Control of kinetic properties of AMPA receptor channels by nuclear RNA editing. Science *266*, 1709-1713.

Louis, D. N. (2006). Molecular pathology of malignant gliomas. Annu Rev Pathol *1*, 97-117.

Lu, J., Getz, G., Miska, E. A., Alvarez-Saavedra, E., Lamb, J., Peck, D., Sweet-Cordero, A., Ebert, B. L., Mak, R. H., Ferrando, A. A.*, et al.* (2005). MicroRNA expression profiles classify human cancers. Nature *435*, 834-838.

Lu, Y., Thomson, J. M., Wong, H. Y., Hammond, S. M., and Hogan, B. L. (2007). Transgenic over-expression of the microRNA miR-17-92 cluster promotes proliferation and inhibits differentiation of lung epithelial progenitor cells. Dev Biol *310*, 442-453.

Luciano, D. J., Mirsky, H., Vendetti, N. J., and Maas, S. (2004). RNA editing of a miRNA precursor. RNA *10*, 1174-1177.

Lujambio, A., Ropero, S., Ballestar, E., Fraga, M. F., Cerrato, C., Setien, F., Casado, S., Suarez-Gauthier, A., Sanchez-Cespedes, M., Git, A*., et al.* (2007). Genetic unmasking of an epigenetically silenced microRNA in human cancer cells. Cancer Res *67*, 1424-1429.

Lytle, J. R., Yario, T. A., and Steitz, J. A. (2007). Target mRNAs are repressed as efficiently by microRNA-binding sites in the 5' UTR as in the 3' UTR. Proc Natl Acad Sci U S A *104*, 9667-9672.

Ma, L., Teruya-Feldstein, J., and Weinberg, R. A. (2007). Tumour invasion and metastasis initiated by microRNA-10b in breast cancer. Nature *449*, 682-688.

Ma, L., and Weinberg, R. A. (2008). Micromanagers of malignancy: role of microRNAs in regulating metastasis. Trends Genet *24*, 448-456.

Maas, S. (2010). Gene regulation through RNA editing. Discov Med *10*, 379-386.

Maas, S., Patt, S., Schrey, M., and Rich, A. (2001). Underediting of glutamate receptor GluR-B mRNA in malignant gliomas. Proc Natl Acad Sci U S A *98*, 14687-14692.

Macbeth, M. R., Schubert, H. L., Vandemark, A. P., Lingam, A. T., Hill, C. P., and Bass, B. L. (2005). Inositol hexakisphosphate is bound in the ADAR2 core and required for RNA editing. Science *309*, 1534-1539.

Maroney, P. A., Yu, Y., Fisher, J., and Nilsen, T. W. (2006). Evidence that microRNAs are associated with translating messenger RNAs in human cells. Nat Struct Mol Biol *13*, 1102-1107.

Martello, G., Rosato, A., Ferrari, F., Manfrin, A., Cordenonsi, M., Dupont, S., Enzo, E., Guzzardo, V., Rondina, M., Spruce, T*., et al.* (2010). A MicroRNA targeting dicer for metastasis control. Cell *141*, 1195-1207.

Maruyama, K., Watanabe, H., Shiozaki, H., Takayama, T., Gofuku, J., Yano, H., Inoue, M., Tamura, S., Raz, A., and Monden, M. (1995). Expression of autocrine motility factor receptor in human esophageal squamous cell carcinoma. Int J Cancer *64*, 316-321.

Mayes, D. A., Hu, Y., Teng, Y., Siegel, E., Wu, X., Panda, K., Tan, F., Yung, W. K., and Zhou, Y. H. (2006). PAX6 suppresses the invasiveness of glioblastoma cells and the expression of the matrix metalloproteinase-2 gene. Cancer Res *66*, 9809-9817.

Mayr, C., Hemann, M. T., and Bartel, D. P. (2007). Disrupting the pairing between let-7 and Hmga2 enhances oncogenic transformation. Science *315*, 1576-1579.

McDonough, W., Tran, N., Giese, A., Norman, S. A., and Berens, M. E. (1998). Altered gene expression in human astrocytoma cells selected for migration: I. Thromboxane synthase. J Neuropathol Exp Neurol *57*, 449-455.

Mehler, M. F., and Mattick, J. S. (2007). Noncoding RNAs and RNA editing in brain development, functional diversification, and neurological disease. Physiol Rev *87*, 799-823.

Meister, G., Landthaler, M., Patkaniowska, A., Dorsett, Y., Teng, G., and Tuschl, T. (2004). Human Argonaute2 mediates RNA cleavage targeted by miRNAs and siRNAs. Mol Cell *15*, 185-197.

Mineno, J., Okamoto, S., Ando, T., Sato, M., Chono, H., Izu, H., Takayama, M., Asada, K., Mirochnitchenko, O., Inouye, M., and Kato, I. (2006). The expression profile of microRNAs in mouse embryos. Nucleic Acids Res *34*, 1765-1771.

Miranda, K. C., Huynh, T., Tay, Y., Ang, Y. S., Tam, W. L., Thomson, A. M., Lim, B., and Rigoutsos, I. (2006). A pattern-based method for the identification of MicroRNA binding sites and their corresponding heteroduplexes. Cell *126*, 1203-1217.

Mizuguchi, Y., Mishima, T., Yokomuro, S., Arima, Y., Kawahigashi, Y., Shigehara, K., Kanda, T., Yoshida, H., Uchida, E., Tajiri, T., and Takizawa, T. (2011). Sequencing and bioinformatics-based analyses of the microRNA transcriptome in hepatitis B-related hepatocellular carcinoma. PLoS One *6*, e15304.

Molina, J. R., Hayashi, Y., Stephens, C., and Georgescu, M. M. (2010). Invasive glioblastoma cells acquire stemness and increased Akt activation. Neoplasia *12*, 453-463.

Moore, L. M., and Zhang, W. (2010). Targeting miR-21 in glioma: a small RNA with big potential. Expert Opin Ther Targets *14*, 1247-1257.

Nakae, A., Tanaka, T., Miyake, K., Hase, M., and Mashimo, T. (2008). Comparing methods of detection and quantitation of RNA editing of rat glycine receptor alpha3. Int J Biol Sci *4*, 397-405.

Nicholas, M. K., Lukas, R. V., Chmura, S., Yamini, B., Lesniak, M., and Pytel, P. (2011). Molecular heterogeneity in glioblastoma: therapeutic opportunities and challenges. Semin Oncol *38*, 243-253.

Nicoloso, M. S., Sun, H., Spizzo, R., Kim, H., Wickramasinghe, P., Shimizu, M., Wojcik, S. E., Ferdin, J., Kunej, T., Xiao, L*., et al.* (2010). Single-nucleotide polymorphisms inside microRNA target sites influence tumor susceptibility. Cancer Res *70*, 2789-2798.

Nielsen, C. B., Shomron, N., Sandberg, R., Hornstein, E., Kitzman, J., and Burge, C. B. (2007). Determinants of targeting by endogenous and exogenous microRNAs and siRNAs. RNA *13*, 1894-1910.

Nilsson, K., Svensson, S., and Landberg, G. (2004). Retinoblastoma protein function and p16INK4a expression in actinic keratosis, squamous cell carcinoma in situ and invasive squamous cell carcinoma of the skin and links between p16INK4a expression and infiltrative behavior. Mod Pathol *17*, 1464-1474.

Nishikura, K. (2006). Editor meets silencer: crosstalk between RNA editing and RNA interference. Nat Rev Mol Cell Biol *7*, 919-931.

Nishikura, K. (2010). Functions and regulation of RNA editing by ADAR deaminases. Annu Rev Biochem *79*, 321-349.

Nowacki, P., and Kojder, I. (2001). Peritumoral angiogenesis around primary and metastatic brain neoplasms. Morphometric analysis. Folia Neuropathol *39*, 95-102.

O'Donnell, K. A., Wentzel, E. A., Zeller, K. I., Dang, C. V., and Mendell, J. T. (2005). c-Myc-regulated microRNAs modulate E2F1 expression. Nature *435*, 839-843.

Okamura, K., Liu, N., and Lai, E. C. (2009). Distinct mechanisms for microRNA strand selection by Drosophila Argonautes. Mol Cell *36*, 431-444.

Okamura, K., Phillips, M. D., Tyler, D. M., Duan, H., Chou, Y. T., and Lai, E. C. (2008). The regulatory activity of microRNA* species has substantial influence on microRNA and 3' UTR evolution. Nat Struct Mol Biol *15*, 354-363.

Osenberg, S., Paz Yaacov, N., Safran, M., Moshkovitz, S., Shtrichman, R., Sherf, O., Jacob-Hirsch, J., Keshet, G., Amariglio, N., Itskovitz-Eldor, J., and Rechavi, G. (2010). Alu sequences in undifferentiated human embryonic stem cells display high levels of A-to-I RNA editing. PLoS One *5*, e11173.

Ovaska, K., Laakso, M., Haapa-Paananen, S., Louhimo, R., Chen, P., Aittomaki, V., Valo, E., Nunez-Fontarnau, J., Rantanen, V., Karinen, S*., et al.* (2010). Large-scale data integration framework provides a comprehensive view on glioblastoma multiforme. Genome Med *2*, 65.

Paschen, W., Dux, E., and Djuricic, B. (1994). Developmental changes in the extent of RNA editing of glutamate receptor subunit GluR5 in rat brain. Neurosci Lett *174*, 109-112.

Patterson, J. B., and Samuel, C. E. (1995). Expression and regulation by interferon of a double-stranded-RNA-specific adenosine deaminase from human cells: evidence for two forms of the deaminase. Mol Cell Biol *15*, 5376-5388.

Paupard, M. C., O'Connell, M. A., Gerber, A. P., and Zukin, R. S. (2000). Patterns of developmental expression of the RNA editing enzyme rADAR2. Neuroscience *95*, 869-879.

Paz, N., Levanon, E. Y., Amariglio, N., Heimberger, A. B., Ram, Z., Constantini, S., Barbash, Z. S., Adamsky, K., Safran, M., Hirschberg, A*., et al.* (2007). Altered adenosine-to-inosine RNA editing in human cancer. Genome Res *17*, 1586-1595.

Petersen, C. P., Bordeleau, M. E., Pelletier, J., and Sharp, P. A. (2006). Short RNAs repress translation after initiation in mammalian cells. Mol Cell *21*, 533-542.

Phillips, H. S., Kharbanda, S., Chen, R., Forrest, W. F., Soriano, R. H., Wu, T. D., Misra, A., Nigro, J. M., Colman, H., Soroceanu, L.*, et al.* (2006). Molecular subclasses of high-grade glioma predict prognosis, delineate a pattern of disease progression, and resemble stages in neurogenesis. Cancer Cell *9*, 157-173.

Piao, Y., Lu, L., and de Groot, J. (2009). AMPA receptors promote perivascular glioma invasion via beta1 integrin-dependent adhesion to the extracellular matrix. Neuro Oncol *11*, 260-273.

Pillai, R. S., Bhattacharyya, S. N., and Filipowicz, W. (2007). Repression of protein synthesis by miRNAs: how many mechanisms? Trends Cell Biol *17*, 118-126.

Radaelli, E., Ceruti, R., Patton, V., Russo, M., Degrassi, A., Croci, V., Caprera, F., Stortini, G., Scanziani, E., Pesenti, E., and Alzani, R. (2009). Immunohistopathological and neuroimaging characterization of murine orthotopic xenograft models of glioblastoma multiforme recapitulating the most salient features of human disease. Histol Histopathol *24*, 879-891.

Rajan, P., and McKay, R. D. (1998). Multiple routes to astrocytic differentiation in the CNS. J Neurosci *18*, 3620-3629.

Raver-Shapira, N., Marciano, E., Meiri, E., Spector, Y., Rosenfeld, N., Moskovits, N., Bentwich, Z., and Oren, M. (2007). Transcriptional activation of miR-34a contributes to p53-mediated apoptosis. Mol Cell *26*, 731-743.

Rivat, C., De Wever, O., Bruyneel, E., Mareel, M., Gespach, C., and Attoub, S. (2004). Disruption of STAT3 signaling leads to tumor cell invasion through alterations of homotypic cell-cell adhesion complexes. Oncogene *23*, 3317-3327.

Rodriguez, A., Griffiths-Jones, S., Ashurst, J. L., and Bradley, A. (2004). Identification of mammalian microRNA host genes and transcription units. Genome Res *14*, 1902-1910.

Rueter, S. M., Dawson, T. R., and Emeson, R. B. (1999). Regulation of alternative splicing by RNA editing. Nature *399*, 75-80.

Ryan, B. M., Robles, A. I., and Harris, C. C. (2010). Genetic variation in microRNA networks: the implications for cancer research. Nat Rev Cancer *10*, 389-402.

Saito, Y., Liang, G., Egger, G., Friedman, J. M., Chuang, J. C., Coetzee, G. A., and Jones, P. A. (2006). Specific activation of microRNA-127 with downregulation of the proto-oncogene BCL6 by chromatin-modifying drugs in human cancer cells. Cancer Cell *9*, 435-443.

Sarver, A. L., Li, L., and Subramanian, S. (2010). MicroRNA miR-183 functions as an oncogene by targeting the transcription factor EGR1 and promoting tumor cell migration. Cancer Res *70*, 9570-9580.

Saunders, M. A., Liang, H., and Li, W. H. (2007). Human polymorphism at microRNAs and microRNA target sites. Proc Natl Acad Sci U S A *104*, 3300-3305.

Schmitt, J., Dux, E., Gissel, C., and Paschen, W. (1996). Regional analysis of developmental changes in the extent of GluR6 mRNA editing in rat brain. Brain Res Dev Brain Res *91*, 153-157.

Schulte, J. H., Marschall, T., Martin, M., Rosenstiel, P., Mestdagh, P., Schlierf, S., Thor, T., Vandesompele, J., Eggert, A., Schreiber, S.*, et al.* (2010). Deep sequencing reveals differential expression of microRNAs in favorable versus unfavorable neuroblastoma. Nucleic Acids Res *38*, 5919-5928.

Schust, J., Sperl, B., Hollis, A., Mayer, T. U., and Berg, T. (2006). Stattic: a small-molecule inhibitor of STAT3 activation and dimerization. Chem Biol *13*, 1235-1242.

Selbach, M., Schwanhausser, B., Thierfelder, N., Fang, Z., Khanin, R., and Rajewsky, N. (2008). Widespread changes in protein synthesis induced by microRNAs. Nature *455*, 58-63.

Senft, C., Priester, M., Polacin, M., Schroder, K., Seifert, V., Kogel, D., and Weissenberger, J. (2011). Inhibition of the JAK-2/STAT3 signaling pathway impedes the migratory and invasive potential of human glioblastoma cells. J Neurooncol *101*, 393-403.

Shen, J., Ambrosone, C. B., and Zhao, H. (2009). Novel genetic variants in microRNA genes and familial breast cancer. Int J Cancer *124*, 1178-1182.

Silber, J., James, C. D., and Hodgson, J. G. (2009). microRNAs in gliomas: small regulators of a big problem. Neuromolecular Med *11*, 208-222.

Silber, J., Lim, D. A., Petritsch, C., Persson, A. I., Maunakea, A. K., Yu, M., Vandenberg, S. R., Ginzinger, D. G., James, C. D., Costello, J. F.*, et al.* (2008). miR-124 and miR-137 inhibit proliferation of glioblastoma multiforme cells and induce differentiation of brain tumor stem cells. BMC Med *6*, 14.

Siomi, H., and Siomi, M. C. (2010). Posttranscriptional regulation of microRNA biogenesis in animals. Mol Cell *38*, 323-332.

Slaby, O., Bienertova-Vasku, J., Svoboda, M., and Vyzula, R. (2011). Genetic polymorphisms and MicroRNAs: new direction in molecular epidemiology of solid cancer. J Cell Mol Med.

Sommer, B., Kohler, M., Sprengel, R., and Seeburg, P. H. (1991). RNA editing in brain controls a determinant of ion flow in glutamate-gated channels. Cell *67*, 11-19.

Sun, G., Yan, J., Noltner, K., Feng, J., Li, H., Sarkis, D. A., Sommer, S. S., and Rossi, J. J. (2009). SNPs in human miRNA genes affect biogenesis and function. RNA *15*, 1640-1651.

Sun, J., Blaskovich, M. A., Jove, R., Livingston, S. K., Coppola, D., and Sebti, S. M. (2005). Cucurbitacin Q: a selective STAT3 activation inhibitor with potent antitumor activity. Oncogene *24*, 3236-3245.

Sun, Q., Gu, H., Zeng, Y., Xia, Y., Wang, Y., Jing, Y., Yang, L., and Wang, B. (2010). Hsa-mir-27a genetic variant contributes to gastric cancer susceptibility through affecting miR-27a and target gene expression. Cancer Sci *101*, 2241-2247.

Takanami, I., Takeuchi, K., Watanabe, H., Yanagawa, T., Takagishi, K., and Raz, A. (2001). Significance of autocrine motility factor receptor gene expression as a prognostic factor in non-small-cell lung cancer. Int J Cancer *95*, 384-387.

Takeda, K., and Akira, S. (2000). STAT family of transcription factors in cytokine-mediated biological responses. Cytokine Growth Factor Rev *11*, 199-207.

Tanizaki, Y., Sato, Y., Oka, H., Utsuki, S., Kondo, K., Miyajima, Y., Nagashio, R., and Fujii, K. (2006). Expression of autocrine motility factor mRNA is a poor prognostic factor in high-grade astrocytoma. Pathol Int *56*, 510-515.

Tavazoie, S. F., Alarcon, C., Oskarsson, T., Padua, D., Wang, Q., Bos, P. D., Gerald, W. L., and Massague, J. (2008). Endogenous human microRNAs that suppress breast cancer metastasis. Nature *451*, 147-152.

Tay, Y., Zhang, J., Thomson, A. M., Lim, B., and Rigoutsos, I. (2008). MicroRNAs to Nanog, Oct4 and Sox2 coding regions modulate embryonic stem cell differentiation. Nature *455*, 1124-1128.

Teferedegne, B., Murata, H., Quinones, M., Peden, K., and Lewis, A. M. (2010). Patterns of microRNA expression in non-human primate cells correlate with neoplastic development in vitro. PLoS One *5*, e14416.

Thomson, J. M., Newman, M., Parker, J. S., Morin-Kensicki, E. M., Wright, T., and Hammond, S. M. (2006). Extensive post-transcriptional regulation of microRNAs and its implications for cancer. Genes Dev *20*, 2202-2207.

Tsai, Y. C., Mendoza, A., Mariano, J. M., Zhou, M., Kostova, Z., Chen, B., Veenstra, T., Hewitt, S. M., Helman, L. J., Khanna, C., and Weissman, A. M. (2007). The ubiquitin ligase gp78 promotes sarcoma metastasis by targeting KAI1 for degradation. Nat Med *13*, 1504-1509.

Vajkoczy, P., Goldbrunner, R., Farhadi, M., Vince, G., Schilling, L., Tonn, J. C., Schmiedek, P., and Menger, M. D. (1999). Glioma cell migration is associated with glioma-induced angiogenesis in vivo. Int J Dev Neurosci *17*, 557-563.

Valastyan, S., Reinhardt, F., Benaich, N., Calogrias, D., Szasz, A. M., Wang, Z. C., Brock, J. E., Richardson, A. L., and Weinberg, R. A. (2009). A pleiotropically acting microRNA, miR-31, inhibits breast cancer metastasis. Cell *137*, 1032-1046.

Valencia-Sanchez, M. A., Liu, J., Hannon, G. J., and Parker, R. (2006). Control of translation and mRNA degradation by miRNAs and siRNAs. Genes Dev *20*, 515-524.

Valente, L., and Nishikura, K. (2005). ADAR gene family and A-to-I RNA editing: diverse roles in posttranscriptional gene regulation. Prog Nucleic Acid Res Mol Biol *79*, 299-338.

Valente, L., and Nishikura, K. (2007). RNA binding-independent dimerization of adenosine deaminases acting on RNA and dominant negative effects of nonfunctional subunits on dimer functions. J Biol Chem *282*, 16054-16061.

Verhaak, R. G., Hoadley, K. A., Purdom, E., Wang, V., Qi, Y., Wilkerson, M. D., Miller, C. R., Ding, L., Golub, T., Mesirov, J. P.*, et al.* (2010). Integrated genomic analysis identifies clinically relevant subtypes of glioblastoma characterized by abnormalities in PDGFRA, IDH1, EGFR, and NF1. Cancer Cell *17*, 98-110.

Voorhoeve, P. M., le Sage, C., Schrier, M., Gillis, A. J., Stoop, H., Nagel, R., Liu, Y. P., van Duijse, J., Drost, J., Griekspoor, A.*, et al.* (2006). A genetic screen implicates miRNA-372 and miRNA-373 as oncogenes in testicular germ cell tumors. Cell *124*, 1169-1181.

Wahlstedt, H., Daniel, C., Enstero, M., and Ohman, M. (2009). Large-scale mRNA sequencing determines global regulation of RNA editing during brain development. Genome Res *19*, 978-986.

Wahlstedt, H., and Öhman, M. (2011). Site-selective versus promiscuous A-to-I editing. Wiley Interdisciplinary Reviews: RNA, n/a-n/a.

Wang, F., Ma, Y. L., Zhang, P., Yang, J. J., Chen, H. Q., Liu, Z. H., Peng, J. Y., Zhou, Y. K., and Qin, H. L. (2011). A genetic variant in microRNA-196a2 is associated with increased cancer risk: a meta-analysis. Mol Biol Rep.

Wang, Q., Miyakoda, M., Yang, W., Khillan, J., Stachura, D. L., Weiss, M. J., and Nishikura, K. (2004). Stress-induced apoptosis associated with null mutation of ADAR1 RNA editing deaminase gene. J Biol Chem *279*, 4952-4961.

Wei, J. S., Song, Y. K., Durinck, S., Chen, Q. R., Cheuk, A. T., Tsang, P., Zhang, Q., Thiele, C. J., Slack, A., Shohet, J., and Khan, J. (2008). The MYCN oncogene is a direct target of miR-34a. Oncogene *27*, 5204-5213.

Weissenberger, J., Priester, M., Bernreuther, C., Rakel, S., Glatzel, M., Seifert, V., and Kogel, D. (2010). Dietary curcumin attenuates glioma growth in a syngeneic mouse model by inhibition of the JAK1,2/STAT3 signaling pathway. Clin Cancer Res *16*, 5781-5795.

Whitney, N. P., Peng, H., Erdmann, N. B., Tian, C., Monaghan, D. T., and Zheng, J. C. (2008). Calcium-permeable AMPA receptors containing Q/R-unedited GluR2 direct human neural progenitor cell differentiation to neurons. FASEB J *22*, 2888-2900.

Winkler, F., Kienast, Y., Fuhrmann, M., Von Baumgarten, L., Burgold, S., Mitteregger, G., Kretzschmar, H., and Herms, J. (2009). Imaging glioma cell invasion in vivo reveals mechanisms of dissemination and peritumoral angiogenesis. Glia *57*, 1306-1315.

Winter, J., Jung, S., Keller, S., Gregory, R. I., and Diederichs, S. (2009). Many roads to maturity: microRNA biogenesis pathways and their regulation. Nat Cell Biol *11*, 228-234.

Wu, C., Lin, J., Hong, M., Choudhury, Y., Balani, P., Leung, D., Dang, L. H., Zhao, Y., Zeng, J., and Wang, S. (2009). Combinatorial control of suicide gene expression by tissue-specific promoter and microRNA regulation for cancer therapy. Mol Ther *17*, 2058-2066.

Wu, L., and Belasco, J. G. (2005). Micro-RNA regulation of the mammalian lin-28 gene during neuronal differentiation of embryonal carcinoma cells. Mol Cell Biol *25*, 9198-9208.

Wu, L., Fan, J., and Belasco, J. G. (2006). MicroRNAs direct rapid deadenylation of mRNA. Proc Natl Acad Sci U S A *103*, 4034-4039.

Wu, M., Jolicoeur, N., Li, Z., Zhang, L., Fortin, Y., L'Abbe, D., Yu, Z., and Shen, S. H. (2008). Genetic variations of microRNAs in human cancer and their effects on the expression of miRNAs. Carcinogenesis *29*, 1710-1716.

Wurdinger, T., Tannous, B. A., Saydam, O., Skog, J., Grau, S., Soutschek, J., Weissleder, R., Breakefield, X. O., and Krichevsky, A. M. (2008). miR-296 regulates growth factor receptor overexpression in angiogenic endothelial cells. Cancer Cell *14*, 382-393.

Xie, Q., Thompson, R., Hardy, K., DeCamp, L., Berghuis, B., Sigler, R., Knudsen, B., Cottingham, S., Zhao, P., Dykema, K.*, et al.* (2008). A highly invasive human glioblastoma pre-clinical model for testing therapeutics. J Transl Med *6*, 77.

Xie, X., Lu, J., Kulbokas, E. J., Golub, T. R., Mootha, V., Lindblad-Toh, K., Lander, E. S., and Kellis, M. (2005). Systematic discovery of regulatory motifs in human promoters and 3' UTRs by comparison of several mammals. Nature *434*, 338-345.

Xu, T., Zhu, Y., Wei, Q. K., Yuan, Y., Zhou, F., Ge, Y. Y., Yang, J. R., Su, H., and Zhuang, S. M. (2008). A functional polymorphism in the miR-146a gene is associated with the risk for hepatocellular carcinoma. Carcinogenesis *29*, 2126-2131.

Yang, J. S., Phillips, M. D., Betel, D., Mu, P., Ventura, A., Siepel, A. C., Chen, K. C., and Lai, E. C. (2011). Widespread regulatory activity of vertebrate microRNA* species. RNA *17*, 312-326.

Yang, W., Chendrimada, T. P., Wang, Q., Higuchi, M., Seeburg, P. H., Shiekhattar, R., and Nishikura, K. (2006). Modulation of microRNA processing and expression through RNA editing by ADAR deaminases. Nat Struct Mol Biol *13*, 13-21.

Ye, G., Fu, G., Cui, S., Zhao, S., Bernaudo, S., Bai, Y., Ding, Y., Zhang, Y., Yang, B. B., and Peng, C. (2011). MicroRNA 376c enhances ovarian cancer cell survival by targeting activin receptor-like kinase 7: implications for chemoresistance. J Cell Sci *124*, 359-368.

Yekta, S., Shih, I. H., and Bartel, D. P. (2004). MicroRNA-directed cleavage of HOXB8 mRNA. Science *304*, 594-596.

Yoshida, M., Kaziro, Y., and Ukita, T. (1968). The modification of nucleosides and nucleotides. X. Evidence for the important role of inosine residue in codon recognition of yeast alanine tRNA. Biochim Biophys Acta *166*, 646-655.

Yu, Z., Li, Z., Jolicoeur, N., Zhang, L., Fortin, Y., Wang, E., Wu, M., and Shen, S. H. (2007). Aberrant allele frequencies of the SNPs located in microRNA target sites are potentially associated with human cancers. Nucleic Acids Res *35*, 4535-4541.

Yuan, X., Liu, C., Yang, P., He, S., Liao, Q., Kang, S., and Zhao, Y. (2009). Clustered microRNAs' coordination in regulating protein-protein interaction network. BMC Syst Biol *3*, 65.

Yuki, K., Natsume, A., Yokoyama, H., Kondo, Y., Ohno, M., Kato, T., Chansakul, P., Ito, M., Kim, S. U., and Wakabayashi, T. (2009). Induction of oligodendrogenesis in glioblastoma-initiating cells by IFN-mediated activation of STAT3 signaling. Cancer Lett *284*, 71-79.

Zeng, Y., and Cullen, B. R. (2003). Sequence requirements for micro RNA processing and function in human cells. RNA *9*, 112-123.

Zhang, L., Huang, J., Yang, N., Greshock, J., Megraw, M. S., Giannakakis, A., Liang, S., Naylor, T. L., Barchetti, A., Ward, M. R.*, et al.* (2006). microRNAs exhibit high frequency genomic alterations in human cancer. Proc Natl Acad Sci U S A *103*, 9136-9141.

Zhou, Y. H., Hess, K. R., Liu, L., Linskey, M. E., and Yung, W. K. (2005). Modeling prognosis for patients with malignant astrocytic gliomas: quantifying the expression of multiple genetic markers and clinical variables. Neuro Oncol *7*, 485-494.

Appendix

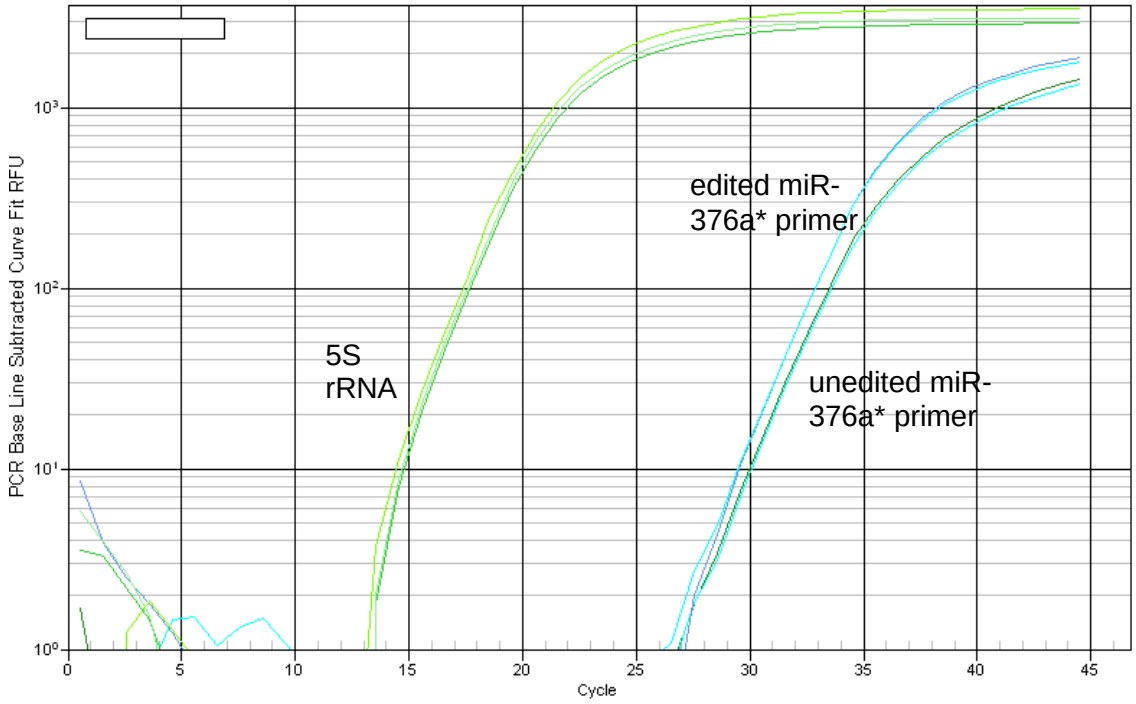

Appendix Figure A1. qRT-PCR amplification of unedited miR-376a* with primers corresponding to unedited miR-376a* (right) and edited miR-376a* (left), differing by a single base. Note the similar Cts for both primers, indicating similar efficiency of amplification and inability to discriminate the single base difference between miRNAs by this method.

Appendix Table A1 Genes downregulated by miR-376a*A in U87 and SW1783 cells representing potential candidate targets of unedited miR-376a* in glioma cells.

Symbol	Description
SEPT10	septin 10
ADAM17	ADAM metallopeptidase domain 17
ALG2	asparagine-linked glycosylation 2, alpha-1,3-mannosyltransferase homolog (S. cerevisiae)
ARL6	ADP-ribosylation factor-like 6
ARMCX5	armadillo repeat containing, X-linked 5
ATP10D	ATPase, class V, type 10D
B3GAT3	beta-1,3-glucuronyltransferase 3 (glucuronosyltransferase I)
BAG5	BCL2-associated athanogene 5
BRI3BP	BRI3 binding protein
BZW1	basic leucine zipper and W2 domains 1
C18orf54	chromosome 18 open reading frame 54
C18orf55	chromosome 18 open reading frame 55
C7orf58	chromosome 7 open reading frame 58
CAST	calpastatin
COMMD2	COMM domain containing 2
DENR	density-regulated protein
DIP2A	DIP2 disco-interacting protein 2 homolog A (Drosophila)
DKFZP564C152	DKFZP564C152 protein
DPYD	dihydropyrimidine dehydrogenase
ELOVL5	ELOVL family member 5, elongation of long chain fatty acids (FEN1/Elo2, SUR4/Elo3-like, yeast)
EPB41L5	erythrocyte membrane protein band 4.1 like 5
ERLIN2	ER lipid raft associated 2
FAM168A	family with sequence similarity 168, member A
FAM18B	family with sequence similarity 18, member B
FAM20B	family with sequence similarity 20, member B
FAM55C	family with sequence similarity 55, member C
FGF2	fibroblast growth factor 2 (basic)
FRMD5	FERM domain containing 5
G3BP2	GTPase activating protein (SH3 domain) binding protein 2
GALNT11	UDP-N-acetyl-alpha-D-galactosamine:polypeptide N-acetylgalactosaminyltransferase 11 (GalNAc-T11)
GFPT1	glutamine-fructose-6-phosphate transaminase 1
GIGYF2	GRB10 interacting GYF protein 2
GLT8D3	glycosyltransferase 8 domain containing 3
GNE	glucosamine (UDP-N-acetyl)-2-epimerase/N-acetylmannosamine kinase
GOLPH3L	golgi phosphoprotein 3-like
HDAC9	histone deacetylase 9
HNRNPAB	heterogeneous nuclear ribonucleoprotein A/B
ISOC1	isochorismatase domain containing 1
KCTD12	potassium channel tetramerisation domain containing 12
KDSR	3-ketodihydrosphingosine reductase
KIF16B	kinesin family member 16B
KPNA6	karyopherin alpha 6 (importin alpha 7)
LARS2	leucyl-tRNA synthetase 2, mitochondrial
LOC643287	similar to prothymosin alpha
LOC727914	BMS1-like, ribosome assembly protein (yeast) pseudogene
LRRFIP2	leucine rich repeat (in FLII) interacting protein 2
LYRM7	Lyrm7 homolog (mouse)
MAP2	microtubule-associated protein 2
MDH1	malate dehydrogenase 1, NAD (soluble)
MED28	Mediator complex subunit 28
MELK	maternal embryonic leucine zipper kinase
MIS12	MIS12, MIND kinetochore complex component, homolog (yeast)
MLF1IP	MLF1 interacting protein
MUS81	MUS81 endonuclease homolog (S. cerevisiae)
MYH9	myosin, heavy chain 9, non-muscle
NAPG	N-ethylmaleimide-sensitive factor attachment protein, gamma
NHLRC3	NHL repeat containing 3
NSUN2	NOL1/NOP2/Sun domain family, member 2
NUDT15	nudix (nucleoside diphosphate linked moiety X)-type motif 15

(Continued)

Symbol	Description
NUP50	nucleoporin 50kDa
ORAI3	ORAI calcium release-activated calcium modulator 3
PANK4	pantothenate kinase 4
PEX19	peroxisomal biogenesis factor 19
PIP4K2A	phosphatidylinositol-5-phosphate 4-kinase, type II, alpha
PITRM1	pitrilysin metallopeptidase 1
POMGNT1	protein O-linked mannose beta1,2-N-acetylglucosaminyltransferase
PPP2R2A	protein phosphatase 2 (formerly 2A), regulatory subunit B, alpha isoform
PTPRJ	protein tyrosine phosphatase, receptor type, J
RAB8B	RAB8B, member RAS oncogene family
RAP2A	RAP2A, member of RAS oncogene family
RAPGEF6	Rap guanine nucleotide exchange factor (GEF) 6
RBM17	RNA binding motif protein 17
RNF138	ring finger protein 138
RNF141	ring finger protein 141
RPS6KA3	ribosomal protein S6 kinase, 90kDa, polypeptide 3
RPS6KB1	ribosomal protein S6 kinase, 70kDa, polypeptide 1
RRAS2	related RAS viral (r-ras) oncogene homolog 2
RSPRY1	ring finger and SPRY domain containing 1
RTN4	reticulon 4
SCML1	sex comb on midleg-like 1 (Drosophila)
SEC23B	Sec23 homolog B (S. cerevisiae)
SKP2	S-phase kinase-associated protein 2 (p45)
SLC25A43	solute carrier family 25, member 43
SLC2A14	solute carrier family 2 (facilitated glucose transporter), member 14
SLC35A1	solute carrier family 35 (CMP-sialic acid transporter), member A1
SLC38A1	solute carrier family 38, member 1
SLC39A10	solute carrier family 39 (zinc transporter), member 10
SLC7A11	solute carrier family 7, (cationic amino acid transporter, y+ system) member 11
SLC7A6OS	solute carrier family 7, member 6 opposite strand
SMN1	survival of motor neuron 1, telomeric
SNRPA1	small nuclear ribonucleoprotein polypeptide A'
SQSTM1	sequestosome 1
STAT3	**signal transducer and activator of transcription 3 (acute-phase response factor)**
SUB1	SUB1 homolog (S. cerevisiae)
TDG	thymine-DNA glycosylase
THUMPD1	THUMP domain containing 1
TOR1B	torsin family 1, member B (torsin B)
TPK1	thiamin pyrophosphokinase 1
TTC39C	tetratricopeptide repeat domain 39C
UGCG	UDP-glucose ceramide glucosyltransferase
USP53	ubiquitin specific peptidase 53
VEZT	vezatin, adherens junctions transmembrane protein
VMA21	VMA21 vacuolar H+-ATPase homolog (S. cerevisiae)
VTA1	Vps20-associated 1 homolog (S. cerevisiae)
WDR37	WD repeat domain 37
YPEL5	yippee-like 5 (Drosophila)
YRDC	yrdC domain containing (E. coli)
ZCCHC10	zinc finger, CCHC domain containing 10
ZFYVE26	zinc finger, FYVE domain containing 26
	Full length insert cDNA clone ZB81B12
	Full-length cDNA clone CS0DK008YI09 of HeLa cells Cot 25-normalized of Homo sapiens (human)
	CDNA FLJ30661 fis, clone DFNES2000526
	Homo sapiens, clone IMAGE:4294444, mRNA
	Full-length cDNA clone CS0DF022YM06 of Fetal brain of Homo sapiens (human)
	MRNA; cDNA DKFZp586F1523 (from clone DKFZp586F1523)
	CDNA FLJ30010 fis, clone 3NB692000154

Appendix Table A2 Genes downregulated by miR-376a*G in U87 and SW1783 cells representing potential candidate targets of edited miR-376a* in glioma cells.

Symbol	Description
AASDHPPT	aminoadipate-semialdehyde dehydrogenase-phosphopantetheinyl transferase
ABHD2	abhydrolase domain containing 2
ABL1	c-abl oncogene 1, receptor tyrosine kinase
ACVR1	activin A receptor, type I
AFF1	AF4/FMR2 family, member 1
AFG3L2	AFG3 ATPase family gene 3-like 2 (yeast)
AHCYL2	S-adenosylhomocysteine hydrolase-like 2
AMFR	**autocrine motility factor receptor**
AP3M1	adaptor-related protein complex 3, mu 1 subunit
APC	adenomatous polyposis coli
ARF1	ADP-ribosylation factor 1
ARHGAP21	Rho GTPase activating protein 21
ARHGAP26	Rho GTPase activating protein 26
ARHGEF7	Rho guanine nucleotide exchange factor (GEF) 7
ARL4C	ADP-ribosylation factor-like 4C
ARMC8	armadillo repeat containing 8
ARNTL	aryl hydrocarbon receptor nuclear translocator-like
ARRDC3	arrestin domain containing 3
BRD3	bromodomain containing 3
C10orf26	chromosome 10 open reading frame 26
C13orf23	chromosome 13 open reading frame 23
C15orf57	chromosome 15 open reading frame 57
C17orf39	chromosome 17 open reading frame 39
C17orf80	chromosome 17 open reading frame 80
C19orf2	chromosome 19 open reading frame 2
C1orf96	chromosome 1 open reading frame 96
C2orf64	chromosome 2 open reading frame 64
C5orf51	chromosome 5 open reading frame 51
C9orf126	chromosome 9 open reading frame 126
CASP7	caspase 7, apoptosis-related cysteine peptidase
CBLB	Cas-Br-M (murine) ecotropic retroviral transforming sequence b
CDC26	cell division cycle 26 homolog (S. cerevisiae)
CHD6	chromodomain helicase DNA binding protein 6
CYB5R4	cytochrome b5 reductase 4
DHTKD1	dehydrogenase E1 and transketolase domain containing 1
DPYSL3	dihydropyrimidinase-like 3
DUSP14	dual specificity phosphatase 14
ELK4	ELK4, ETS-domain protein (SRF accessory protein 1)
EML4	echinoderm microtubule associated protein like 4
EMP2	epithelial membrane protein 2
EZH1	enhancer of zeste homolog 1 (Drosophila)
FAM120B	Family with sequence similarity 120B
FAM122B	family with sequence similarity 122B
FAM171A1	family with sequence similarity 171, member A1
FBXO46	F-box protein 46
FNIP2	folliculin interacting protein 2
FOXJ3	forkhead box J3
FZD5	frizzled homolog 5 (Drosophila)
GAS2L3	Growth arrest-specific 2 like 3
GDAP1	ganglioside-induced differentiation-associated protein 1
GLOD4	glyoxalase domain containing 4
GPR157	G protein-coupled receptor 157
GPR180	G protein-coupled receptor 180
GRK5	G protein-coupled receptor kinase 5
HDAC4	histone deacetylase 4
HIPK2	homeodomain interacting protein kinase 2
HRSP12	heat-responsive protein 12
IL6R	interleukin 6 receptor
IMPA2	inositol(myo)-1(or 4)-monophosphatase 2
IRGQ	immunity-related GTPase family, Q
IRS1	insulin receptor substrate 1

(Continued)

Symbol	Description
JMJD6	jumonji domain containing 6
JOSD1	Josephin domain containing 1
KIAA2018	KIAA2018
KIF1B	kinesin family member 1B
KIRREL	kin of IRRE like (Drosophila)
KLF13	Kruppel-like factor 13
LMAN2L	lectin, mannose-binding 2-like
LMLN	leishmanolysin-like (metallopeptidase M8 family)
LOC149832	hypothetical protein LOC149832
LPP	LIM domain containing preferred translocation partner in lipoma
LRRC58	leucine rich repeat containing 58
MALT1	mucosa associated lymphoid tissue lymphoma translocation gene 1
MAP2K4	mitogen-activated protein kinase kinase 4
MCC	mutated in colorectal cancers
MED14	mediator complex subunit 14
MLXIP	MLX interacting protein
MOBKL1B	MOB1, Mps One Binder kinase activator-like 1B (yeast)
MYCBP	c-myc binding protein
NAV1	neuron navigator 1
NRN1	neuritin 1
NUCKS1	nuclear casein kinase and cyclin-dependent kinase substrate 1
NUCKS1	Nuclear casein kinase and cyclin-dependent kinase substrate 1
OXSR1	oxidative-stress responsive 1
PAFAH1B1	platelet-activating factor acetylhydrolase, isoform Ib, subunit 1 (45kDa)
PDLIM5	PDZ and LIM domain 5
PEG10	paternally expressed 10
PI4K2A	phosphatidylinositol 4-kinase type 2 alpha
PLS1	plastin 1 (I isoform)
PPFIA1	protein tyrosine phosphatase, receptor type, f polypeptide (PTPRF), interacting protein (liprin), alpha 1
PRICKLE2	prickle homolog 2 (Drosophila)
PRKAB2	protein kinase, AMP-activated, beta 2 non-catalytic subunit
PRKACB	protein kinase, cAMP-dependent, catalytic, beta
PRNP	prion protein
PRRC1	proline-rich coiled-coil 1
PRSS23	Protease, serine, 23
PSEN1	presenilin 1
PTCH1	patched homolog 1 (Drosophila)
RAB31	RAB31, member RAS oncogene family
RBM23	RNA binding motif protein 23
SCLY	selenocysteine lyase
SEC22B	SEC22 vesicle trafficking protein homolog B (S. cerevisiae)
SETBP1	SET binding protein 1
SLC1A1	solute carrier family 1 (neuronal/epithelial high affinity glutamate transporter, system Xag), member 1
SLC30A6	solute carrier family 30 (zinc transporter), member 6
SLC38A7	solute carrier family 38, member 7
SNX21	sorting nexin family member 21
SOCS3	suppressor of cytokine signaling 3
ST5	suppression of tumorigenicity 5
SYT1	synaptotagmin I
TCF7	transcription factor 7 (T-cell specific, HMG-box)
TFG	TRK-fused gene
TMEM183A	transmembrane protein 183A
TMEM33	transmembrane protein 33
TNFRSF10B	tumor necrosis factor receptor superfamily, member 10b
TNFRSF21	tumor necrosis factor receptor superfamily, member 21
TPRG1L	tumor protein p63 regulated 1-like
TRIM69	tripartite motif-containing 69
TTC7B	tetratricopeptide repeat domain 7B
TWSG1	twisted gastrulation homolog 1 (Drosophila)
UBE2I	Ubiquitin-conjugating enzyme E2I (UBC9 homolog, yeast)
UBE2Z	ubiquitin-conjugating enzyme E2Z

(Continued)

Symbol	Description
UBP1	upstream binding protein 1 (LBP-1a)
UFM1	ubiquitin-fold modifier 1
UNC13B	unc-13 homolog B (C. elegans)
WAPAL	wings apart-like homolog (Drosophila)
WBP4	WW domain binding protein 4 (formin binding protein 21)
XPNPEP3	X-prolyl aminopeptidase (aminopeptidase P) 3, putative
YIPF6	Yip1 domain family, member 6
ZAK	sterile alpha motif and leucine zipper containing kinase AZK
ZCCHC24	zinc finger, CCHC domain containing 24
ZDHHC5	zinc finger, DHHC-type containing 5
ZNF23	zinc finger protein 23 (KOX 16)
ZNF271	zinc finger protein 271
ZNF317	zinc finger protein 317
ZNF35	zinc finger protein 35
ZXDB	zinc finger, X-linked, duplicated B
	CDNA FLJ30652 fis, clone DFNES2000011
	CDNA FLJ39585 fis, clone SKMUS2006633
	CDNA FLJ31233 fis, clone KIDNE2004579
	CDNA FLJ37302 fis, clone BRAMY2016009
	CDNA FLJ34250 fis, clone FCBBF4000529